Development of a Flame Spread Screening Tool for Fiber Reinforced Polymers

A Major Qualifying Project Report
submitted to the Faculty of
WORCESTER POLYTECHNIC INSTITUTE
in partial fulfillment of the requirements for the
Degree of Bachelor of Science
By:

_____

Valerie Boutin

_____

Andrew Eng

_____

Michael Gorgone

_____

Matthew Guilfoyle

_____

Craig Mitchell

_____

Chelsea Tuttle

May 2012
Project number: NAD FM11

_____

Professor Nicholas A. Dembsey, Advisor

Table of Contents

List of Figures

List of Tables

1. Organization of this MQP

This MQP is a compilation of two 15-page conference papers focusing on flame spread modeling of fiber reinforced polymers. Chapter two is the first of the two papers and focuses on interior testing. Chapter three is the second of the papers and focuses on exterior testing as well as a capstone design exercise. Abstract and references are included with each respective chapter. The MQP also contains a series of appendices to cover material in a complexity not covered in the conference style paper.

2. Development of a Flame Spread Screening Tool for Fiber Reinforced Polymers for Interior Applications

2.1. Abstract

The International Building Code (IBC) is often referenced in the United States to establish requirements for new construction. Based on performance criteria established in the IBC, interior finish materials are rated Class A, B, or C or pass/fail. The uses of materials are limited to particular building areas and applications according to their classification. To obtain a classification, materials must undergo full-scale standardized tests: Tunnel Test and Room Corner Test (ASTM E 84 or NFPA 286 respectively). The Tunnel Test is beneficial because it is less expensive to conduct, provides a greater range of classification, and is a traditional test in the field of fire protection. The Room Corner Test is advantageous because the conditions are more realistic and comparable to true fire scenarios. Both of these tests impose a potentially significant economic penalty for material development. Currently there is no IBC process for screening materials based on economical bench-scale standardized testing (ASTM E 1354) to assess materials performance in full-scale tests. Fiber reinforced polymers (FRPs) are of growing interest in building construction due to their customizability. An initial flame spread model was developed relating Cone Calorimeter (ASTM E 1354) test data to full-scale test scenarios in the Tunnel Test and Room Corner Test. The flame spread model is capable of screening new materials to suggest performance levels in full-scale testing based on material properties of FRP systems.

2.2. Introduction

Material developers are faced with the challenge of creating new materials that fit both an architect's vision and the Authority Having Jurisdiction's (AHJ's) safety requirements. The International Building Code (IBC) [1] is often referenced in the United States by the AHJ to establish safety requirements for new construction. The IBC requires any new interior finish material to undergo a full-scale standardized test, either the Tunnel Test (ASTM E84) [2] (Appendix G) or the Room Corner Test (NFPA 286) [3] (Appendix F). The Tunnel Test will result in a classification (A, B, or C), and this classification will determine where the material can be used inside the building. The Room Corner Test results are reported as pass/fail. If the material passes it can be used virtually anywhere inside the building. These tests are both time

consuming and costly. If the desired result is not attained, the material developer must make changes and submit the material for retesting. Additional testing imposes a potentially significant economic penalty for material development. Currently, there is no process for screening materials based on the more economical bench-scale standardized tests such as the Cone Calorimeter (ASTM E 1354) [4] (Appendix A) to assess performance in full-scale tests.

This project studied the relationship between the material properties measured in the Cone Calorimeter of fiber reinforced polymers (FRPs) and their performance in full-scale tests. These materials are of growing interest in building construction due to their customizability. An initial flame spread model was developed relating Cone Calorimeter material properties to full-scale test scenarios in the Tunnel Test and Room Corner Test. The Tunnel Test model was based on previous work by Mowrer and Williamson [5] and the Room Corner Test model used this work in conjunction with Schebel's work [6]. Fourteen FRP systems, each with a change in one component (e.g. resin type, aggregate type, etc.) were screened using the model.

In going forward, manufacturers will be able to use this initial model to screen materials relative to full-scale standardized test performance, and determine in which applications their material can be used. This will enable them to make changes to the material to obtain optimum performance without wasting time and resources on multiple full-scale tests.

2.3. Interior Finishes

The IBC divides all parts of a building into three sections as seen in Figure 1. Depending on what section of the building (exit enclosure/exit passageway, corridor, or room/enclosed space) and the primary use of the building the required classification of the material will change (Appendix I). For areas that are important to the means of egress, life safety becomes a concern. The code requirements are stricter because the material needs to be able to withstand a fire long enough for people to safely exit. Table 2-1 summarizes the code requirements for non-sprinklered buildings. The code requirements change if the building is fitted with an automatic suppression system.
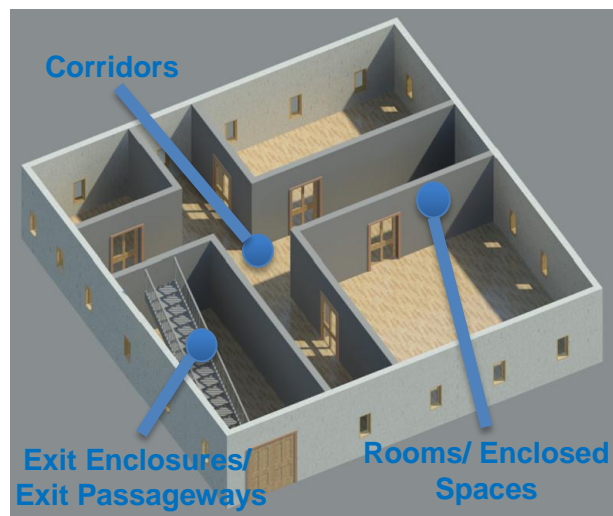

Figure 2-1: Areas of a Building

Table 2-1: IBC Interior Finish Requirements

Occupancy	Example	Exit Enclosures & Exit Passageways	Corridors	Rooms & Enclosed Spaces
Assembly-1 & Assembly 2	Theater & Restaurant	A	A	B
Assembly-3, Assembly-4, & Assembly 5	Community Hall, Arena, & Stadium	A	A	C
Business, Educational, Mercantile, & Residential-1	Office, School, Retail Store, & Hotel	A	B	C
Residential-4	Assisted Living (6-15 people)	A	B	B
Factory	Millwork	B	C	C
High Hazard	Storage of Toxic Materials	A	A	B
Institutional-1	Assisted Living Facility	A	B	B
Institutional-2	Hospital	A	A	B
Institutional-3	Prison	A	A	B
Institutional-4	Child Daycare Facility	A	A	B
Residential-2	Apartment	B	B	C
Residential-3	Adult Care Facility (<5 people)	C	C	C
Storage	Warehouse	B	B	C

2.4. Database

Fourteen (14) FRP systems provided by Kreysler & Associates were designed for interior applications. The Baseline FRP Figure 2-2 was a 0.06in (1.5mm) thick polymer concrete layer that contained a resin, alumina trihydrate, and sand aggregate. The substrate was a 0.1875in (4.8mm) layer consisting of a resin and 4 layers of glass in a chopped strand mat mixed in a glass to resin ratio range of 25:75 to 35:65 by weight. The resin used in both layers was Norsodyne with intumescent additives. The other FRP systems were modifications of the Baseline, each with one variation of a component: sand aggregate was replaced by specified fillers, the size of sand aggregate was altered, various pigments were added to the polymer concrete, and the surface layer was changed to Norsodyne without an aggregate and the substrate layer was changed to DCPD. Additionally, three FRP systems were sandwich panels Figure 2-2 with the Baseline FRP on the top face, varying materials in the core, and an identical substrate layer on the bottom face. A complete table of FRP systems can be seen in Table 2-2: FRP System .
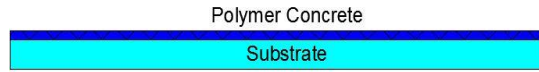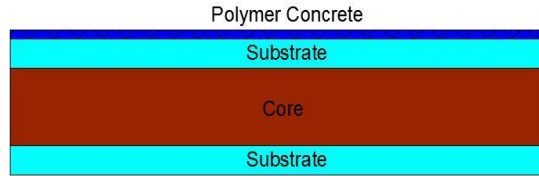
Figure 2-2: Baseline FRP

Figure 2-3: Sandwich Panel FRP

Table 2-2: FRP System Modifications

Filler	Aggregate	Pigment	Resin	Core
Bronze	#0/30	White	Norsodyne	Plywood
Aluminum	#0/60	Grey	DCPD	Balsa
	#2/16	Beige		Foam

Following ASTM E 1354 (See Appendix A), the fourteen FRP specimens were tested in the Cone Calorimeter to obtain bench-scale material properties. Incident heat fluxes of 25, 50, and 75kW/m^2 were selected for testing. Various material properties were obtained including the heat release rate per unit area (HRRPUA), time to ignition (t_f), and mass loss rate. Qualitative observations were made during the test to determine other parameters required for large-scale prediction (e.g. time to burn out). A database was developed to organize the information by specimen type and document each specimen's characteristics. Typical variation in heat release rate caused by changes to the incident heat flux of the Cone is shown in Figure 2-4. A complete compilation of Cone data can be found in Appendix J and Appendix K.
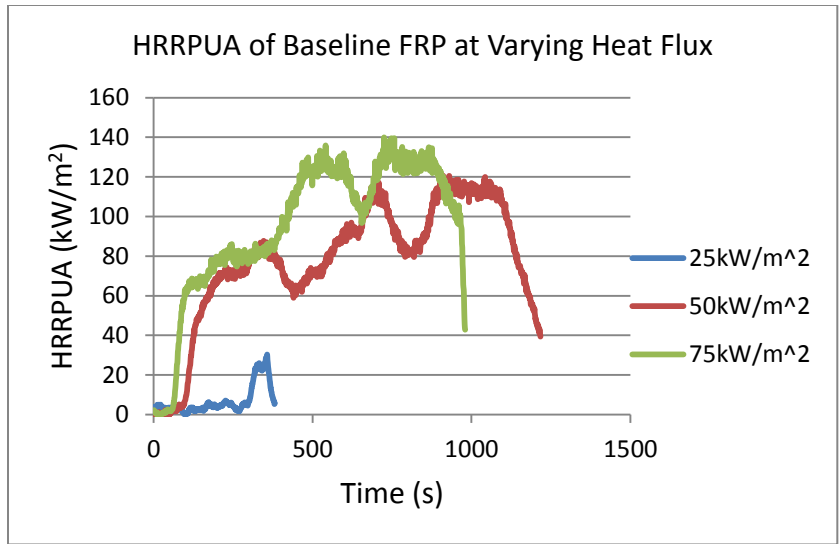
Figure 2-4: HRRPUA of Baseline FRP at Variable Heat Fluxes

A significant drop in heat release rate was seen at an incident heat flux of $25kW/m^2$. This suggests that this value is near the minimum heat flux for ignition of the material. This is further illustrated by the significant increase in time to ignition at the lower heat flux as seen in Figure 2-5.

Figure 2-5: Baseline FRP time to Ignition vs Incident Heat Flux

The Database of inputs each system from the Cone Calorimeter is highlighted in Table 2-3. These inputs will be used in the Modeling Section below.

Table 2-3: Model Inputs at 65kW/m^2

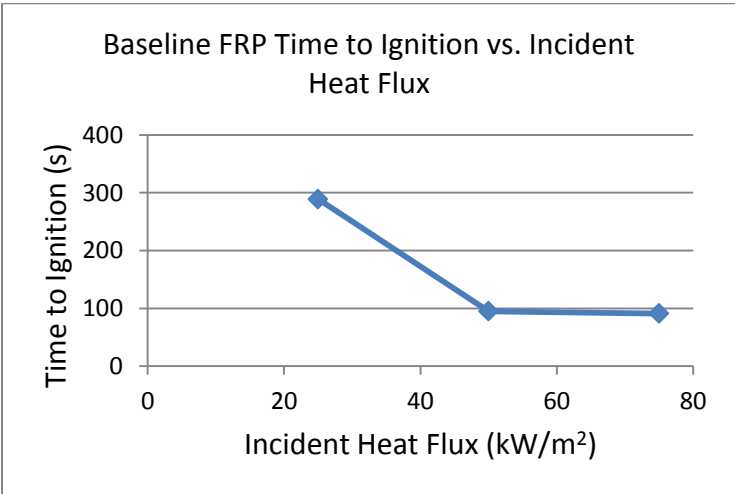| System	HRRPUA (kW/m^2)	T$_f$ (sec)
Baseline	110	150
Core_Plywood	60	140
Core_Balsa	50	130
Core_Foam	120	60
Filler_Bronze	110	50
Filler_Aluminum	110	50
Pigment_White	110	60
Pigment_Grey	90	60
Pigment_Beige	101	60
Aggregate_030	101	60
Aggregate_060	110	60
Aggregate_216	70	70
Resin_Norsodyne	101	50
Resin_DCPD	120	30

2.5. The Model

The model being used is an adaptation of Mower and Williamson's simple flame spread model for thin interior materials [5] (Appendix B). The model uses the parameters measured in the Cone to predict the propagation of the pyrolysis front and the burnout front during the test. While the pyrolysis front starts at the ignition time, the burnout front beings after a set burnout time for the model. Mower and Williamson's simplified model simulates flame spread through the advance of the pyrolysis front which is shown below (Figure 2-6):
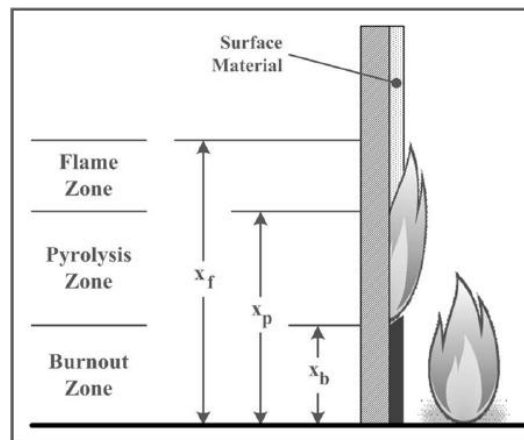

Figure 2-6: Mowrer and Williamson Flame Spread Model

$$\frac{dx_p}{dt} = V_p = \frac{x_f(t) - x_p(t)}{t_f} \tag{2-1}$$

The advancement of the pyrolysis front is based on flame height, pyrolysis height and ignition time. Once burnout begins this value is shown by:

$$\frac{dx_b}{dt} = V_b = \frac{x_p(t) - x_b(t)}{t_{bo}} \tag{2-2}$$

Mower and Williamson finish their derivation by integrating the equations within specific bounds to gain relationships for x_p and x_b. However, since the source fire plays a significant role in the flame spread of standardized tests, the equations have been adapted to incorporate the source fire. The driving force behind the model is the forward heating zone, represented by the flame length. The flame length is calculated using a linearized approximation suggested by Quintiere et. Al [7]. The flame length approximation before burnout therefor becomes:

$$x_f = k_f \dot{E}'' x_p + k_f \dot{Q}_s' \tag{2-3}$$

A similar flame length approximation is used for times after burnout:

$$x_f = k_f \dot{E}'' (x_p - x_b) + k_f \dot{Q}_s' + x_b \tag{2-4}$$

Using the flame length approximation including the source fire, Equation 2-.1 can be rewritten using Equation 2-3 as:

$$\frac{dx_p}{dt} = \frac{k_f \dot{Q}_s' + (k_f \dot{E}'' - 1) x_p}{t_f} \tag{2-5}$$

Using Equation 2-5, a relationship is derived for x_p before burnout by integrating with the bounds of $x_p = x_{po}$ at t=0 and $x_p = x_p$ at t=t. With these bounds Equation 2-5 can be integrated and rearranged:

$$x_p = \left(\frac{k_f \dot{Q}_s'}{k_f \dot{E}'' - 1} + x_{po} \right) * e^{k_f \dot{E}'' - 1 * \left(\frac{t}{t_f} \right)} - \frac{k_f \dot{Q}_s'}{k_f \dot{E}'' - 1} \tag{2-6}$$

According to Mower and Williamson [5], the flame spread can be expressed as the advancement of the pyrolysis zone, V_p-V_b. Combining Equations 2-1 and 2-2 with Equation 2-4, we get a relationship for the advancement of the pyrolysis zone after burnout begins, shown below:

$$V_p(t) - V_b(t) = \frac{d(x_p - x_b)}{dt} = \frac{k_f \dot{Q}_s' + k_f \dot{E}'' (x_p - x_b) + x_b - x_p}{t_f} - \frac{x_p - x_b}{t_{bo}} \tag{2-7}$$

Integrating Equation 2-7 with the bounds of x_p-x_b=x_{p1}-x_{po} at t=t_b and x_p-x_b= x_p-x_b at t=t a relationship between the pyrolysis zone and time can be seen below:

$$x_p - x_b = \frac{\left((x_{p1} - x_{po}) C_4 + C_3 \right) e^{C_1(t - t_b)} - C_3}{C_4} \tag{2-8}$$

2-11

An expression for x_b can be derived in a similar fashion by following the work of Schebel [6]. Combining Equations 2-2 and 2-8 an expression for V_b is developed:

$$V_b = \frac{dx_b}{dt} = \frac{\left((x_{p1}-x_{po})C_4+C_3\right)e^{C_1(t-t_b)}-C_3}{C_4} + x_b - x_b \tag{2-9}$$

Integrating Equation 2-9 within the bounds of burnout, $x_b=x_{po}$ at $t=t_b$ and $x_b=x_b$ at $t=t$, we obtain an expression for the advancement of the burnout front after t_b:

$$x_b = \left(\frac{C_2}{C_1} + \frac{C_3}{C_1 C_4 t_{bo}}\right)\left(e^{C_1(t-t_b)} - 1\right) - \frac{C_3(t-t_b)}{C_4 t_{bo}} + x_{po} \tag{2-10}$$

Where: $\qquad C_1 = \dfrac{\left(k_f \dot{E}'' - \frac{t_f}{t_b} - 1\right)}{t_f} \qquad\qquad\qquad C_3 = k_f \dot{Q}_s' t_{bo}$

$\qquad\qquad\qquad C_2 = \dfrac{x_{p1}-x_{po}}{t_{bo}} \qquad\qquad\qquad\qquad C_4 = \left(k_f \dot{E}'' - 1\right)t_{bo} - t_f$

Combining Equations 2-9 and 2-10, an expression for x_p after burnout can be found.

There are 3 different sets of inputs for the model being used. The source fire heat release rate, flame length coefficient, and the initial burn zone make up the first set of inputs. These values come directly from the literature for the respective tests and are taken to be constants. The second set of inputs comes directly from the material database: the ignition time and HRRPUA. The last set of inputs contains the calibration parameters: time to burnout and material burnout time. These parameters were calibrated based on full-scale test data.

For the Room Corner test we assumed a burn area similar to the work of Schebel [6]. Equation 2-11 describes the area of the wall burning while both x_p and x_b are on the wall. Equation 2-12 is effective once x_p reaches the ceiling and begins to spread along the walls in the T-shape pattern. The T-shaped pattern is represented as 8% of the ceiling height. Equation 2-13 represents the burn area once both x_p and x_b have exceeded the ceiling height. The model assumes the fire advances radially across the ceiling.

For $x_p < H$ and $x_b < H$

$$HRR \; vs. Time = (x_p - x_b)(2x_{pow})(\dot{E}'') \tag{2-11}$$

For $x_p > H$ and $x_b < H$

$$HRR \; vs. Time = \left[(H - x_b)2x_{pow} + 2D(x_p - H) + \frac{\pi}{4}\left(\frac{x_{pow}}{2} + (x_p - H)\right)^2\right]\dot{E}'' \tag{2-12}$$

For $x_p > H$ and $x_b > H$

$$HRR \; vs. Time = \left[2D(x_p - x_b) + \frac{\pi}{4}\left(\frac{x_{pow}}{2} + (x_p - H)\right)^2 - \frac{\pi}{4}\left(\frac{x_{pow}}{2} + (x_b - H)\right)^2\right]\dot{E}'' \tag{2-13}$$

2.6. Tunnel Test Calibration Inputs

The input parameter x_{p0} represents the length of the initial pyrolysis zone in meters. For the Tunnel Test model it is taken as equal to 0.6m. This value was estimated for the Tunnel Test based on a heat flux map for ASTM E 84 [8], and the assumption that x_{p0} would represent an ignition length where the heat fluxes are above 30kW/m^2, which is consistent with the observation in the Cone testing that the critical heat flux of the FRP systems is approximately 25kW/m^2. The maximum heat flux from the heat flux map was approximately 44kW/m^2. The average heat flux over the estimated 0.6m was 36kW/m^2 which was rounded to 40kW/m^2. The input $\dot{E}''$ represents the heat release rate per unit area of the baseline FRP system at a characteristic heat flux composed of the source fire and the insult from wall flames. To obtain this characteristic heat flux, the value from the burner (40kW/m^2) is added to 25kW/m^2. The 25kW/m^2 is the estimated heat flux from the burning specimen according to the wall [9]. This results in a total incident heat flux of 65kW/m^2. From a graph of HRRPUA vs. heat flux from the Cone data, and the characteristic heat flux of 65kW/m^2, an interpolated value for HRRPUA was 110kW. The same method of interpolation was used to calculate a time to ignition at a heat flux of 65kW/m^2 (Similar to Figure 2-5). The input k_f is a constant and the value 0.011 is used. This value is increased from the suggested 0.01 value due to the forced flow effects in the tunnel. Based on the work of Fernandez-Pello [10], forced flow increases the heat transfer between the flame and ceiling (this is further detailed in Appendix C). The inputs t_b and t_{bo} were calibration parameters adjusted during calibration. Ultimately both inputs were assigned a value of 60 seconds which yielded model results consistent with the actual full-scale test results. After 60 seconds the flame spread has advanced outside of the source fire heat affected zone. The model reflects this by neglecting the source fire after 60 seconds. All calibration inputs are outlined in Table 2-4.

2.7. Room Corner Test Calibration Inputs

In the room corner test, the initial burn zone is equal to 0.5m. This was estimated using the work of Williamson and Revenaugh [11]. The input k_f is a flame length parameter. As outlined in Clearey and Quintiere's paper [7] a value 0 .01 is used for buoyant flow. The input $\dot{E}''$ represents the characteristic heat release per unit area which consists of the heat from the source fire to the wall and from the burning material to the wall. The value used was 85kW/m^2. An approximate value of 60kW/m^2 was used for the heat from the source fire to the wall. An additional 25kW/m^2 was added to account for the heat from the burning material to the wall [9]. Since the cone data was only available for a maximum incident heat flux of 75kW/m^2, these values were used. The time to ignition, t_f, was selected based on the cone data at 75kW/m^2. Similar to the tunnel test calibration, t_b and t_{bo} were calibration parameters adjusted during calibration. Ultimately, t_{bo} was assigned a value of 400s, and t_b was assigned a value of 60s, in order to yield the best fit from the model to the actual full-scale test results.

Table 2-4: Calibration Inputs

Inputs		ASTM E 84 Tunnel Test Calibration Inputs		NFPA 286 Room Corner Test Calibration Inputs	
			Units		Units
Initial burn zone	X_{po}	0.6	m	0.5	m
Flame length parameter	K_f	0.011	m^2/kW	0.010	m^2/kW
HRRPUA Material	$\dot{E}''$	110	kW/m^2	110	kW/m^2
HRRPUA Source	Q	120	kW/m	230	kW/m
Time to ignition	t_f	150	seconds	50	seconds
Material burnout	t_{bo}	60	seconds	400	seconds
Test burnout	t_b	60	seconds	60	seconds

2.8. Results

The outcome of the Tunnel Test is a flame-spread index (FSI) that classifies materials based on burning behavior on surfaces such as walls and ceilings. Flame-spread index is a number calculated according to the total area under a flame-spread curve. The Baseline FRP system was used to calibrate the model against Tunnel Test results provided by Kreysler & Associates. The final result of the calibration procedure of the model for the Tunnel Test indicates an FSI of 15 (shown in Figure 2-7) while the experimental data suggests a rating of 20. Using the Law of Propagation of Uncertainty, the uncertainty of the calibration process was calculated as $\pm$ 0.5m (Appendix D). It is calculated that a fluctuation of 0.5m reflects a change in FSI of $\pm$ 5. The experimental FSI falls within the uncertainty boundaries of the calculated model. With the calibration parameters determined from the Baseline, the model was run for all FRP systems.
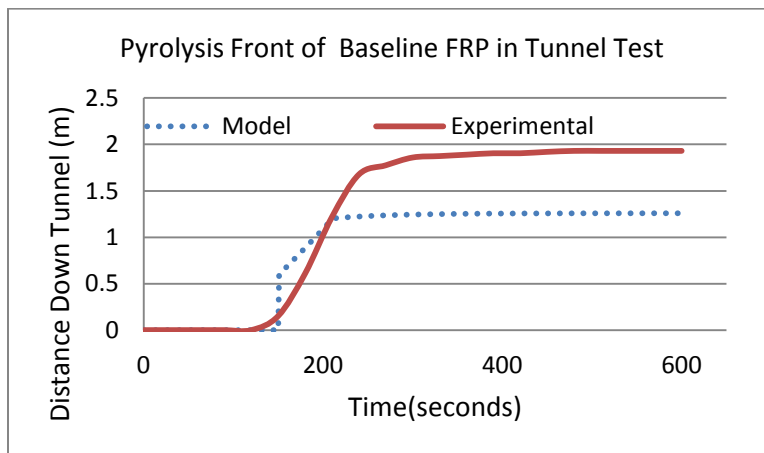
Figure 2-7: Pyrolysis Front of Baseline FRP in Tunnel Test

The outcome of the NFPA 286 Room Corner Test is a pass/fail grade based on the heat release rate (HRR). Materials that produce less than 800kW are considered passing and have no application restrictions, similar to a Class A material [3] (See appendix F). The two step burner

regime of 286 was used where the HRR of the burner starts at 40kW for 5 minutes followed immediately by 160 kW for 10 minutes. The experimental room corner tests were not run in exact accordance with NFPA 286. There were four tests each with variations. The first two tests (one with the baseline FRP and one with the Norsodyne resin FRP) were run as screening tools. Panels were placed vertically up the corner and horizontally across where the wall meets the ceiling. In addition, two panels were placed on the ceiling. For the second two tests, these ceiling panels were removed. These configurations can be seen in Figure 2-8 and Figure 2-9. For a screening specimen to be considered valid, the pyrolysis zone cannot reach the end of the panels. In these experiments, the ends of the specimens were reached indicating that further flame spread would be expected and greater HRRs would be produced. These greater HRRs indicate that the two FRP systems on the walls and ceiling will not pass a NFPA 286 test using a full specimen. To simplify the model calibration, two additional experiments were conducted using a constant burner HRR of 160kW for 10 minutes. In one experiment the Baseline FRP was used with no ceiling panels, and in the other experiment the surface coating Norsodyne resin FRP with ceiling panels was used. As with the Tunnel Test, this model was calibrated against the Baseline and Norsodyne surface layer experimental results. The results of these two experiments are shown in Figure 2-10 and Figure 2-11. The experimental results without the ceiling (Figure 2-10) indicate a maximum HRR of 340kW (prior to compartment effect) while our model suggests a maximum of 310kW. Using the Law of Propagation of Uncertainty, the uncertainty of the calibration process was calculated as ± 40kW (Appendix D). The experimental results for the test with a ceiling indicate a maximum heat release rate of 780kW/m^2 while the model suggests a maximum of 2000kW/m^2 with an uncertainty of ± 40kW.
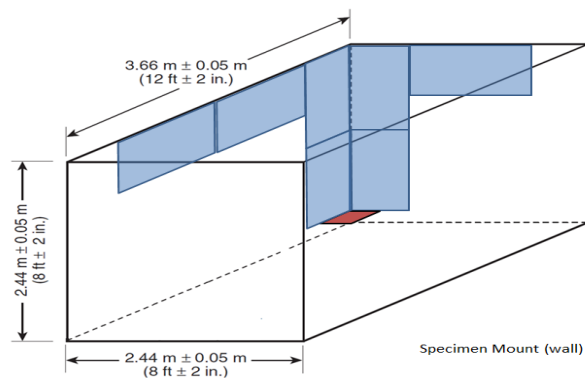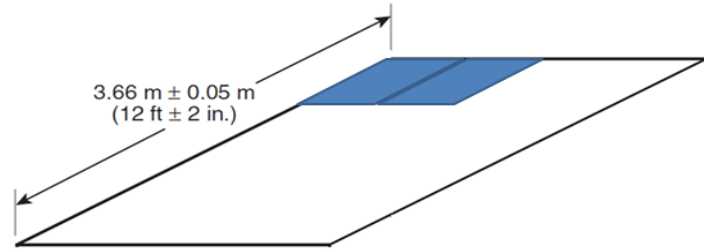

Figure 2-8: Room Corner Test Wall Configuration

Specimen Mount (ceiling)

Figure 2-9: Room Corner Test Ceiling Configuration
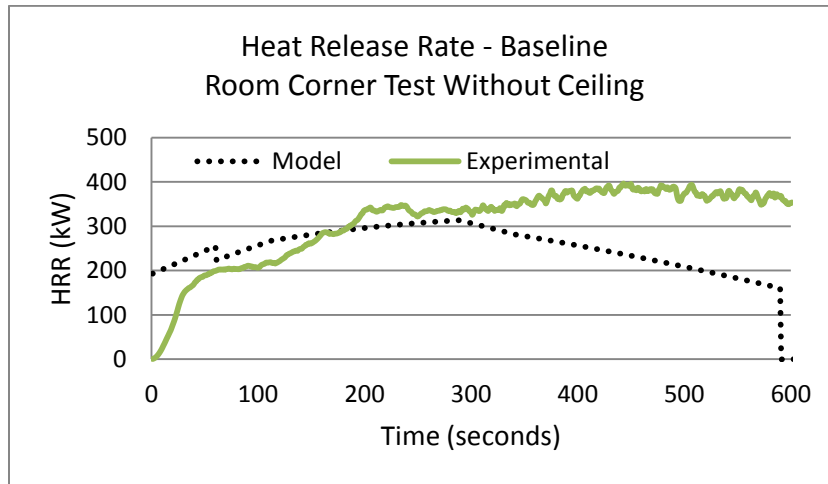

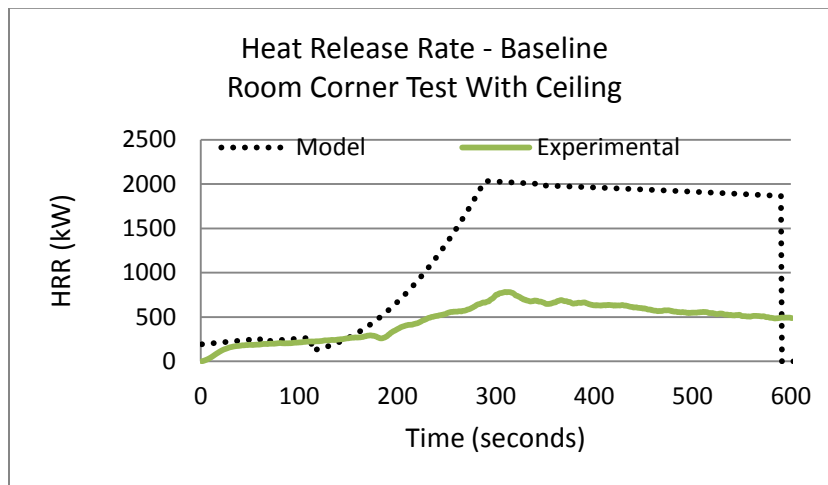Figure 2-10: Baseline HRR Calibration Results With No Ceiling

Figure 2-11: Baseline HRR Calibration Results With Ceiling

Table 2-5: Simulated Test Results

Specimen	ASTM E84 Tunnel Test		NFPA 286 Room Corner Test No Ceiling		NFPA 286 Room Corner Test With Ceiling	
	FSI	Class	HRR (kW)	Pass	HRR (kW)	Pass
Baseline	15	A	310	Yes	2040	No
Bronze Filler	45	B	460	Yes	2690	No
Al Filler	45	B	510	Yes	2740	No
0/30 Aggregate	30	B	480	Yes	2550	No
0/60 Aggregate	35	B	410	Yes	2300	No
2/16 aggregate	20	A	370	Yes	2100	No
White Pigment	40	B	280	Yes	1310	No
Grey Pigment	25	A	410	Yes	2120	No
Beige Pigment	30	B	400	Yes	2300	No
Norsodyne Resin	40	B	420	Yes	2310	No
DCPD Resin*	180 / 20	C / A	480	Yes	2550	No
Plywood Core	15	A	260	Yes	1380	No
Balsa Core	15	A	350	Yes	2070	No
Foam Core	15	A	290	Yes	1660	No

DCPD Resin has two reported FSIs because there was a large discrepancy in the cone data for time to ignition

As seen in Table 2-5, all of the FRP systems received an A or B classification in the Tunnel Test and passed the Room Corner Test if the FRP is not placed on the ceiling. If the FRP were to be used on the ceiling, the model predicts the specimen will not meet the passing requirements.

Even though all FRPs passed the tests, the different groups of systems performed differently. Changing the fillers had a significant negative effect on HRR, with these systems having an FSI of 45. This change from the baseline FSI of 15 is significant because it is exceeds the bounds of uncertainty of our model. Changing the aggregates had a less significant effect, with FSI values ranging from 20 to 35, but several of these are outside the bounds of our uncertainty. Changing the pigments also had a less significant effect, with FSI values ranging from 25 to 40, but several of these are outside the bounds of our uncertainty as well. The addition of cores had little to no impact on the FSI. As seen in Table 2-5, there are similar trends between tests within the groups of systems. The systems with different fillers had the highest HRR, the ones with different pigments had the next highest HRR, the ones with the different aggregate sizes had lower HRR, and the systems with the different cores had little to no change in HRR. The screening tool was unable to accurately represent the systems with resin changes the Norsodyne surface layer and the DCPD substrate layer because their initial burning behaviors were outside the paradigm of model.

2.9. Conclusion and Recommendations

The recommendations of the team are that none of the FRP systems should be used on the ceiling. If a class A rating is desired, the FRPs with different fillers should not be used, and systems with different aggregate sizes or pigments should be carefully considered before use. The systems with added cores behave similarly to the Baseline FRPs and therefore should be able to be used in the same applications. During our analysis it was determined that the driving factor behind changes in performance was the time to ignition. The systems that ignited the quickest had the highest FSI in the Tunnel Test and the highest HRR in the Room Corner Test. This should be taken into consideration when analyzing different FRP systems. In conclusion, this project created a simple, easy to use flame spread model for different FRPs that gives a better indication of performance of the modified FRPs without spending money on full-scale testing. This allows manufacturers to know where different systems could be used in a building. In the future we hope the framework of this project can be used to facilitate further research.

2.10.   Nomenclature

$t = time$
$t_f = ignition\ time$
$t_b = time\ to\ burnout$
$t_{bo} = material\ burnout\ time$
$x_{po} = intial\ burn\ zone$
$x_{p1} = burn\ zone\ when\ burnout\ begins$
$k_f = flame\ length\ correlation$
$\dot{E}'' = Heat\ realase\ rate\ per\ unit\ area\ of\ material$ (HRRPUA)
$\dot{Q}'_s = source\ fire$
$V_p = velocity\ of\ pyrolysis\ front$
$V_b = velocity\ of\ burnout\ front$
$x_{pow} = Initial\ source\ fire\ width$
$H = Ceiling\ Height$
$D = .08H\ (Representative\ T - Shape\ depth)$

2.11.   References

(1) International Building Code, 5th Edition.

(2) ASTM E 84, "Standard Test Method for Surface Burning Characteristics of Building Materials," ASTM International, West Conshohocken, PA

(3) NFPA 286, Standard Methods of Fire Tests for Evaluating Contribution of Wall and Ceiling Interior Finish to Room Fire Growth, 2011 Edition

(4) ASTME E 1354, "Standard Test Method for Heat and Visible Smoke Release Rates for Materials and Products Using an Oxygen Consumpiton Calorimeter," ASTM International, West Conshohocken, PA

(5) Mowrer, F.W., and Williamson, R.B.. "Flame Spread Evaluation for Thin Interior Finish Materials". *Fire Safety Science-Proceedings of the Third International Symposium*, p. 689-698.

(6) Schebel, K., Dembsey, N.A., Meacham, B.J., Johann, M., Tubbs, J., and Alston, J. "Fire Growth Simulation in Passenger Rail Vehicles Using a Simplified Flame Spread Model Coupled with a CFD Fire Model".

(7) Cleary, T.G., and Quintiere, J.G.. "A Framework for Utilizing Fire Property Tests". *Fire Safety Science-Proceedings of the Third International Symposium*, p. 647-656.

(8) Society of Fire Protection Engineering Handbook, 3rd edition: 2-14.59

(9) Society of Fire Protection Engineering Handbook, 3rd edition: 2-14.34

(10) Fernandez-Pello, C., & Zhou, L. "Turbulent, Concurrent, Ceiling flame spread: The Effect of Buoyancy." Combustion and Flame 92:45-49 (1993).

(11) Williamson,R, Revenaugh, A "Ignition Sources in Room Fire Tests and Some Implications for Flame Spread Evaluation"

3. Development of a Flame Spread Screening Tool for Fiber Reinforced Polymers for Interior Applications

3.1. Abstract

The International Building Code (IBC) is often referenced in the United States to establish requirements for new construction. Based on performance criteria, exterior cladding materials are classified as pass or fail, and require a pass in order to be used on the exterior of a building (with some exceptions listed in the IBC). To obtain this classification, materials must undergo a full-scale standardized test, NFPA 285, which imposes an economic penalty for materials development. Currently there is no process for screening materials based on economical bench-scale standardized testing such as the Cone Calorimeter (ASTM E 1354) to assess materials' performance in full-scale tests.

This study investigated the relationship between bench-scale material properties of various fiber reinforced polymers (FRPs) and their performance in full-scale tests. A flame

spread model was developed relating Cone Calorimeter (ASTM E 1354) test data to the full-scale Multi Story Building Test (NFPA 285). Initial evaluation shows the model to be a useful tool for screening materials. In going forward, manufacturers will be able to use this model to screen materials relative to full-scale standardized test performance, and determine if their material can be used. This will enable them to make changes to the material to obtain optimum performance without wasting time and resources on multiple full-scale tests. Additionally, an alternative test method was designed as a screening test for NFPA 285 using the dimensions of a standard fire test compartment. The accessible test facility will enable more laboratories to run the test and predict how the material will behave in the Multi Story Building Test.

3.2.Introduction

In the United States the International Building Code (IBC) [1], or similar adaptations, is referenced to govern new construction projects. The IBC dictates where and how certain materials can be used, and therefore influences decisions made by architects and contractors. Specifically, it requires that exterior wall assemblies be tested in accordance with and comply with the acceptance criteria of the test standard NFPA 285 [12] (Appendix E). However, the Multi Story Building Test (NFPA 285) requires a large test facility as well as large testing specimens, which limit the number of facilities that can conduct this test for material developers. Due to this limitation and the potential economic penalty, when a developer is ready to test his product, failure of NFPA 285 is extremely undesirable.

It was the goal of this project to develop a screening tool to predict behavior of materials in the NFPA 285 test using bench-scale material properties obtained from a Cone Calorimeter test (ASTM E 1354) [4] (Appendix A). Similar work has been done by the Building Research Association of New Zealand (Branz) and is reported in Development of a vertical channel test method for regulatory control of combustible exterior cladding system [13]. Branz suggests an intermediate test, which would act as a screening test to larger scale exterior test methods similar to NFPA 285. The initial model used as a screening tool was adapted from the work done by Mowrer and Williamson [5] and was calibrated using the data from Chapter 2 - Interior Finishes. When used correctly, the model is able to use input parameters derived from cone calorimeter results to calculate the length of flame spread for a specific material in the NFPA 285 test. The success of this model would allow material developers to run multiple bench-scale tests to refine their materials before spending time, money, and resources on a large-scale test such as NFPA 285.

Finally, this project designed an alternative test method for screening NFPA 285. This Exterior Screening Test will provide data to determine whether or not a material will pass or fail the NFPA 285 test. The test is developed to mimic the heat fluxes and flame spread associated

with NFPA 285 while using smaller room dimensions.

3.3. Database

      The FRPs used for this project were provided by Kreysler and Associates. They are designed for both interior and exterior use and can be modified to possess desired aesthetic traits. The Baseline FRP (Figure 3-1) consists of a polymer concrete layer on the top face of a substrate. The polymer concrete contains Norsodyne resin, alumina trihydrate, and sand aggregate. The substrate contains Norsodyne resin with 4 layers of chopped strand mat glass. There were thirteen other FRP systems, each with a change in one component. As portrayed in Table 3-1: the sand aggregate was replaced by specified fillers, affecting the reflectivity of the FRP; the size of the aggregate was varied, affecting the texture; and various pigments were added to the polymer concrete, affecting the color. They also experimented with the resins in the FRP. In one sample, the alumina trihydrate and sand aggregate were removed from the polymer concrete, leaving the top layer a resin-rich surface of Norsodyne. This mimicked a gel coat surface, which could have desirable characteristics to an architect. The final sample was experimental: the substrate resin was replaced with a DCPD laminate resin, which is more combustible then Norosdyne, to observe the fire protective properties of the Baseline polymer concrete. Additionally, as shown in Figure 3-2, three FRP systems were sandwich panels, with the Baseline FRP on the top face, varying cores in the middle, and an identical substrate layer on the bottom face. These cores were added to increase strength and bending resistance.
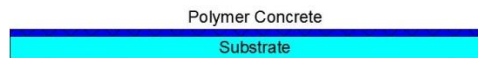
Figure 3-1: Baseline FRP
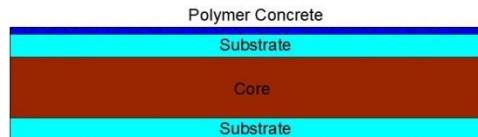
Figure 3-2: FRP Sandwich Panel

Table 3-1: FRP System Modifications

Filler	Aggregate	Pigment	Resin	Core
• Bronze • Aluminum	• #0/30 • #0/60 • #2/16	• White • Grey • Beige	• Resin rich surface • DCPD Laminate	• Plywood • Balsa • Foam

3.4. Cone

The FRP systems were tested using the Cone Calorimeter in accordance with ASTM E1354 (Appendix A) to create a material database of the 14 systems (Cone data found in Appendix J). The material database contains information about these systems at three incident heat fluxes: 25kW/m^2, 50kW/m^2, and 75kW/m^2. Shown below (Figure 3-3) is the typical heat release rate per unit area (HRRPUA) of the Baseline FRP system at 50kW/m^2. Using the material database, values can be interpolated at the desired incident heat flux. The material properties used in the model come directly from the Cone data, including average ignition time and average HRRPUA. Shown in Table 3-2, these parameters where taken at an incident heat flux of 65 kW/m2, which is consistent with the incident heat flux of NFPA 285.
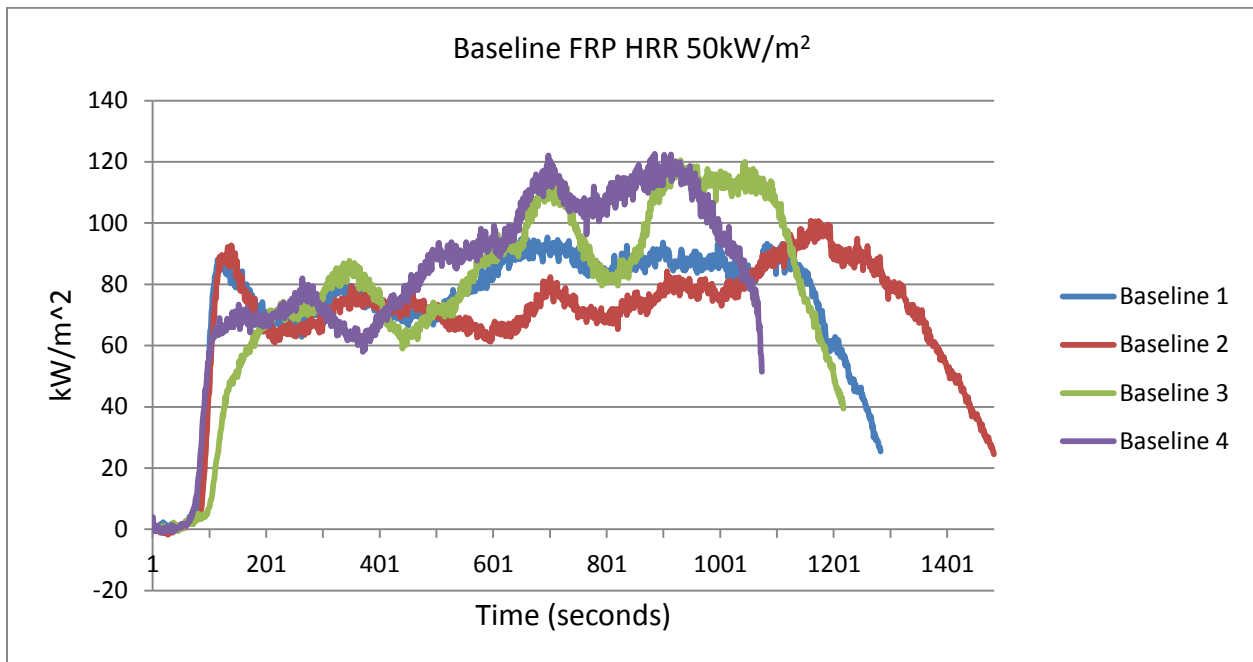
Figure 3-3: Repeat Runs of Baseline FRP at 50kW/m^2

Table 3-2: Model Inputs at 65kW/m^2

System	HRRPUA (kW/m^2)	T$_f$ (sec)
Baseline	110	150
Core_Plywood	60	140
Core_Balsa	50	130
Core_Foam	120	60
Filler_Bronze	110	50
Filler_Aluminum	*110*	*50*
Pigment_White	110	60
Pigment_Grey	90	60
Pigment_Beige	101	60
Aggregate_030	101	60
Aggregate_060	110	60
Aggregate_216	70	70
Resin_Norsodyne	101	50
Resin_DCPD	120	30

3.5. Model

The model being used is an adaptation of Mowrer and Williamson's [5] simple flame spread model for thin interior materials (for more information see Appendix B). The model uses the parameters measured in the Cone to predict the propagation of the pyrolysis front and the burnout front during the test. While the pyrolysis front starts at the ignition time, the burnout front begins after a set burnout time for the model. Mowrer and Williamson's simplified model simulates flame spread through the advance of the pyrolysis front:

$$\frac{dx_p}{dt} = V_p = \frac{x_f(t) - x_p(t)}{t_f} \tag{3-1}$$

The advancement of the pyrolysis front is based on the flame height, the pyrolysis height and the ignition time. Once burnout begins this value is shown by:

$$\frac{dx_b}{dt} = V_b = \frac{x_p(t) - x_b(t)}{t_{bo}} \tag{3-2}$$

Mowrer and Williamson finish their derivation by integrating the equations within specific bounds to gain relationships for x_p and x_b. However, since the source fire plays a significant role in the flame spread of standardized tests, the equations have been adapted to incorporate the source fire. The driving force behind the model is the forward heating zone, represented by flame length. The flame length is calculated using a linearized approximation suggested by Mowrer and Williamson [5]. The flame length approximation before burnout therefore becomes:

$$x_f = k_f \dot{E}'' x_p + k_f \dot{Q_s}' \tag{3-3}$$

A similar flame length approximation is used for times after burnout:

$$x_f = k_f \dot{E}'' (x_p - x_b) + k_f \dot{Q_s}' + x_b \tag{3-4}$$

Using the flame length approximation including the source fire, Equation 3-1 can be rewritten using Equation 3-3 as:

$$\frac{dx_p}{dt} = \frac{k_f \dot{Q}_s{}' + (k_f \dot{E}'' - 1)x_p}{t_f}$$ (3-5)

Using Equation 3-5, a relationship is derived for x_p before burnout by integrating with the bounds of $x=x_{po}$ at t=0 and $x=x_{p1}$ at $t=t_b$. With these bounds, Equation 3-5 can be integrated and rearranged:

$$x_p = \left(\frac{k_f \dot{Q}_s{}'}{k_f \dot{E}'' - 1} + x_{po}\right) * e^{k_f \dot{E}'' - 1 * \left(\frac{t}{t_f}\right)} - \frac{k_f \dot{Q}_s{}'}{k_f \dot{E}'' - 1}$$ (3-6)

According to Mowrer and Williamson [5], the flame spread can be expressed as the advancement of the pyrolysis zone, V_p-V_b. Combining Equations 3-1 and 3-2 with Equation 3-4, we get a relationship for the advancement of the pyrolysis zone after burnout begins, shown below:

$$V_p(t) - V_b(t) = \frac{d(x_p - x_b)}{dt} = \frac{k_f \dot{Q}_s{}' + k_f \dot{E}''(x_p - x_b) + x_b - x_p}{t_f} - \frac{x_p - x_b}{t_{bo}}$$ (3-7)

Integrating Equation 3-7 with the bounds of x_p-x_b=x_{p1}-x_{po} at $t=t_b$ and x_p-x_b= x_p-x_b at t=t a relationship between the pyrolysis zone and time can be seen below:

$$x_p - x_b = \frac{\left((x_{p1} - x_{po})C_4 + C_3\right)e^{C_1(t - t_b)} - C_3}{C_4}$$ (3-8)

An expression for x_b can be derived in a similar fashion by following the work of Schebel [6]. Combining Equations 3-2 and 3-8, an expression for V_b is developed:

$$V_b = \frac{dx_b}{dt} = \frac{\left((x_{p1} - x_{po})C_4 + C_3\right)e^{C_1(t - t_b)} - C_3}{C_4} + x_b - x_b$$ (3-9)

Integrating Equation 3-9 within the bounds of burnout, x_b=x_{po} at $t=t_b$ and x_b=x_b at t=t, we obtain an expression for the advancement of the burnout front after t_b:

$$x_b = \left(\frac{C_2}{C_1} + \frac{C_3}{C_1 C_4 t_{bo}}\right)\left(e^{C_1(t - t_b)} - 1\right) - \frac{C_3(t - t_b)}{C_4 t_{bo}} + x_{po}$$ (3-10)

Where:
$$C_1 = \frac{\left(k_f \dot{E}'' - \frac{t_f}{t_b} - 1\right)}{t_f} \qquad\qquad C_3 = k_f \dot{Q}_s' t_{bo}$$

$$C_2 = \frac{x_{p1} - x_{po}}{t_{bo}} \qquad\qquad C_4 = \left(k_f \dot{E}'' - 1\right)t_{bo} - t_f$$

Combining Equations 3-9 and 3-10, an expression for x_p after burnout can be found.

There are 3 different sets of inputs for the model being used. The source fire heat release rate, flame length correlation, and the initial burn zone make up the first set of inputs.

These values come directly from literature regarding NFPA 285 and are taken to be constants for each test. The second set of inputs comes directly from the material database: the ignition time and HRRPUA. The last set of inputs contains the calibration parameters: time to burnout and material burnout time. These parameters were taken to be equal because of their nature and were adjusted during the calibration process.

3.6. Results

The model was calibrated and simulates NFPA 285 based on the calibration process used for NFPA 286 and ASTM E 84 (Chapter 2 – Interior Finishes) as well as information presented by Ron Alpert [14]. The input parameters are shown in Table 3-3. The value of 75kW/m was used based on a flame length of 2.5ft on an inert wall, using the flame length correlation shown in Equation 3.3. Since there is buoyant flow flame spread present in NFPA 285, the value of $0.01 m^2/kW$ is used for k_f as suggested by Cleary [15]. Values of ignition time and HRRUPA of the material can be interpolated at an incident heat flux of $65kW/m^2$ using the data in the material database. Work by Ron Alpert [14] suggests an incident heat flux of $40kW/m^2$ from the source fire, and a value of $25kW/m^2$ is assumed for the flame heat flux characteristic to the material itself. For NFPA 285, x_{po} was taken to be 1m based on the heat-affected zone shown by Ron Alpert [14]. The reasoning behind this is that the source fire has a flame length of 1m, and regardless of the material this 1-meter zone is affected. The flame spread, which causes a pass or fail of NFPA 285, occurs above this zone. The last model inputs are the calibration parameters, which were adjusted based on the test being simulated. Since there was no full-scale testing results for the model to be calibrated against, these values were taken to be 60 seconds (similar to the calibration process of ASTM E 84 in Chapter 2 – Interior Finishes). This data came from the knowledge that the source fire was a driving force of the flame spread in the heat-affected zone of the source fire. The source fire was turned off after burnout began because it is believed that the source fire intensity is a main component of the initial flame spread of the model but not significant above this zone. The uncertainty of the model was calculated using the Law of Propagation of Uncertainty as described in Appendix D. It was found that the uncertainty of the model results is +/- 1 foot. This uncertainty is consistent with the uncertainty found in the Tunnel test and takes into account the change of input parameters for NFPA 285.

Table 3-3: NFPA 285 Inputs for Baseline System

Input	t_f	t_b	t_{bo}	x_{po}	$\dot{E}''$	k_f	$\dot{Q_s}'$
Value	150s	60s	60s	1m	$110kW/m^2$	$0.01 m^2/kW$	75kW/m

The 14 FRP systems can be broken up into five different categories based on the changes made to their composition. The five categories are: cores, fillers, aggregate, pigments, and resin changes.
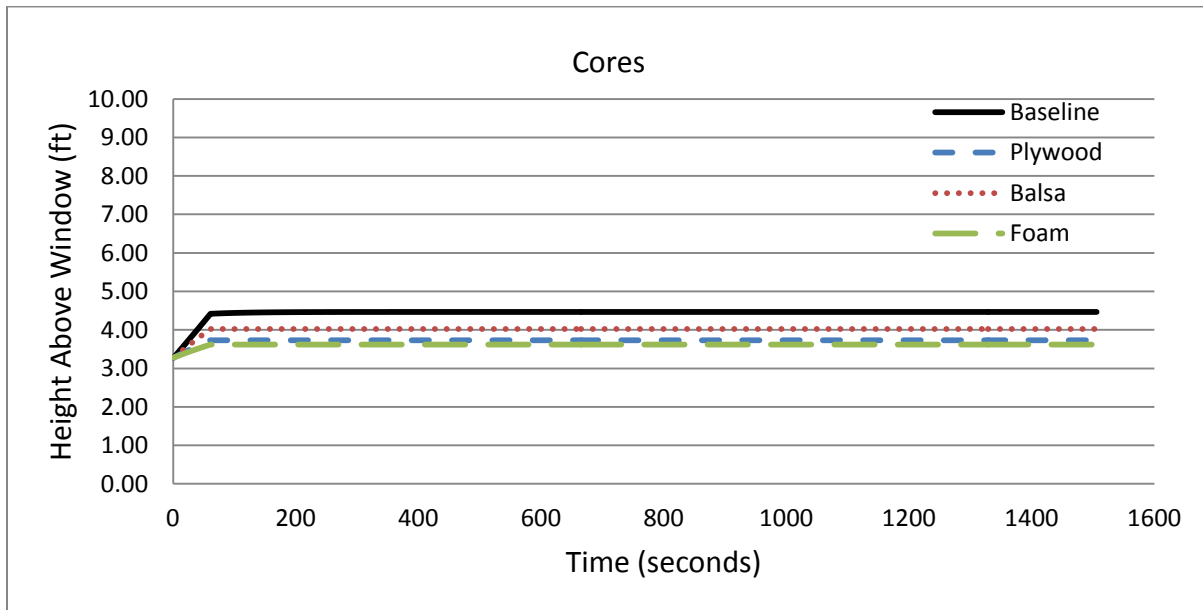
Figure 3-4: NFPA 285 Model Results Cores
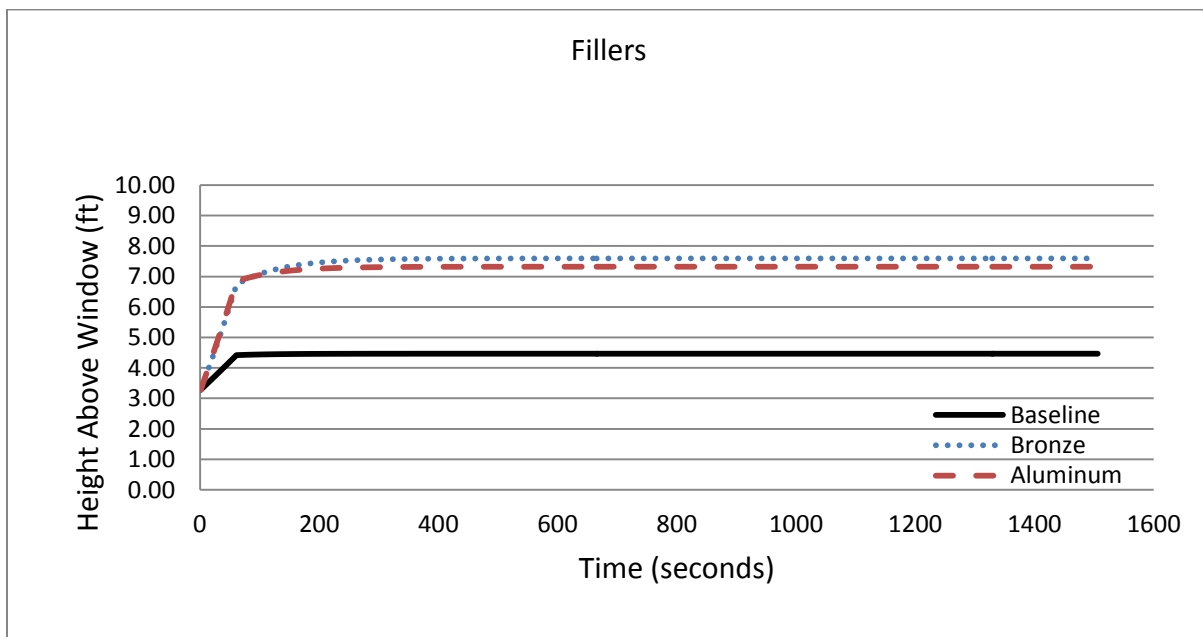
Figure 3-5: NFPA 285 Model Results Fillers
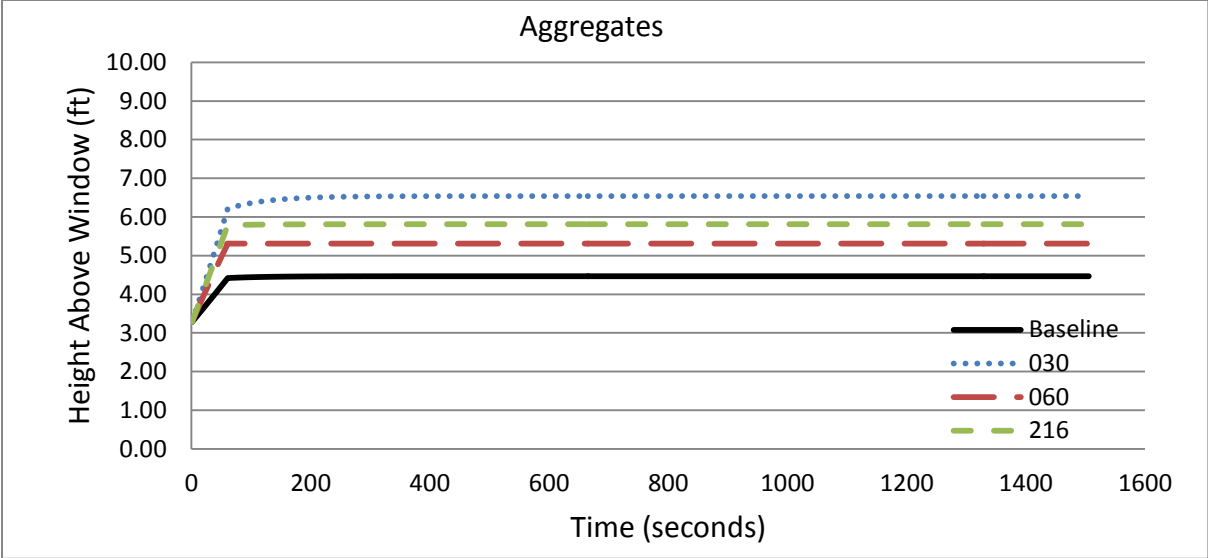
Figure 3-6: NFPA 285 Model Results Aggregates
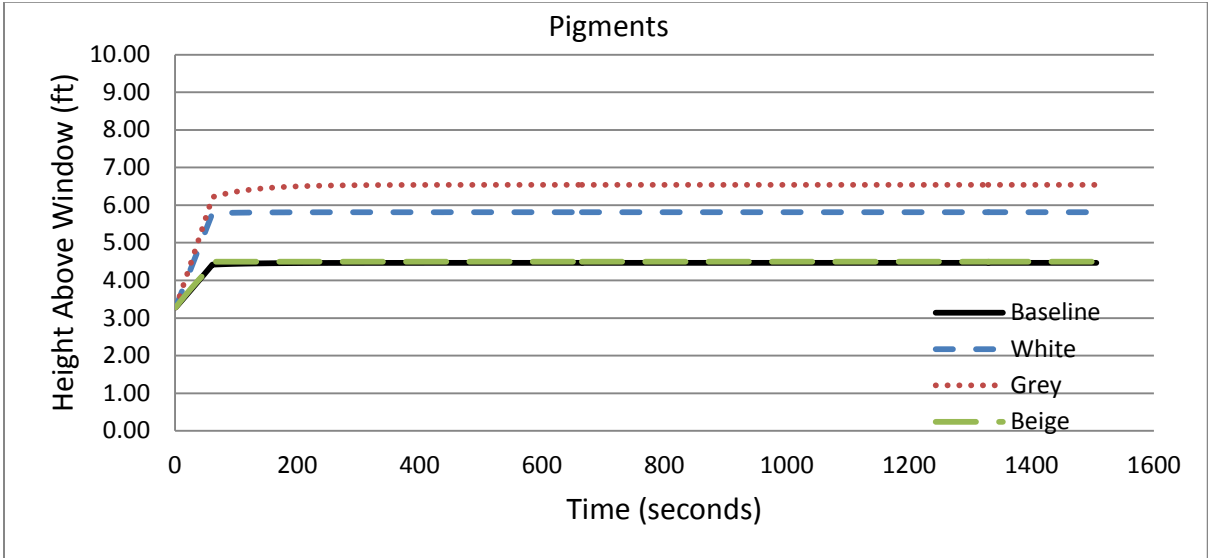
Figure 3-7: NFPA 285 Model Results Pigments
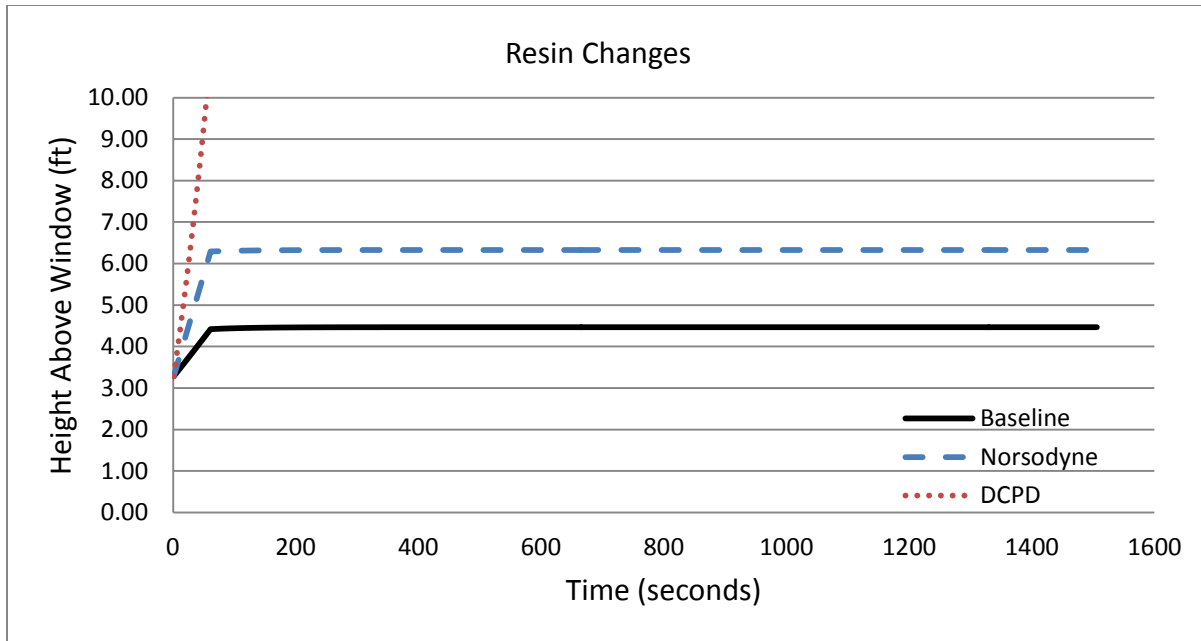
Figure 3-8: NFPA 285 Model Results Resin Changes

In Figure 3-4 through Figure 3-8, the results can be seen for each category of FRPs. The charts display the flame spread above the top of the window. It is observed that changes made to the fillers of the polymer concrete will have the most negative effects on flame spread. It is also observed that changing the core of the sandwich panel will have little to no effect since the top face is the Baseline FRP. The aggregate and pigment changes experience various changes in flame spread. The changes in resin have vastly different effects. Through data obtained in the Tunnel Test Model (Chapter 2 – Interior Finishes), it was decided that these two FRP systems were outside the paradigm of the NFPA 285 Model. This conclusion was consistent with the erratic behavior of the FRPs in the Cone Calorimeter data reports. With the exception of the DCPD resin change, all of the systems propagated to a distance below 10 feet. Therefore it is predicted that these systems would pass an NFPA 285 standardized test.

3.7. Design

This project also designed a screening test method for NFPA 285 [12], the Standard Fire Test Method for Evaluation of Fire Propagation Characteristics of Exterior Non-Load-Bearing Wall Assemblies Containing Combustible Components. It was the goal of this test (Exterior Screening Test) to be a screening test for the Multi Story Building Test, with smaller required dimensions. A standard compartment is used for the test facilities (same as the one used in NFPA 286 [3]), with one short wall removed. The specimen shall be 8 feet tall and 2 feet wide

and mounted on the middle of the other short wall. 1-inch steel angles shall be installed on each side of the specimen. A slot burner shall be located along the width of the specimen. The slot burner is constructed from a 2-foot long, 1-inch, schedule 40 steel pipe with a ½-inch slot cut down the top (a mesh screen is placed below the slot to diffuse the gas). Gas shall be run into both ends of the slot burner via two 90-degree elbows. Methane gas lines are installed at each elbow, with flow controls on each side to ensure a balanced flame. The flame produced by the slot burner will be no higher than 1ft from the floor of the room. This size flame will produce a HRRPUW of 12kW/m as seen in the SFPE Handbook [16]. A radiant panel will be located one inch behind the slot burner set at 35kW/m^2, which takes into account the absorptivity of the slot burner flame. This panel should be approximately 2ft wide and 3ft tall. The predicted heat flux distribution of the Exterior Screening Test is shown in Figure 3-9 the Exterior Screening Test attempts to mimic the upper 8ft of NFPA 285 by using the radiant panel and slot burner to produce this heating regime in the standard compartment. The upper 8ft is the focus of this test because it is the area where the flame spread will occur, and will determine whether or not a material passes or fails. The slot burner will mimic the top of the source fire and the radiant heat burner will add in the additional heat flux, which is lost by not including the source fire. The test shall be run for 25 minutes in accordance with NFPA 285 disregarding the preheating of the room [3]. Figure 3-10 and Figure 3-11 show the layout of this test with required dimensions.
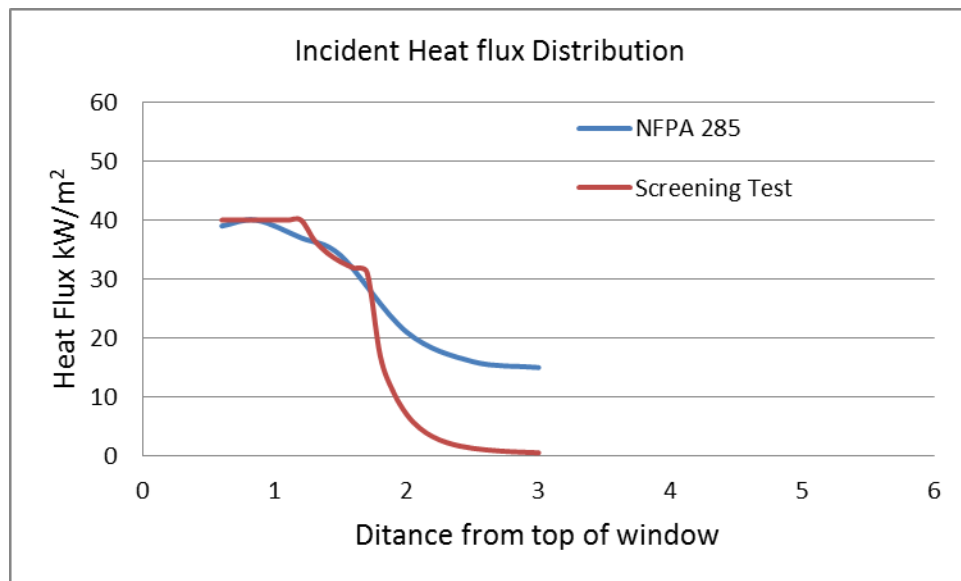
Figure 3-9: Incident Heat Flux Distribution
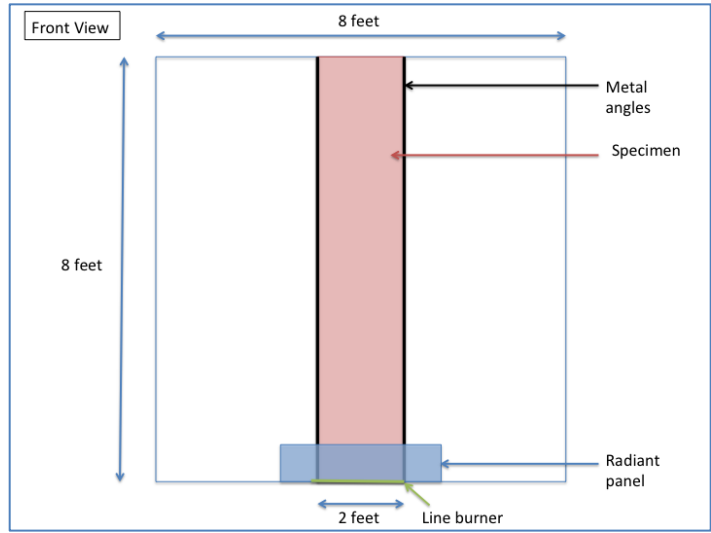
Figure 3-10: Equivalent Screening Test Front View
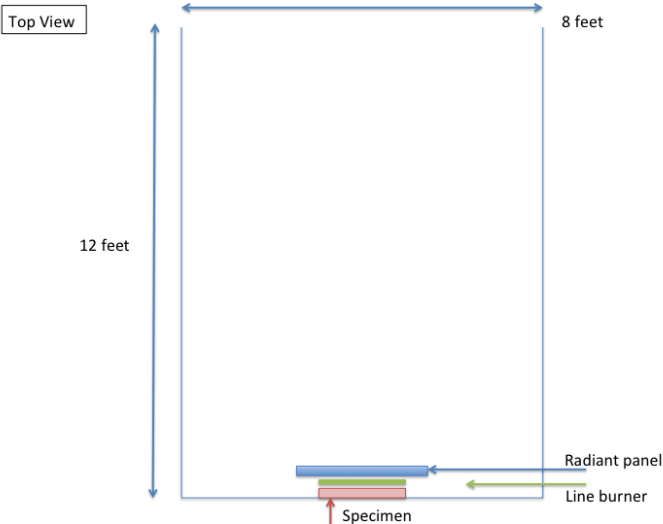
Figure 3-11: Equivalent Screening Test Top View

3.8. Compartment Effects

Because this test is conducted within a partially enclosed compartment, it is necessary to understand the impacts the compartment will have on the screening test specimen. The following equation (3-14) and values (Table 3-4) were used to determine the change in the upper gas layer from the ambient conditions. The change in temperature is estimated to be 72K, which gives an upper layer temperature of 367K.

$$DT_g = 480 \left(\frac{\dot{Q}}{\sqrt{g}c_p r_\infty T_\infty A_0 \sqrt{H_0}} \right)^{2/3} \left(\frac{h_k A_T}{\sqrt{g}c_p r_\infty A_0 \sqrt{H_0}} \right)^{-1/3} \tag{3-14}$$

Inputs	ΔT	Rho	k	Delta	g	A$_0$	H$_0$	C$_p$	Q	T$_{amb}$	h$_k$	A$_t$
Values	72	1440 kg/m^3	0.00028 kW/mK	0.05m	9.8m/s^2	5m^2	2m	1.05 kJ/kgK	90 kW	295 K	0.106 kW/mK	41.7 m^2

Table 3-4: Compartment Effects

It can be observed that the compartment has a minimal effect on the wall specimen due to the low increase in upper layer gas temperature. This method is developed by McCaffrey, Quintiere, and Harkleroad in the SFPE Handbook [17] and is referenced in Appendix H.

3.9. Conclusion

While the model followed the same calibration procedures as the successful screening models in Chapter 2, there are still many limitations involved. The model is only capable of screening the vertical flame spread component of NFPA 285. It does not take into consideration the horizontal flame spread, and overall temperature requirements for passing NFPA 285, nor can it completely model the effect of the flashed over room as a source of heat flux as seen in 285. Another limitation is that there was no NFPA 285 test data for the 14 FRP systems to compare and calibrate the model against. An area of future work would be to run NFPA 285 tests on the Baseline system (at least) in order to obtain a calibration.

As seen in the results, some FRP systems performed better than others. This is due to the changes in components. These changes effect the time to ignition, which is the driving force of how fast and far a flame front will propagate on a material. Therefore, it is suggested that material developers focus on achieving longer times to ignition in order to have the best chance of passing a Multi Story Building Test. Through the anaylsis of this model it is observed that bench-scale material properties have a dominating affect on full-scale test performance.

3.10. Nomenclature

$t = time$
$t_f = ignition\ time$
$t_b = time\ to\ burnout$
$t_{bo} = material\ burnout\ time$
$x_{po} = intial\ burn\ zone$

x_{p1} = burn zone when burnout begins
k_f = flame length correlation
$\dot{E}''$ = Heat realase rate per unit area of material (HRRPUA)
$\dot{Q}'_s$ = source fire
V_p = velocity of pyrolysis front
V_b = velocity of burnout front
$\dot{Q}$ = heat release rate (HRR)
g = acceleration due to gravity
c_p = specific heat of gas
ρ_∞ = ambient air density
T_∞ = ambient air temperature
A_0 = area of opening
H_0 = height of opening
h_k = effective heat transfer coefficient
A_T = total area of the compartment enclosing surfaces

3.11.   References

(1) International Building Code, 5th Edition.

(2) ASTM E 84, "Standard Test Method for Surface Burning Characteristics of Building Materials," ASTM International, West Conshohocken, PA

(3) NFPA 286, Standard Methods of Fire Tests for Evaluating Contribution of Wall and Ceiling Interior Finish to Room Fire Growth, 2011 Edition

 (4) ASTME E 1354, "Standard Test Method for Heat and Visible Smoke Release Rates for Materials and Products Using an Oxygen Consumpiton Calorimeter," ASTM International, West Conshohocken, PA

(5) Mowrer, F.W., and Williamson, R.B.. "Flame Spread Evaluation for Thin Interior Finish Materials". *Fire Safety Science-Proceedings of the Third International Symposium*, p. 689-698.

(6) Schebel, K., Dembsey, N.A., Meacham, B.J., Johann, M., Tubbs, J., and Alston, J. "Fire Growth Simulation in Passenger Rail Vehicles Using a Simplified Flame Spread Model Coupled with a CFD Fire Model".

(7) Cleary, T.G., and Quintiere, J.G.. "A Framework for Utilizing Fire Property Tests". *Fire Safety Science-Proceedings of the Third International Symposium*, p. 647-656.

 (8) Society of Fire Protection Engineering Handbook, 3rd edition: 2-14.59

(9) Society of Fire Protection Engineering Handbook, 3rd edition: 2-14.34

(10) Fernandez-Pello, C., & Zhou, L. "Turbulent, Concurrent, Ceiling flame spread: The Effect of Buoyancy." Combustion and Flame 92:45-49 (1993).

(11) Williamson,R, Revenaugh, A "Ignition Sources in Room Fire Tests and Some Implications for Flame Spread Evaluation"

(12) NFPA 285, Standard Fire Test Method for Evaluation of Fire Propagation Characteristics of Exterior Non-Load-Bearing Wall Assemblies Containing Combustible Components, 2012 Edition

(13) Whiting, P.N. "Development of the Vertical Channel Test Method for Regulatory Control Of Combustible Exterior Cladding Systems." BRANZ Study Report No. 137. (2005).

(14) Alpert, Ron. "Evaluation of Exterior Insulation and Finish System Fire Hazard for Commercial Applications." Journal of Fire Protection engineering, Vol. 12, Novemeber 2002, p. 245-256

(15) Cleary, T.G., and Quintiere, J.G.. "A Framework for Utilizing Fire Property Tests". *Fire Safety Science-Proceedings of the Third International Symposium*, p. 647-656.

(16) Society of Fire Protection Engineering Handbook, 3rd edition: 2-14

(17) McCaffrey, Quintiere, and Harkleroad. Society of Fire Protection Engineering Handbook, 3rd edition: 3

4. Conclusion

This project succeeded in creating an initial flame spread modeling tool for FRPs that is simple and easy to use. The model uses material properties from bench-scale tests to predict behavior in full-scale tests within reasonable uncertainty. The full-scale tests modeled in this project were the ASTM E84 Tunnel Test, the NFPA 286 Room Corner Test, and the NFPA 285 Multi Story Building Test. This is useful to materials developers because it allows them to have a better idea of how their FRP systems will perform in expensive full-scale tests while only needing to conduct economical bench-scale tests. This project is also significant because it will serve as the base for future work in the field. Limitations of the model and various input parameters will serve as a starting point for future work. Specific recommendations follow:

- Additional full-scale test data to refine model calibration.
- Further study of FRP intumescent behavior to better define material properties such as time to ignition for use in model simulation.
- Further study of how the flame spread model represents the forward heating zone for materials with low heat release rates per unit area.
- Refinement of the NFPA 285 compartment based screening test.

5. Acknowledgements

Appendix A   Cone Calorimeter

Cone Calorimeter

The cone calorimeter is a fire-testing instrument used to quantify the burn characteristics of small test samples (100mm x 100mm per ASTM E1354). The main component is a conical radiant electrical heater that simulates real fire development by producing a range of heat fluxes. The characteristics measured by the cone calorimeter include:

- Heat release rate per unit area
- Cumulative heat released
- Effective heat of combustion
- Mass loss rate
- Total mass loss
- Smoke obscuration

While the results from cone calorimeter testing are determined on small specimens, they are an accurate representation of the intended product in end use as long as all data obtained during edge burning is disregarded. This test method is the starting point for the development of materials with desirable fire resistant, flame retardant, and smoke suppressant properties.

Oxygen Consumption

Oxygen consumption calorimetry is the basis for determining heat characteristics of the sample. Using an oxygen analyzer, the cone calorimeter determines the amount of oxygen consumed during the burn. For every 1 kilogram of oxygen consumed during the burn, approximately $13.1*10^3$ kilojoules of heat are released (ASTM E1354-10a). Heat release rate per unit area and cumulative heat released are calculated from this data.

Load Cell

The load cell is instrumental to cone calorimetry in that it provides data necessary to characterize the burn sample. During the test, the sample is secured on the load cell which measures and records mass every second. This data is compiled to calculate total mass loss and mass loss rate. Change in mass and heat release rate are needed to calculate effective heat of combustion.

Products Of Combustion

Products of combustion are directed through a duct where a helium-neon laser, silicon photodiodes, and reference detectors are positioned and programmed to measure smoke obscuration. The initial intensity of the laser is recorded using a sample of clean air. This value is compared to the instantaneous intensity measurements as the products of combustion flow through the duct. Changes in intensity correlate to the density of the products of combustion.

Mowrer and Williamson

Mowrer and Williamson used a simplified flame spread model in order to evaluate upward flame spread. This model is used to evaluate the flame spread on thin lining materials which are adhered to noncombustible substrates.

Assumptions

In Mowrer and Williamson's flame spread model there are a number of assumptions which are made. The first is that the heat flux is considered to be constant in the vicinity of the exposed area and zero in the areas which are not exposed. The overall heat flux imposed on the wall by the wall flame is treated as a constant value of approximately 25-30 kW/m2 in the pyrolysis and flame zones and zero in the other areas. The external heat flux is assumed to be 50-60 kW/m2, which is based on the room fire tests which are being considered. Once the wall fuel in the vicinity of the external ignition source burns out, the external source no longer plays a role in the overall heat flux, and the additional wall fuel is considered to be exposed only to the heat flux produced by the wall flame. The next assumption is that a linearized flame length approximation is used. There are two models which are used to measure this, one before burnout begins and one after burnout.

Nomenclature

E - Energy release (kJ)
$\dot{E}$ - Energy release rate (kW)
kpc - Thermal inertia [(kW/m^2-K)^2-s]
k - Flame length parameter
m - Mass (kg)
$\dot{q}$" - Heat flux (kW/m2)
t - Time (s)
T - Temperature (K or C)
V - Velocity (rn/s)
x - Length parameter (m)

Subscripts

b - Burnout zone
bo - Burning duration
e - External
f - Flame zone
ig - Ignition
p - Pyrolysis zone
s - Surface

Superscripts

' Per unit length (m^{-1})
'' Per unit area (m^{-2})
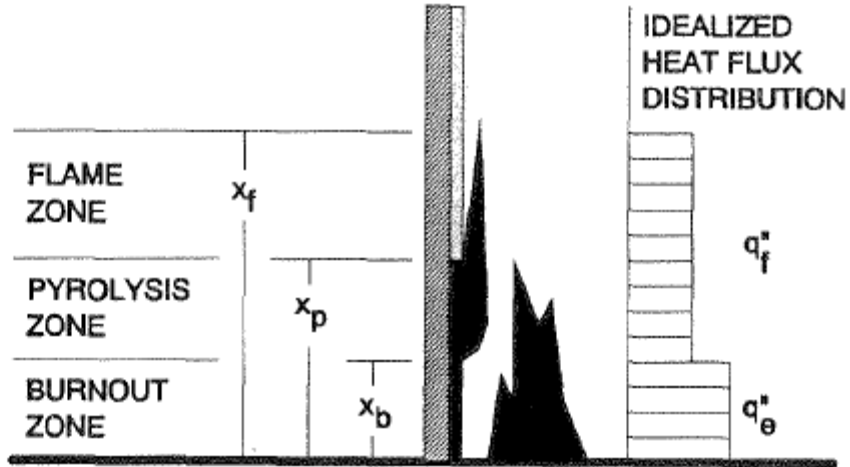
FIGURE 1. Schematic illustration of the upward flame spread model.

Figure one is a schematic of the variables and measurements used in this model.

Equations

The equations which are used in the flame spread model are outlined and explained below.

(1) – Rate of pyrolysis front advance

$$V_p = \frac{dx_p}{dt} = \frac{x_p(t + t_f) - x_p(t)}{t_f} = \frac{x_f(t) - x_p(t)}{t_f}$$

In this model, the flame spread rate is defined as the rate of pyrolysis front advance. This is the change in the height of the pyrolysis zone (x_p) over time.

(2) – Thermal model of heating an inert wall with constant properties

$$t_f = k\rho c \left[\frac{T_{ig} - T_g}{\dot{q}''} \right]^2$$

This formula defines the variable t_f, which is used in equation (1). $k\rho c$ is defined as the thermal inertia, which is a property intrinsic to the material on the wall. t_f is the time that the material takes to heat to the point where ignition is possible.

(3) – Rate of fuel burnout

$$V_b = \frac{dx_b}{dt} = \frac{x_b - (t + t_{bo}) - x_b(t)}{t_{bo}} = \frac{x_p(t) - x_b(t)}{t_{bo}}$$

In this formula, rate of fuel burnout is defined as the velocity of the burnout zone. This is the change in the height of the burnout zone (x_b) over time.

(4) – Linearized flame length approximation before burnout

$$\frac{x_f}{x_p} = k_f \dot{E}''$$

This formula defines the flame length before burnout begins, which is the area from the top of the pyrolysis zone to the top of the flame. K_f is a correlating factor used to approximate this. Cleary and Quintiere suggest a value of $.01 m^2/kW$ for k_f. $\dot{E}''$ is the heat release rate per unit area.

(5) – Dimensionless flame length after burnout begins

$$\frac{(x_f - x_b)}{(x_p - x_b)} = k_f \dot{E}''$$

This formula defines the flame length after burnout begins, which is the area from the top of the pyrolysis zone to the top of the flame. This formula adjusts for the fact that the flame is no longer at the floor level and is rising up the wall.

(6) – Using equation (4) for times $t < t_b$, equation (1) can be written as:

$$\frac{dx_p}{dt} = \left(k_f \dot{E}'' - 1\right) * \frac{x_p}{t_f}$$

(7) – Equation (6) can be integrated with the limits that $x = x_{po}$ at $t = 0$ and $x = x_p$ at $t = t$ as:

$$\frac{dx_p}{dt} = \left(k_f \dot{E}'' - 1\right) * \frac{x_p}{t_f}$$

$$\downarrow$$

$$\int_{x_{po}}^{x_p} \frac{dx_p}{x_p} = \int_0^t (k_f \dot{E}'' - 1) \frac{dt}{t_f}$$

$$\downarrow$$

$$\ln \frac{x_p}{x_{p0}} = \ln(k_f \dot{E}'' - 1) \frac{dt}{t_f}$$

$$\downarrow$$

$$x_p = x_{po} * e^{(k_f \dot{E}'' - 1) * \frac{t}{t_f}}$$

(8) – After burnout begins, at times $t > t_b$, the net rate of flame propagation can be expressed as the difference between the pyrolysis front velocity and the burnout front velocity:

$$V_p(t) - V_b(t) = \frac{d}{dt}(x_p - x_b) = \frac{x_f - x_p}{t_f} - \frac{x_p - x_b}{t_{bo}}$$

(9) – Solving equation (5) for x_f and substituting it into equation (8), it can be rearranged to:

$$\frac{d}{dt}(x_p - x_b) = \frac{k_f E''(x_p - \dot{x}_b) + (x_b - x_p)}{t_f} - \frac{x_p - x_b}{t_{bo}}$$

$$\downarrow$$

$$\frac{d}{dt}(x_p - x_b) = (x_p - x_b)\left(\frac{k_f \dot{E}'' - 1}{t_f} - \frac{1}{t_{bo}}\right)$$

$$\downarrow$$

$$\frac{d}{dt}(x_p - x_b) = (x_p - x_b) * \left(\frac{\left((k_f \dot{E}'' - 1) * t_{bo} - t_f\right)}{t_f t_{bo}}\right)$$

(10) – Equation (9) can be integrated, with the limits of $(x_p - x_b) = (x_{p1} - x_{po})$ at $t = t_b$ and $(x_p - x_b) = (x_p - x_b)$ at time $t = t$, to yield the pyrolysis zone length at any time:

$$\frac{d}{dt}(x_p - x_b) = (x_p - x_b) * \left(\frac{\left((k_f \dot{E}'' - 1) * t_{bo} - t_f\right)}{t_f t_{bo}}\right)$$

$$\downarrow$$

$$\int_{x_{p1} - x_{po}}^{x_p - x_b} \frac{d(x_p - x_b)}{x_p - x_b} = \int_{t_b}^{t} \left(\frac{\left((k_f \dot{E}'' - 1) * t_{bo} - t_f\right)}{t_f t_{bo}}\right) dt$$

$$\downarrow$$

$$\ln \frac{(x_p - x_b)}{x_{p1} - x_{po}} = \left(\frac{\left((k_f \dot{E}'' - 1) * t_{bo} - t_f\right)}{t_f t_{bo}}\right) t$$

$$\downarrow$$

$$x_p - x_b = (x_{p1} - x_{po})e^{\left(k_f \dot{E}'' - \frac{t_f}{t_{bo}} - 1\right) * \frac{t - t_b}{t_f}}$$

Schebel

Schebel applies the flame spread model which is presented in Mowrer and Williamson in order to model flame spread in a train car. In this model Schebel makes a few more assumptions in order to apply the model to his work

Assumptions

The first assumption which Schebel makes is that there is no preheating of the upper gas layer caused by convection and radiation. The heat flux which is used in the cone calorimeter is used as both the external heat flux as well as the wall flame heat flux. The areas of which are preheated and spread pattern of the flame are based on an expected, predetermined burn pattern (shown below). Any lateral spread across the walls is considered to be minimal and therefore it is neglected. However, a region of wall along the ceiling will experience lateral flame spread. The depth of this region is estimated as .08h, where h is the ceiling height. Mowrer and Williamson's model is used to establish a pyrolysis area. With this pyrolysis area and the expected burn areas, Heat Release Rates can be established.

Equations

Based on the assumptions made, HRR values are established using pyrolysis areas based on $x_p - x_b$, using three different equations, based on whether the pyrolysis area is on the wall, the ceiling, or both.
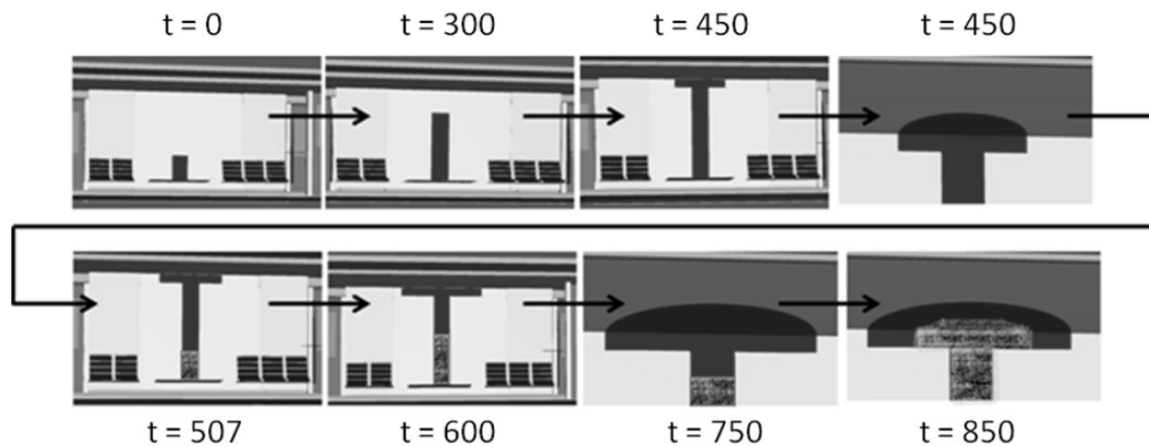
Figure 4 - Representative Flame Spread

For $x_p < H$ and $x_b < H$

$$HRR\ vs.\ Time = (x_p - x_b)(x_{pow})(\dot{E}'')$$

For $x_p > H$ and $x_b < H$

$$HRR\ vs.\ Time = \left[(H - x_b)x_{pow} + 2D(x_p - H) + \frac{\pi}{2}\left(\frac{x_{pow}}{2} + (x_p - H)\right)^2\right]\dot{E}''$$

For $x_p > H$ and $x_b > H$

$$HRR\ vs.\ Time = \left[2D\left(x_p - x_b\right) + \frac{\pi}{2}\left(\frac{x_{pow}}{2} + (x_p - H)\right)^2 - \frac{\pi}{2}\left(\frac{x_{pow}}{2} + (x_b - H)\right)^2\right]\dot{E}''$$

Where

X_{pow} = Initial source fire width

H = Ceiling Height

D = .08H (Representative T-shape depth)

Inputs

When doing his calculations, Schebel uses several inputs taken from Cone Calorimeter tests in order to simplify the use of the Mowrer and Williamson flame spread model. The first variable taken from cone testing data is the characteristic flame spread time, or t_{ig}. This simplifies the model by directly incorporating parameters such as the ignition temperature and the thermal inertia. Schebel also based his heat flux measurements off of data from Cone Calorimeter tests. He found that the pyrolysis zone flame heat flux is 20 kW/m^2 greater than the heat flux generated by the cone calorimeter. As another simplification, Schebel assumes that the burnout time is the time of source fire burnout, and is taken to be the burnout time observed in the Cone Calorimeter.

Application to other tests

The methods used by Schebel to adapt the Mowrer and Williamson flame spread model can be used to adapt the model to other tests. The main difference between the tests will be the geometry used to determine the HRR vs. Time.

ASTM E84 Tunnel test

The geometry of the Tunnel Test is similar to the geometry of the Schebel test before it reaches the ceiling, except that the fire travels horizontally along a tunnel instead of vertically up a wall.
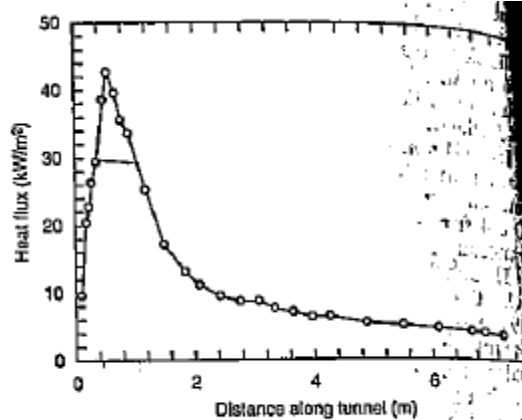
Figure 2-14.59. *Calculated incident heat flux along length of the ASTM E84 tunnel.*

The critical heat fluxes of FRPs tested in the Cone Calorimeter were found to be approximately 25 kW/m2. Any distance along the graph with a heat flux above 30 kW/m2 was taken to be the initial burn height to provide a margin of safety. This distance is approximately .6m down the tunnel. This is confirmed to be reasonable when compared to the total length of the burner flame, which is approximately 1.4m. For the purposes of the model, once this area ignites the source fire is to be ignored.

$$HRR\ vs.\ Time = (x_p - x_b)(W)(\dot{E}")$$

Where
W = Width of the tunnel (20in)
X_{po} = .6m

NFPA 286 room corner test

The geometry in the room corner test is very similar to that in the Schebel test. The main difference is that the fire travels up the corner of a room rather than a flat wall. This means that the width of the burning wall area will be twice as wide, because there will be an area as wide as the source fire on both walls. The initial heat release rate of the burner is 40 kW for the first 5 minutes and 160 kW for the next 10 minutes.

For $x_p < H$ and $x_b < H$

$$HRR\ vs.\ Time = (x_p - x_b)(2x_{pow})(\dot{E}")$$

For $x_p > H$ and $x_b < H$

B-42

$$HRR\ vs.\,Time = \left[(H - x_b)2x_{pow} + 2D(x_p - H) + \frac{\pi}{4}\left(\frac{x_{pow}}{2} + (x_p - H)\right)^2\right]\dot{E}''$$

For $x_p > H$ and $x_b > H$

$$HRR\ vs.\,Time = \left[2D(x_p - x_b) + \frac{\pi}{4}\left(\frac{x_{pow}}{2} + (x_p - H)\right)^2 - \frac{\pi}{4}\left(\frac{x_{pow}}{2} + (x_b - H)\right)^2\right]\dot{E}''$$

Where

X_{pow} = Initial source fire width (in the room corner test the burner width is 12in)
H = Ceiling Height (in the room corner test the ceiling height is 8ft)
D = .08H (Representative T-shape depth)
X_{po} = .5m

ISO 9705 Room Corner Test

The geometry in the ISO 9705 room corner test is very similar to that in the Schebel test. The main difference is that the fire travels up the corner of a room rather than a flat wall. This means that the width of the burning wall area will be twice as wide, because there will be an area as wide as the source fire on both walls. The initial heat release rate is 100kW for the first 10 minutes and 300 kW for the next 10 minutes.

Figure 8. 8: Incident Heat Flux Distribution to the Walls and Ceiling from a 17 cm Square Corner Ignition Burner at 100 kW: Fire Plume Plus Cold Surface Correction Factor.
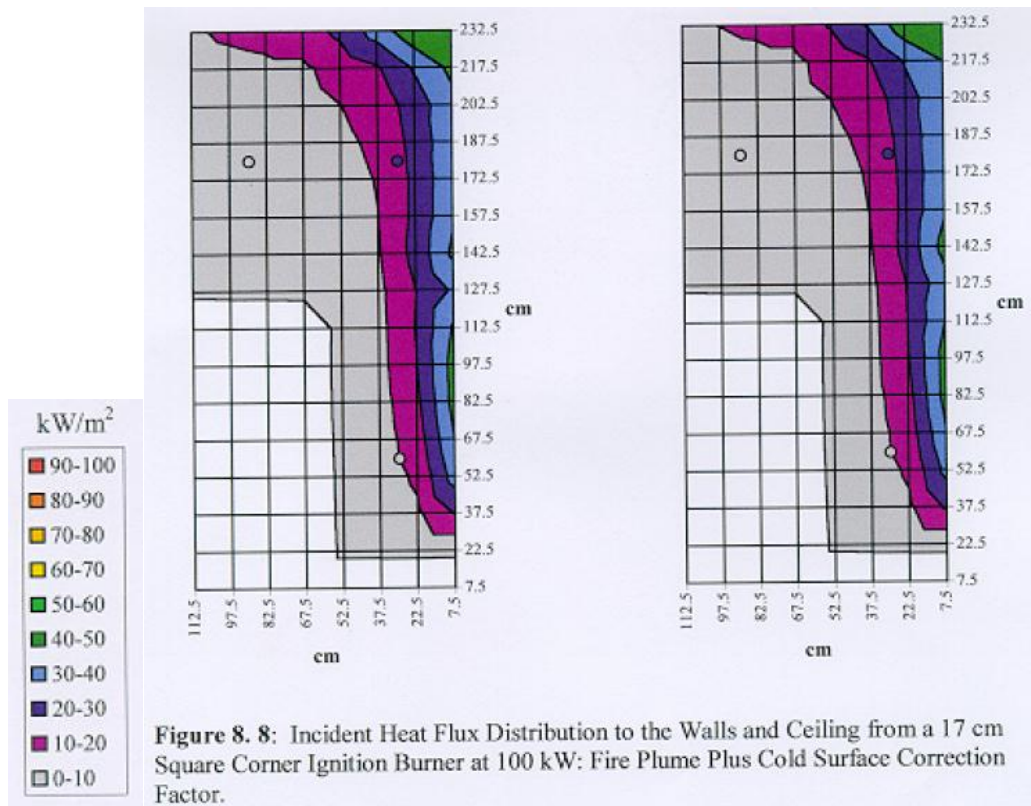
Based on the heat flux maps shown above, the initial burn height is estimated to be the distance of the highest heat flux (40-50 kW/m2) nearest to the burner. This height is approximately .45m. For the purposes of the model it is assumed that once this area ignites the source fire is ignored.

For x_p < H and x_b < H

$$HRR \; vs. Time = (x_p - x_b)(2x_{pow})(\dot{E}")$$

For x_p > H and x_b < H

$$HRR \; vs. Time = \left[(H - x_b)2x_{pow} + 2D(x_p - H) + \frac{\pi}{4}\left(\frac{x_{pow}}{2} + (x_p - H)\right)^2\right]\dot{E}"$$

For x_p > H and x_b > H

$$HRR \; vs. Time = \left[2D(x_p - x_b) + \frac{\pi}{4}\left(\frac{x_{pow}}{2} + (x_p - H)\right)^2 - \frac{\pi}{4}\left(\frac{x_{pow}}{2} + (x_b - H)\right)^2\right]\dot{E}"$$

Where

X_{pow} = Initial source fire width (in the room corner test the burner width is 17cm)
H = Ceiling Height (in the room corner test the ceiling height is 2.4m)
D = .08H (Representative T-shape depth)
X_{po} = .45m

NFPA 285

The geometry of the NFPA 285 test is similar to the geometry of the Schebel test before it reaches the ceiling, with the source fire width being the width of the window burner.
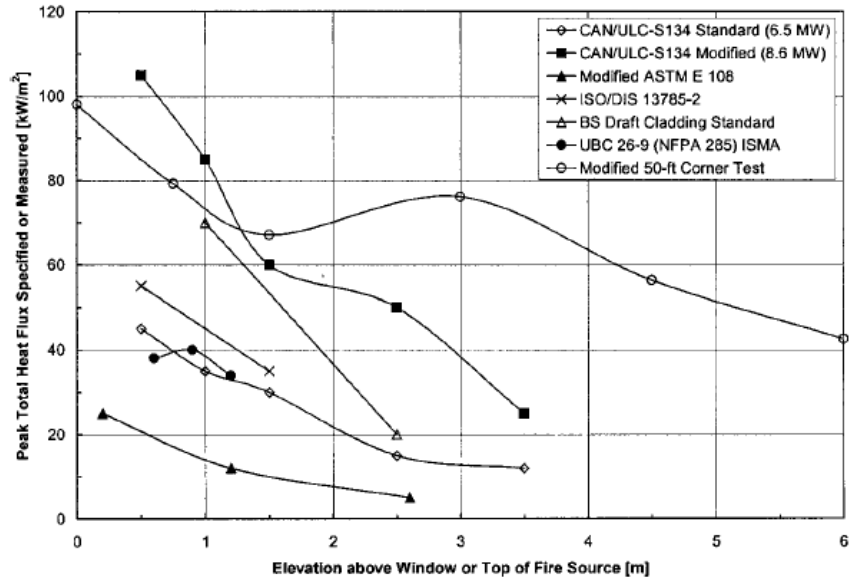
Figure 5. Comparison of total heat flux profiles for existing facade test methods.

The critical heat fluxes of FRPs tested in the Cone Calorimeter were found to be approximately 25 kW/m2. Any distance along the NFPA 286 line on the graph with a heat flux above 30 kW/m2 was taken to be the initial burn height to provide a margin of safety. This distance is approximately 1m. For the purposes of the model, once this area ignites the source fire is to be ignored.

$$HRR \ vs. Time = (x_p - x_b)(W)(\dot{E}'')$$

Where

W = Width of the window burner (60in)
X_{po} = 1m

The Effect of Tunnel Velocity on Flame kf

William Parker's investigation of the fire environment in the ASTM E84 tunnel test reveals the air flow information necessary to draw correlations between the E 84 tunnel test and the Zhou & Fernandez-Pello study of forced flow flame spread across a ceiling. Parker's paper reveals airflow velocities in various stages of the tunnel at ambient air temperatures as well as with the burner on for differing amounts of time. As determined in the Zhou study, airflow velocity 1< V < 5 (m/s) will accelerate flamespread across the ceiling by reducing the distance between the flame front and the material surface. A shorter distance between the flame front and the fuel source enhances heat transfer in the forward heating zone. In Parker's testing of the tunnel configuration, average airflows were consistently in range for an accelerated spread both with and without the burner ignited. Figures 12 through 15 serve to illustrate these findings in several iterations of the experiment .
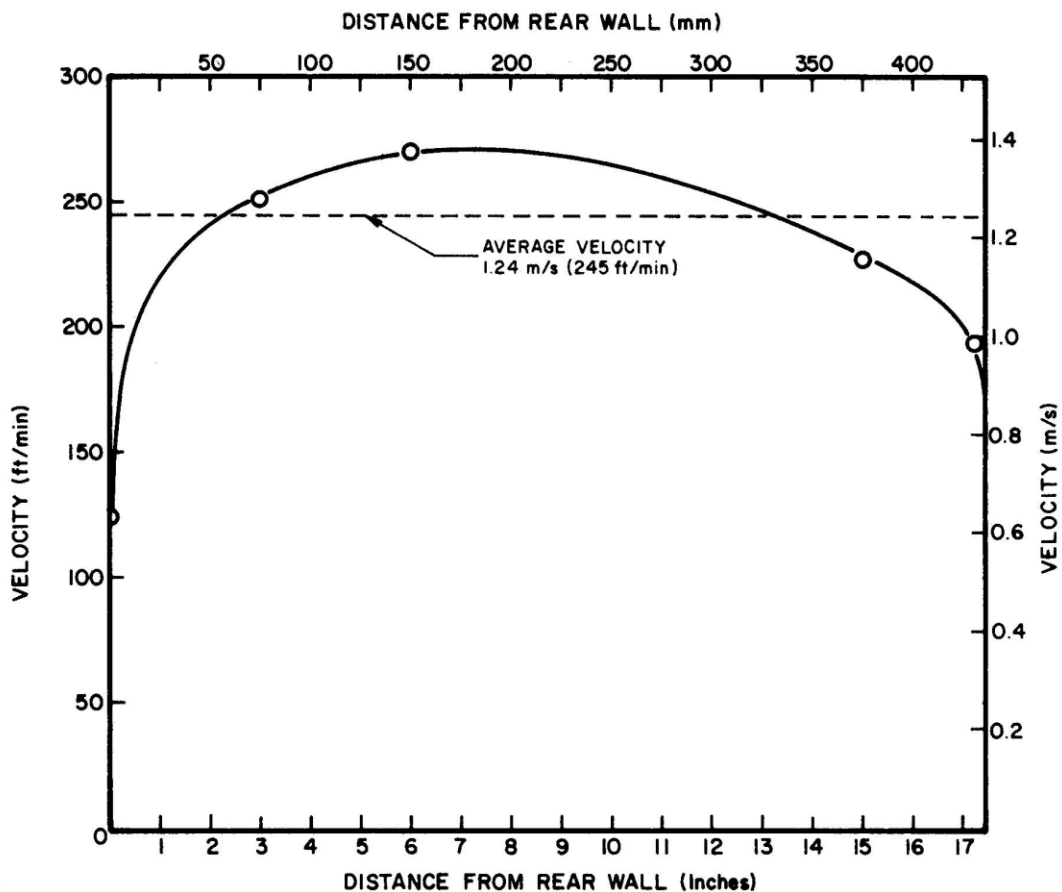
Figure 12.　Horizontal Velocity Distribution of the Ambient Air Along the Midheight at the End of the Tunnel
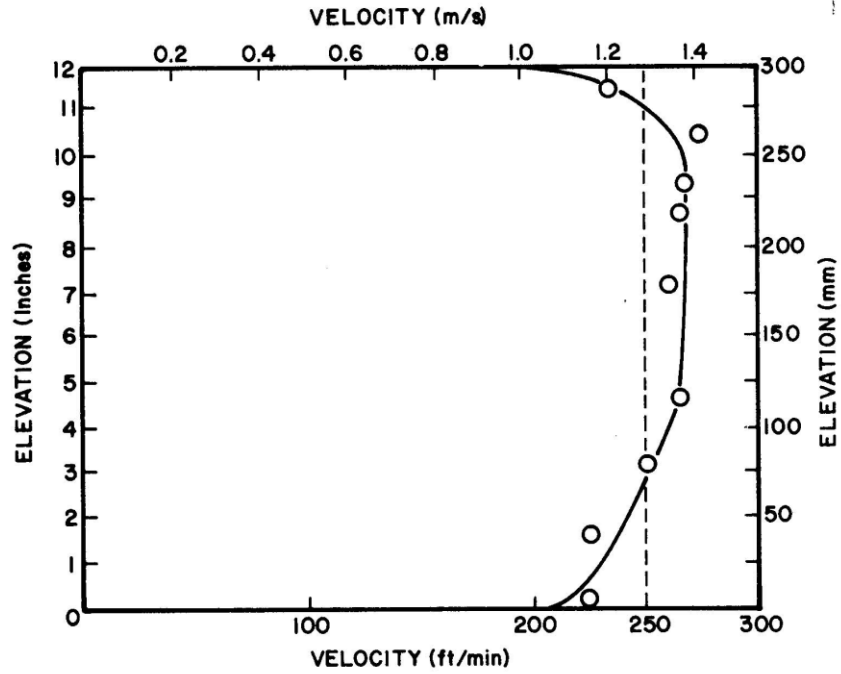
Figure 13. Vertical Velocity Profile Through the Centerline
at Nine Feet with the Burner Off (1 foot = 0.305 meters)
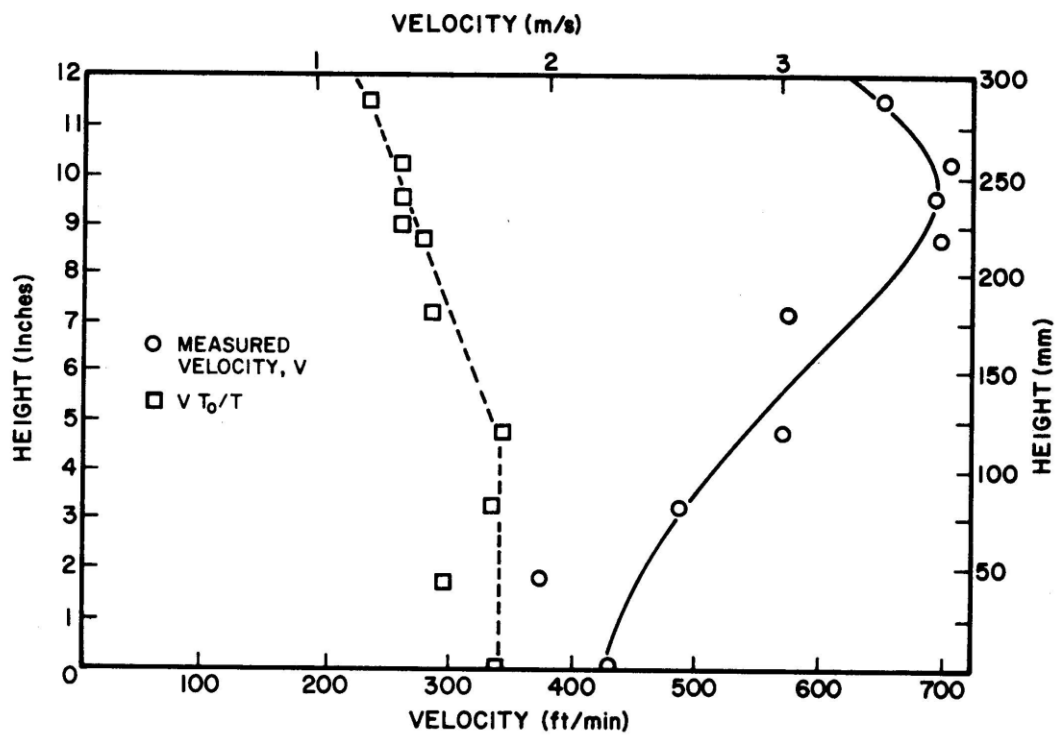
Figure 14. Vertical Velocity Profile through the Centerline at Nine Feet with the Burner On for 4 Minutes
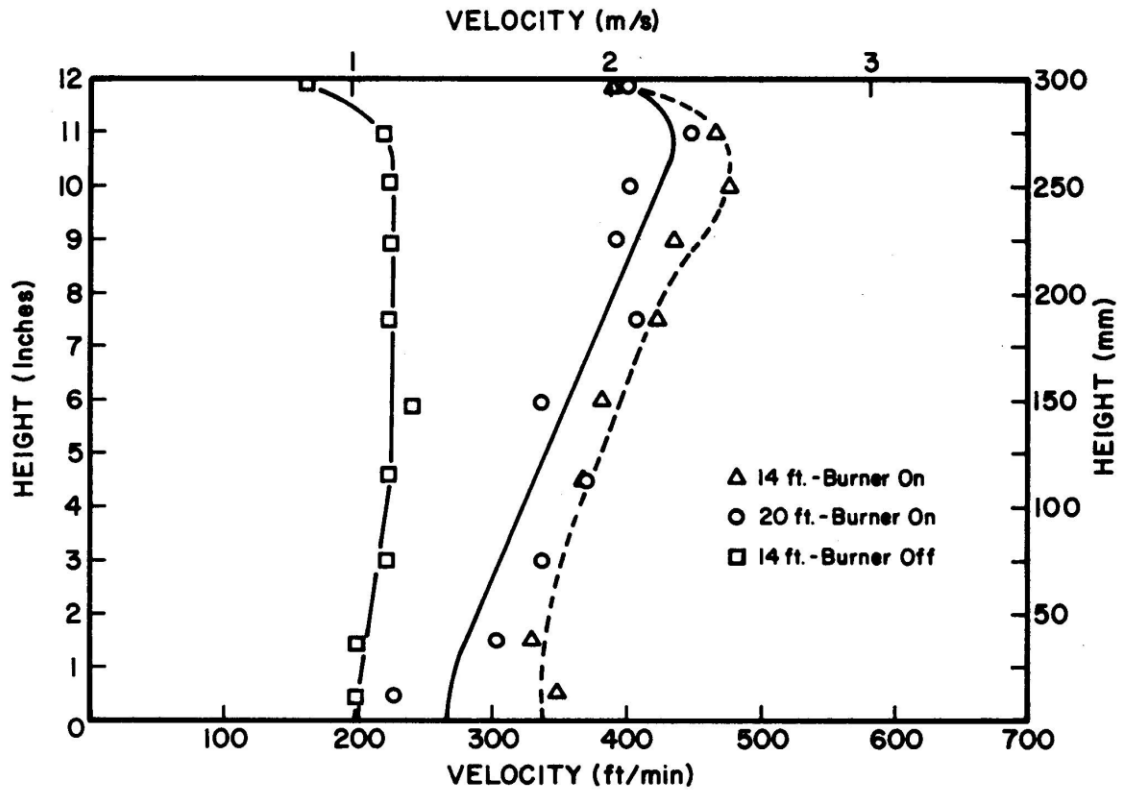
Figure 15. Vertical Velocity Profile through Centerline at 14 and 20 Feet for ACB with the Burner On and for 20 Feet with Burner Off

To determine the amount of uncertainty associated with the flame spread model the team conducted an analysis using the Propagation of Uncertainty theory. This method states that the uncertainty of an equation can be derived from the equation:

$$U(f) = \sqrt{\left(\frac{\delta f}{\delta a}\right)^2 \sigma_a^2 + \left(\frac{\delta f}{\delta b}\right)^2 \sigma_b^2 + \left(\frac{\delta f}{\delta c}\right)^2 \sigma_c^2} \qquad (1)$$

$\frac{\delta f}{\delta a}$ Is the partial differentiation of the equation f with respect to n, and S_n is the standard deviation of the parameter n. Since the model uses a different equation once burnout begins, the uncertainty must be calculated for both of these equations. Due to a lack of sufficient data, the standard deviation (σ) values for each input parameter were determined by normalizing the experimental data rather than a standard formula.

Algebraic Constants

$$C_1 = (k_f \dot{E}'' - \frac{t_f}{t_b} - 1)t_f^{-1}$$

$$C_2 = \frac{x_{p1} - x_{po}}{t_{bo}}$$

$$C_3 = k_f \dot{Q}_s t_{bo}$$

$$C_4 = \left(k_f \dot{E}'' - 1\right)t_{bo} - t_f$$

Before Burnout

$$\frac{\delta x_p}{\delta \dot{E}''} = -\left(\frac{k_f^2 \dot{Q}_s}{(k_f \dot{E}'')^2}\right)e^{(k_f E''-1)\frac{t}{t_f}} + \left(\frac{k_f t}{t_f}e^{(k_f E''-1)\frac{t}{t_f}}\right)\left(\frac{k_f \dot{Q}_s}{k_f \dot{E}''-1} + x_{po}\right) + \frac{k_f^2 \dot{Q}_s}{(k_f \dot{E}'')^2} \qquad (2)$$

$$\frac{\delta x_p}{\delta t_f} = -\left(\frac{k_f \dot{Q}_s}{k_f \dot{E}''-1} + x_{po}\right)\left(\frac{k_f t}{t_f^2}\right)e^{(k_f E''-1)\frac{t}{t_f}} \qquad (3)$$

$$U(x_p) = \sqrt{\left(\frac{\delta x_p}{\delta \dot{E}''}\right)^2 \sigma_{\dot{E}''}^2 + \left(\frac{\delta x_p}{\delta t_f}\right)^2 \sigma_{t_f}^2} \qquad (1)$$

The resulting U(x_p) value is the uncertainty of x_p before burnout.

After Burnout

$$\frac{\delta x_p}{\delta \dot{E}''} = \left(\frac{-k_f \dot{Q}_s t_{bo}(k_f t_{bo})}{((k_f \dot{E}''-1)t_{bo}-t_f)^2}\right)e^{(k_f \dot{E}''-\frac{t}{t_f}-1)\frac{t-t_b}{t_f}} + (x_{p1}-x_{po}) + \left[\frac{k_f \dot{Q}_s t_{bo}}{(k_f \dot{E}''-1)t_{bo}-t_f}\right]k_f\left(\frac{t-t_b}{t_f}\right)e^{(k_f \dot{E}''-\frac{t}{t_f}-1)\frac{t-t_b}{t_f}} +$$

$$\frac{k_f \dot{Q}_s t_{bo}(k_f t_{bo})}{((k_f \dot{E}''-1)t_{bo}-t_f)^2} + \frac{-k_f C_2 t_f}{(k_f \dot{E}''-\frac{t_f}{t_{bo}}-t_f)^2} + \frac{C_3}{t_{bo}}\left[\frac{k_f}{(k_f \dot{E}''-\frac{t_f}{t_{bo}}-t_f)^2}\left(\frac{1}{(k_f \dot{E}''-1)t_{bo}-t_f}\right)\right] -$$

$$\left[\frac{k_f t_{bo}}{((k_f \dot{E}''-1)t_{bo}-t_f)^2}\left(\frac{1}{k_f \dot{E}''-\frac{t_f}{t_{bo}}-1}\right)\right]\left(e^{(k_f \dot{E}''-\frac{t}{t_f}-1)\frac{t-t_b}{t_f}}-1\right) + k_f\left(\frac{t-t_b}{t_f}\right)e^{(k_f \dot{E}''-\frac{t}{t_f}-1)\frac{t-t_b}{t_f}}\left[C_2\frac{t_f}{k_f \dot{E}''-\frac{t_f}{t_{bo}}-1} +\right.$$

$$\left.\frac{C_3 t_f}{\left(k_f \dot{E}''-\frac{t_f}{t_{bo}}-1\right)((k_f \dot{E}''-1)t_{bo}-t_f)t_{bo}}\right]C_3\left(\frac{t-t_b}{t_{bo}}\right)\left(\frac{k_f t_{bo}}{((k_f \dot{E}''-1)t_{bo}-t_f)^2}\right) \qquad (4)$$

$$\frac{\delta x_p}{\delta t_b} = \left(\frac{C_3}{((k_f \dot{E}''-1)t_{bo}-t_f)^2}\right)e^{(k_f \dot{E}''-\frac{t}{bo}-\frac{1}{t_f})(t-t_b)} + \left(\frac{-k_f \dot{E}''}{t_f^2}+\frac{1}{t_f^2}\right)(t-t_b)e^{(k_f \dot{E}''-\frac{t_f}{t_{bo}}-1)\frac{t-t_b}{t_f}}\left((x_{p1}-x_p)+\right.$$

$$\frac{C_3}{(k_f \dot{E}''-1)t_{bo}-t_f} - \frac{C_3}{((k_f \dot{E}''-1)t_{bo}-t_f)^2} + \left[\frac{C_2(k_f E''-1)}{t_f^2\left(\frac{k_f \dot{E}''-1}{t_f}-\frac{1}{t_{bo}}\right)^2}+\frac{C_3}{t_{bo}}\left[\left(\frac{(k_f \dot{E}''-1)}{t_f^2\left(\frac{k_f \dot{E}''-1}{t_f}-\frac{1}{t_{bo}}\right)^2}\right)\left(\frac{1}{(k_f \dot{E}''-1)t_b-t_f}\right)+\right.\right.$$

$$\left.\left.\left(\frac{1}{((k_f \dot{E}''-1)t_b-t_f)^2}\right)\left(\frac{1}{\frac{k_f \dot{E}''-1}{t_f}-\frac{1}{t_{bo}}}\right)\right]\right]\left(e^{\left(\frac{k_f \dot{E}''-1}{t_f}-\frac{1}{t_b}\right)(t-t_b)}-1\right) -$$

$$\left[\left(\frac{(k_f \dot{E}''-1)(t-t_b)}{t_f^2}\right)\left(e^{\left(\frac{k_f \dot{E}''-1}{t_f}-\frac{1}{t_b}\right)(t-t_b)}\right)\left(\frac{C_2}{\frac{k_f \dot{E}''-1}{t_f}-\frac{1}{t_{bo}}}+\frac{C_3}{\left(\frac{k_f \dot{E}''-1}{t_f}-\frac{1}{t_{bo}}\right)((k_f \dot{E}''-1)t_b-t_f)t_{bo}}\right)\right] -$$

$$\left(\frac{C_3(t-t_b)}{t_{bo}}\frac{1}{((k_f \dot{E}''-1)t_{bo}-t_f)^2}\right) \qquad (5)$$

$$U(x_p) = \sqrt{\left(\frac{\delta x_p}{\delta \dot{E}''}\right)^2 \sigma_{\dot{E}''}^2 + \left(\frac{\delta x_p}{\delta t_b}\right)^2 \sigma_{t_f}^2} \qquad (1)$$

The resulting $U(x_p)$ value is the uncertainty of x_p after burnout.

NFPA 285

This test is used to evaluate the following propagation characteristics: (1) the ability of the wall assembly to resist flame propagation over the exterior face of the wall assembly, (2) the ability of the wall assembly to resist vertical flame propagation within the combustible components from one story to the next, (3) the ability of the wall assembly to resist vertical flame propagation over the interior surface of the wall assembly from one story to the next, and (4) the ability of the wall assembly to resist lateral flame propagation from the compartment of origin to adjacent compartments or spaces. (NFPA 285, 2012: 1.3.1)

Geometry

The NFPA 285 test apparatus shall be located in test facility having minimum dimensions of 30 feet wide by 30 feet deep by 23 feet high. The facility is designed to protect the apparatus and test specimen from exposure to wind and precipitation. The test apparatus is a two-story structure with three permanent walls and a movable test frame. Each story shall have a height of 15 feet 8 inches and each shall contain a test room. Each test room shall have an unfinished inside dimension of 10 feet wide by 10 feet deep and an unfinished floor-to-ceiling height of 7 feet. Each story will have one access opening 3.5 feet wide by 6.75 feet high, and access on the first floor shall be closed off during the test.

Test Apparatus:
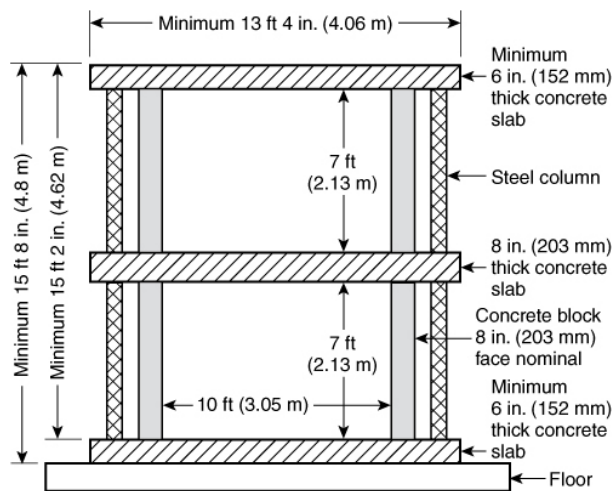
FIGURE 4.2.3
Front View of Test Apparatus Structure (not to scale). For exact dimensions, see 4.2.1 through 4.2.7.

Movable Wall Frame:

Lifting mechanism

1 ft 4 in. (4.06 m)

2 ft (0.61 m)

Minimum 7 ft 6 in. (2.29 m)

Steel frame— top member 8 in. (203 mm) H beam

4 in. x 4 in. (102 mm x 102 mm) angle

7 ft 8 in. (2.34 m)

18 ft 8 in. (5.69 m)

Steel frame 6 in. (152 mm) H beam

8 in. (203 mm)

6 in. (152 mm)

2 in. (51 mm)

15 ft (4.57 m)

16 ft (4.88 m)

FIGURE 4.3.1.3
Front View of Movable Wall Frame (not to scale).

(NFPA 285, 2012: Chapter 4)

Minimum 2 ft (0.61 m)

Wall height minimum 17 ft 6 in. (5.33 m)

7 ft 8 in. (2.34 m)

Test wall system

4 in. (102 mm) angle

7 ft 8 in. (2.34 m)

30 in. (762 mm)

30 in. (762 mm)

Ȼ

Window opening 78 in. (1981 mm)

2 in. to 6 in. (51 mm to 152 mm)

Wall width minimum 13 ft 4 in. (4.06 m)

15 ft (4.57 m)

FIGURE 5.2(b)
Front View of Test Specimen in Movable Test Frame (not to scale).

(NFPA 285, 2012: Chapter 5)

Location of thermocouples on front view of test specimen:

E-53

Thermocouples — 1 in. (25 mm) from exterior wall surface

○ Thermocouples — In the wall cavity air space or the insulation, or both, as shown in Figure 6.1(b) Details A through I.

( ) Thermocouples — Additional thermocouples in the insulation or the stud cavity, or both, where required for the test specimen construction being tested, as shown in Figure 6.1(b) Details C through I.

Fuel Package

The test requires two natural gas-fired burners: one placed inside the first-story test room and other near the top of the first-story window opening of the test specimen. The burners shall be constructed of nominal 2 in outside diameter steel pipe. (NFPA 285, 2012: 4.4)

Test Duration

Five minutes after ignition of the test room burner, the gas supply to the window burner shall be turned on and burner ignited. Thirty minutes after ignition of the test room burner, the gas supply to both burners shall be shut off. Residual burning on the test specimen shall not be extinguished until not less than 10 minutes after the gas supply is shut off. Therefore the total test duration is at least 40 minutes long. (NFPA 285, 2012: Chapter 8)

Thermal Insult

Room burner at 900kW, window burner at 400 kW

Pass/Fail Criteria

In order to pass the fire test, the specimen needs to meet the determined performance criteria during the 30-minute fire exposure portion of the test in order to pass (NFPA 285, 2012: 10.2). The performance criteria specifies that flame propagation on the exterior face of the test specimen shall not occur either vertically or horizontally beyond the area of the flame plume impingement by the window burner flames. NFPA 285 defines this propagation in Chapter 10. Additionally, flames shall not occur in second-story test room, and the temperature in the second-story test room shall not exceed 500 degrees Fahrenheit above the ambient air temperature at beginning of test. Flames shall also not occur beyond the intersection of the test specimen and the side walls of the test apparatus. (NFPA 285, 2012: Chapter 10)

Types of Assemblies

NFPA 285 is designed to test exterior non-load-bearing wall assemblies and panels used as components of curtain wall assemblies that are constructed using combustible materials or that incorporate combustible components, and that are intended to be installed on buildings required to have exterior walls of noncombustible construction (NFPA, 285, 2012: 1.1.1). Test specimens shall be at minimum 17.5 feet high and 13.3 feet wide. There shall be a window opening 30 inches high and 78 inches wide with a sill height 30 inches above the top of the first-story test room slab. The specimen shall completely cover the front face of the test apparatus expect for the window opening. (NFPA 285, 2012: Chapter 5)

Many different wall assembly systems can be tested using NFPA 285. Most assemblies contain some sort of insulation at the core of the system protected by at least one layer of exterior material. An example is extruded polystyrene insulation under various exterior finishes, including brick, stone, concrete, EIFS, etc.

NFPA 286

This section describes NFPA 286, *Standard Methods of Fire Tests for Evaluating Contribution of Wall and Ceiling Interior Finish to Room Fire Growth* (2011 Edition). This standard provides testing procedures to determine how interior finish materials will react when exposed to fire conditions.

Geometry

The test occurs in a fire test room that measures 8 ft x 12 ft x 8 ft. The fire room shall be inside a larger room and consist of four walls each at right angles. Area surrounding the fire test room shall be $20^{\circ}C \pm 10^{\circ}C$ with a relative humidity less than 75%. One doorway measuring 30.75 in x 79.5 in. for ventilation is required in the fire test room. The material being tested is mounted on the walls, ceiling, or both (depending on where it is going to be used).
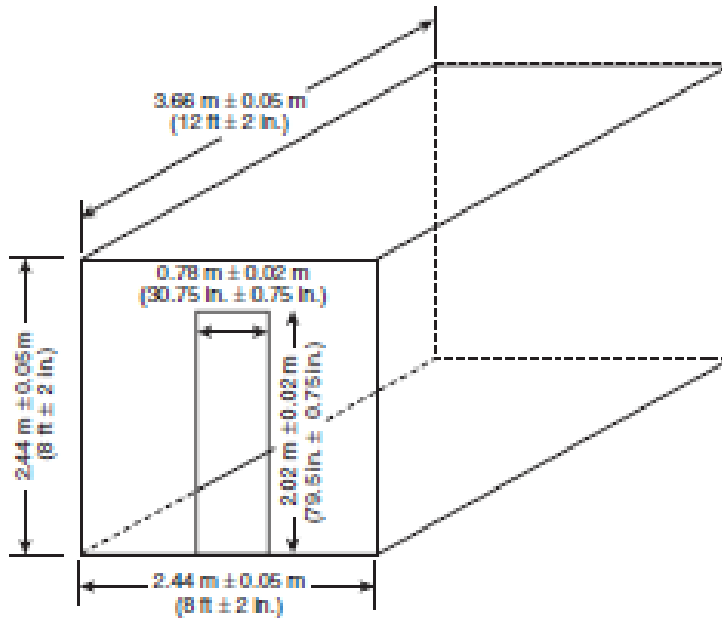
Figure 1: Interior Dimensions of Fire Test Room

Fuel Package

The fuel is provided by a burner, which supplies propane gas of 99% purity. The top of the burner is 12 in. ±2 in. above the floor. The burner shall switch from the 40kW heat output to the 160kW output within 10 seconds. Ignition of the burner will be by a pilot burner or a remotely controlled spark igniter. If flameout occurs the burner shall be capable of automatic shutoff of the gas supply.

Test Duration

The test is run for a total of fifteen minutes. The room is exposed to a heat release of 40 kW from the burner for 5 minutes, then a heat release of 160 kW for an additional ten minutes. The ignition is turned off after the ten minutes at 160 kW and the test is terminated (unless safety concerns make it necessary to terminate earlier).

Thermal Insult

40kW for 5 minutes, 160kW for an additional 10 minutes

Report Criteria

A material is assessed based on:
- Incident heat flux on the center of the floor
- Temperature of the gases in the upper part of the fire test room
- Rate of heat release
- Smoke release
- Time to flashover

A material is said to have passed if all of the following requirements are met:

During the 40 kW exposure:
- Flames do not reach the ceiling

During the 160 kW exposure:
- Flames do not reach the outer extremity of the sample on any wall or ceiling
- Flashover does not occur
- Peak heat release rate never exceeds 800 kW
- Total smoke released does not exceed 1000 m^2

Flashover is said to occur when two of the following conditions have occurred:
- Heat release rate exceeds 1 MW
- Heat flux at the floor exceeds 20 kW/m^2
- Average upper layer temperature exceed 600°C
- Flames exit doorway
- Autoignition of a paper target on the floor occurs

Types of Specimen

This test is used for interior finish materials. Materials can be tested three different ways; on three walls (if the material will only be used on the walls), on three walls and the ceiling (if the materials will be used on the walls and ceiling), and only on the ceiling (for those materials only to be used on the ceiling). The material being tested shall be mounted in the fire room as it would be mounted for actual use. The material will be placed on panels and there will be two panels on the end wall, three panels on each side wall, and three on the ceiling.

Appendix G   ASTM E84 Review

ASTM E 84

This section describes ASTM E84 *Standard Test Method for Surface Burning Characteristics of Building Materials* (2012 Edition). This is a standard for the comparative surface burning behavior of building materials and applies to exposed surfaces such as walls and ceilings. The purpose of this test method is to determine the relative burning behavior of the material based on flame spread along the sample as well as smoke production. Results of this test provide comparative measurements of surface flame spread and smoke density relative to red oak and fiber cement boards.

Geometry

A 24-ft long by 20-in wide specimen is secured as the ceiling (downward facing surface) in a fire test chamber (17.75-in x 12.0-in x 25-ft).
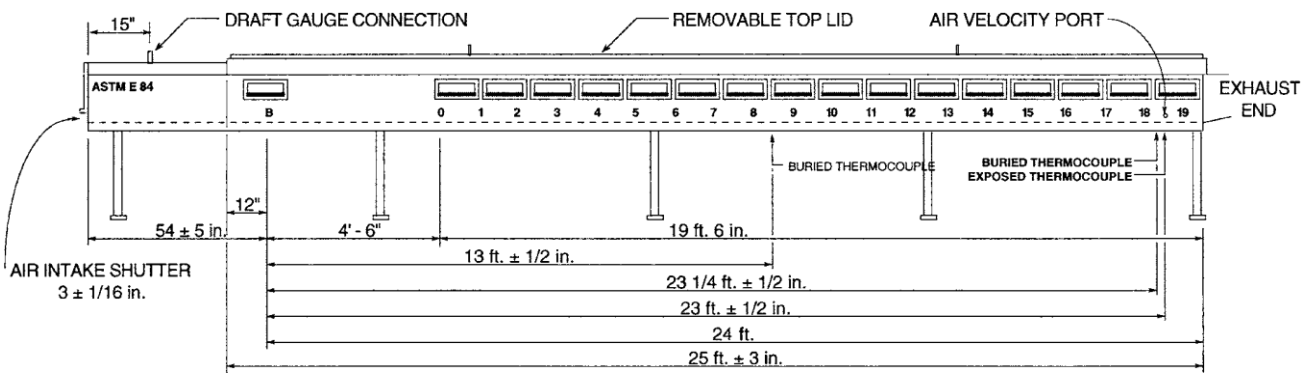
Fuel Package

One end of the test chamber will have two gas burners directed upward, creating flames against the surface of the test specimen. The two gas burners are spaced 12-in from the end of the test chamber and 7 ½ +/- ½ in . below the specimen surface. The burners are fed by one gas inlet split in a tee section to supply each burner.

An air intake shutter is located 54 +/- 5in. upstream of the burner. To provide the proper air turbulence for combustion, six refractory fire bricks are located along the side wall of the chamber to provide turbulence baffling.

Test Duration

The test is to run a total of 10 minutes from the ignition of the burners. The test may be concluded early if the specimen is completely consumed in the fire area and no further progressive burning is evident and the photoelectric cell reading has returned to the baseline. (section 8 procedure)

Pass/Fail Criteria

When the test is completed, flame spread distance vs time is plotted and the area under the curve is calculated. In the event that the flame recedes during the test duration, a horizontal line is drawn from the point of recession for the remainder of the test or until the flame front continues past the original recession point. If the total area under the curve is less than or equal to 97.5, the area is multiplied by .515 to obtain the flame spread index (FSI). FSI = 0.515 $*A_T$. If the total area is greater than 97.5 the FSI is calculated as $4900/(195-A_T)$. The FSI is rounded to the nearest multiple of 5. (See ASTM E84 appendix X2 for derivations)

Types of Assemblies

This test is designed to test building materials that will be used as finishing surfaces such as walls or ceilings. The test assembly must be a downward facing surface in the ceiling position of the test chamber. The test assembly or material has to be capable of mounting in this position by means of self-support or holding in place by supports along the test surface or by securing the specimen from the back. Specimen with supports exhibit lower flame spread index than those able to be tested without additional support. Also materials with dripping and delaminating qualities severe enough to alter the flame front will also display lower flame spread indexes.

Appendix H   Compartment Effect

Because this test is conducted within a partially enclosed compartment, it is necessary to understand the impacts the compartment will have on the fire temperatures. In this case, the fire starts about 2.4 meters below the ceiling. The hot products of combustion will create a plume, which will rise toward the ceiling due to buoyancy. As it rises, the plume will draw in cooler air from the compartment, therefore decreasing the temperature of the plume and increasing its volumetric flow rate. Upon reaching the ceiling, the plume will spread out and form a hot gas layer that descends in the room with time. Eventually this layer will reach the openings in the room where the hot gas will flow out of the room and the outside air will flow into the room. This is known as the two layer or zone model and can be seen in the figure below.
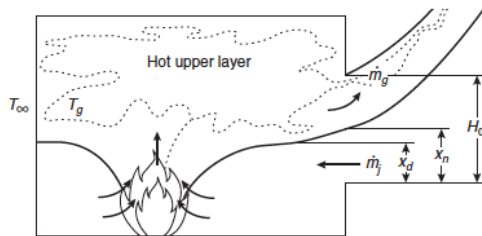
Figure 3-6.2.   Two-layer model with no exchange between layers except the plume.

MQH Method

Many assumptions are made for this model. It is assumed that the only interchange between the air in the lower part of the room and the hot upper gas layer is through the plume. It is also assumed that the compositions and temperatures of each layer is uniform, and that the temperature of the upper layer will always be greater than the lower layer. The basic governing principle used to calculate the temperature in a compartment fire is the conservation of energy. It states that the energy added to the upper layer by the fire is equal to the energy lost from the upper layer from radiation and convection plus the energy convected out of the compartment openings. Throughout this test, flashover conditions

were never attained, this section focuses on predicting compartment fire temperatures for preflashover fires. Specifically, the method of McCaffrey, Quintiere, and Harkleroad was used. These hand calculations are an approximate solution that use a limiting set of assumptions for calculating the upper gas layer temperature. Based on a simple conservation of energy equation and multiple substitutions, the following power-law relationship can be used to solve for this change in temperature:

$$\Delta T_g = 480 \left(\frac{\dot{Q}}{\sqrt{g} c_p \rho_\infty T_\infty A_0 \sqrt{H_0}} \right)^{\frac{2}{3}} \left(\frac{h_k A_T}{\sqrt{g} c_p \rho_\infty A_0 \sqrt{H_0}} \right)^{-\frac{1}{3}}$$

Heat Transfer Coefficient

As stated in the above assumptions, the heat transfer coefficient is determined based on the thermal penetration time. The equation for calculating the thermal penetration time is as follows:

$$t_p = \left(\frac{\rho c}{k} \right) \left(\frac{d}{2} \right)^2$$

Consequently, the following equations are used to determine the heat transfer coefficient necessary for the above analysis.

$$h_k = \frac{k}{d} \text{ for times greater than the thermal penetration time.}$$

$$h_k = \left(\frac{k \rho c}{t} \right)^{\frac{1}{2}} \text{ for times less than or equal to the thermal penetration time.}$$

Limitations

The following limitation exist for this method:

- The correlation holds for compartment upper layer gas temperatures up to approximately 600°C.

- The correlation applies to steady-state as well as time-dependent fires as long as the transient response is the wall conduction phenomenon.

- The correlation is not applicable to rapidly developing fires in large enclosures in which significant fire growth has occurred before the combustion products have exited the compartment.

- The energy release rate of the fire must be determined from data or other correlations.

- The characteristic fire growth time and thermal penetration time of the room-lining materials must be determined in order to evaluate the effective heat transfer coefficient.

- The correlation is based on data from a limited number of experiments and does not contain extensive data on ventilation-controlled fire nor data on combustible walls or ceilings. Most of the fuel n the test fires was near the center of the room.

(SFPE Handbook, Third Edition: 3-6)

Appendix I   International Building Code Review

Building Code Regulations

The interior wall and ceiling finish requirements are dependent on two main factors. The first is the type of building or "occupancy" as the building code refers to it and the second is where in the building the material is going. There are ten main types of building occupancies. The occupancy is determined based on the main use/purpose of the building. Some occupancies are further classified (as 1, 2, 3, etc.) based on a more specific use.

Types of Occupancies

The main occupancy types are:
- Assembly (A)
- Business (B)
- Educational (E)
- Factory (F)
- High-Hazard (H)
- Institutional (I)
- Mercantile (M)
- Residential (R)
- Storage (S)
- Utility and Miscellaneous (U)

As described above, to determine a building's occupancy classification the main purpose of the building is used. Some occupancies types are broken down further with sub-classes. For interior wall and ceiling finish requirements the sub-classes of Assembly, Institutional, and Residential impact the code requirements.

The building is considered an assembly occupancy when many people gather in the building for any reason (i.e. religious, social, awaiting transportation, food, drink, etc.). Since there are such a variety of buildings that fall under the assembly occupancy there are sub categories, A-1, A-2, A-3, A-4, and A-5.   A-1 occupancies typically have fixed seating and are used for performance or viewing performance (i.e. movie theater). Buildings that are meant for the consumption of food or beverages are given an A-2 classification. A-3 occupancy is given to any other assembly type building except for those used for indoor or outdoor sporting events (i.e. place of religious worship, lecture hall, museum, pool hall, etc). Buildings that house indoor sporting events and have spectator seating are considered A-4 occupancies while structures used for outdoor sporting events are considered A-5 occupancies.

Institutional occupancies are buildings in which people live or are cared for because of physical limitations (health or age), medical treatment, or because they "are detained for penal or correctional purposes". The sub-classes of Institutional occupancies are I-1, I-2, I-3, I-4. An I-1 occupancy refers to a building in which people (more than 16) reside and are supervised. *Personal care services* are provided. Residents are capable of reacting to emergency situations without physical assistance (i.e. alcohol and drug centers, assisted living facilities, etc.). I-2 occupancies are buildings used for any type of 24 hour care (physical, mental, or custodial) of people who are not capable of responding to emergency situations on their own (i.e. child care facilities (more than 5 children under the age of 2 ½), hospitals, nursing homes, etc.).   Buildings in which more than five people reside who are incapable of self preservation because of security restraints are considered I-3 occupancies (i.e. jails). I-4 occupancies are

buildings in which people, regardless of age are cared for (for less than 24 hours) by someone other than relatives/guardians.

Residential occupancies are buildings in which people sleep in, but are not considered institutional occupancies. The sub-classes of Residential occupancies are R-1, R-2, R-3, and R-4. R-1 occupancies are building where people do not stay permanently (less than 30 consecutive days). These would include things like hotels or motels. R-2 occupancies are building in which more than two sleeping/dwelling units are present. The occupants tend to be permanent. This would include apartments, dormitories, fraternities, monasteries, etc. R-3 occupancies are building where the occupants are normally permanent but are not classified as R-1, R-2, R-4, or I. R-4 occupancies are building used for assisted living of more than 5 people but no more than 16.

For Business, Educational, Factory, High-Hazard, Mercantile, Storage, Utility and Miscellaneous occupancies any sub-classes that may exist do not matter for the interior wall and ceiling finish requirements. A business occupancy is a building used as an office, for professional services, or other equivalent purposes (i.e. print shop, post office, educational occupancies above the 12th grade, etc.). An educational occupancy is a building used for educational purposes until the 12th grade. Factory assemblies are buildings used for any type or process in manufacturing excluding those classified as High-Hazard or Storage. This includes assembling, disassembling, fabricating, finishing, etc. High-Hazard occupancies are buildings used for the same purpose as a factory assembly except the materials being manufactured constitute physical or health hazards. Mercantile occupancies are comprised of buildings used for the display of goods for sale. Storage occupancies are buildings used for storage purposes. Utility and Miscellaneous buildings are those that cannot be classified under any other category.

Material Classifications and Building Areas

The International Building Code classifies materials based on results from ASTM E 84 or UL 723 testing. There are three different classifications, Class A, Class B, or Class C. The different classes are determined by the flame spread index and smoke-developed during the tests. The following table details the different classifications:

Class	Flame Spread Index	Smoke Developed Index
A	0-25	0-450
B	26-75	0-450
C	76-200	0-450

The code gives a minimum requirement. If the code says that a class B material is needed, then either a class A or class B material can be used. A class C material would not be allowed in that particular section of that type of occupancy. A class C requirement means a class A, B, or C material may be used. When the code says class A material is needed, only a class A material can be used.

Requirements for interior finishes depend on where in the building the material is going to be. The International Building Code divides buildings into three sections: exit enclosures, corridors, and rooms and enclosed spaces. The occupancy type will also affect the material requirements.

Class C materials

Class C materials are only permitted in exit enclosures in F, R-2, R-3, and S occupancies. They are permitted in corridors in B, E, M, R-1, R-4, I-1, F, R-2, R-3, and S occupancies. For rooms and enclosed spaces class C materials are allowed in all assembly and residential occupancies, B, E, M, H, F, S, I-1, and I-3 occupancies.

Class B Materials

Class B materials are permitted wherever class C materials are allowed as well as in exit enclosures in all assembly, B, E, M, R-1, R-4, H, I-1, I-2, and I-4 occupancies. They are permitted in corridors in all assembly, H, I-2, and I-4 occupancies. For rooms and enclosed spaces class B materials are allowed in I-2, and I-4 occupancies.

Class A Materials

Class A materials are permitted wherever class B and C materials are allowed as well as in exit enclosures in I-3 occupancies. They are permitted in corridors in I-3 occupancies.

Non-Sprinklered Buildings

All of the above requirements are assuming the building is sprinklered. If the occupancy is not protected by an automatic sprinkler system the interior finish requirements change. Essentially any area that had a class B requirement in a sprinklered building would require a class A material in a non-sprinklered building. Many class C requirements in sprinklered buildings become class B requirements for non-sprinklered buildings. All of the requirements are increased by a class in the exit enclosure sections for a non-sprinklered building. The only corridor requirement that does not increase in a non-sprinklered building is in the F occupancies. There were more requirements that remained the same for rooms and enclosed spaces for non-sprinklered buildings. These included A-3, A-3, A-4, A-5, B, E, M, R-1, F, I-2, I-4, R-2, S occupancies. No requirements changed for R-3 occupancies regardless of whether the building was sprinklered or not. There are no restrictions for U occupancies in a sprinklered or non-sprinklered building.

Appendix J   Cone: Heat Release Rate Histories

25 kw/m² Heat Release rate analysis

Thirteen FRP systems are analyzed in the context of heat release rate. This briefing highlights all thirteen systems as well as groups the systems in terms of pigments, filler, gel, and aggregate composition for comparison purposes.

Baseline FRP System
No gelcoat
Polymer concrete: Norsodyne H 81269 TF with 6% cobalt & DDM-9
Alumina Trihydrate: 10% of resin by weight
Sand: 150% of resin by weight, split evenly between #0/30 and #2/16
1-1/2 parts sand to 1 part resin
No pigment
Approximately 60 mil thickness (aggregate dependent)
3/16" single skin laminate: Norsodyne H 81269 TF with 6% cobalt & DDM-9
4 layers of 1.5 ounce chopped strand mat
Glass to resin ratio range: 25:75 to 35:65 by weight

System 1 – Addition of 1/2" plywood core & 3/16" rear skin (Note that core separation was observed in several samples)
System 2 – Addition of 3/4" balsa core & 3/16" rear skin
System 3 – Addition of 1/2" polyurethane foam core & 3/16" rear skin
System 4 – Bronze filler instead of sand: 1 part bronze powder to 1 part resin by weight
System 5 – Aluminum filler instead of sand: 1 part aluminum powder to 2 parts resin by weight
System 6 – Straight Norsodyne H 81269 TF as gelcoat in place of resin based polymer concrete
System 7 – Addition of white pigment to polymer concrete
System 8 – Addition of grey pigment to polymer concrete
System 9 – Addition of beige pigment to polymer concrete
System 10 – #0/30 aggregate only
System 11 – #0/60 aggregate only
System 12 – #2/16 aggregate only
**System 13** – DCPD Laminate resin (with 6 layers of glass) instead of Norsodyne

Baseline HRR 25kW/m²

Kreysler Sample 1 HRR 25 kW/m²

Kreysler Sample 2 HRR 25kW/m²
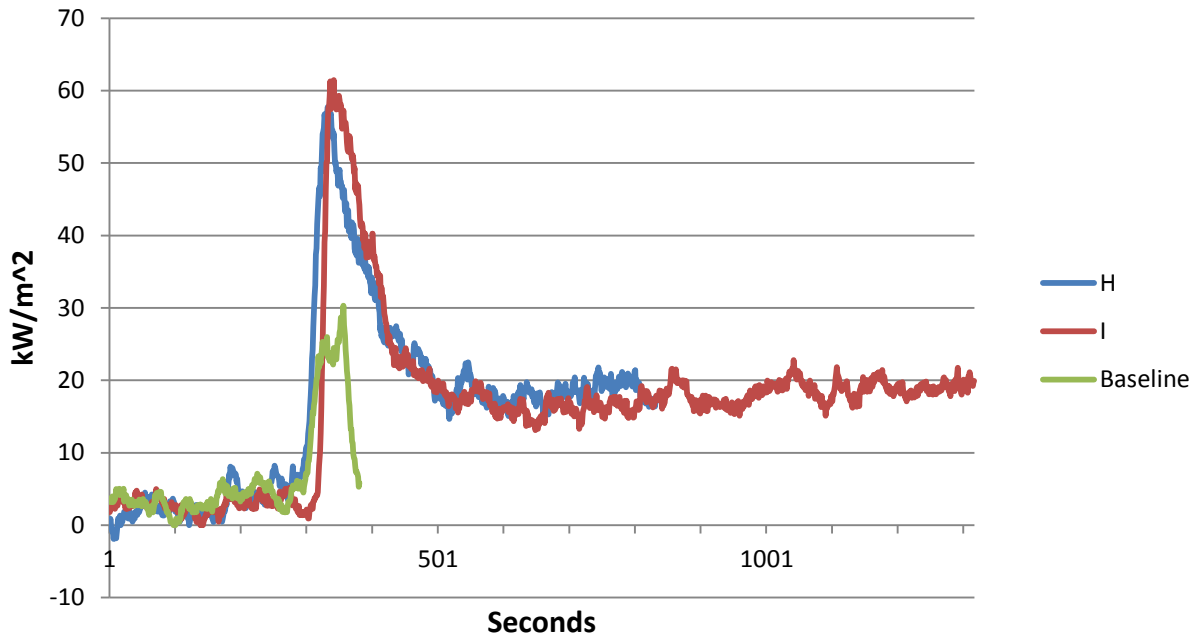
Kreysler Sample 3 HRR 25kW/m²
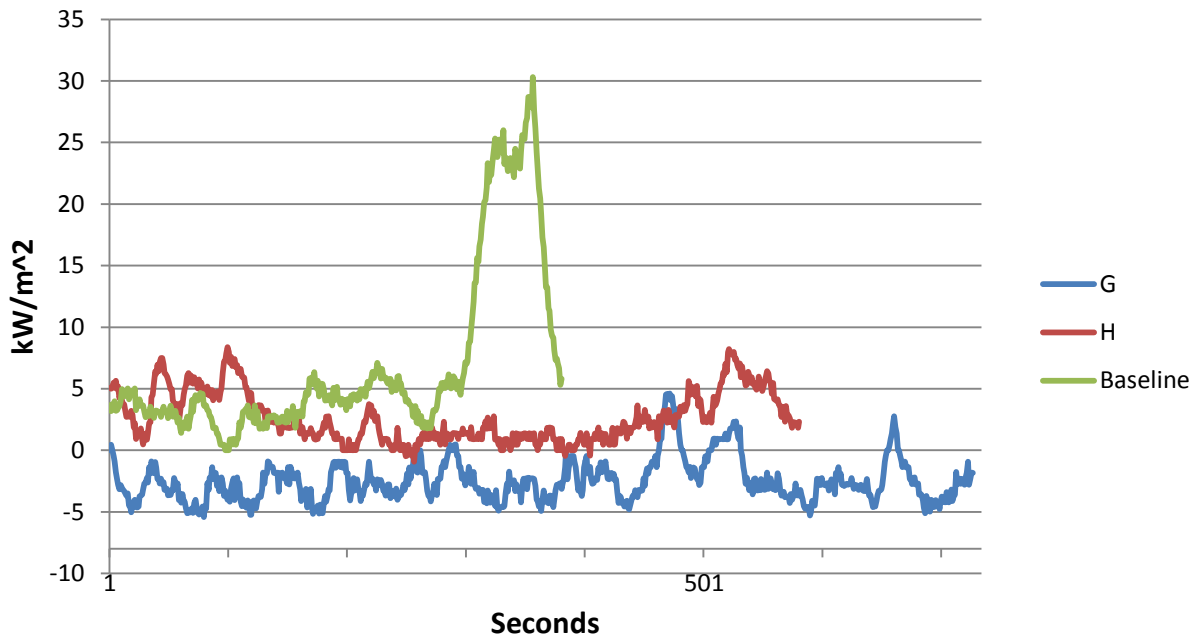
Kreysler Sample 4 HRR 25kW/m²
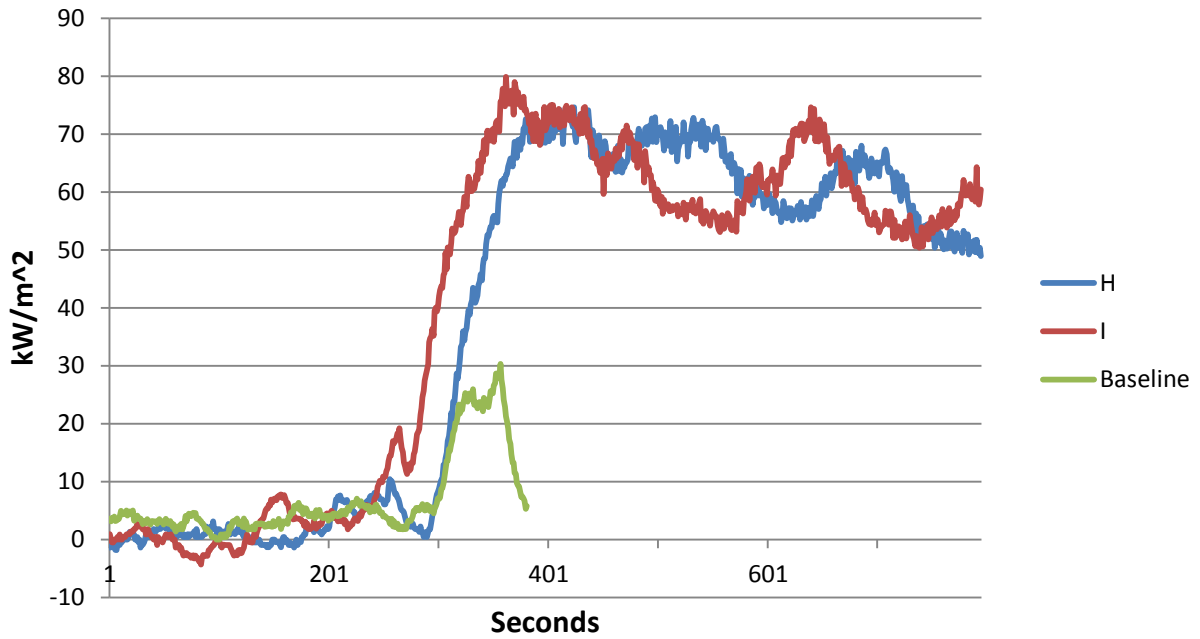
Kreysler Sample 5 HRR 25kW/m²
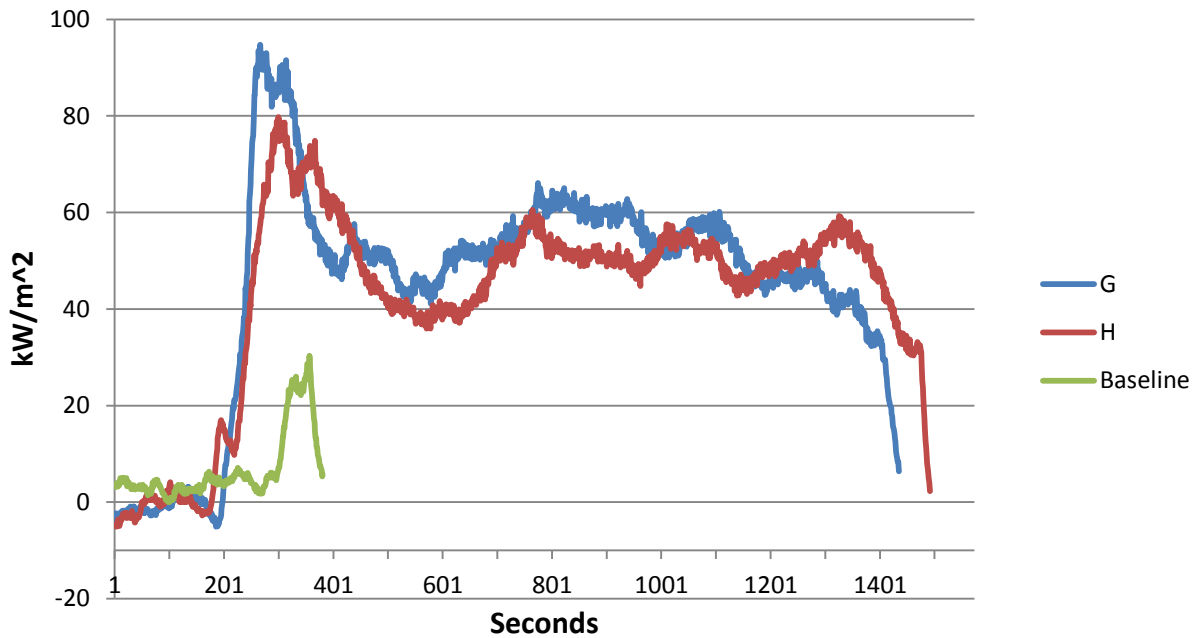
Kreysler Sample 6 HRR 25kW/m²
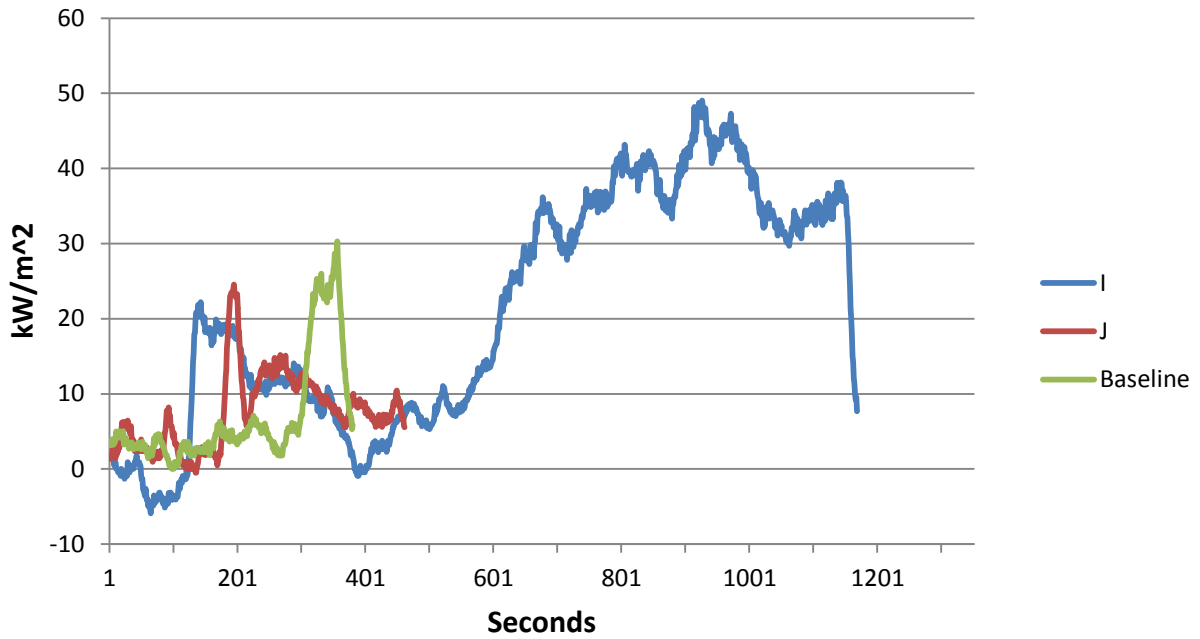
Kreysler Sample 7 HRR 25kW/m²

Kreysler Sample 8 HRR 25kW/m²

Kreysler Sample 9 HRR 25kW/m²
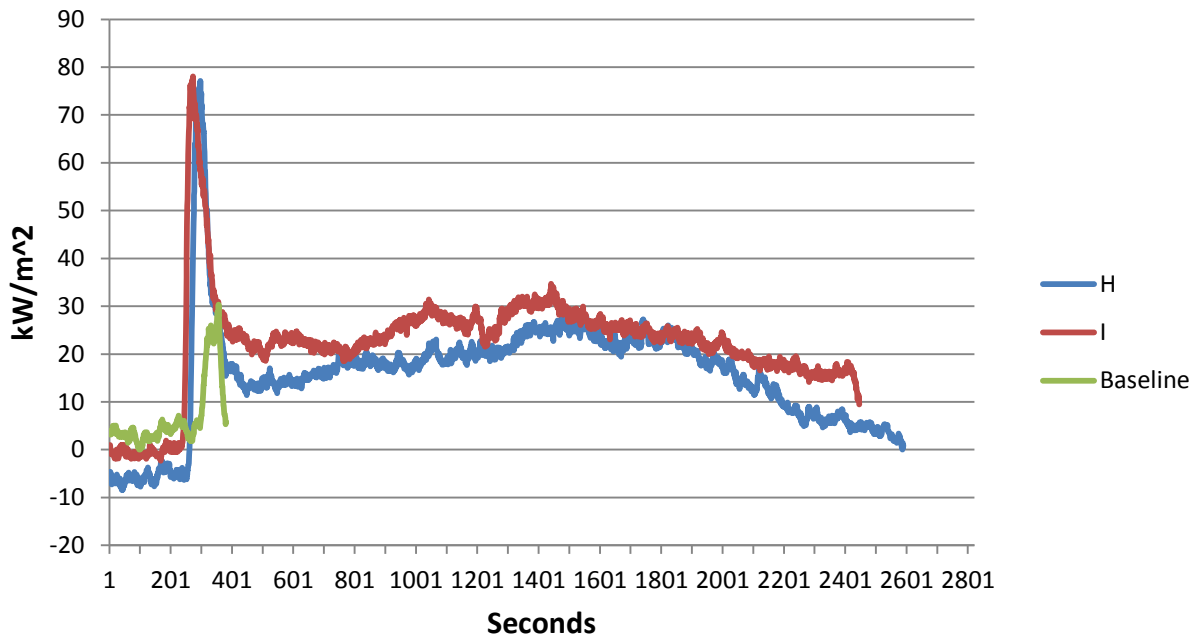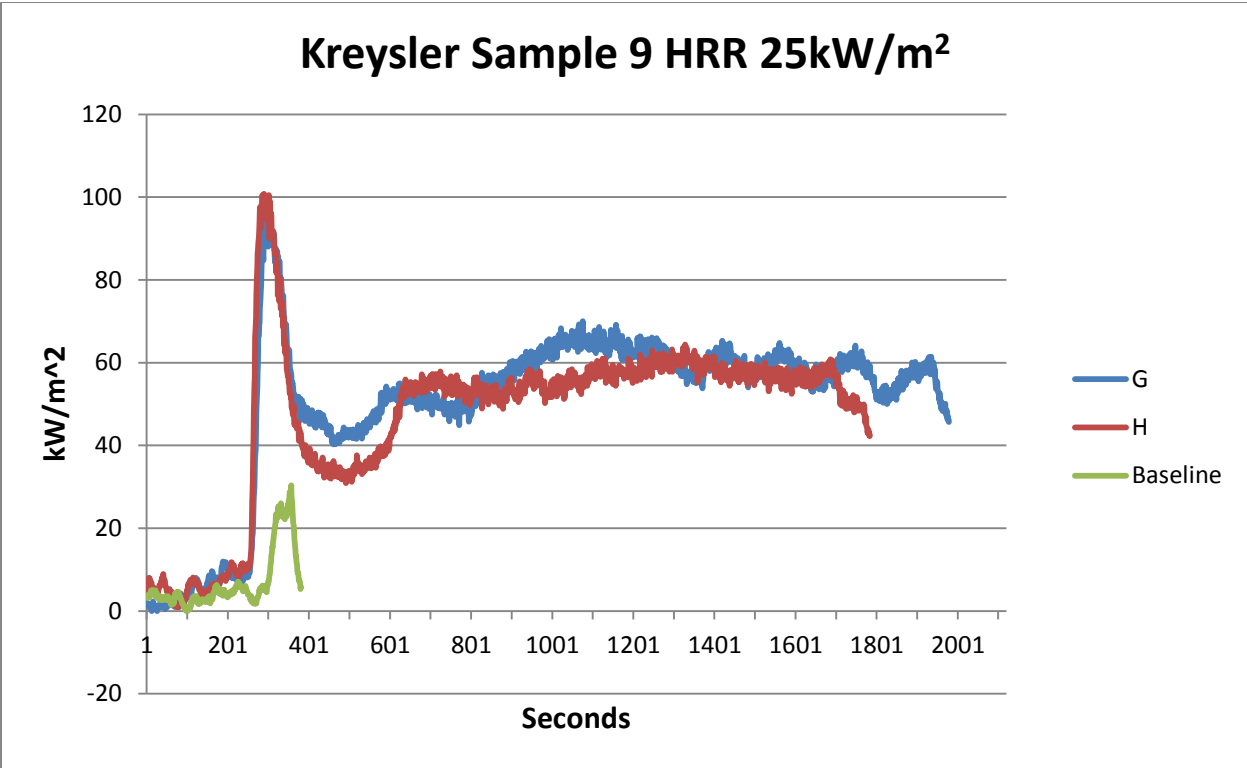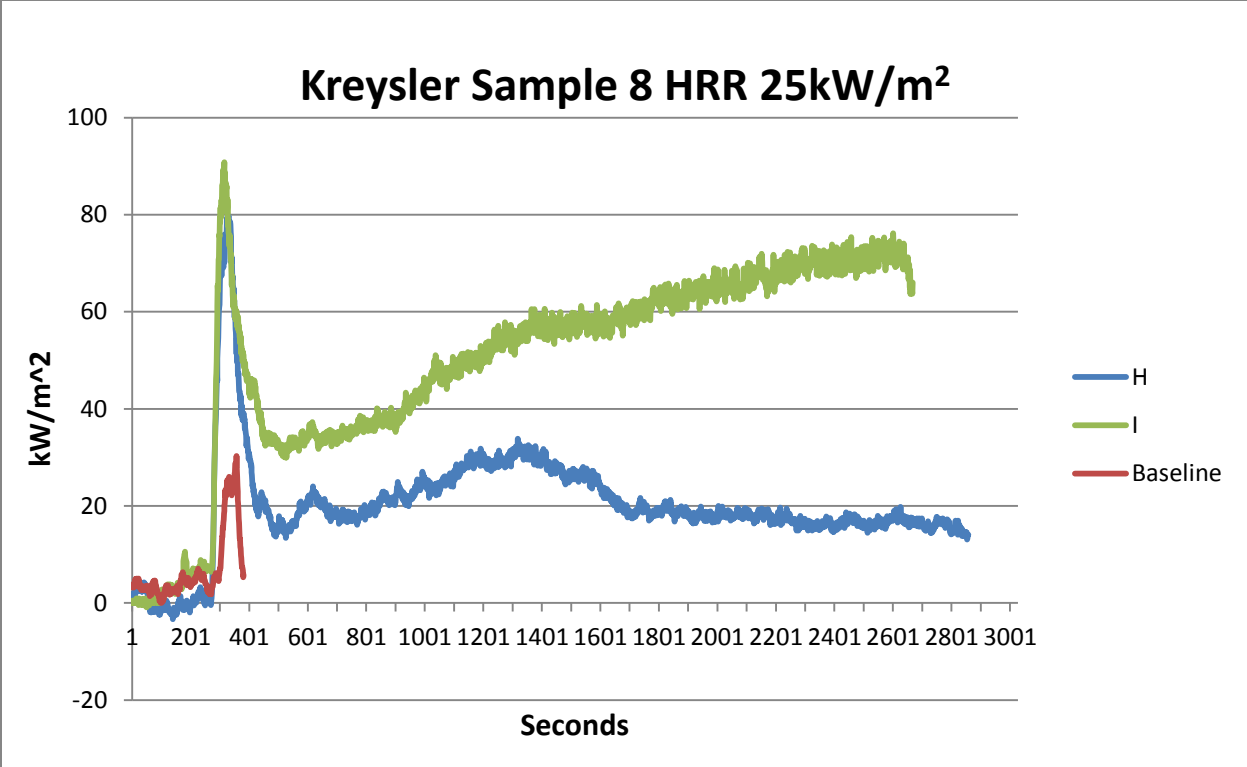
Kreysler Sample 10 HRR 25kW/m²
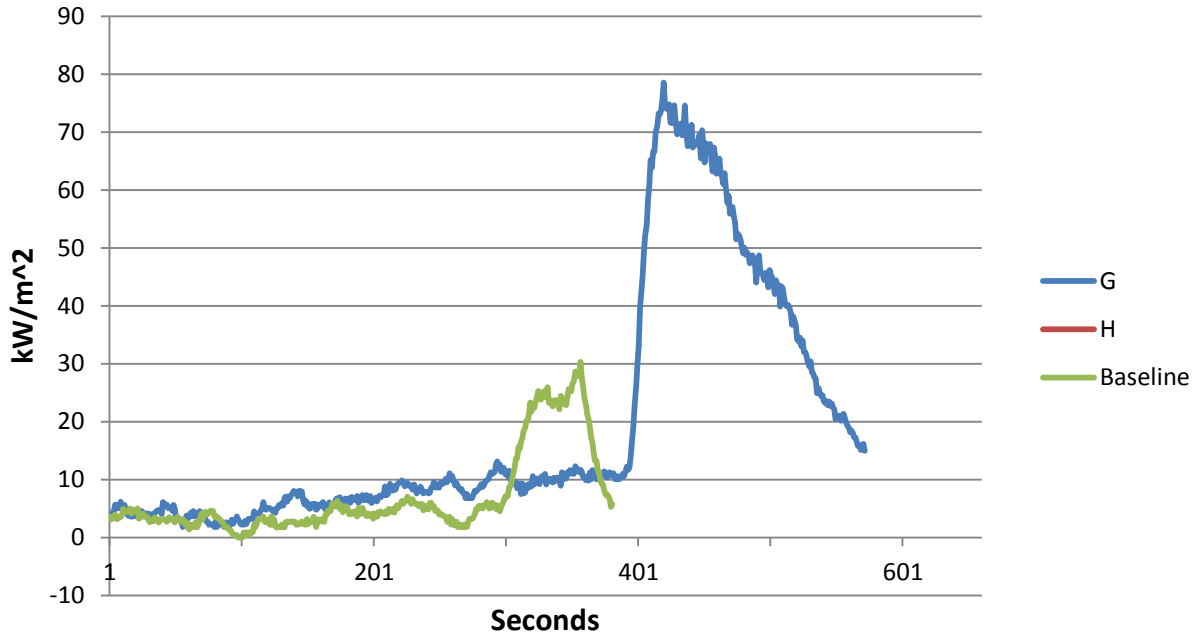
Kreysler Sample 11 HRR 25kW/m²
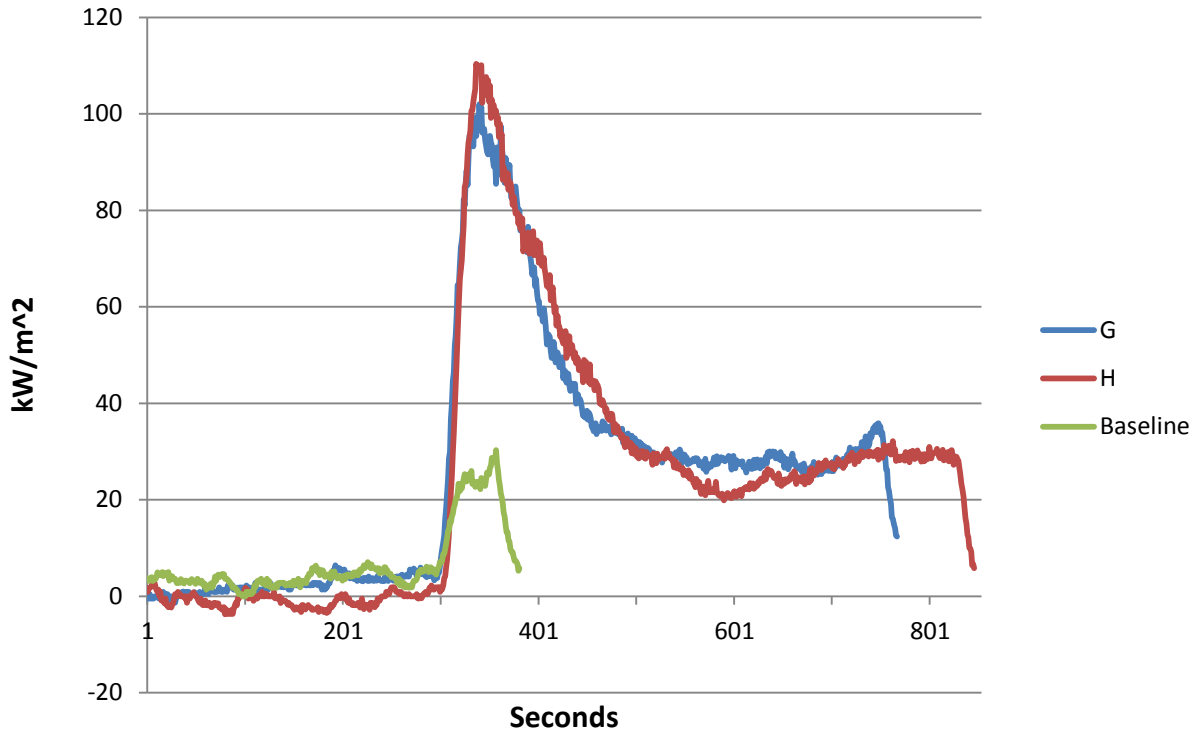
Kreysler Sample 12 HRR 25kW/m²
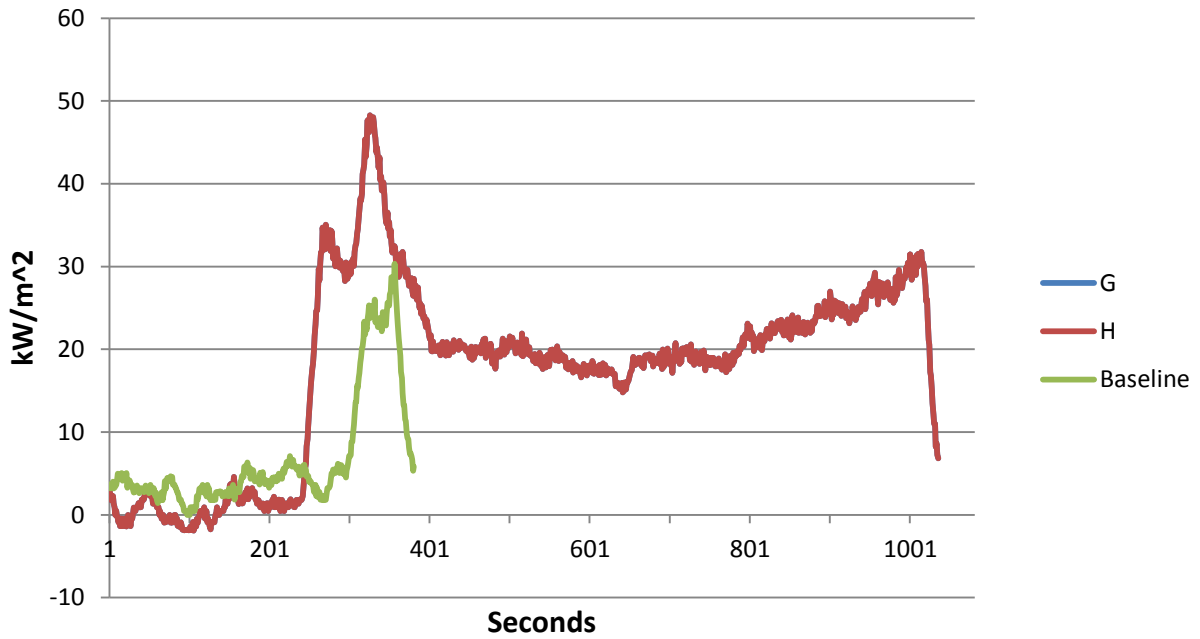
Kreysler Sample 13 HRR 25kW/m²
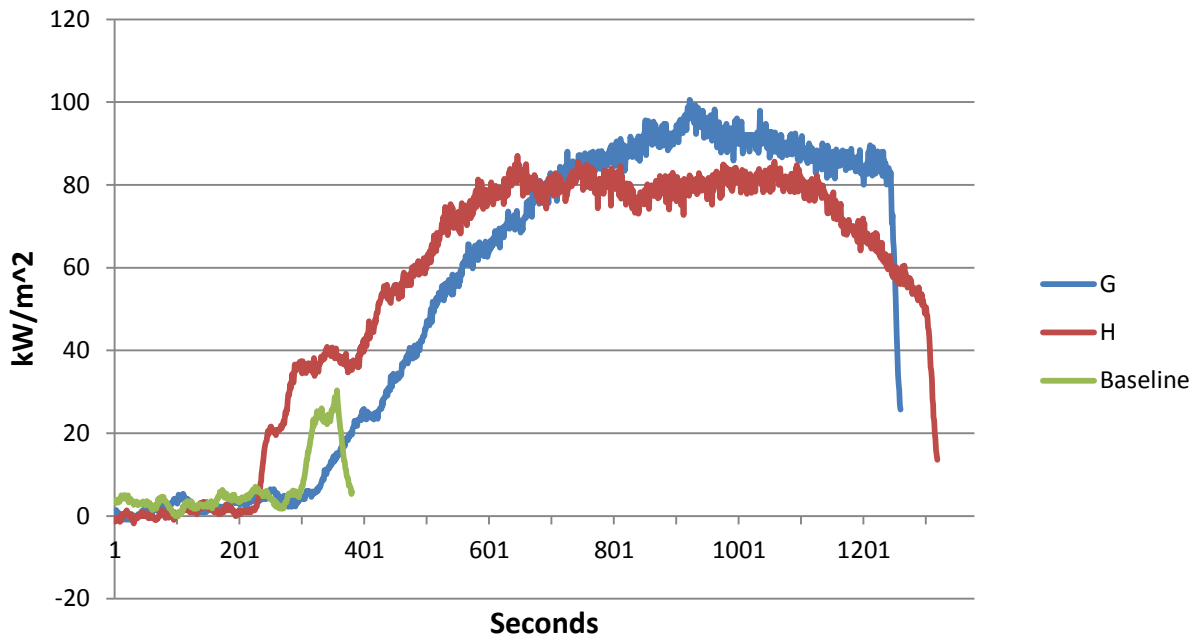
Pigment HRR Comparisons 25kW/m²

Legend: (White) 7H, (Grey) 8H, (Beige) 9G, Baseline

Aggregate HRR Comparison 25kW/m²

Legend: (#0/30) 10G, (#0/60) 11G, (#2/16) 12G, Baseline

Filler HRR Comparison 25kW/m²

- (Bronze) 4H
- (Aluminum) 5G
- Baseline

Gel HRR Comparison 25kW/m²

- Norsodyne 6I
- DCPD 13G
- Baseline
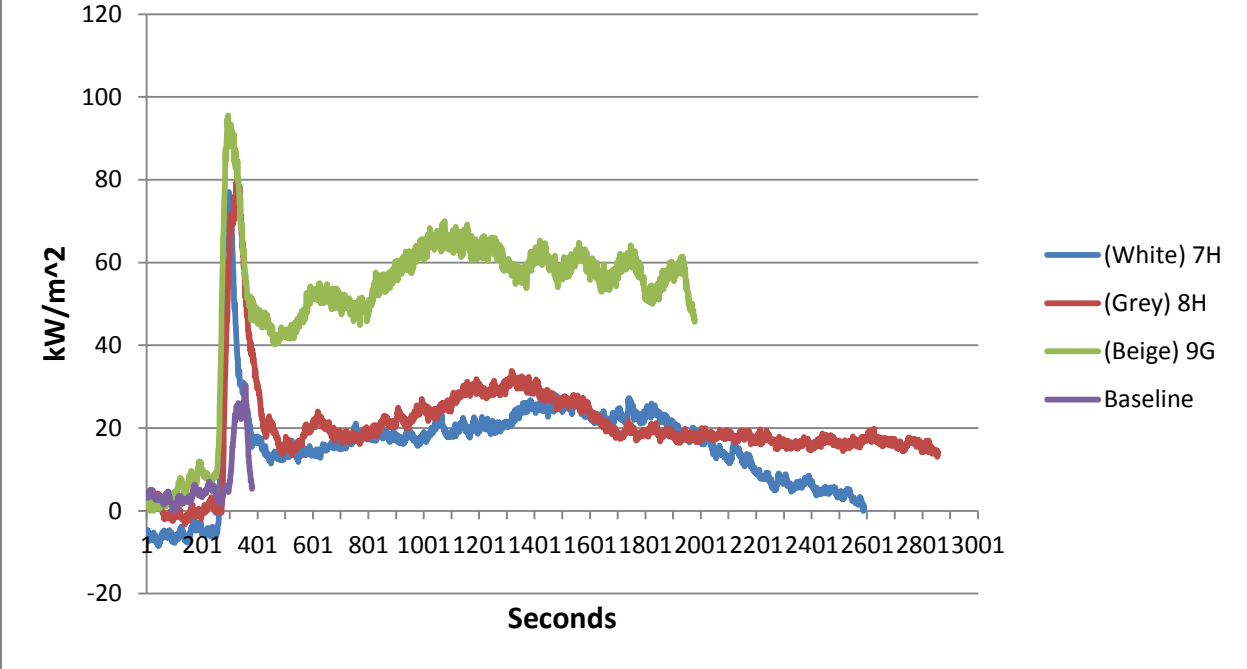
Cores HRR Comparison 25kW/m²
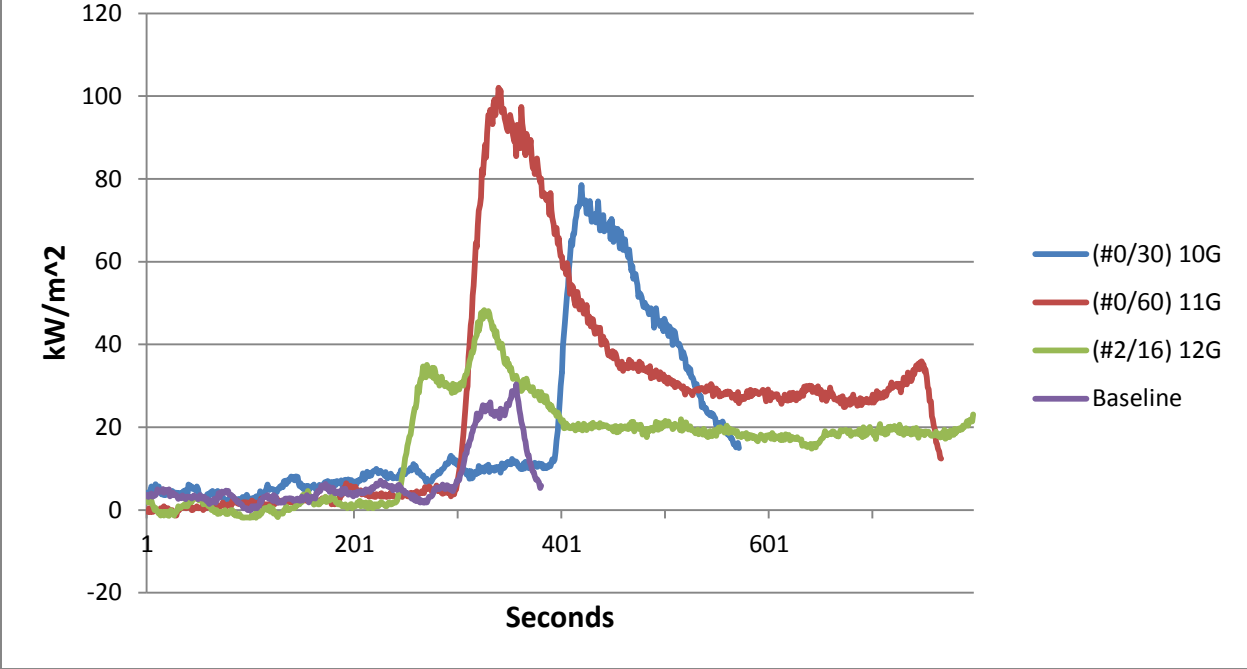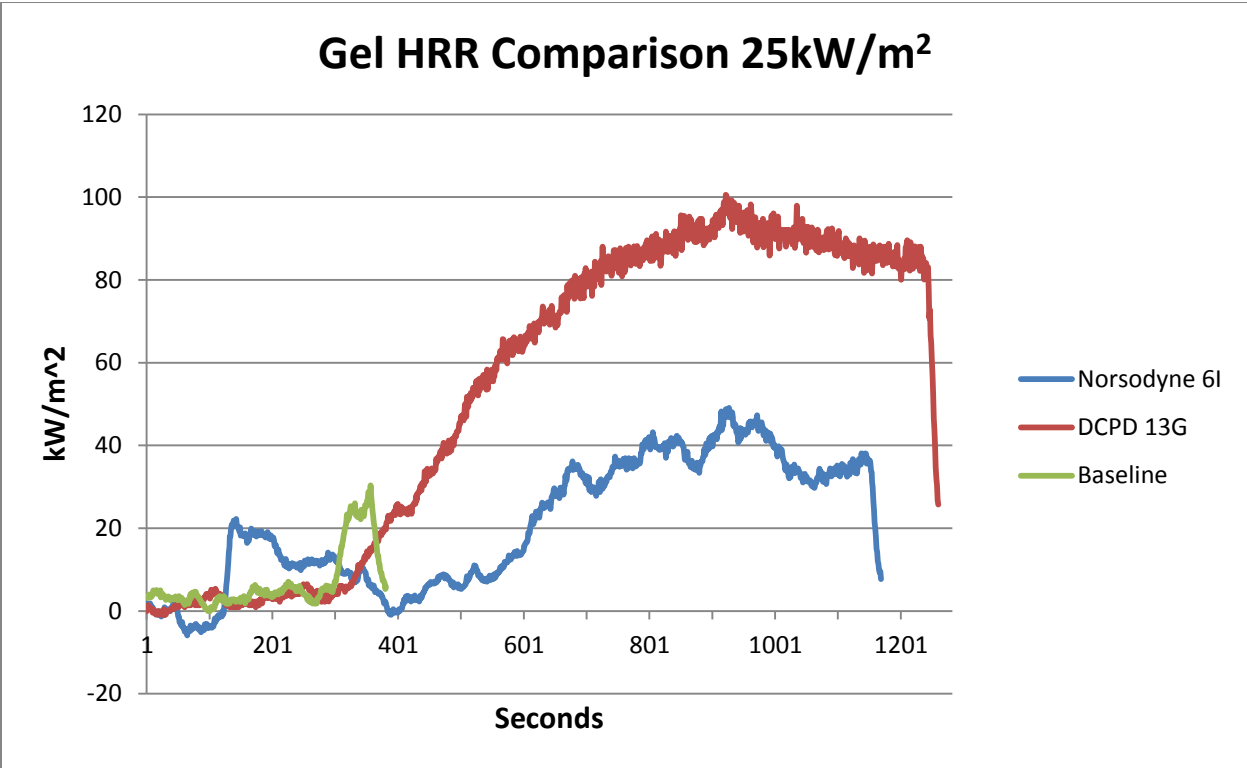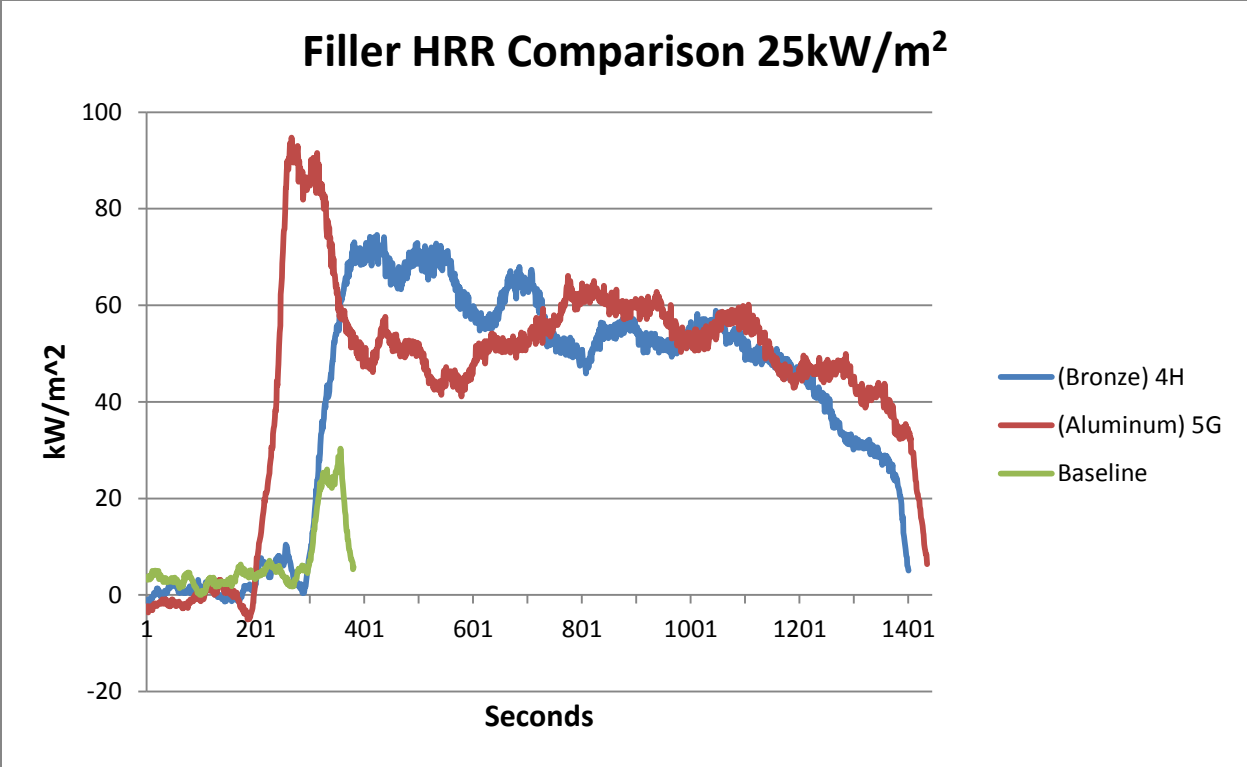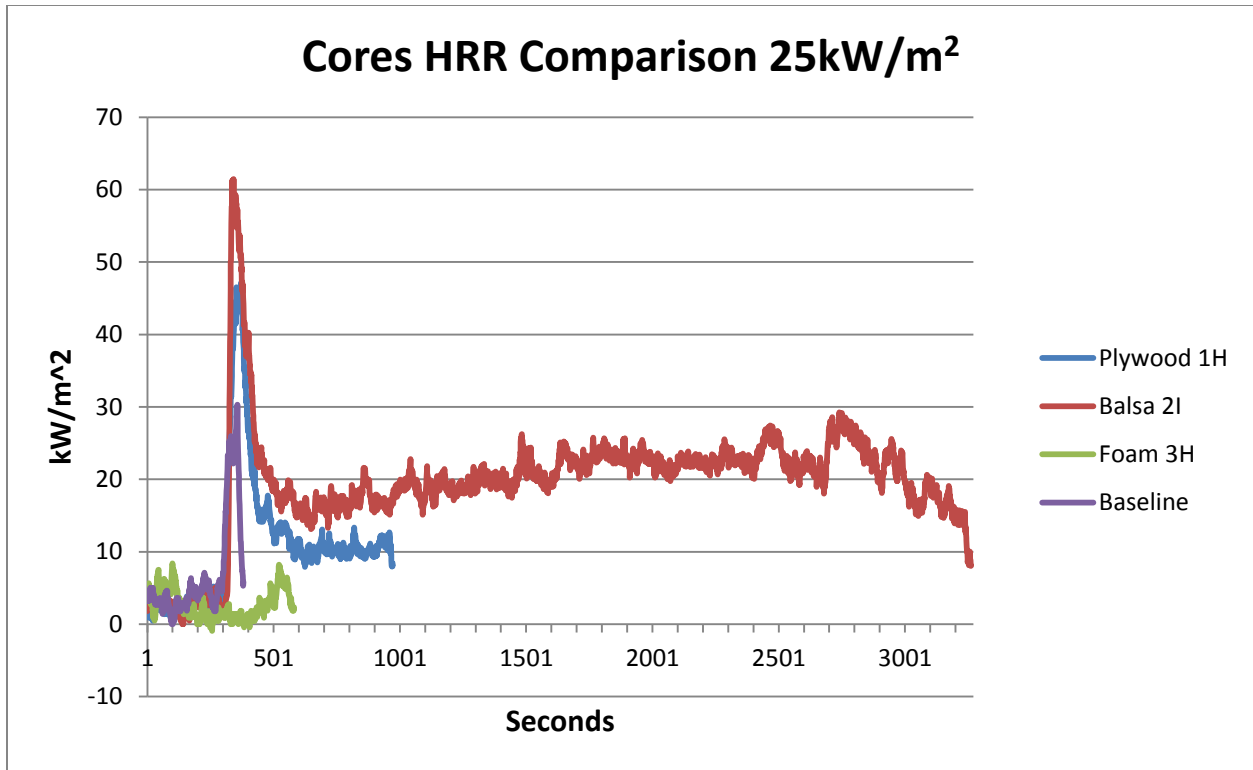
50 kw/m^2 Heat Release rate analysis

Thirteen FRP systems are analyzed in the context of heat release rate. This briefing highlights all thirteen systems as well as groups the systems in terms of pigments, filler, gel, and aggregate composition for comparison purposes.

Additionally, Samples 5, 7, 10, and 13 were selected for further testing with an alternate test method with no sample frame for comparison purposes.

Baseline FRP System

No gelcoat
Polymer concrete: Norsodyne H 81269 TF with 6% cobalt & DDM-9
Alumina Trihydrate: 10% of resin by weight
Sand: 150% of resin by weight, split evenly between #0/30 and #2/16
1-1/2 parts sand to 1 part resin
No pigment
Approximately 60 mil thickness (aggregate dependent)
3/16" single skin laminate: Norsodyne H 81269 TF with 6% cobalt & DDM-9
4 layers of 1.5 ounce chopped strand mat
Glass to resin ratio range: 25:75 to 35:65 by weight

System 1 – Addition of 1/2" plywood core & 3/16" rear skin (Note that core separation was observed in several samples)

System 2 – Addition of 3/4" balsa core & 3/16" rear skin

System 3 – Addition of 1/2" polyurethane foam core & 3/16" rear skin

System 4 – Bronze filler instead of sand: 1 part bronze powder to 1 part resin by weight

System 5 – Aluminum filler instead of sand: 1 part aluminum powder to 2 parts resin by weight

System 6 – Straight Norsodyne H 81269 TF as gelcoat in place of resin based polymer concrete

System 7 – Addition of white pigment to polymer concrete

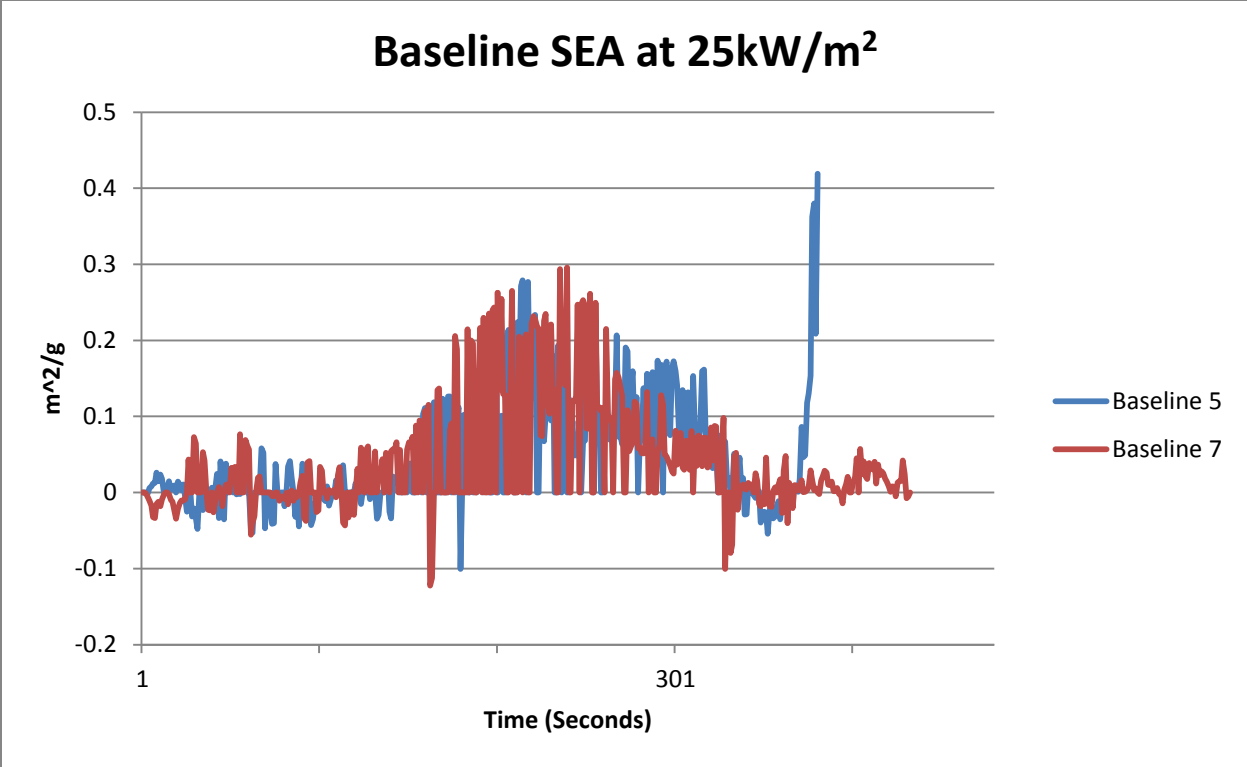**System 8** – Addition of grey pigment to polymer concrete

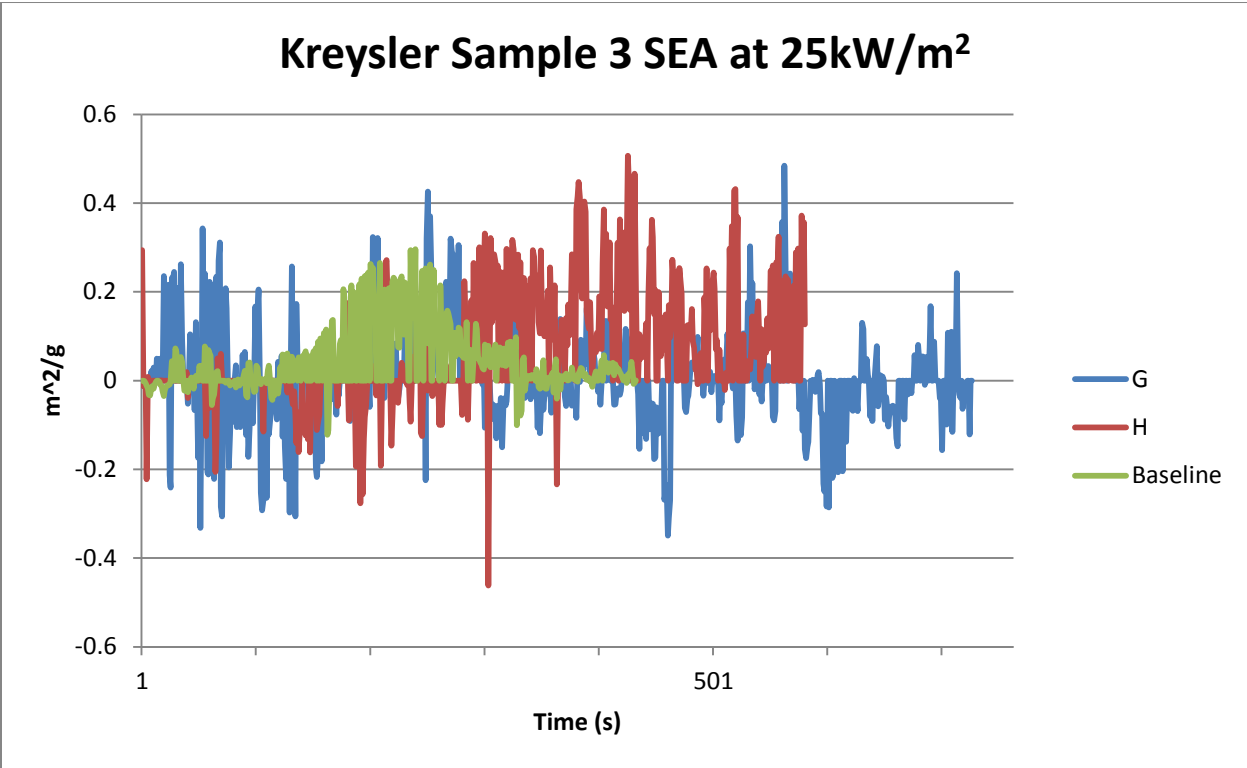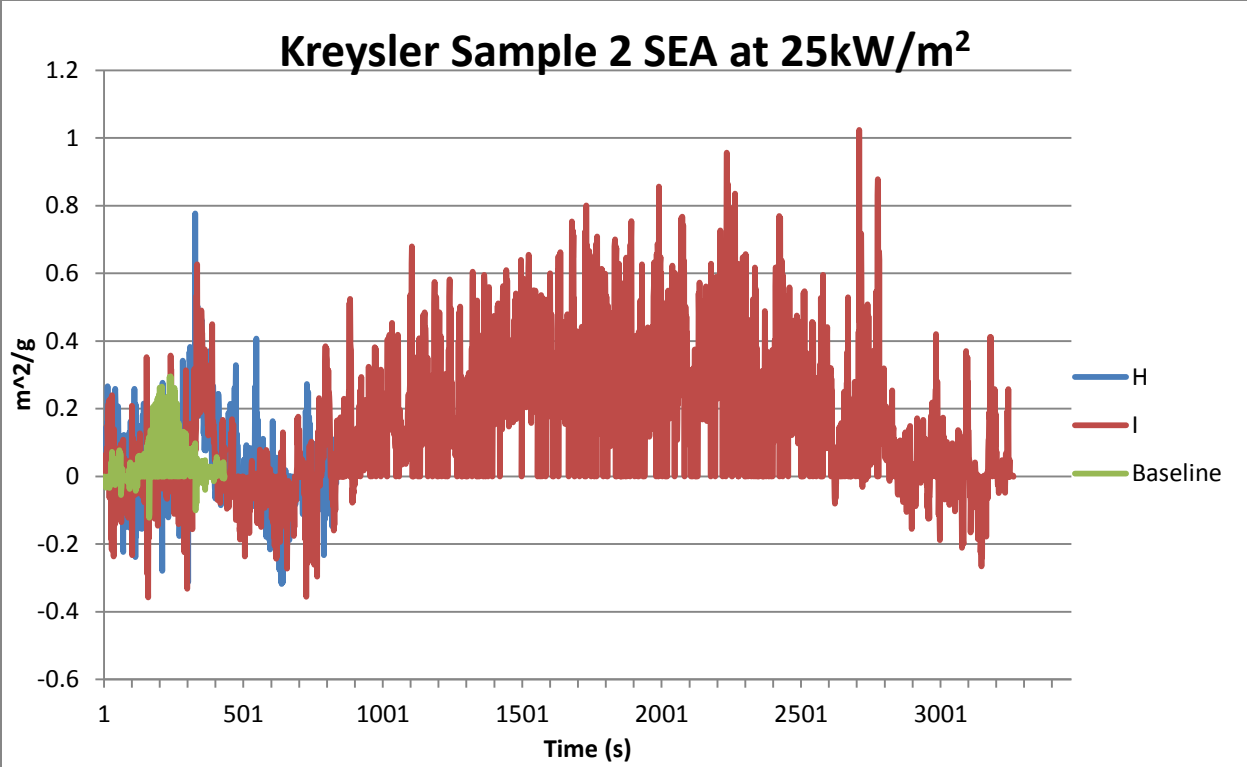**System 9** – Addition of beige pigment to polymer concrete

**System 10** – #0/30 aggregate only

System 11 – #0/60 aggregate only

System 12 – #2/16 aggregate only

System 13 – DCPD Laminate resin (with 6 layers of glass) instead of Norsodyne

Baseline HRR 50kW/m²

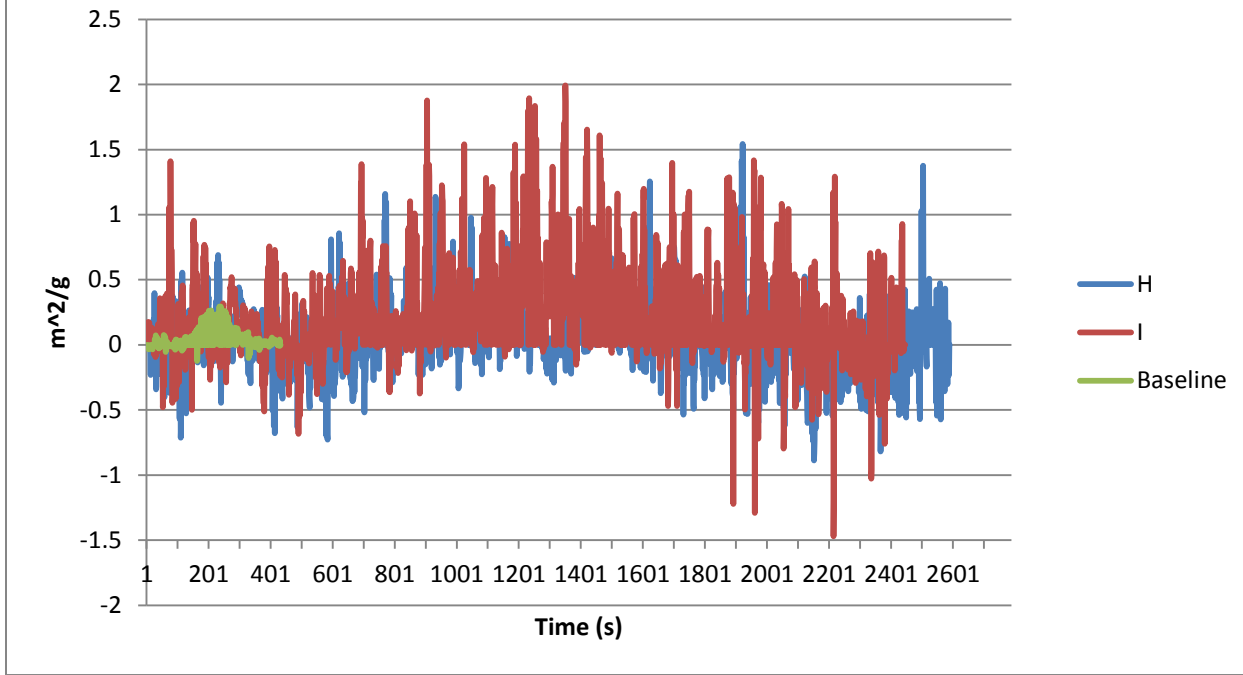**Kreysler Sample 1 HRR 50kW/m²**

Kreysler Sample 2 HRR 50kW/m²

Legend: A, B, C, D, Baseline
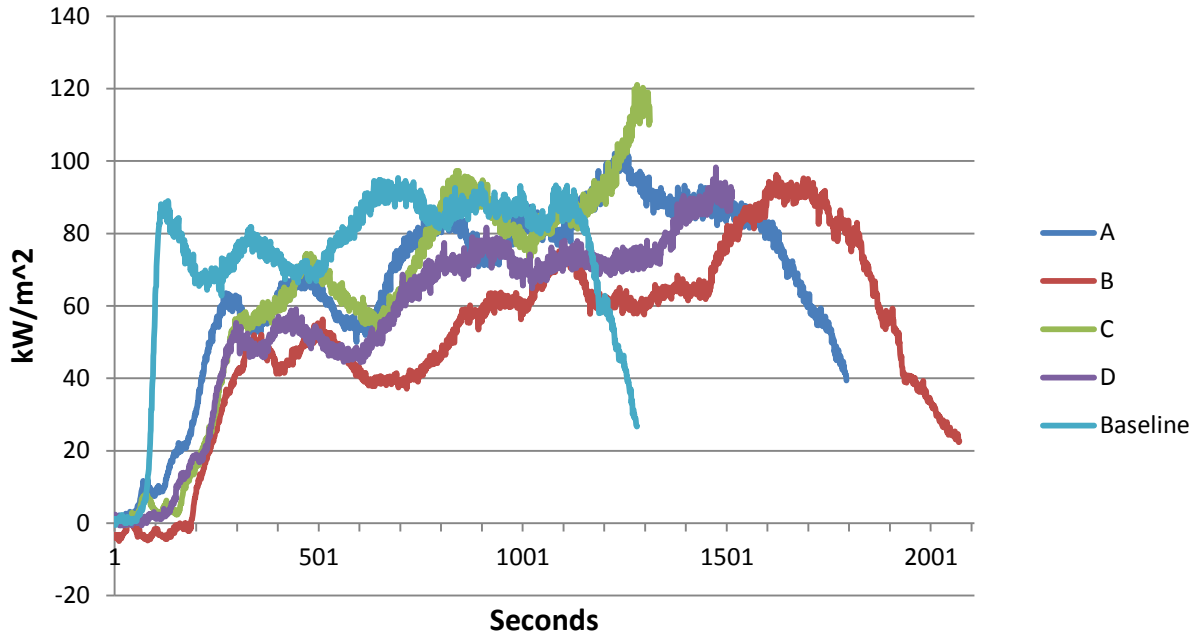
Kreysler Sample 3 HRR 50kW/m²

Legend: A, B, C, D, Baseline
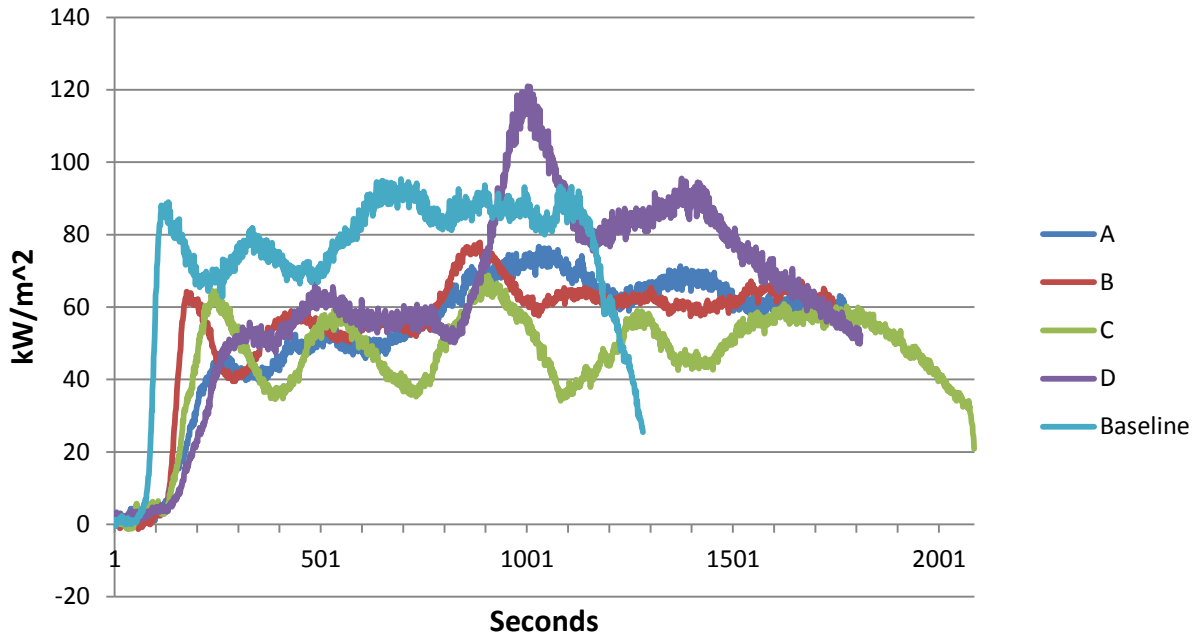
Kreysler Sample 4 HRR 50kW/m²
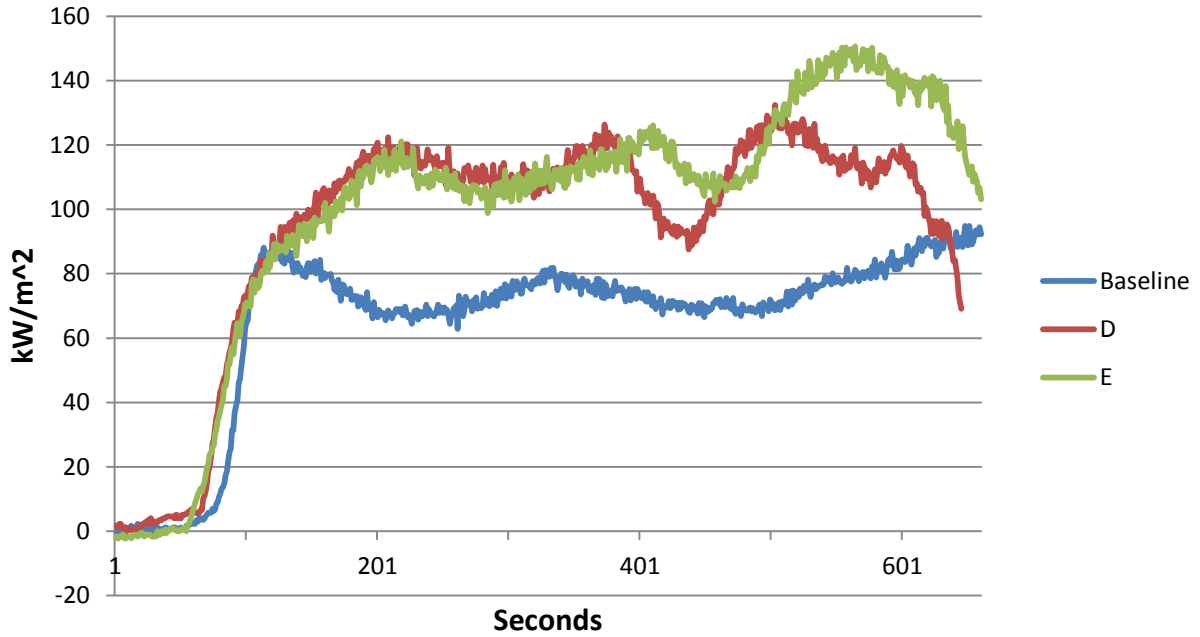
Kreysler Sample 5 HRR/m²
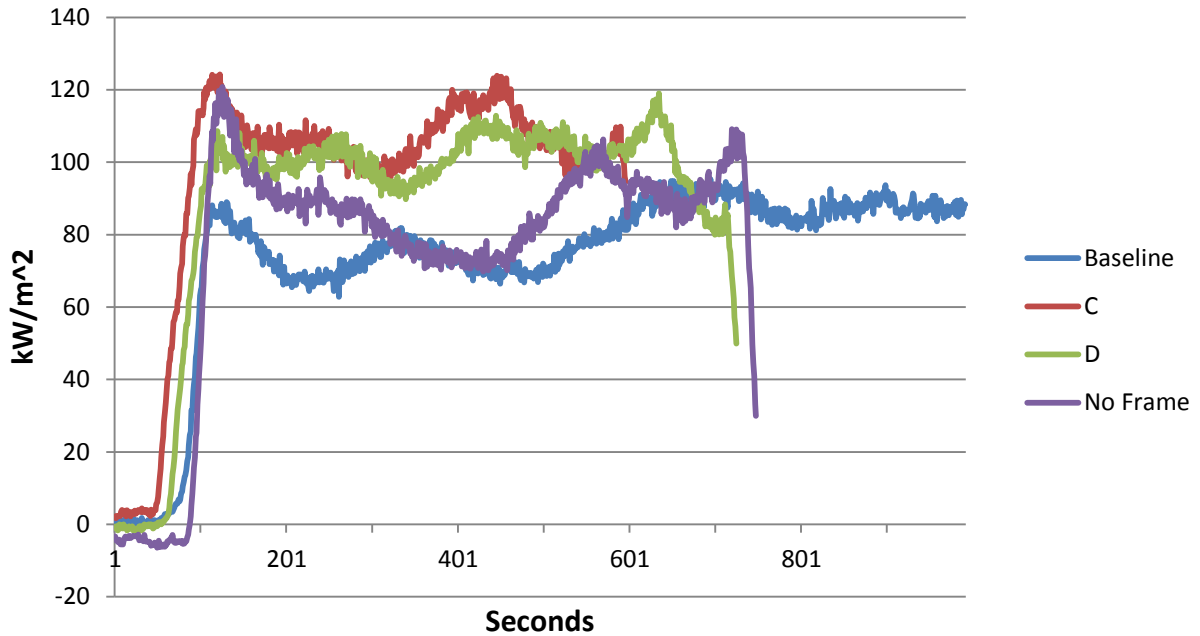
Kreysler Sample 6 HRR 50kW/m²
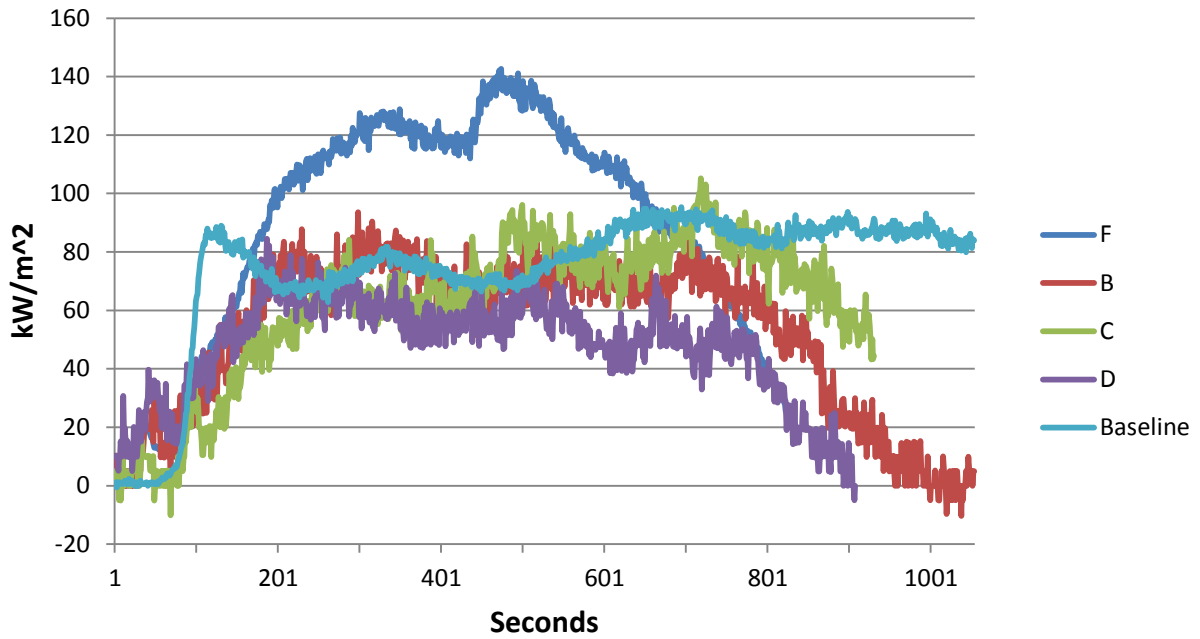
Kreysler Sample 7 HRR/m²

Kreysler Sample 8 HRR 50kW/m²

Kreysler Sample 9 HRR 50kW/m²
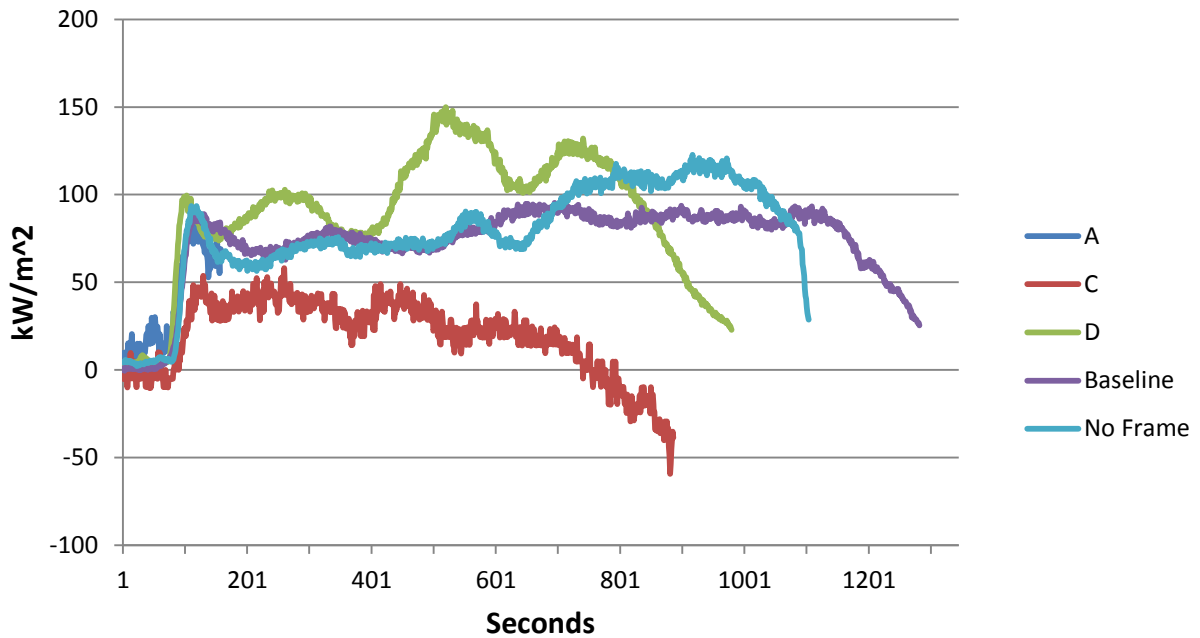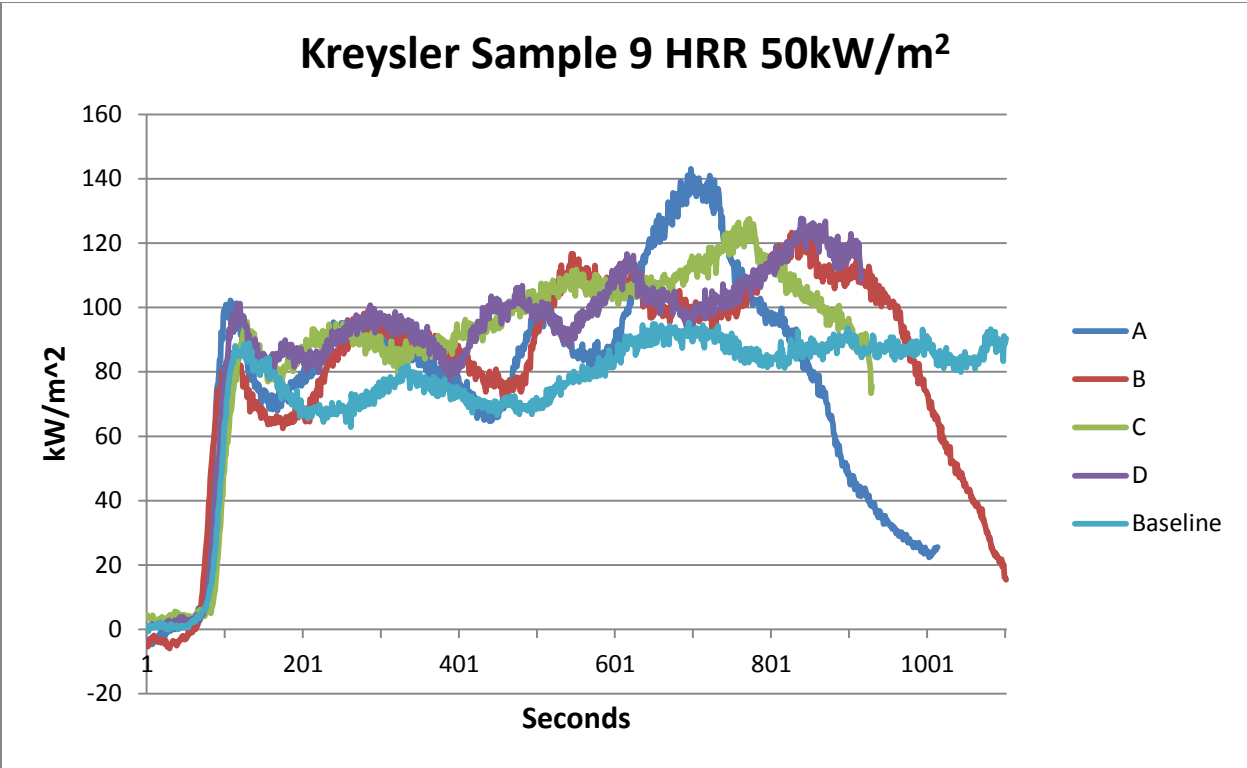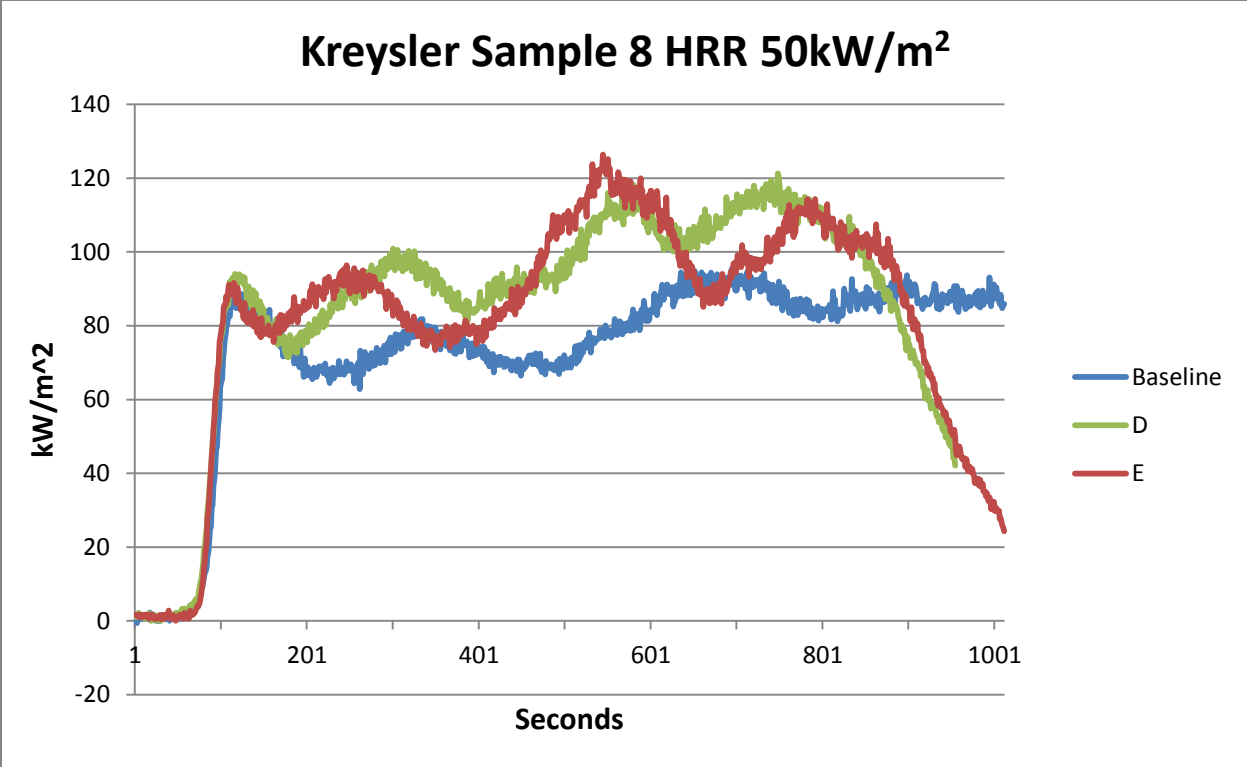
Kreysler Sample 10 HRR/m²
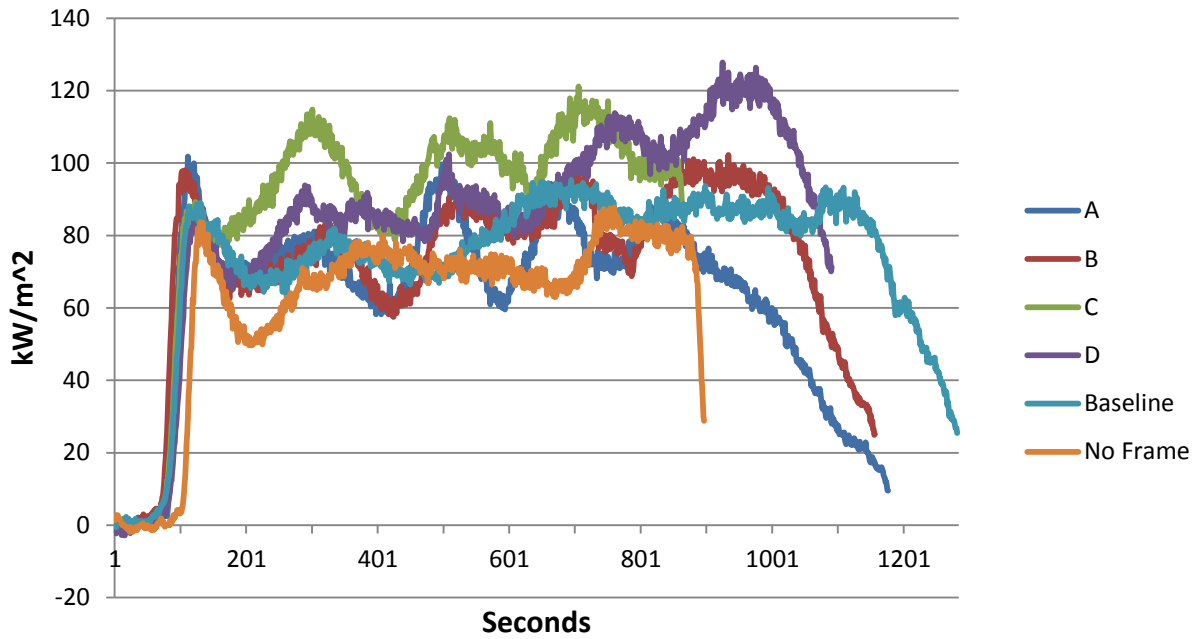
Kreysler Sample 11 HRR 50kW/m²
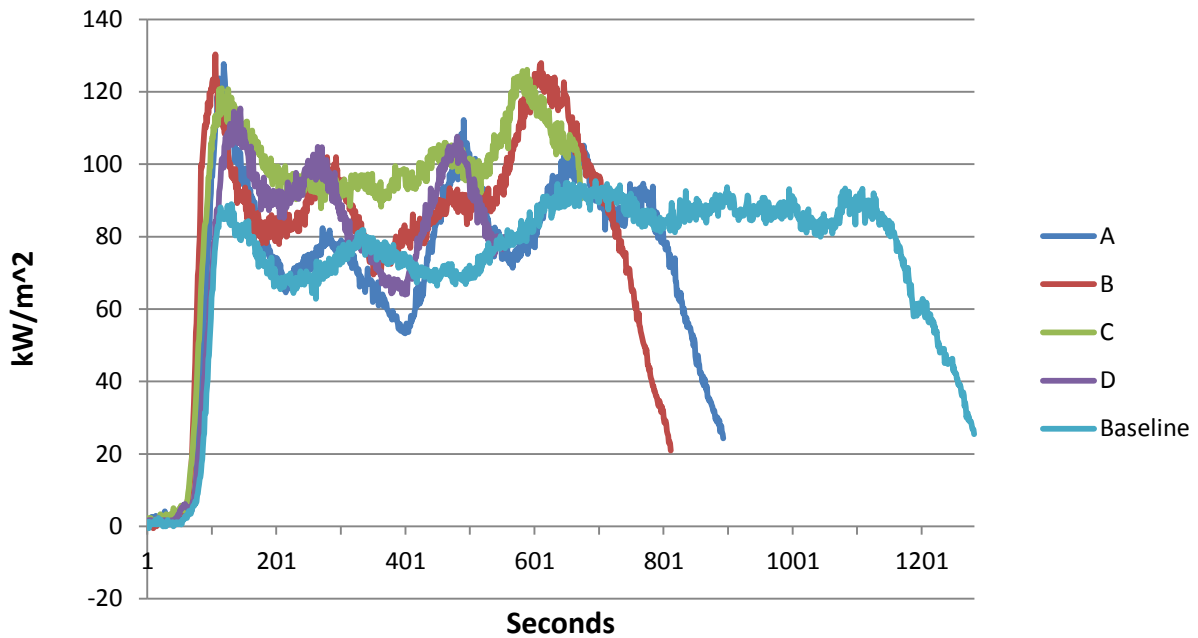
Kreysler Sample 12 HRR 50kW/m²
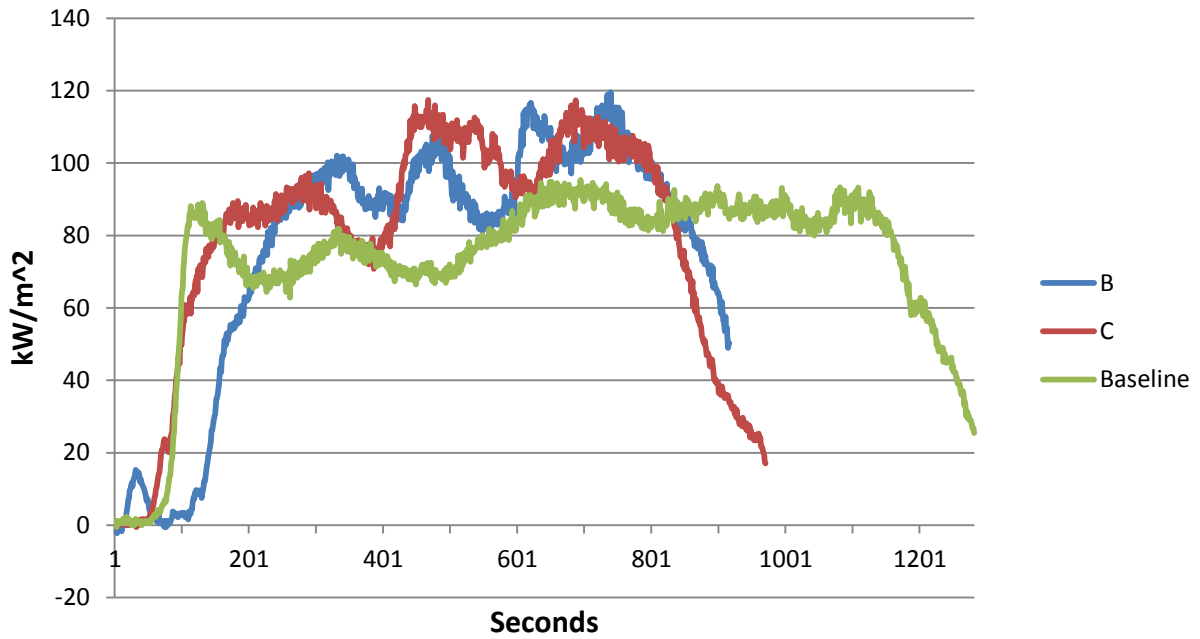
Kreysler Sample 13 HRR/m²

Pigment HRR Comparisons 50kW/m²

Legend:
- (White) 7D
- (Grey) 8D
- (Beige) 9B
- Baseline

Aggregate HRR Comparison 50kW/m²

Legend:
- (#0/30) 10B
- (#0/60) 11B
- (#2/16) 12B
- Baseline

Filler HRR Comparison 50kW/m²

Legend: (Bronze) 4D, (Aluminum) 5D, Baseline

Gel HRR Comparison 50kW/m²

Legend: Norsodyne 6B, DCPD 13C, Baseline

Cores HRR Comparison 50kW/m²

Legend:
— Plywood 1B
— Balsa 2A
— Foam 3B
— Baseline

y-axis: kW/m^2
x-axis: Seconds

75 kw/m^2 Heat Release rate analysis

Thirteen FRP systems are analyzed in the context of heat release rate. This briefing highlights all thirteen systems as well as groups the systems in terms of pigments, filler, gel, and aggregate composition for comparison purposes.

Baseline FRP System
No gelcoat
Polymer concrete: Norsodyne H 81269 TF with 6% cobalt & DDM-9
Alumina Trihydrate: 10% of resin by weight
Sand: 150% of resin by weight, split evenly between #0/30 and #2/16
1-1/2 parts sand to 1 part resin
No pigment
Approximately 60 mil thickness (aggregate dependent)
3/16" single skin laminate: Norsodyne H 81269 TF with 6% cobalt & DDM-9
4 layers of 1.5 ounce chopped strand mat
Glass to resin ratio range: 25:75 to 35:65 by weight

System 1 – Addition of 1/2" plywood core & 3/16" rear skin (Note that core separation was observed in several samples)
System 2 – Addition of 3/4" balsa core & 3/16" rear skin

System 3 – Addition of 1/2" polyurethane foam core & 3/16" rear skin

System 4 – Bronze filler instead of sand: 1 part bronze powder to 1 part resin by weight

System 5 – Aluminum filler instead of sand: 1 part aluminum powder to 2 parts resin by weight

System 6 – Straight Norsodyne H 81269 TF as gelcoat in place of resin based polymer concrete

System 7 – Addition of white pigment to polymer concrete

System 8 – Addition of grey pigment to polymer concrete

System 9 – Addition of beige pigment to polymer concrete

System 10 – #0/30 aggregate only

System 11 – #0/60 aggregate only

System 12 – #2/16 aggregate only

System 13 – DCPD Laminate resin (with 6 layers of glass) instead of Norsodyne

Baseline HRR 75kW/m²

Kreysler Sample 1 HRR 75kW/m²

Kreysler Sample 2 HRR 75kW/m²

kW/m^2 vs *Seconds*

E
F
Baseline
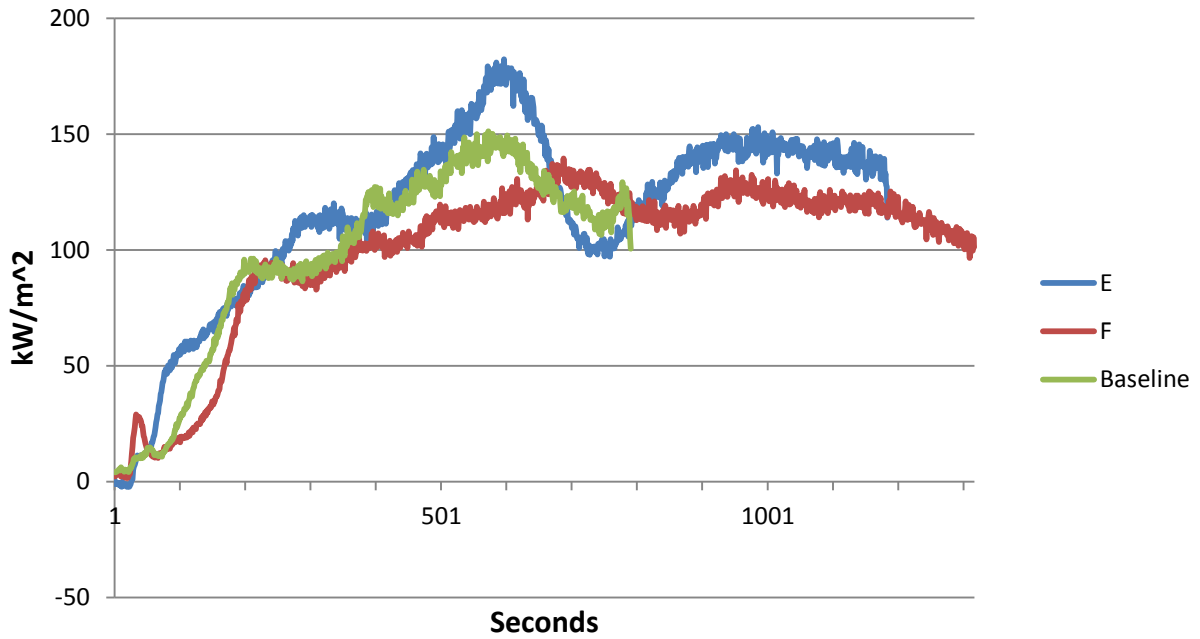
Kreysler Sample 3 HRR 75kW/m²

kW/m^2 vs *Seconds*

E
F
Baseline
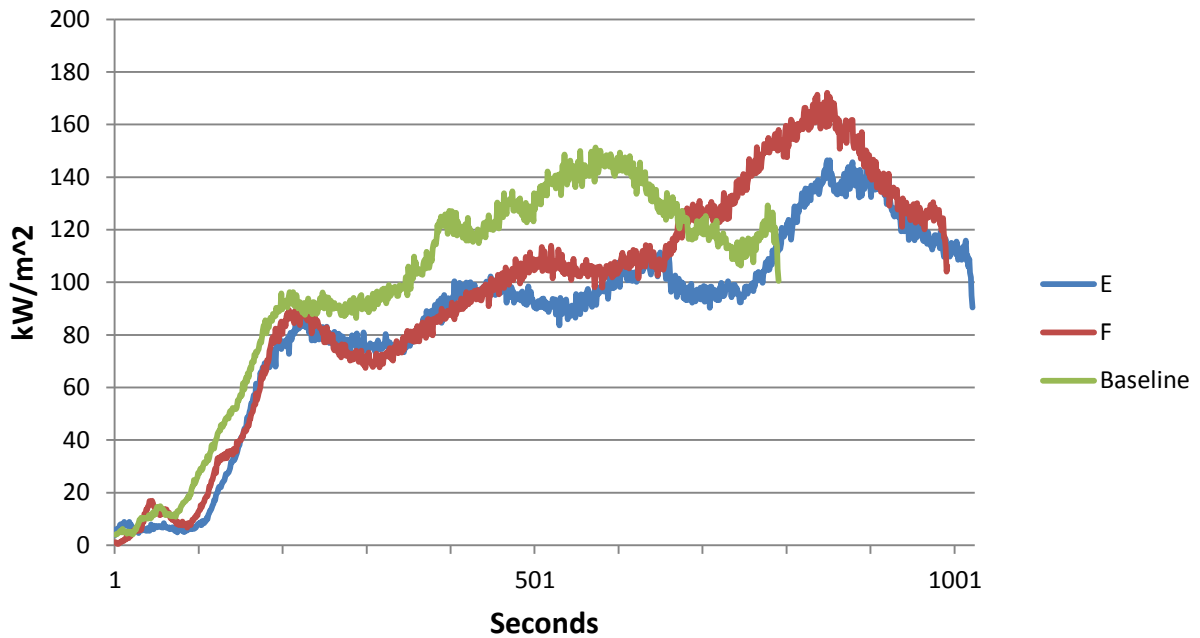
Kreysler Sample 4 HRR 75kW/m²
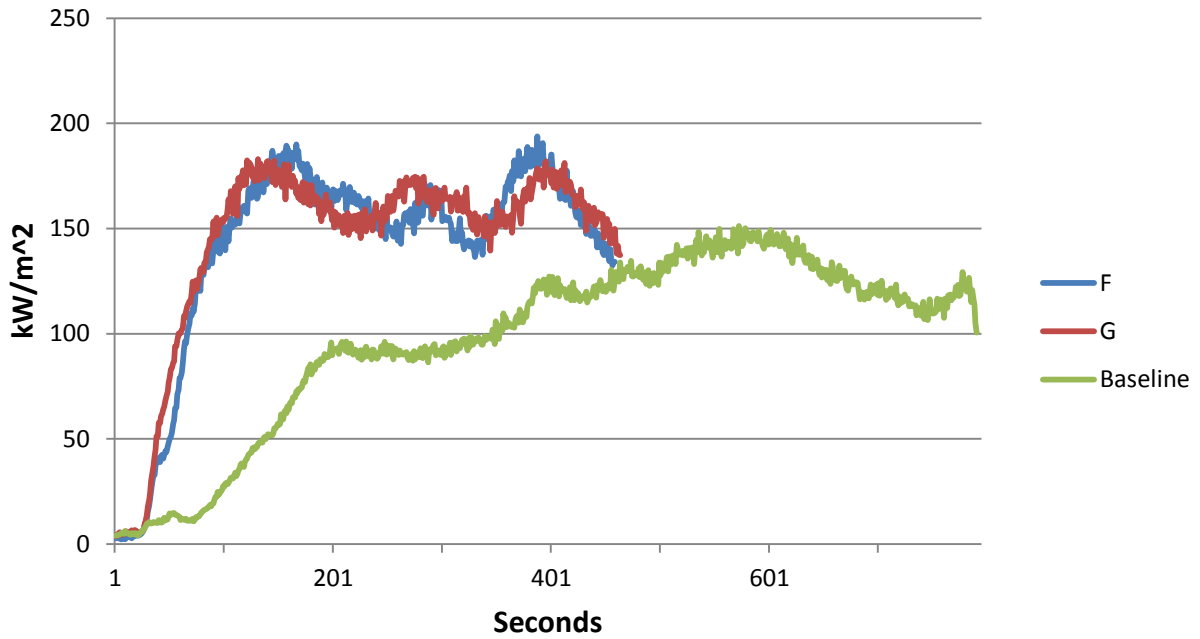
Kreysler Sample 5 HRR 75kW/m²
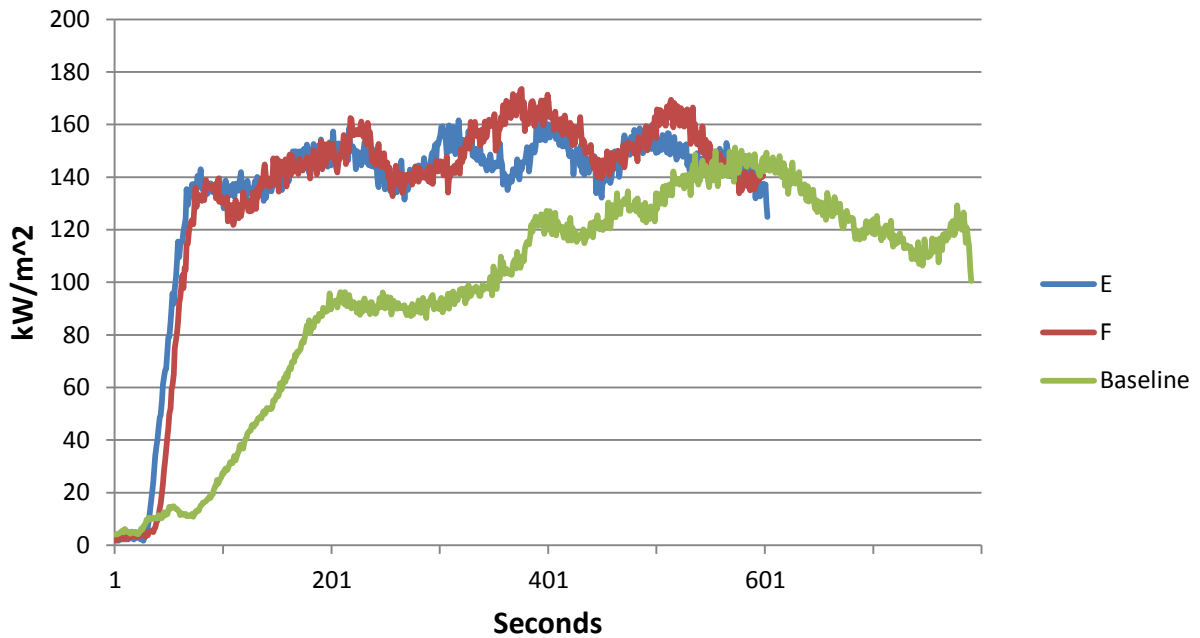
Kreysler Sample 6 HRR 75kW/m²
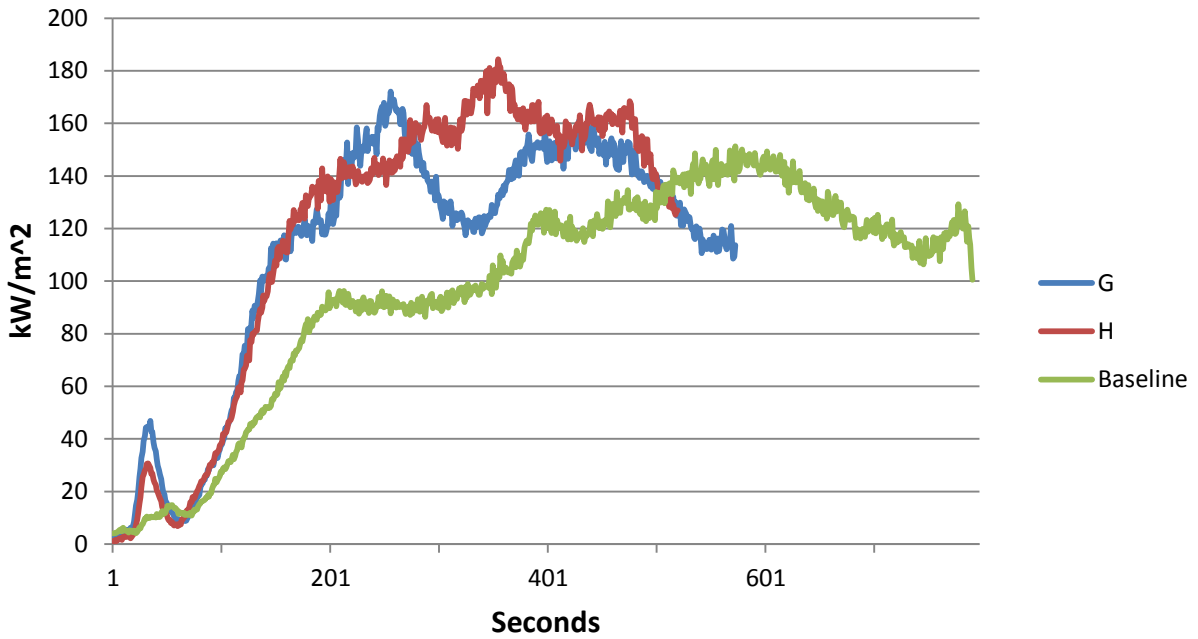
Kreysler Sample 7 HRR 75kW/m²
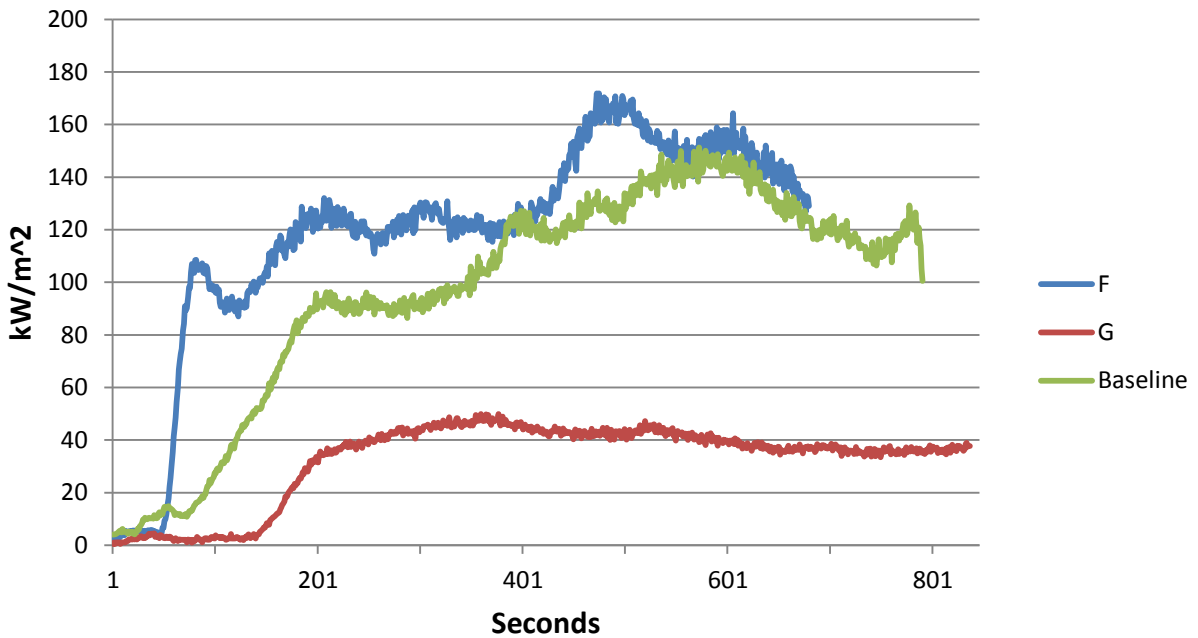
Kreysler Sample 8 HRR 75kW/m²
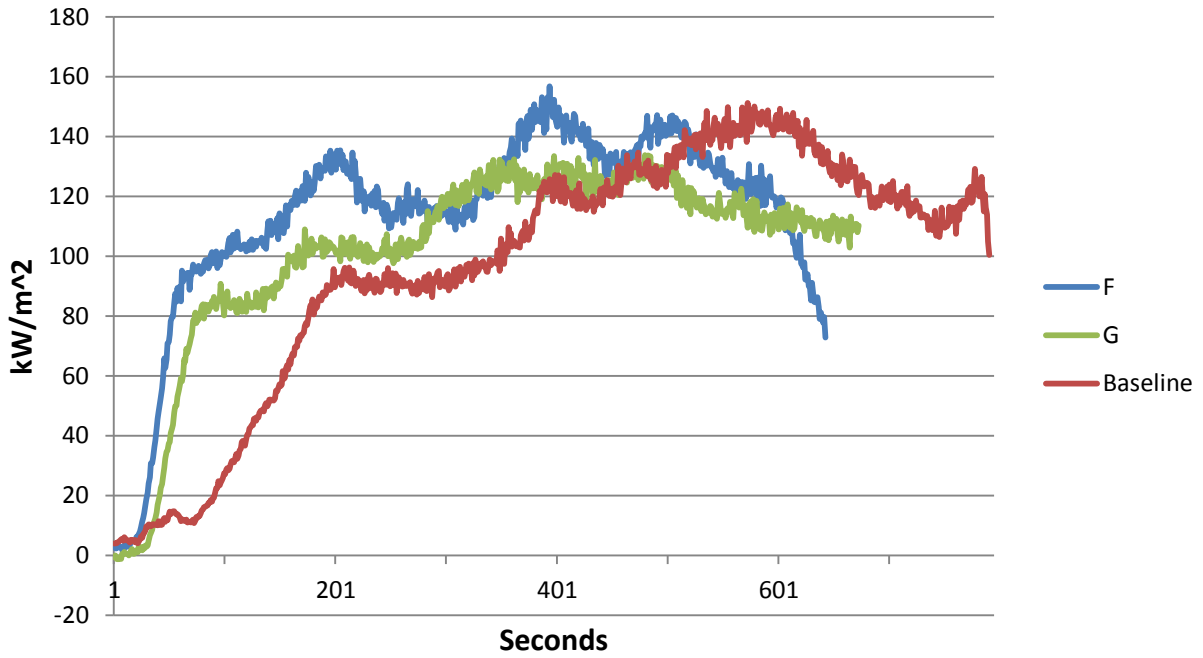
Kreysler Sample 9 HRR 75kW/m²
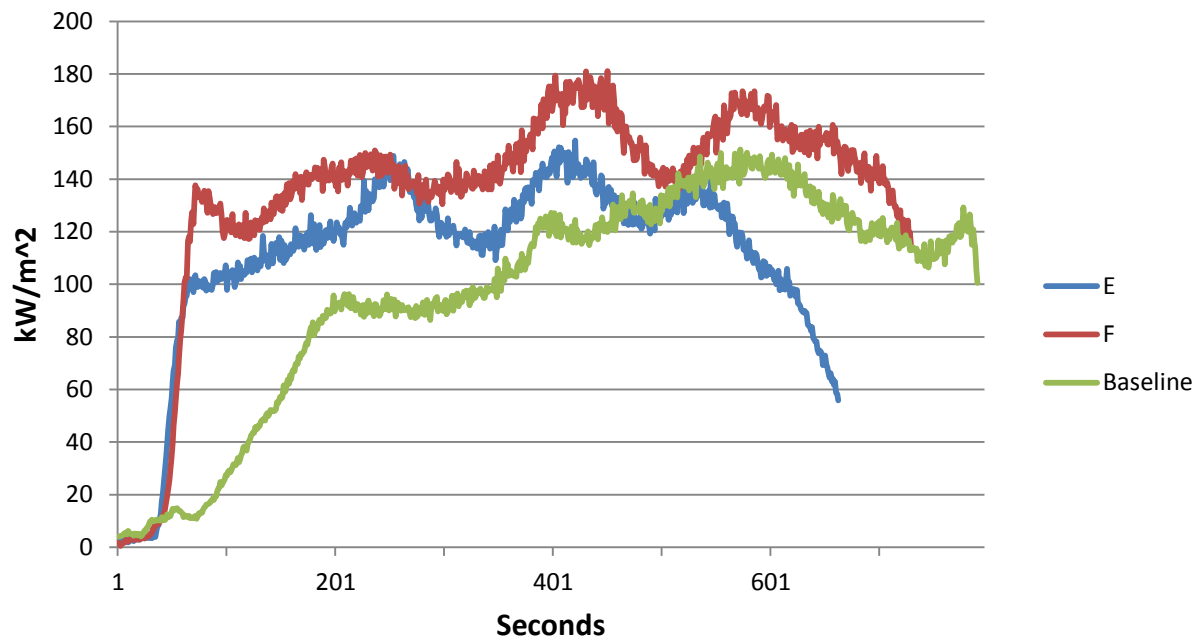
Kreysler Sample 10 HRR 75kW/m²
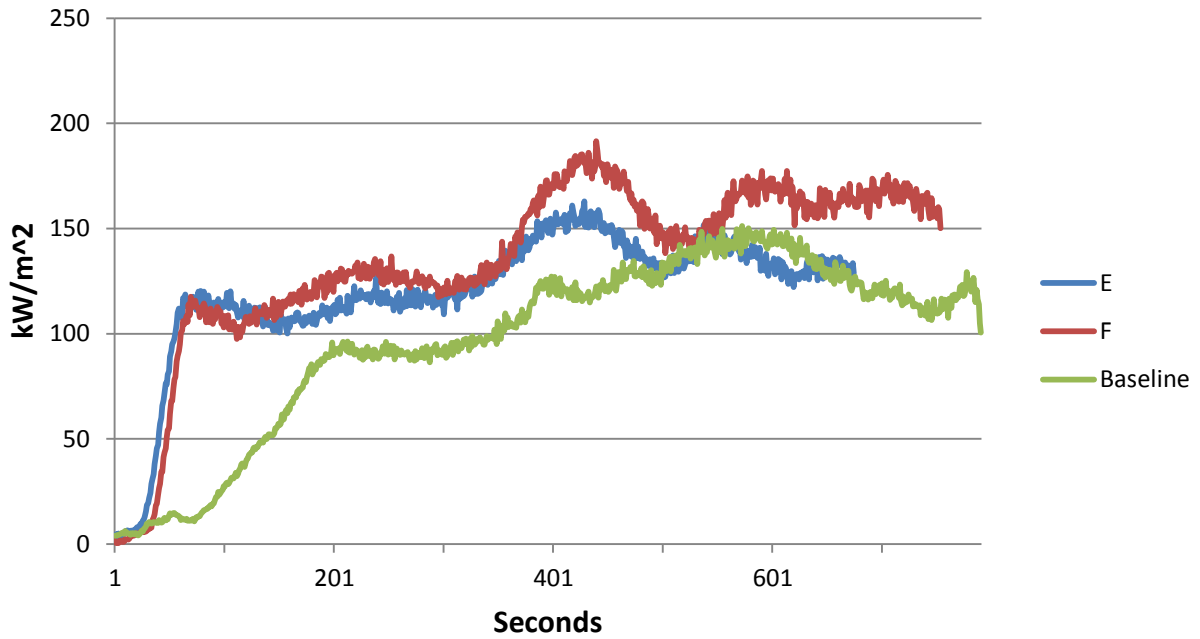
Kreysler Sample 11 HRR 75kW/m²
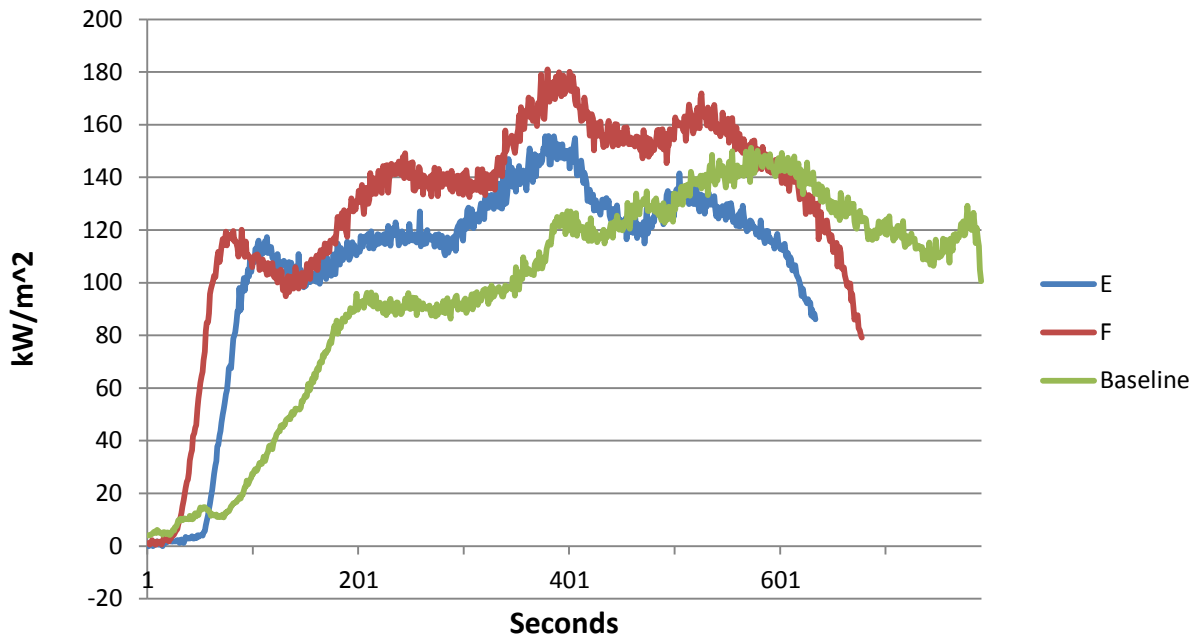
Kreysler Sample 12 HRR 75kW/m²
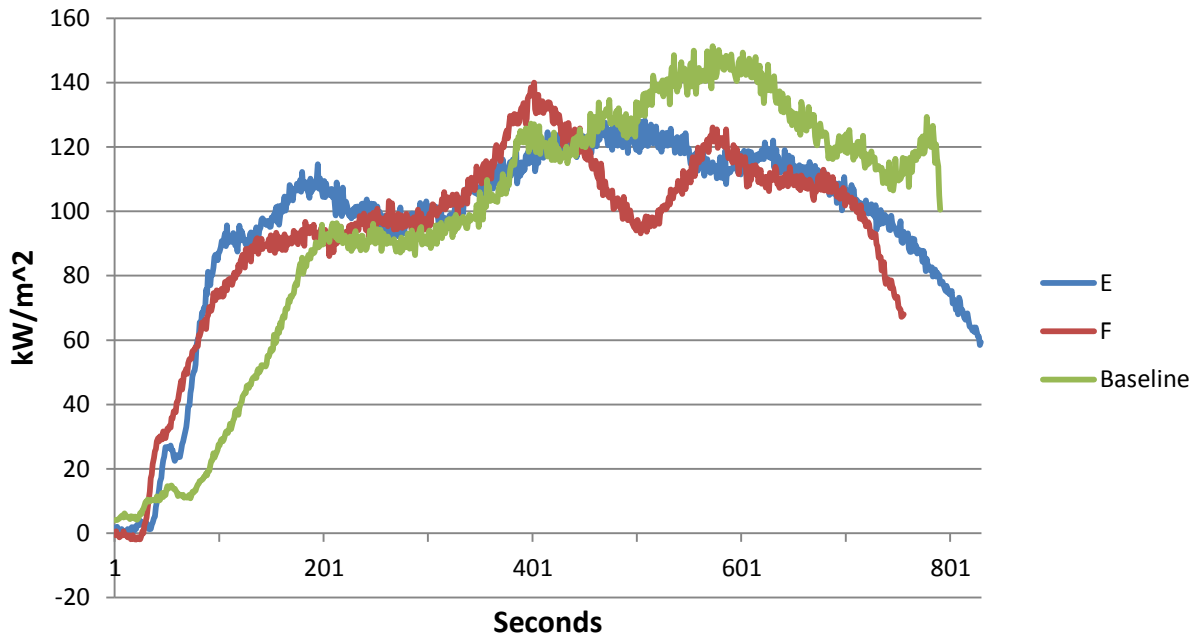
Kreysler Sample 13 HRR 75kW/m²
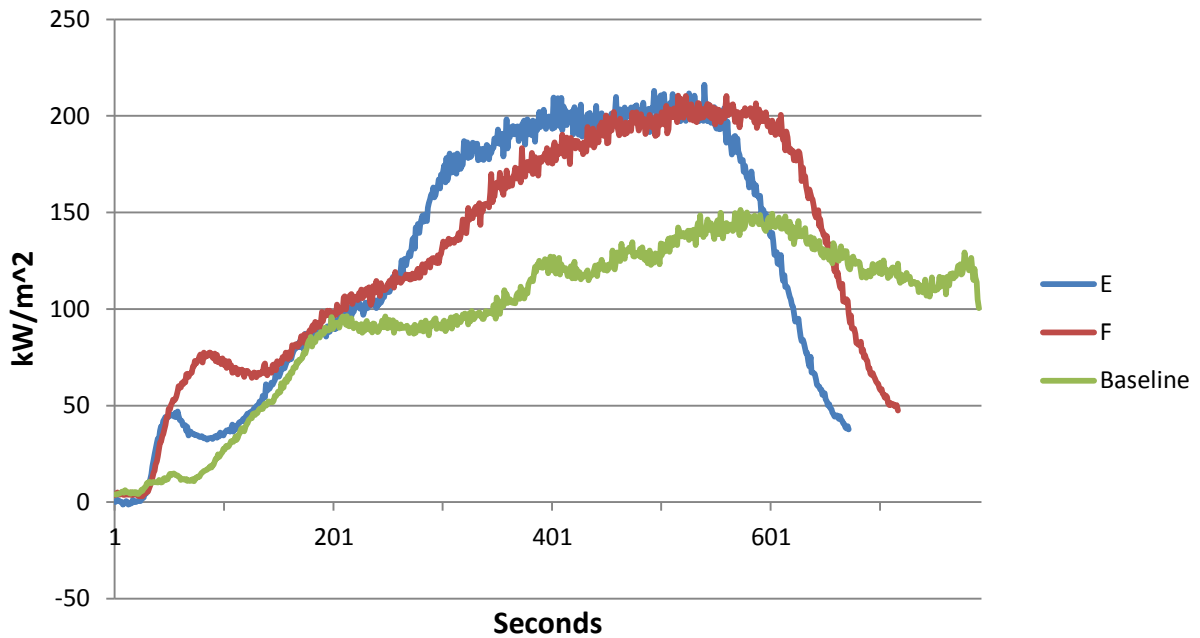
Pigment HRR Comparisons 75kW/m²

Aggregate HRR Comparison 75kW/m²

Filler HRR Comparison 75kW/m²

- (Bronze) 4F
- (Aluminum) 5F
- Baseline

Gel HRR Comparison 75kW/m²

- Norsodyne 6G
- DCPD 13F
- Baseline

Cores HRR Comparison 75kW/m²

Legend: Plywood 1F, Balsa 2F, Foam 3F, Baseline
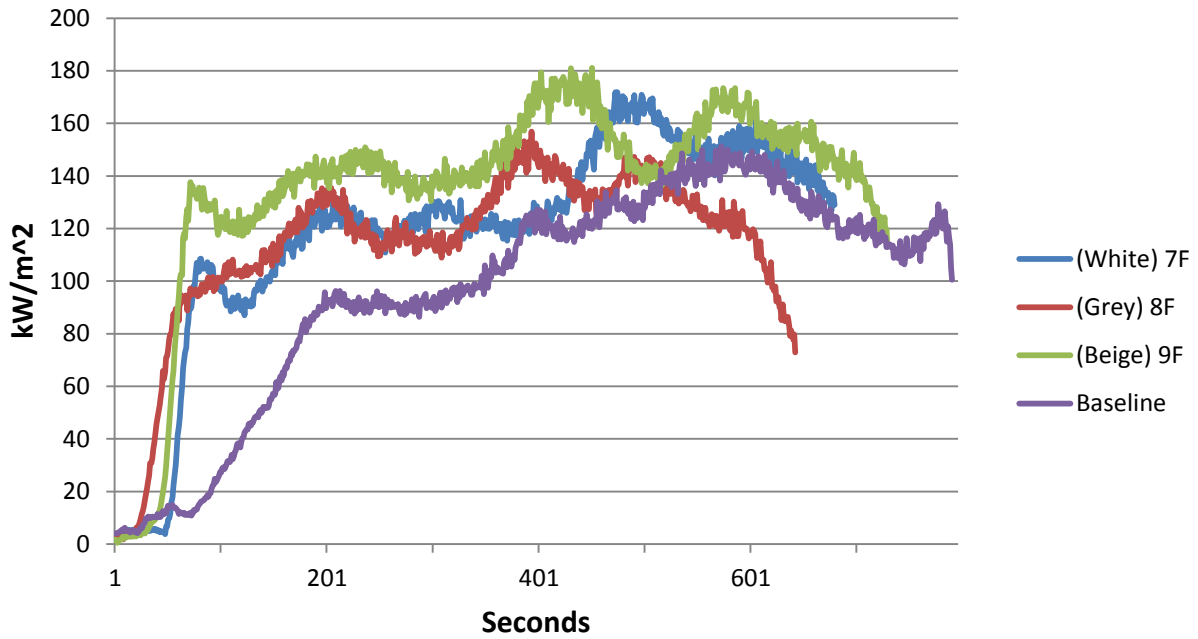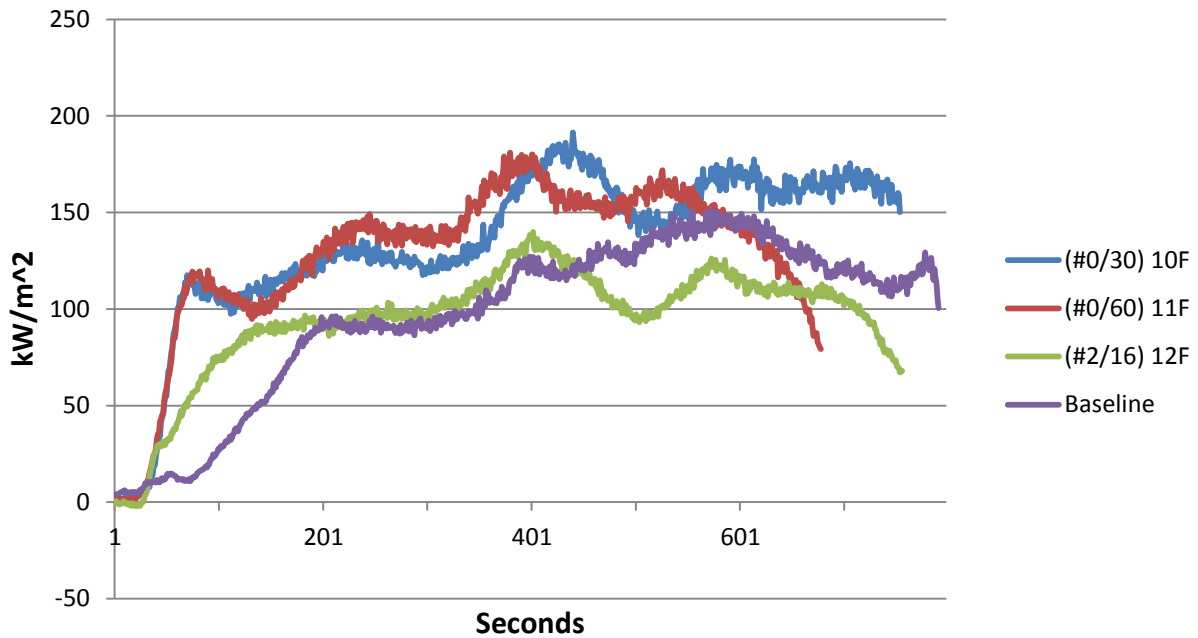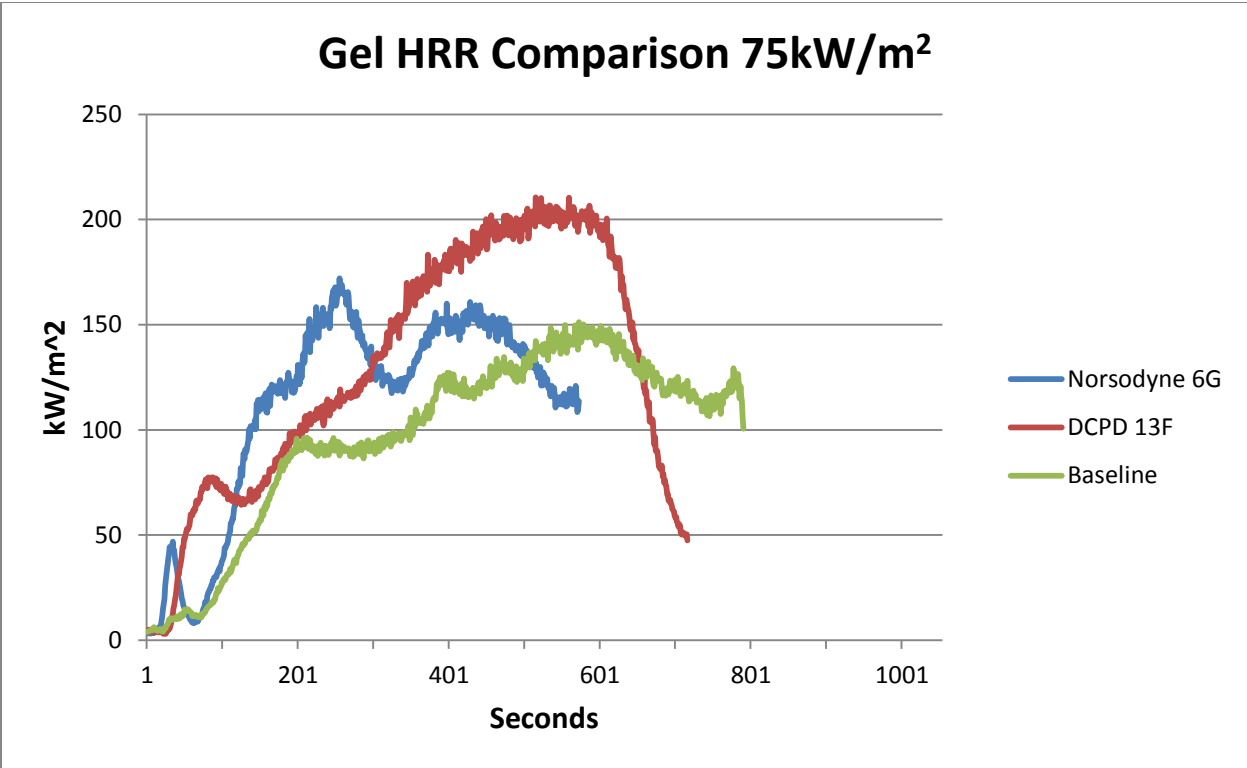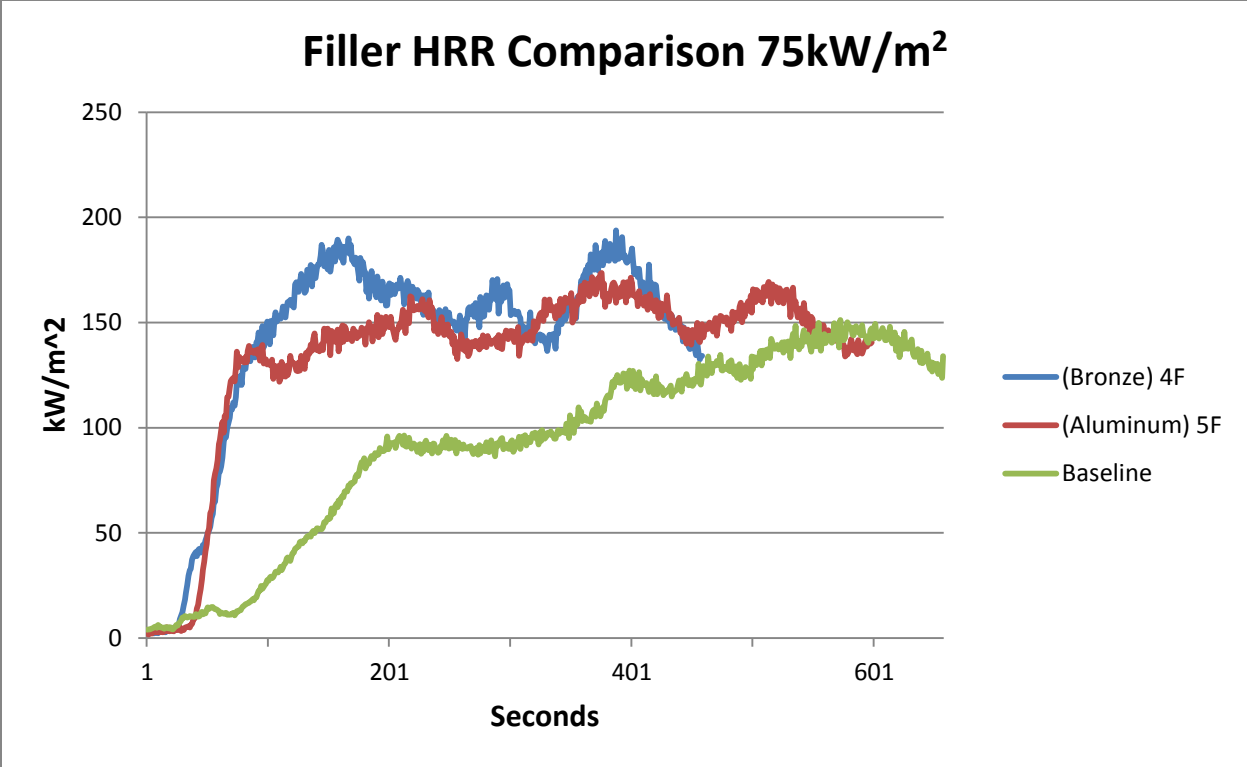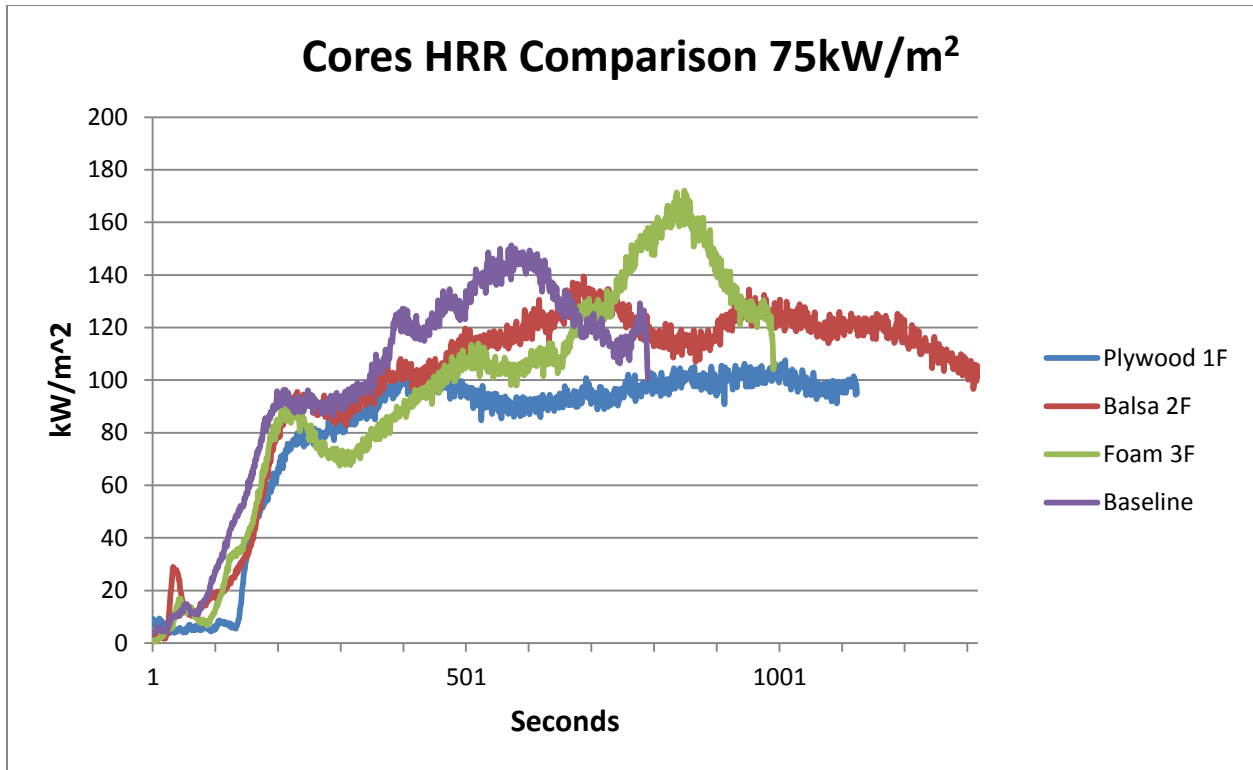
Heat Release rate analysis At variable heat flux

Thirteen FRP systems are analyzed in the context of heat release rate. This briefing highlights all thirteen systems as well as groups the systems in terms of pigments, filler, gel, and aggregate composition for comparison purposes.

Baseline FRP System
No gelcoat
Polymer concrete: Norsodyne H 81269 TF with 6% cobalt & DDM-9
Alumina Trihydrate: 10% of resin by weight
Sand: 150% of resin by weight, split evenly between #0/30 and #2/16
1-1/2 parts sand to 1 part resin
No pigment
Approximately 60 mil thickness (aggregate dependent)
3/16" single skin laminate: Norsodyne H 81269 TF with 6% cobalt & DDM-9
4 layers of 1.5 ounce chopped strand mat
Glass to resin ratio range: 25:75 to 35:65 by weight

System 1 – Addition of 1/2" plywood core & 3/16" rear skin (Note that core separation was observed in several samples)
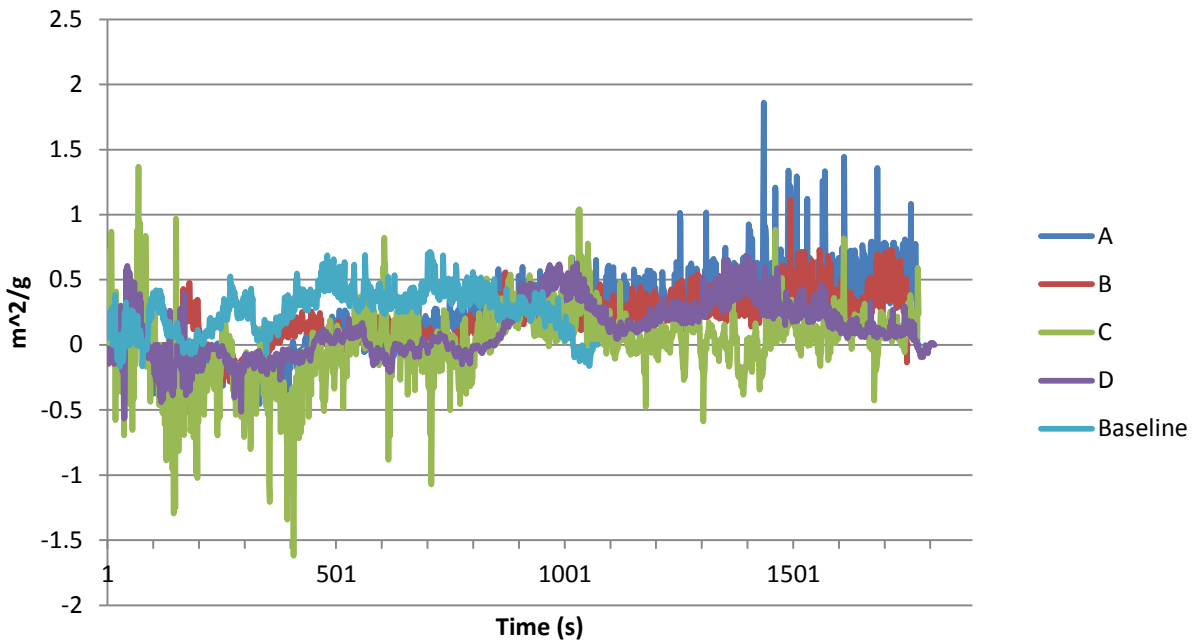**System 2** – Addition of 3/4" balsa core & 3/16" rear skin

System 3 – Addition of 1/2" polyurethane foam core & 3/16" rear skin

System 4 – Bronze filler instead of sand: 1 part bronze powder to 1 part resin by weight

System 5 – Aluminum filler instead of sand: 1 part aluminum powder to 2 parts resin by weight

System 6 – Straight Norsodyne H 81269 TF as gelcoat in place of resin based polymer concrete

System 7 – Addition of white pigment to polymer concrete

System 8 – Addition of grey pigment to polymer concrete

System 9 – Addition of beige pigment to polymer concrete

System 10 – #0/30 aggregate only

System 11 – #0/60 aggregate only

System 12 – #2/16 aggregate only

System 13 – DCPD Laminate resin (with 6 layers of glass) instead of Norsodyne

Kreysler Sample 2 HRR
Variable Heat Flux

Kreysler Sample 2 HRR
Variable Heat Flux

Kreysler Sample 3 HRR Variable Heat Flux

- 25 kW/m^2
- 50 kW/m^2
- 75 kW/m^2
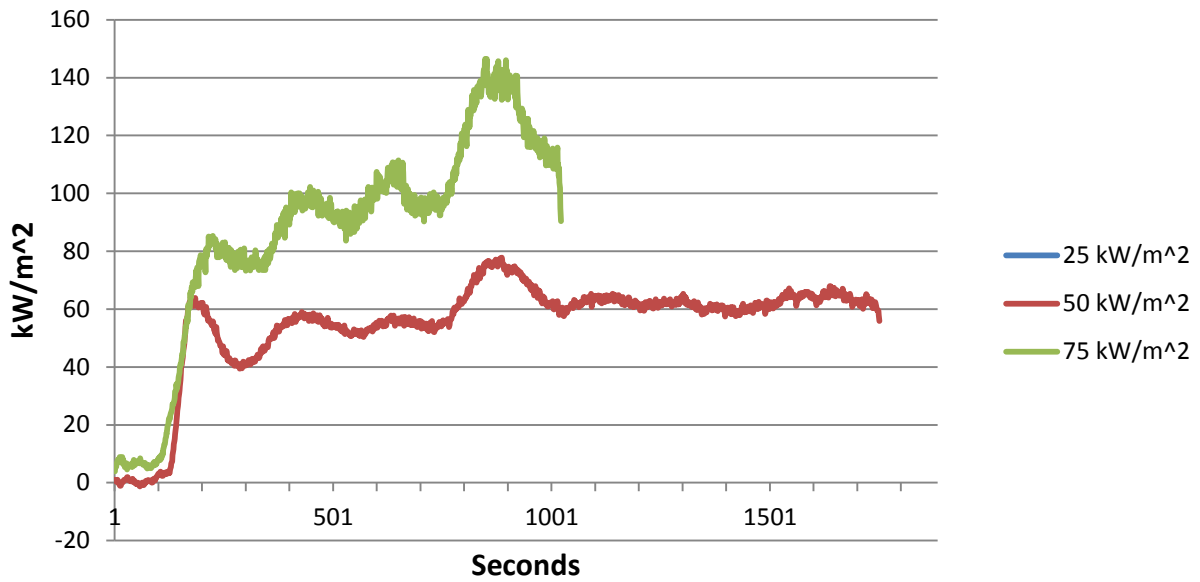
Kreysler Sample 4 HRR Variable Heat Flux

- 25 kW/m^2
- 50 kW/m^2
- 75 kW/m^2
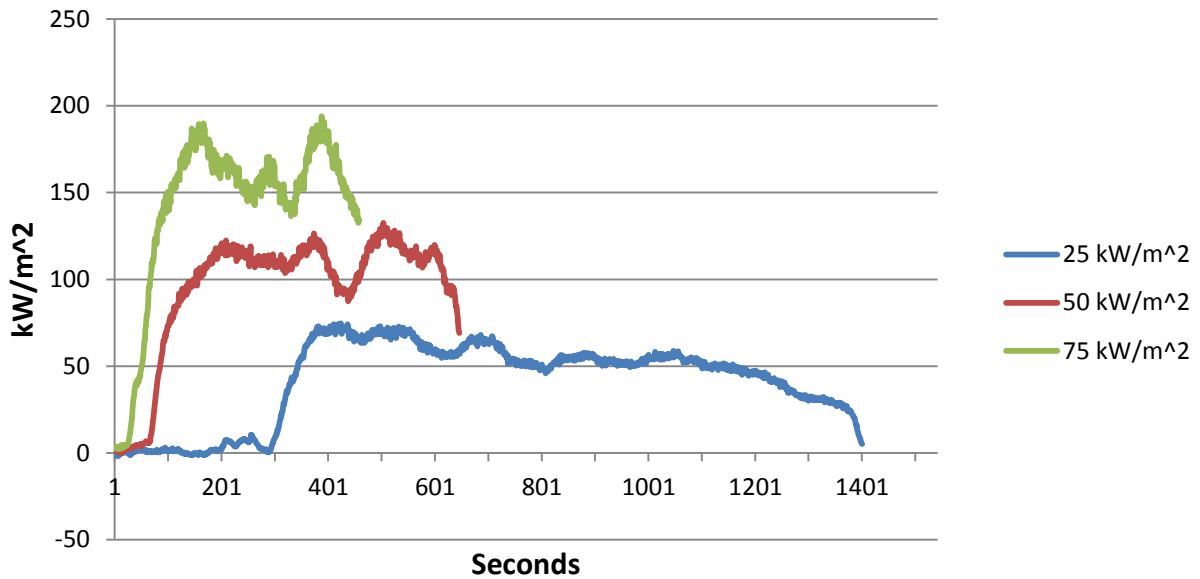
Kreysler Sample 5 HRR
Variable Heat Flux

- 25 kW/m^2
- 50 kW/m^2
- 75 kW/m^2
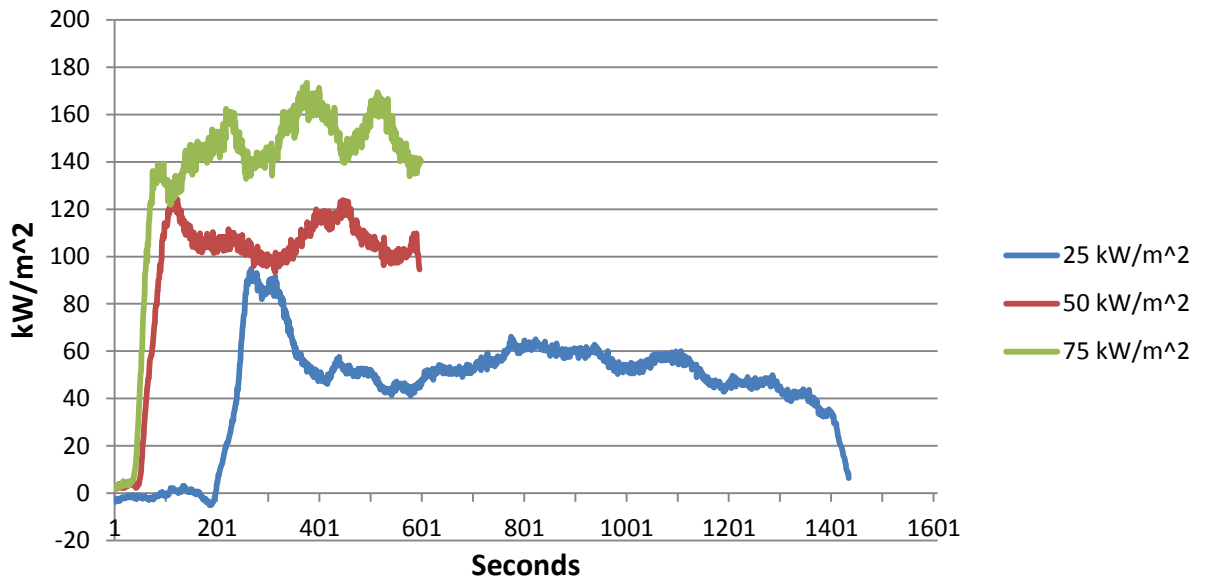
Kreysler Sample 6 HRR
Variable Heat Flux

- 25 kW/m^2
- 50 kW/m^2
- 75 kW/m^2
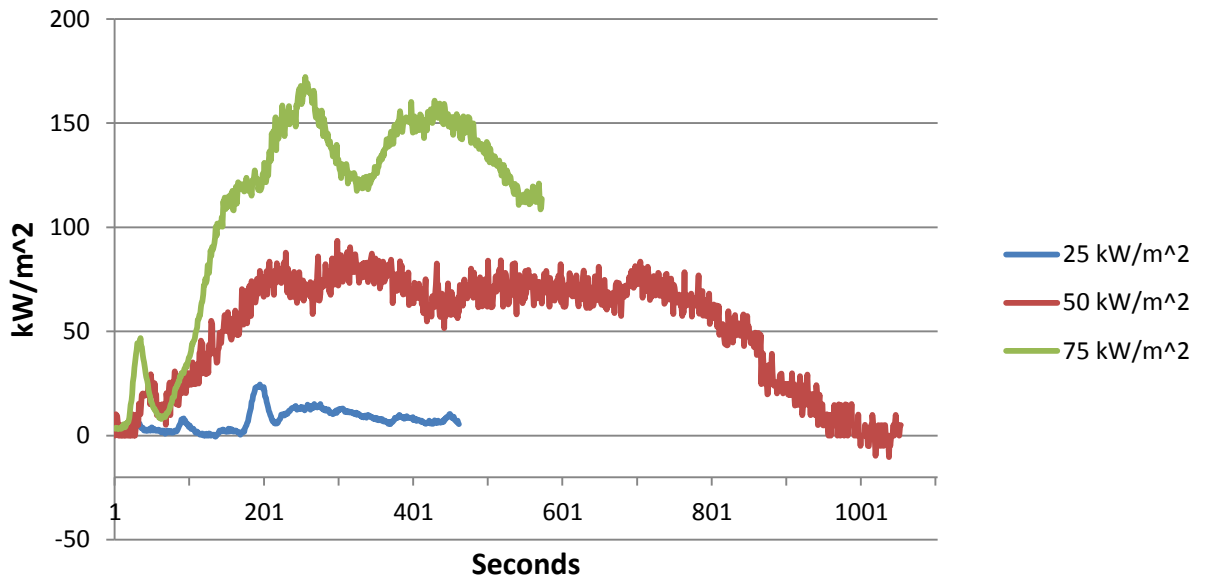
**Kreysler Sample 7 HRR
Variable Heat Flux**

25 kW/m^2
50 kW/m^2
75 kW/m^2
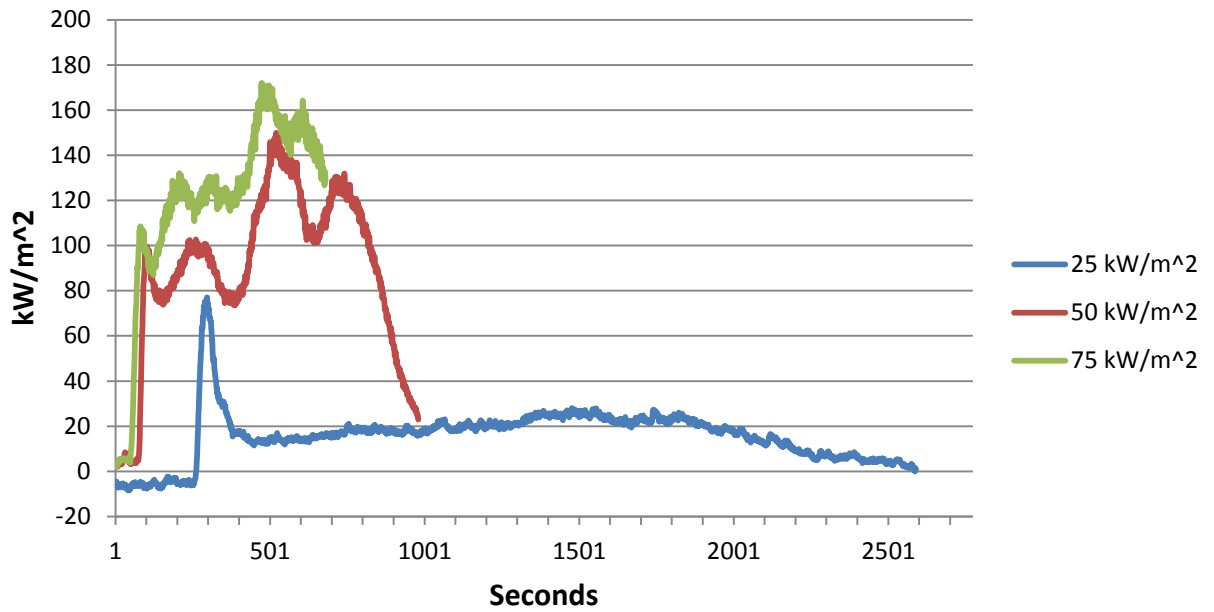
**Kreysler Sample 8 HRR
Variable Heat Flux**

25 kW/m^2
50 kW/m^2
75 kW/m^2
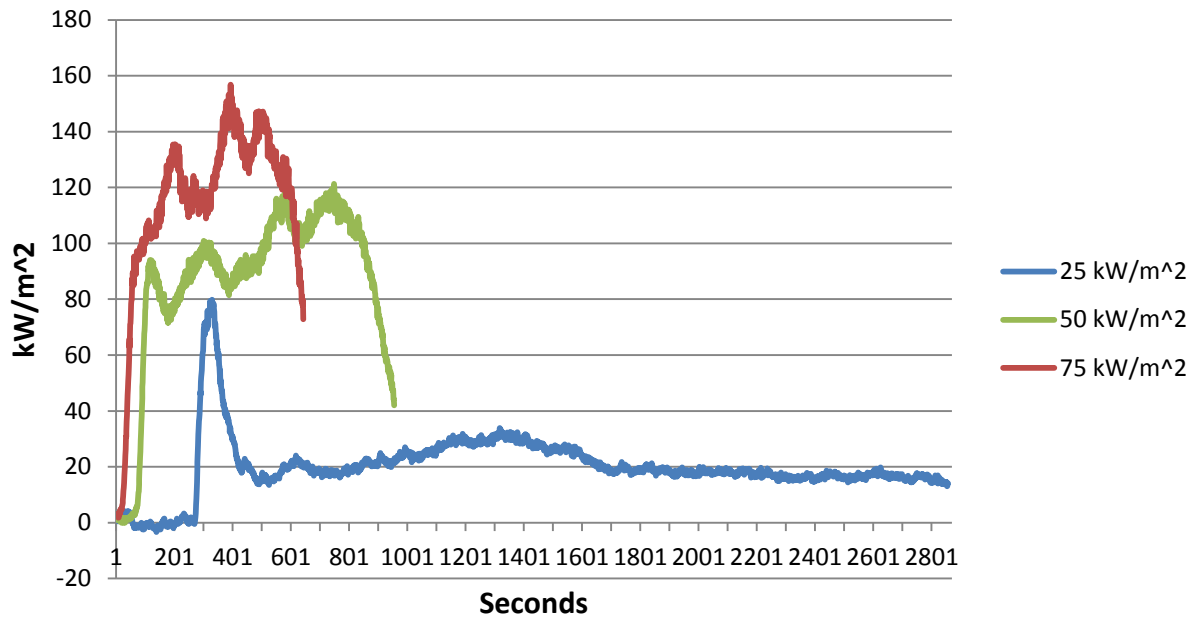
Kreysler Sample 9 HRR
Variable Heat Flux
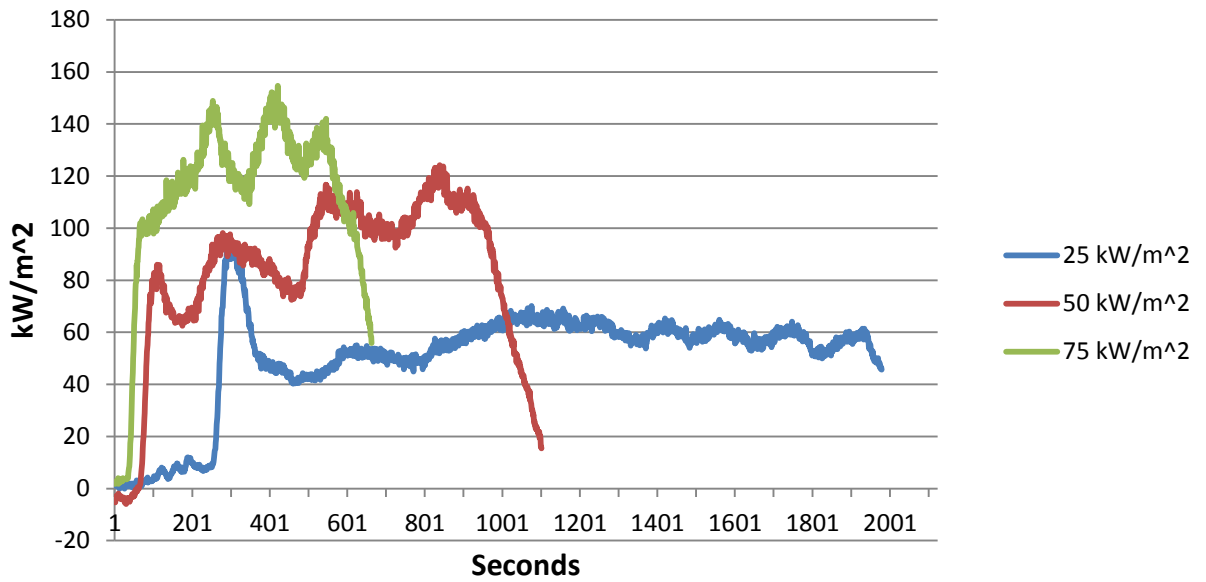
Kreysler Sample 10 HRR
Variable Heat Flux
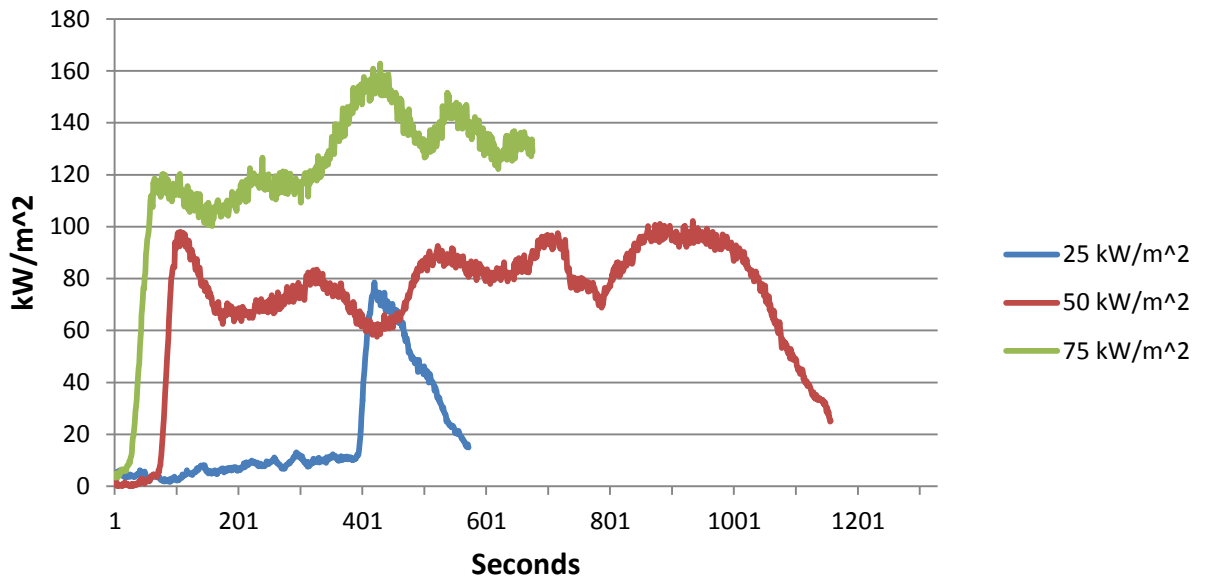
Kreysler Sample 11 HRR
Variable Heat Flux
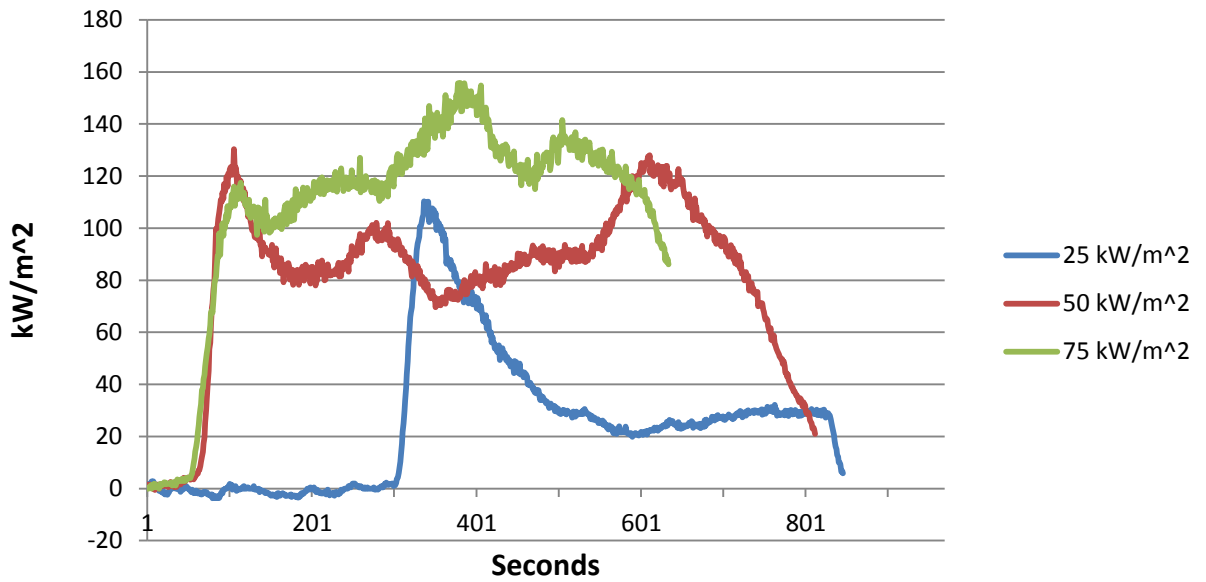
Kreysler Sample 12 HRR
Variable Heat Flux
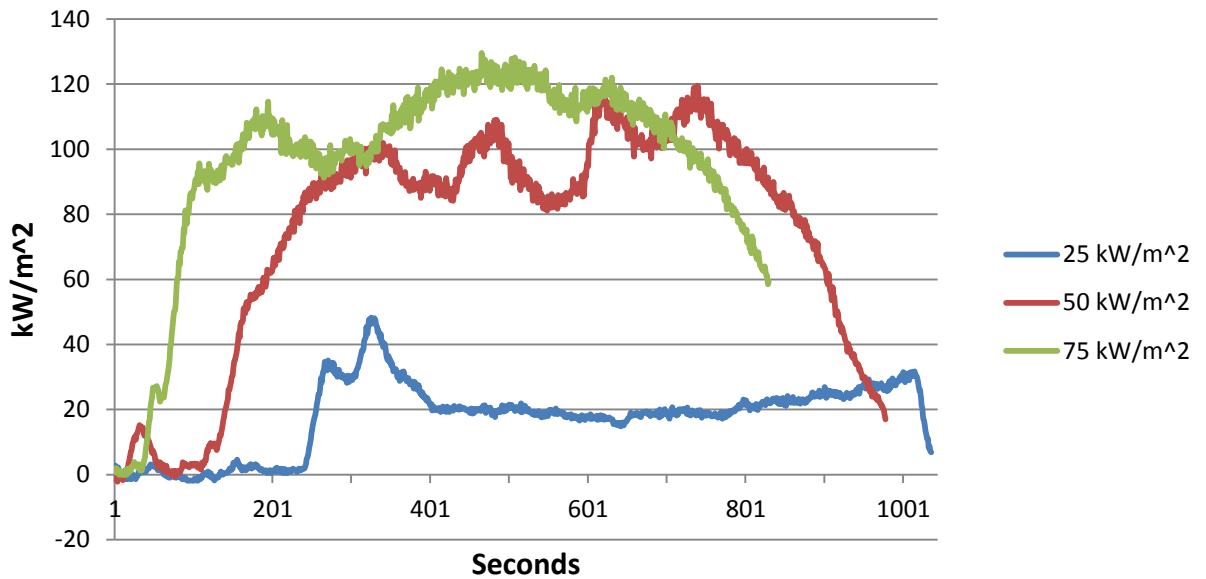
Kreysler Sample 13 HRR
Variable Heat Flux
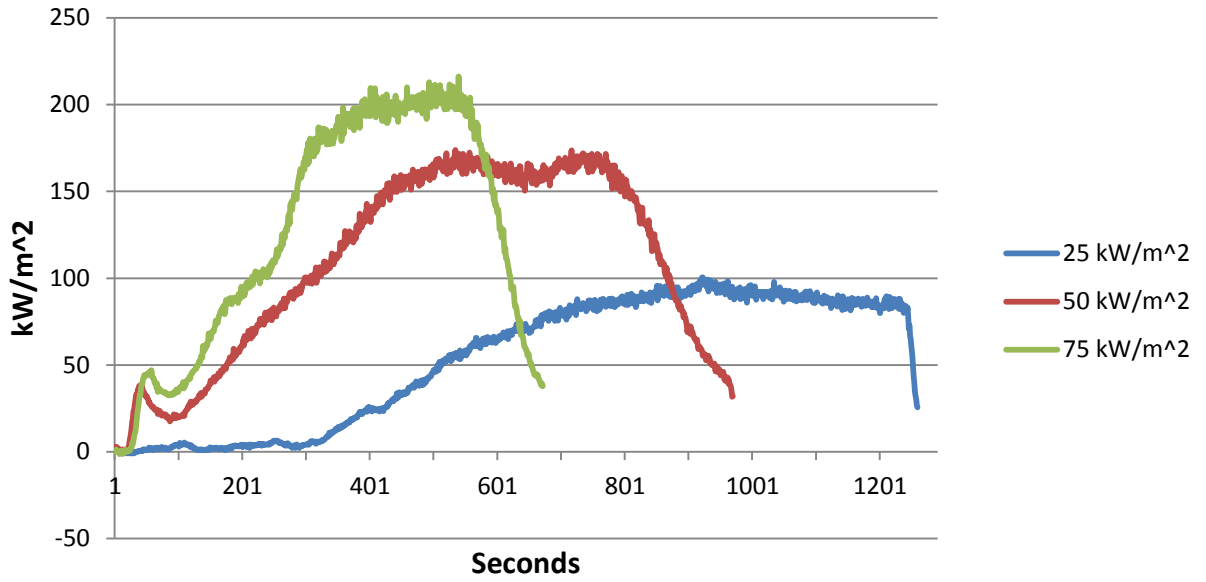
Appendix K   Cone: Specific Extinction Area Histories

Specific Extinction Area analysis – 25kW/M²

Thirteen FRP systems are analyzed in the context of specific extinction area. This briefing highlights all thirteen systems as well as groups the systems in terms of pigments, filler, gel, and aggregate composition for comparison purposes.

Baseline FRP System
No gelcoat
Polymer concrete: Norsodyne H 81269 TF with 6% cobalt & DDM-9
Alumina Trihydrate: 10% of resin by weight
Sand: 150% of resin by weight, split evenly between #0/30 and #2/16
1-1/2 parts sand to 1 part resin
No pigment
Approximately 60 mil thickness (aggregate dependent)
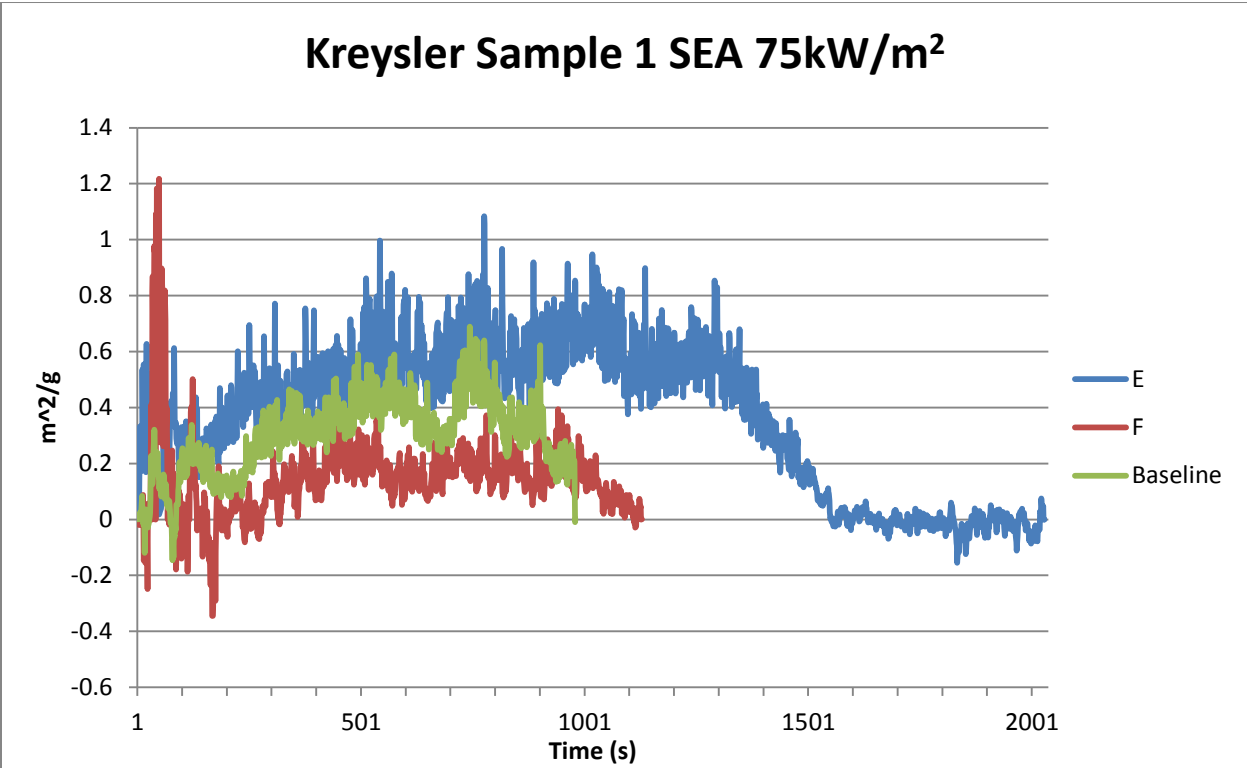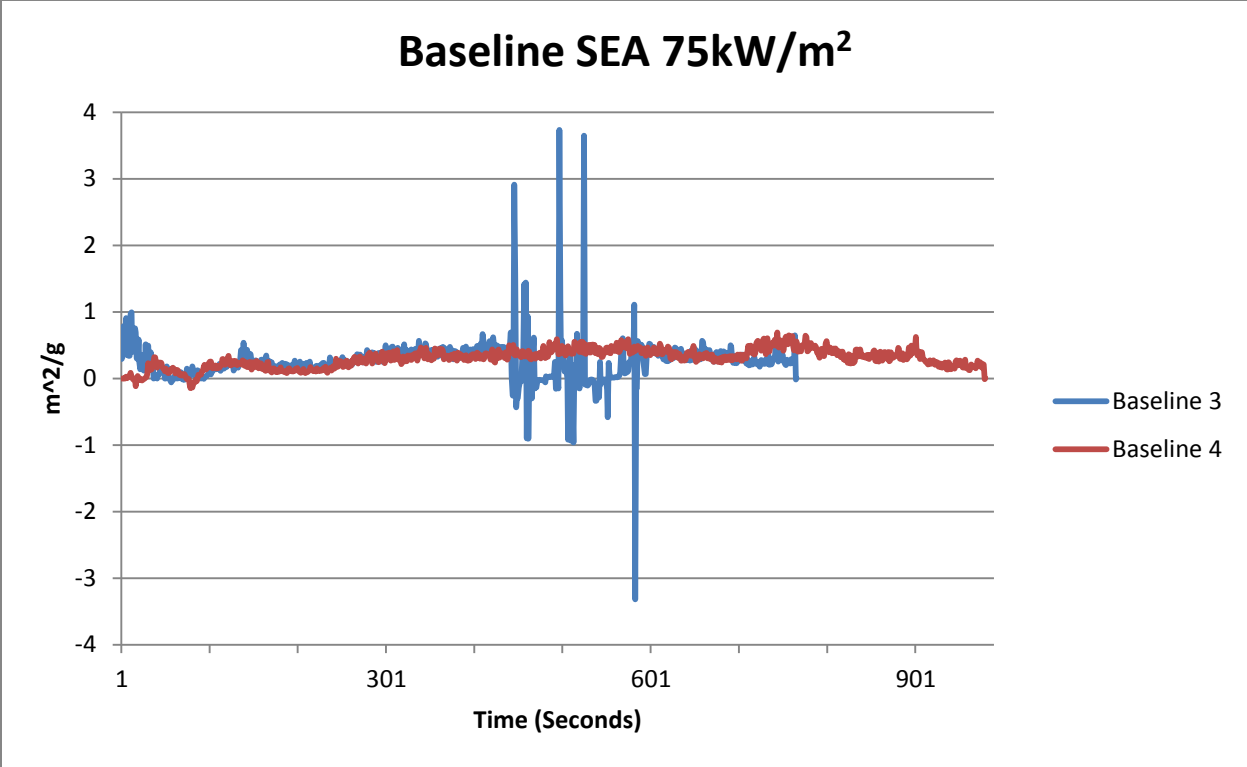3/16" single skin laminate: Norsodyne H 81269 TF with 6% cobalt & DDM-9
4 layers of 1.5 ounce chopped strand mat
Glass to resin ratio range: 25:75 to 35:65 by weight

System 1 – Addition of 1/2" plywood core & 3/16" rear skin (Note that core separation was observed in several samples)
**System 2** – Addition of 3/4" balsa core & 3/16" rear skin
System 3 – Addition of 1/2" polyurethane foam core & 3/16" rear skin
System 4 – Bronze filler instead of sand: 1 part bronze powder to 1 part resin by weight
System 5 – Aluminum filler instead of sand: 1 part aluminum powder to 2 parts resin by weight
System 6 – Straight Norsodyne H 81269 TF as gelcoat in place of resin based polymer concrete
System 7 – Addition of white pigment to polymer concrete
System 8 – Addition of grey pigment to polymer concrete
System 9 – Addition of beige pigment to polymer concrete
System 10 – #0/30 aggregate only
System 11 – #0/60 aggregate only
System 12 – #2/16 aggregate only
System 13 – DCPD Laminate resin (with 6 layers of glass) instead of Norsodyne

Baseline SEA at 25kW/m²

Kreysler Sample 1 SEA at 25kW/m²

Kreysler Sample 2 SEA at 25kW/m²

Kreysler Sample 3 SEA at 25kW/m²

Kreysler Sample 4 SEA at 25kW/m²
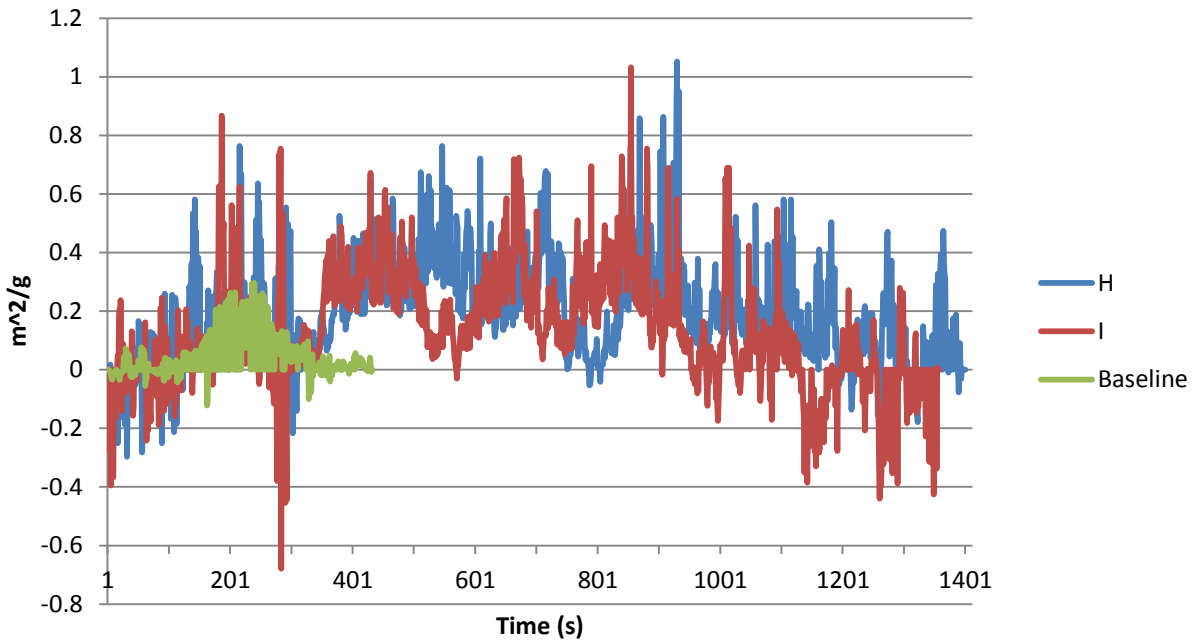
Kreysler Sample 5 SEA at 25kW/m²
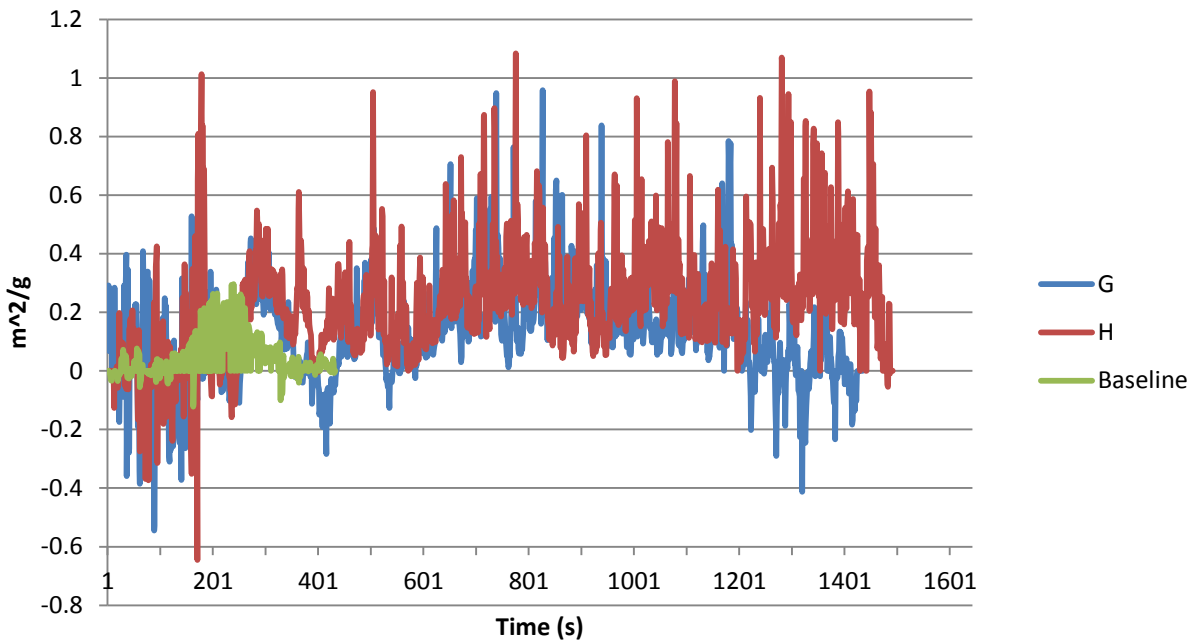
Kreysler Sample 6 SEA at 25kW/m²
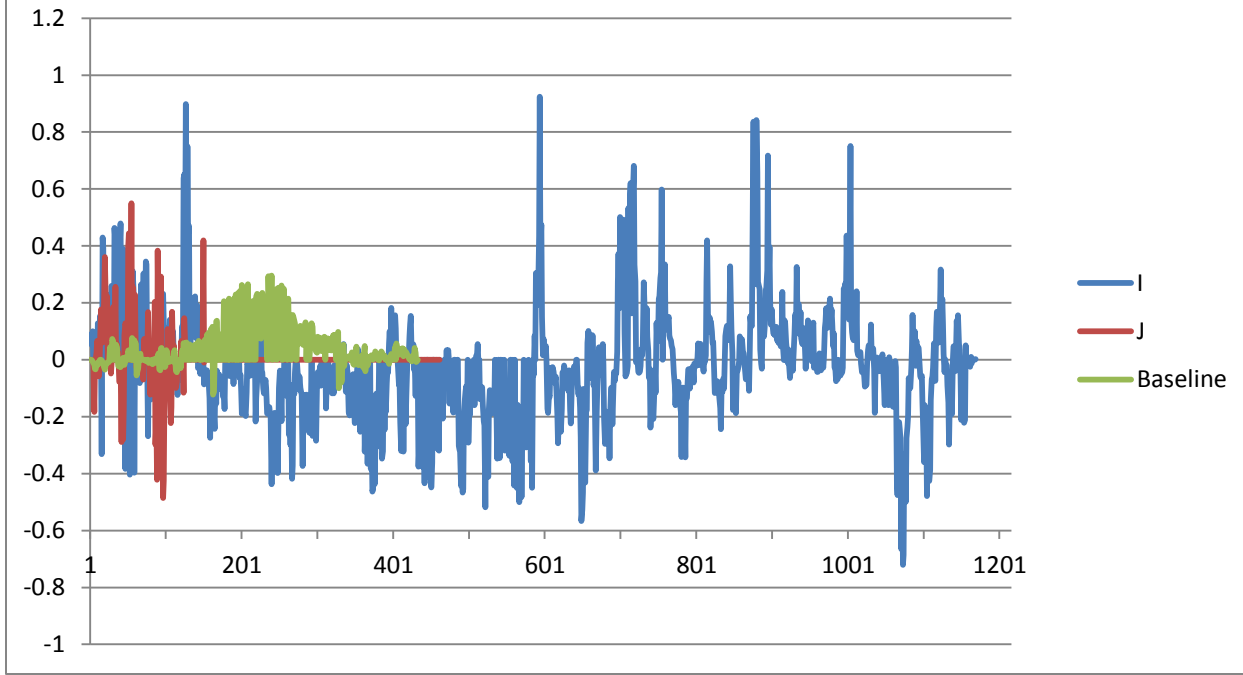
Kreysler Sample 7 SEA at 25kW/m²

Kreysler Sample 8 SEA at 25kW/m²
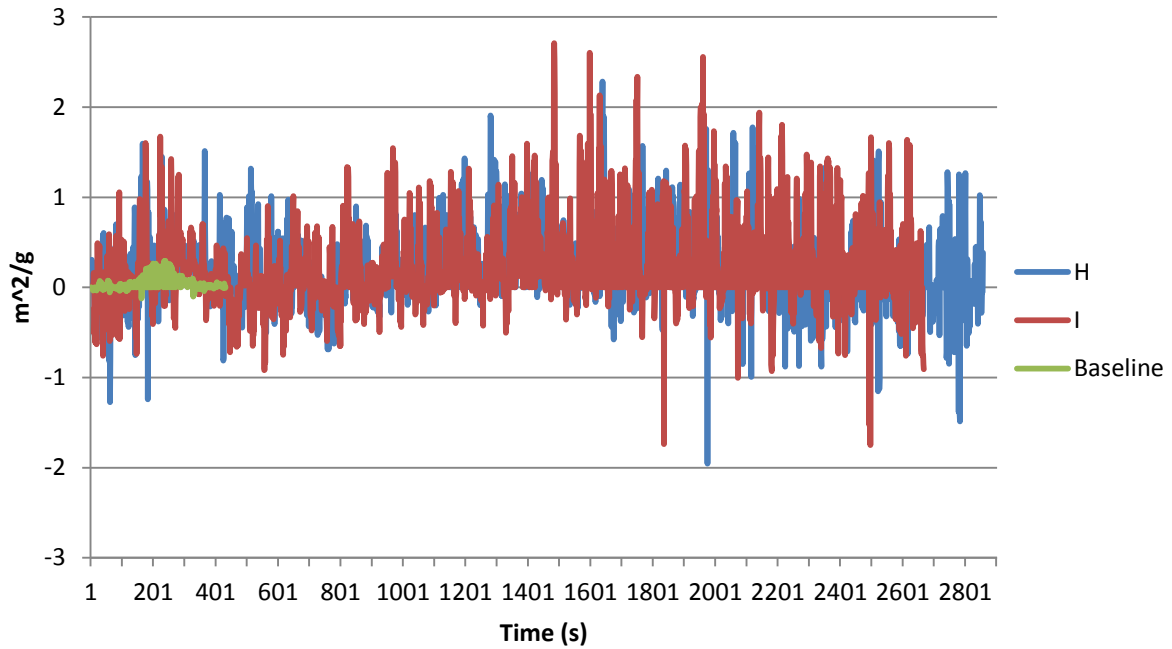
Kreysler Sample 9 SEA at 25kW/m²
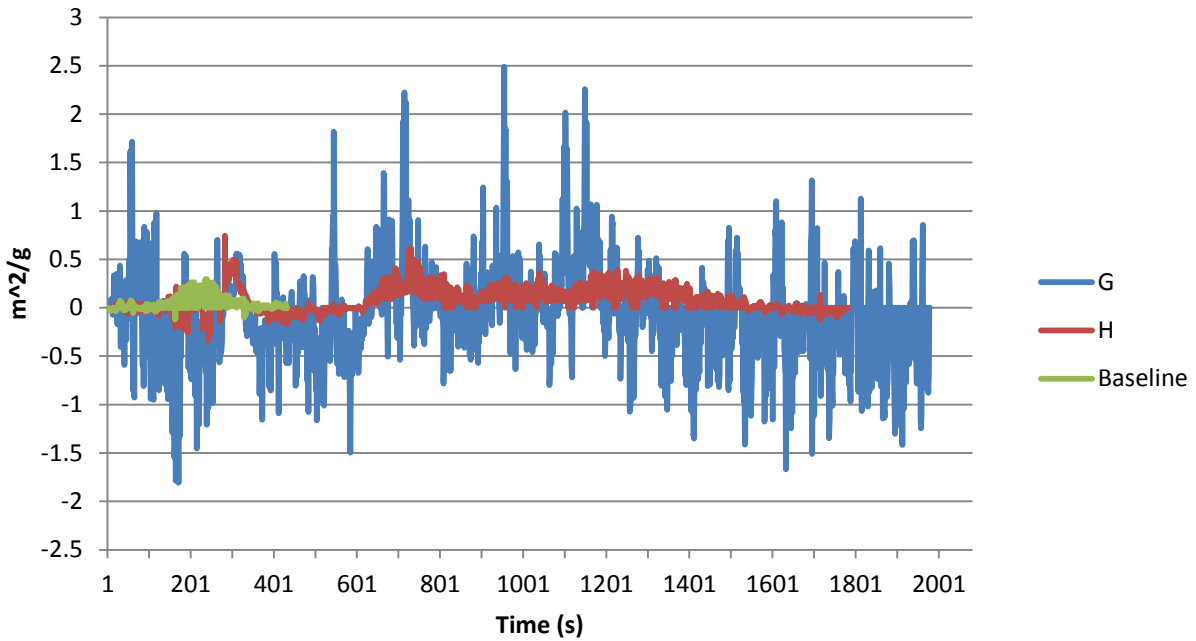
Kreysler Sample 10 SEA at 25kW/m²
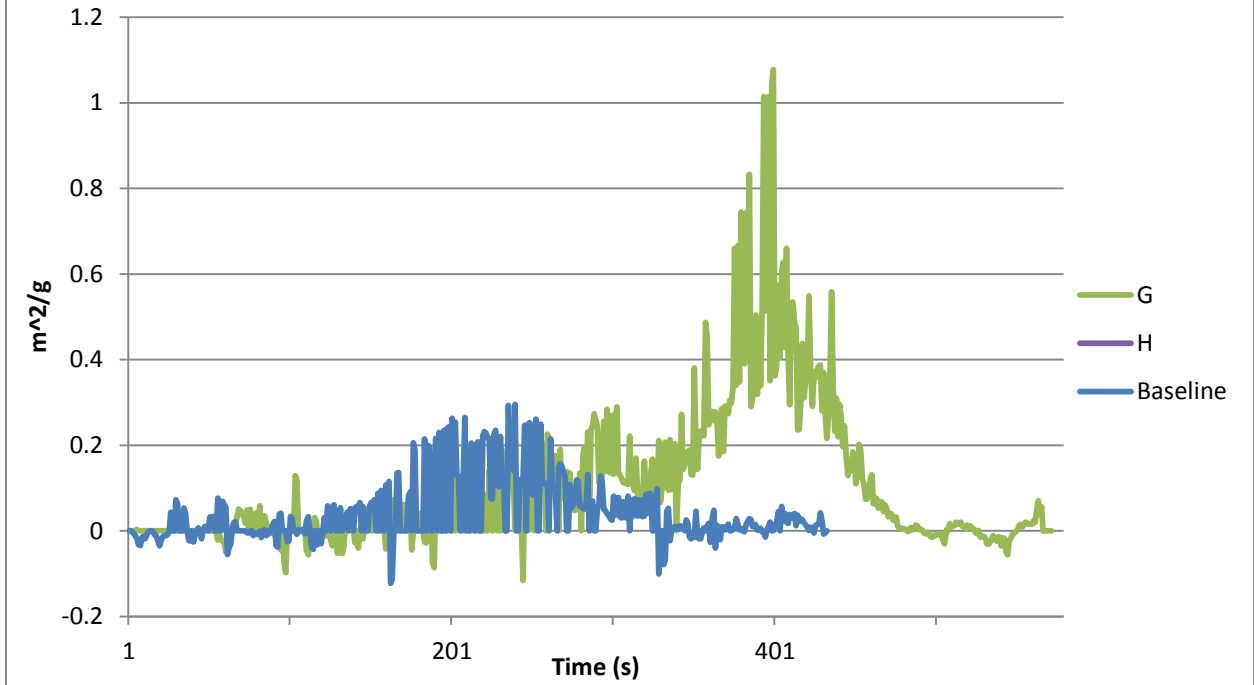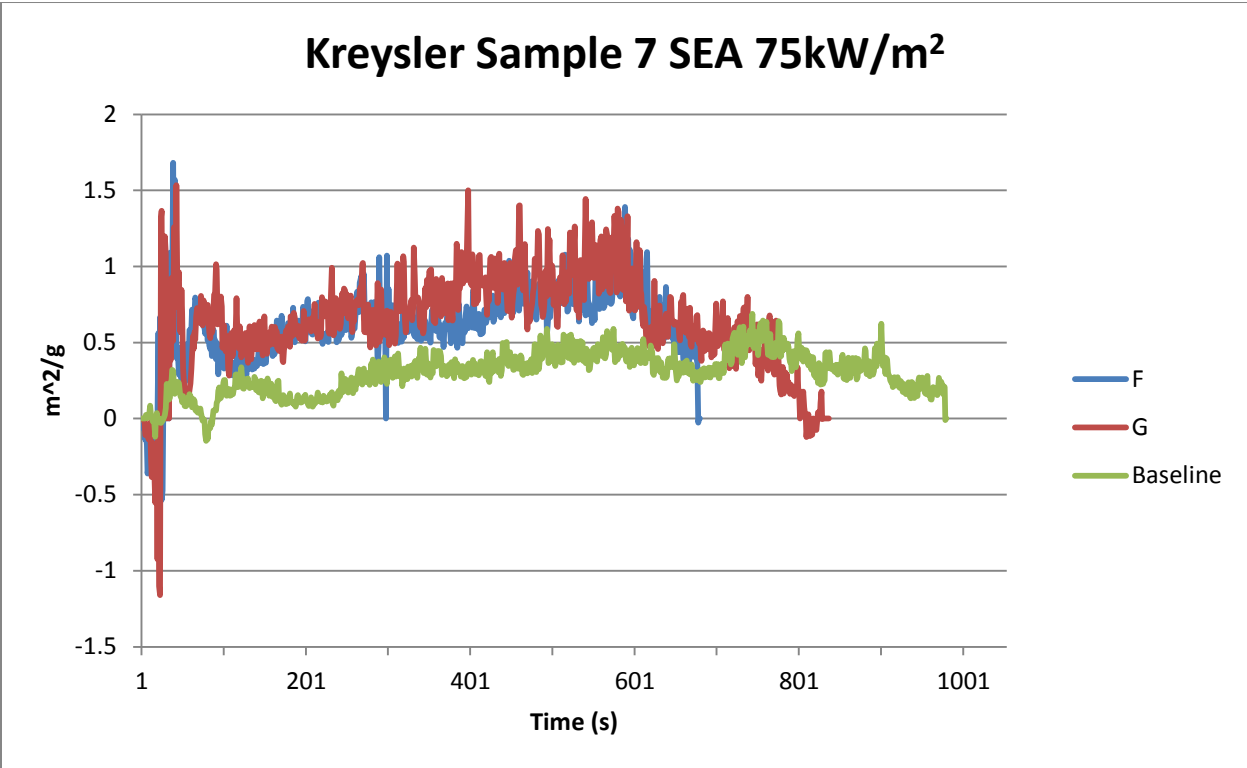
Kreysler Sample 11 SEA at 25kW/m²
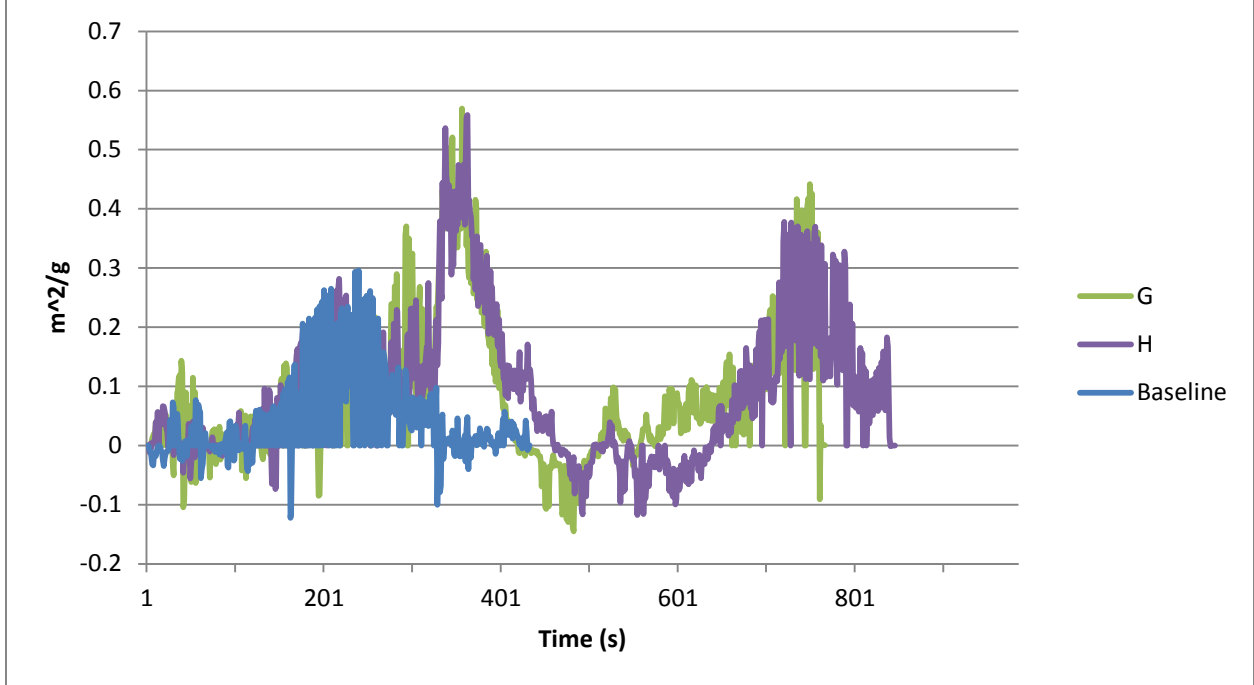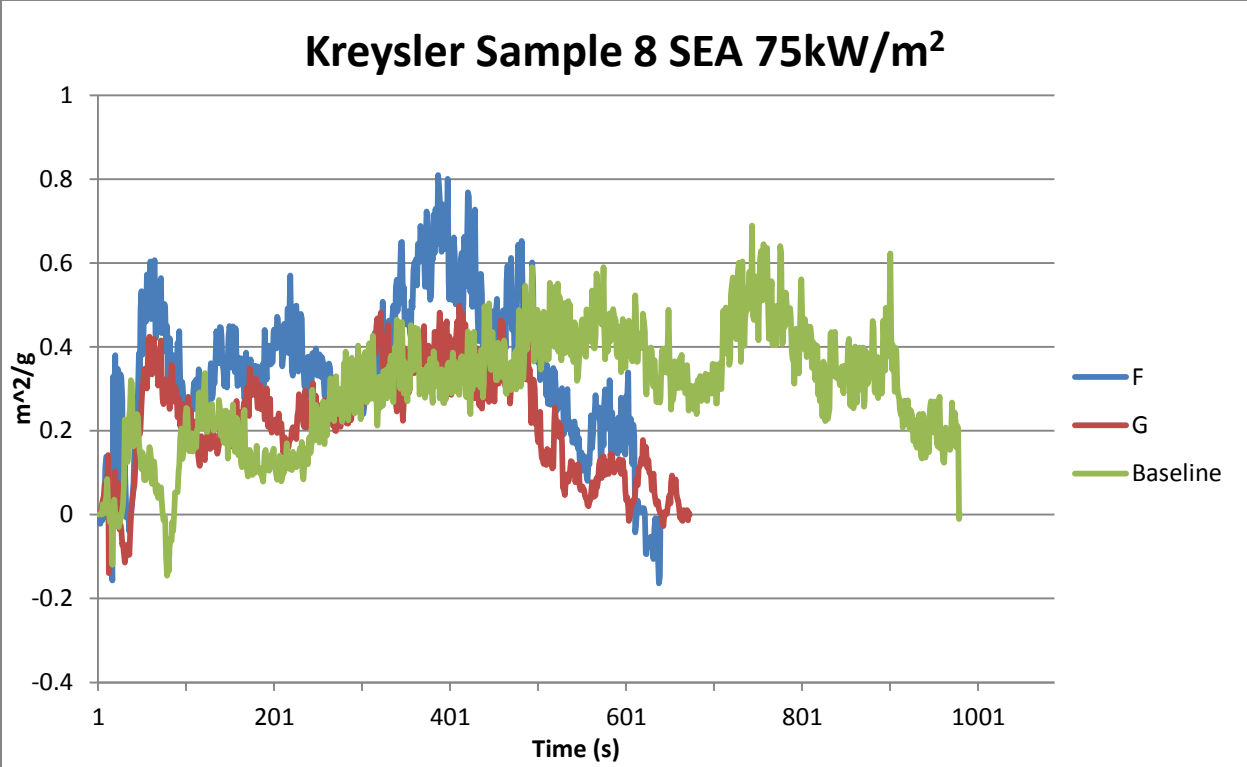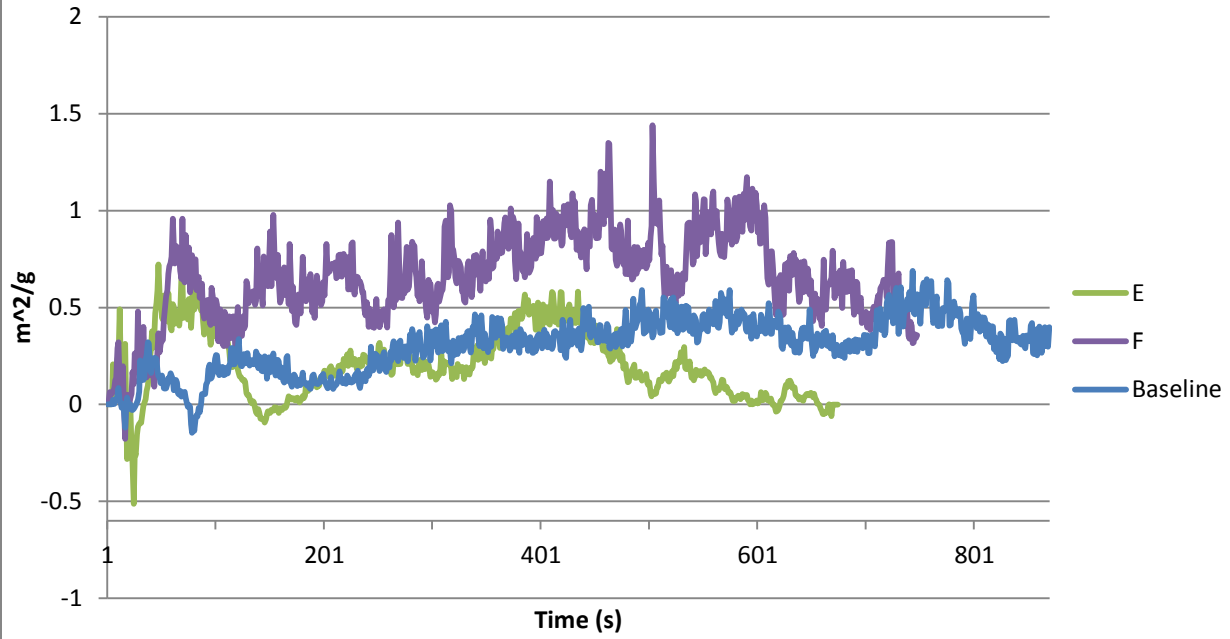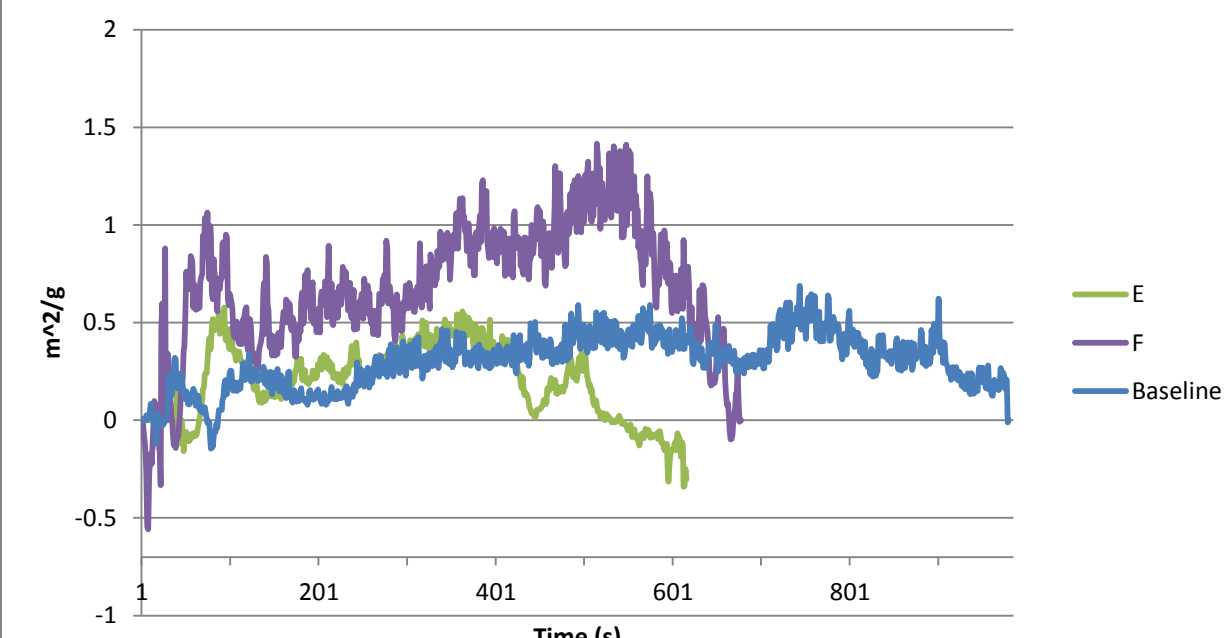
Kreysler Sample 12 SEA at 25kW/m²
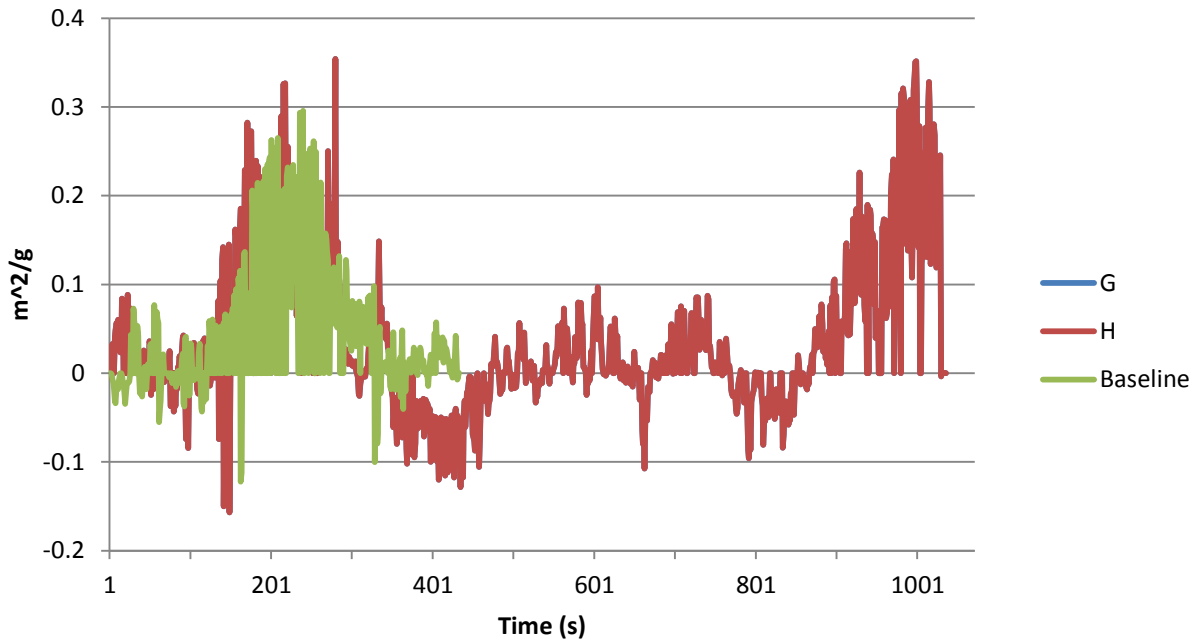
Kreysler Sample 13 SEA at 25kW/m²
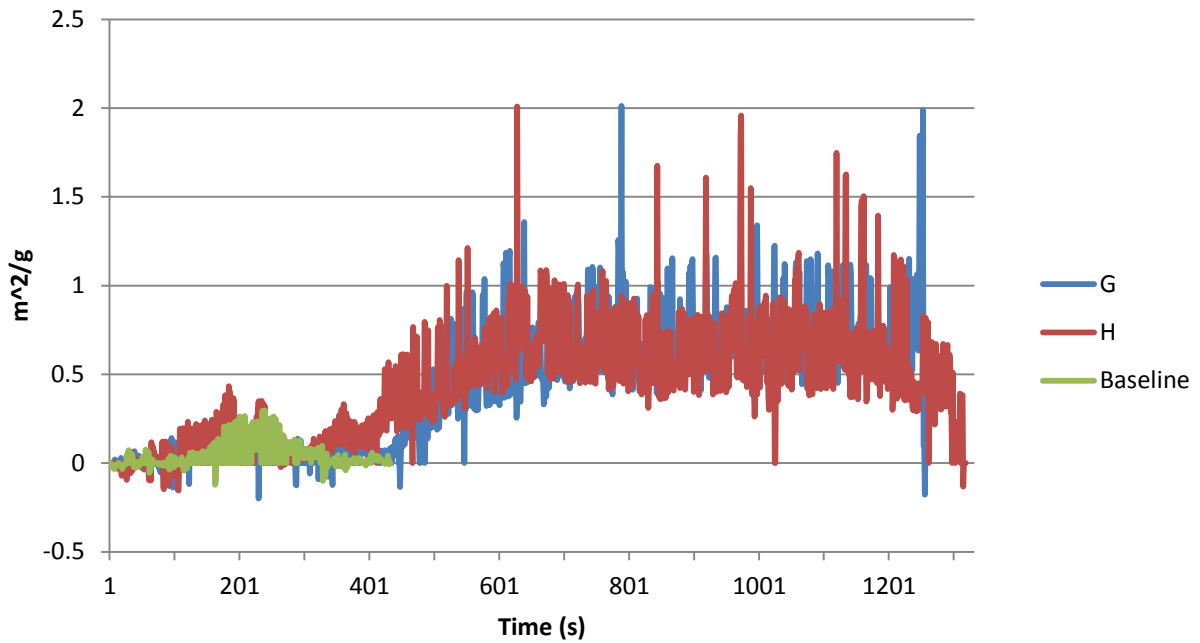
SEA Pigment Comparisons at 25kW/m²

Legend:
- (White) 7H
- (Grey) 8H
- (Beige) 9H
- Baseline
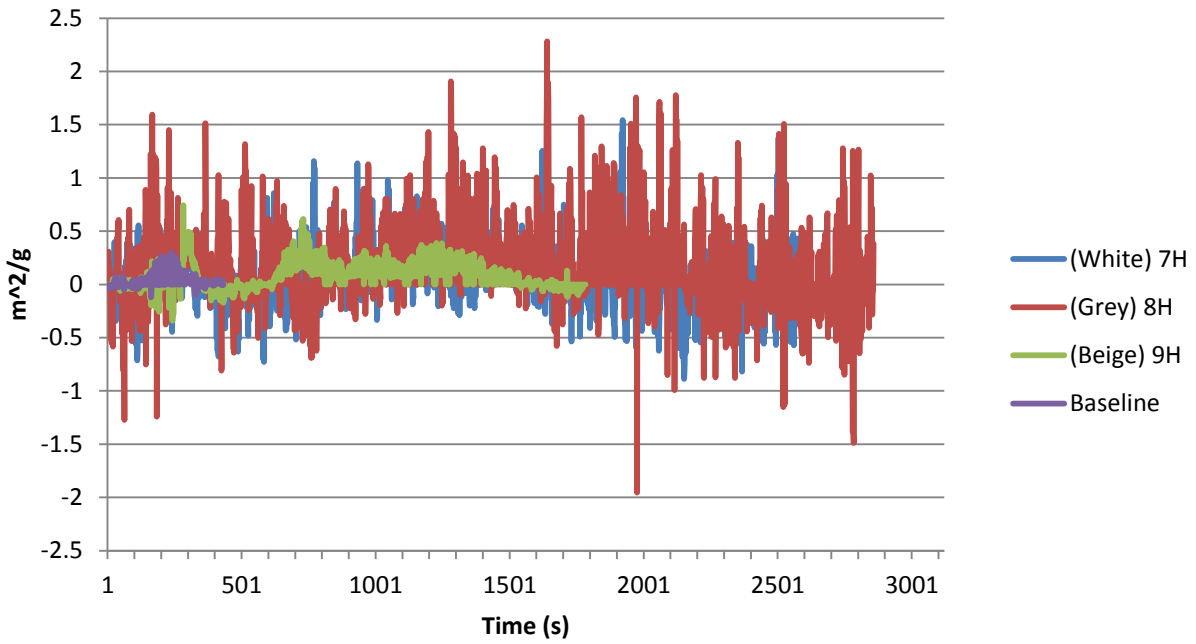
SEA Aggregate Comparison at 25kW/m²

Legend:
- (#0/30) 10G
- (#0/60) 11G
- (#2/16) 12G
- Baseline
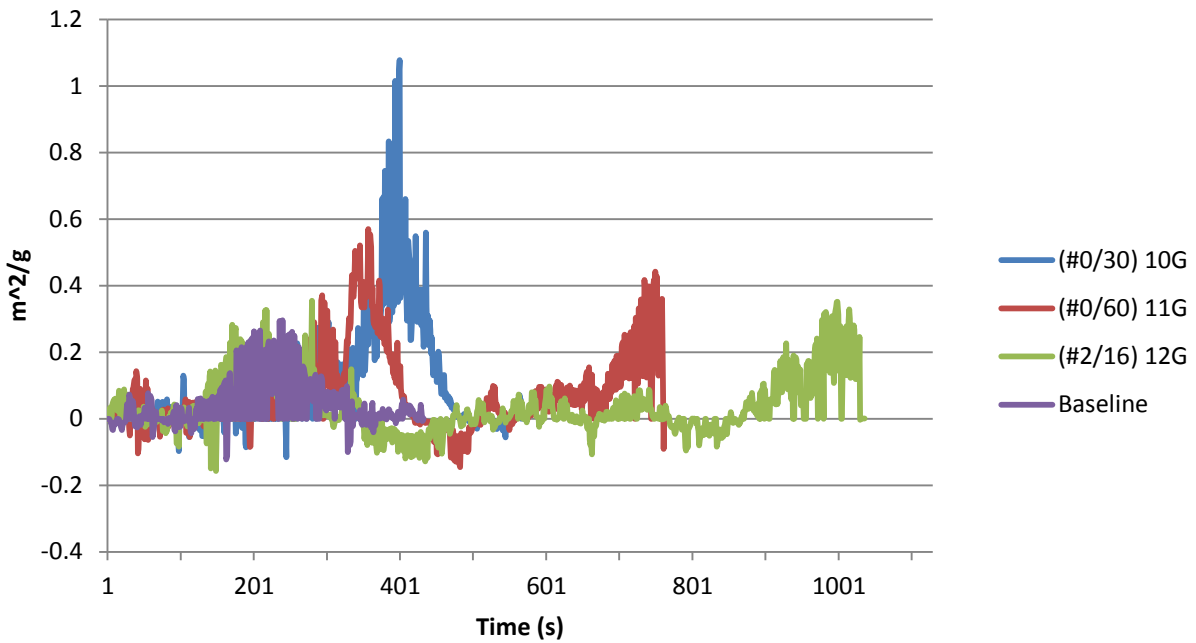
SEA Filler Comparison at 25kW/m²
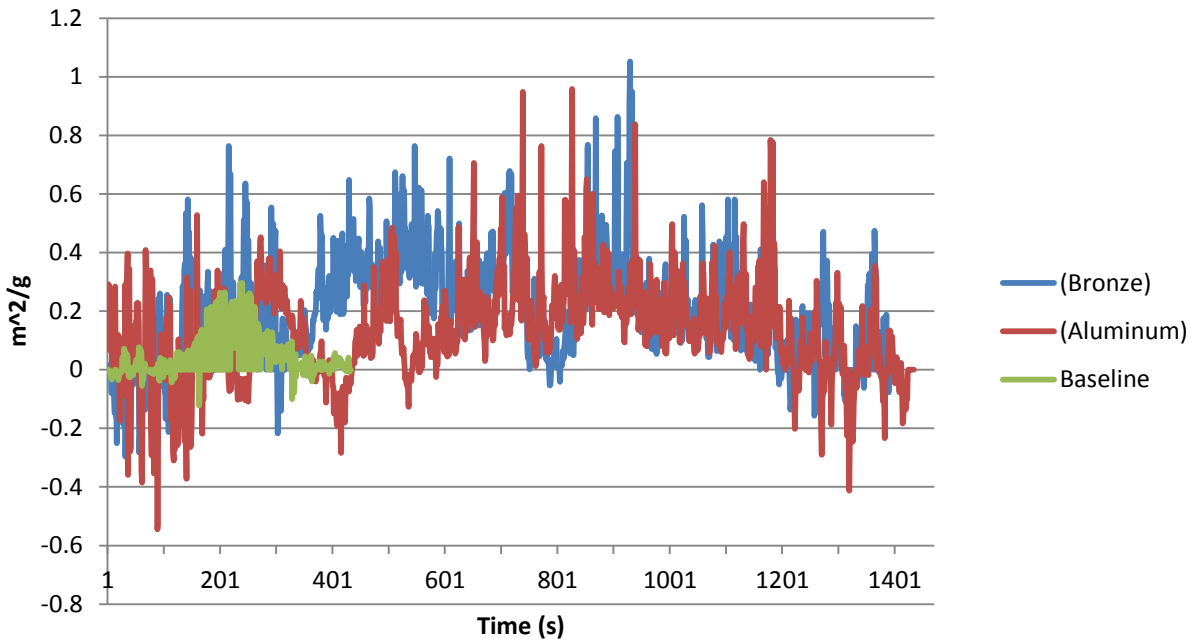
SEA Gel Comparison at 25kW/m²

SEA Cores Comparison at 25kW/m²
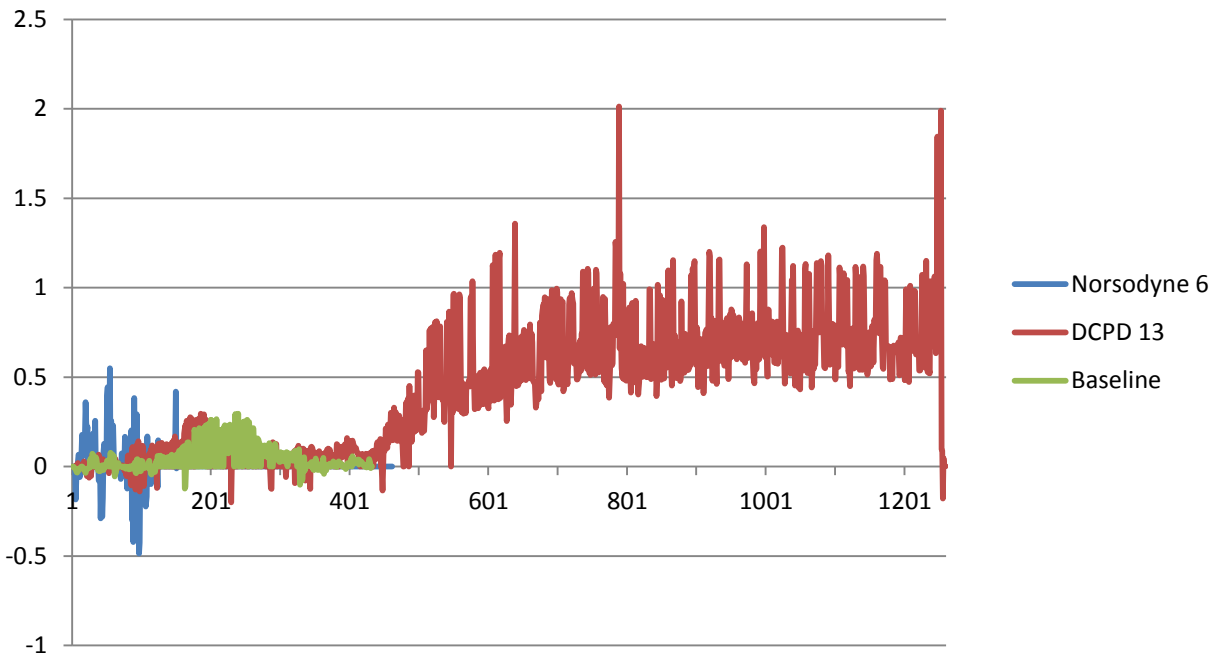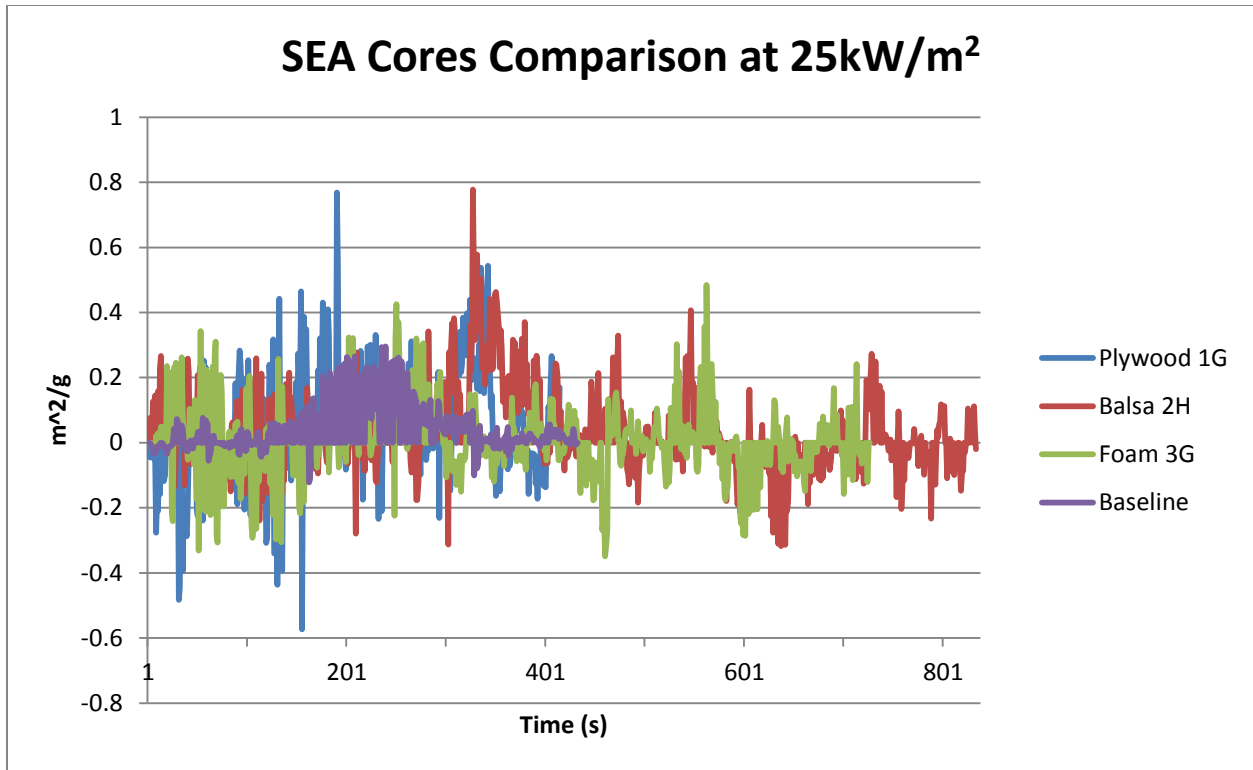
Specific Extinction Area analysis – 50kW /m²

Thirteen FRP systems are analyzed in the context of specific extinction area. This briefing highlights all thirteen systems as well as groups the systems in terms of pigments, filler, gel, and aggregate composition for comparison purposes.

Baseline FRP System
No gelcoat
Polymer concrete: Norsodyne H 81269 TF with 6% cobalt & DDM-9
Alumina Trihydrate: 10% of resin by weight
Sand: 150% of resin by weight, split evenly between #0/30 and #2/16
1-1/2 parts sand to 1 part resin
No pigment
Approximately 60 mil thickness (aggregate dependent)
3/16" single skin laminate: Norsodyne H 81269 TF with 6% cobalt & DDM-9
4 layers of 1.5 ounce chopped strand mat
Glass to resin ratio range: 25:75 to 35:65 by weight

System 1 – Addition of 1/2" plywood core & 3/16" rear skin (Note that core separation was observed in several samples)
System 2 – Addition of 3/4" balsa core & 3/16" rear skin

System 3 – Addition of 1/2" polyurethane foam core & 3/16" rear skin

System 4 – Bronze filler instead of sand: 1 part bronze powder to 1 part resin by weight

System 5 – Aluminum filler instead of sand: 1 part aluminum powder to 2 parts resin by weight

System 6 – Straight Norsodyne H 81269 TF as gelcoat in place of resin based polymer concrete

System 7 – Addition of white pigment to polymer concrete

System 8 – Addition of grey pigment to polymer concrete

System 9 – Addition of beige pigment to polymer concrete

System 10 – #0/30 aggregate only

System 11 – #0/60 aggregate only

System 12 – #2/16 aggregate only

System 13 – DCPD Laminate resin (with 6 layers of glass) instead of Norsodyne

Baseline SEA 50kW/m²

m^2/g vs Time (Seconds)

Baseline 1
Baseline 2
Baseline 3
Baseline4

Kreysler Sample 1 SEA 50kW/m²

m^2/g vs Time (s)

A
B
C
D
Baseline

Kreysler Sample 2 SEA 50kW/m²
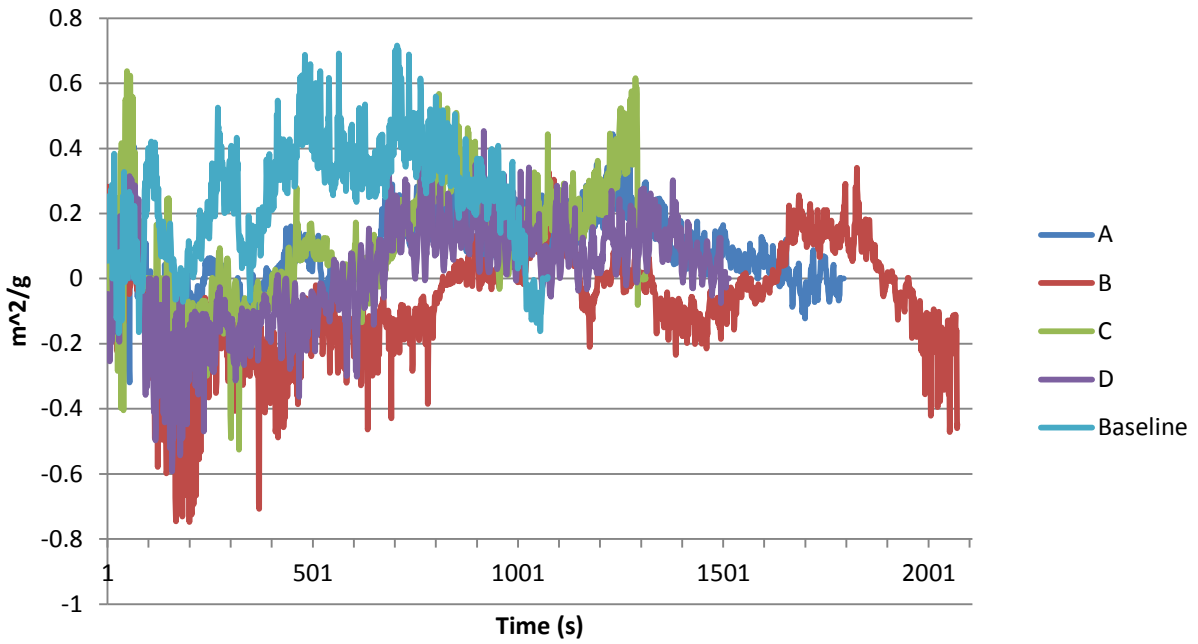
Kreysler Sample 3 SEA 50kW/m²

Kreysler Sample 4 SEA 50kW/m²
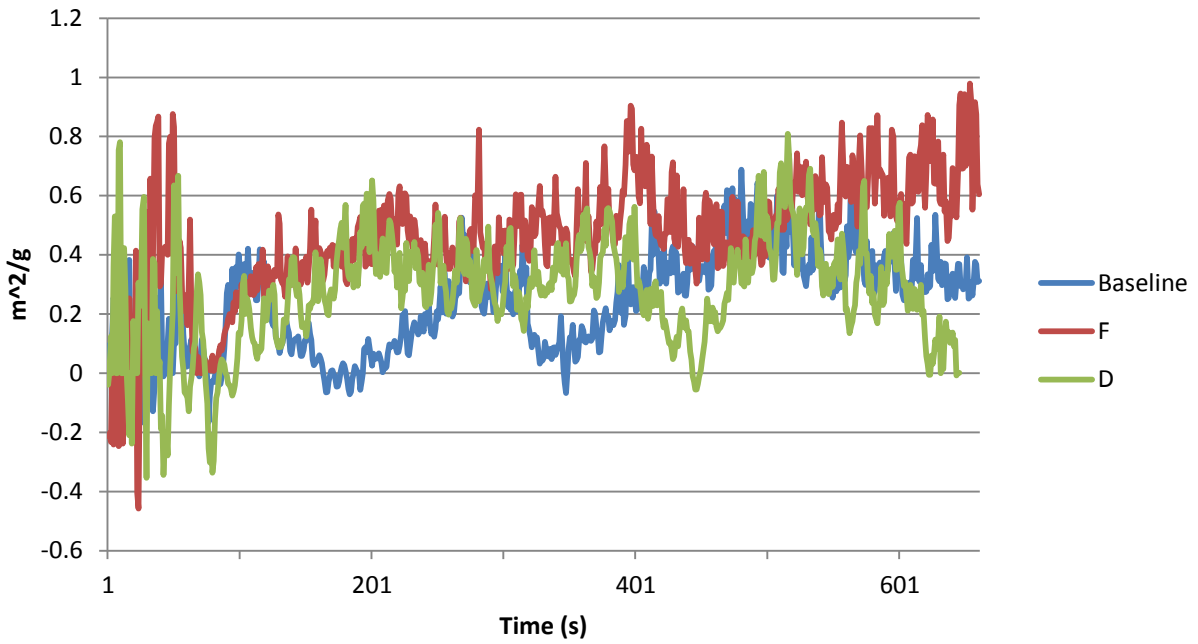
Kreysler Sample 5 SEA 50kW/m²
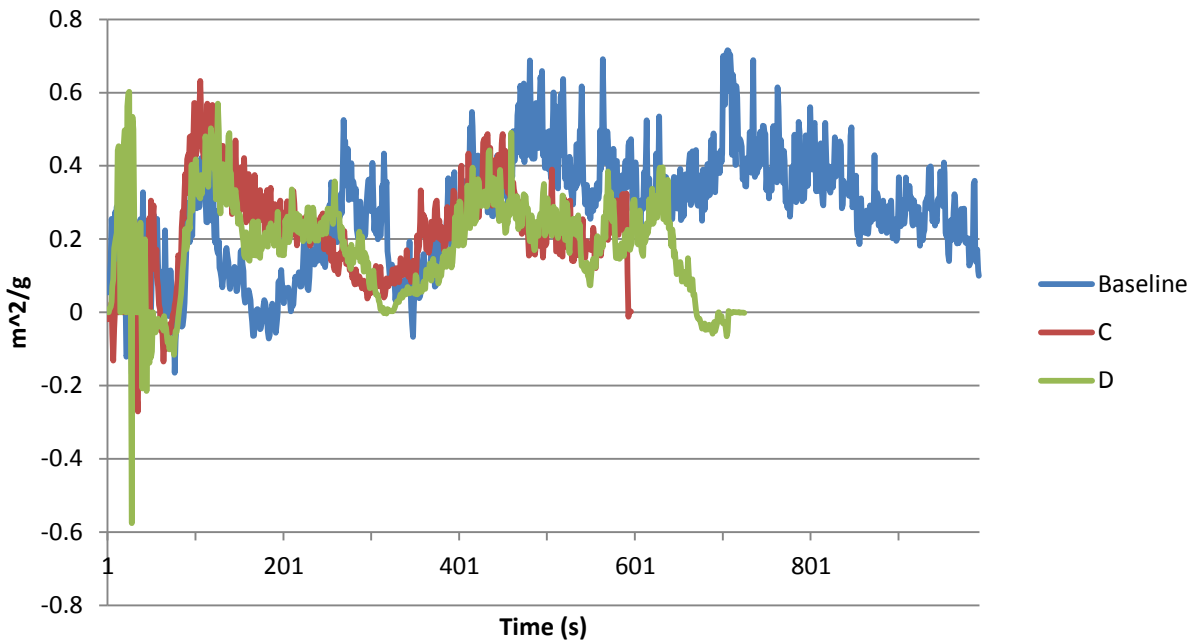
Kreysler Sample 7 SEA 50kW/m²
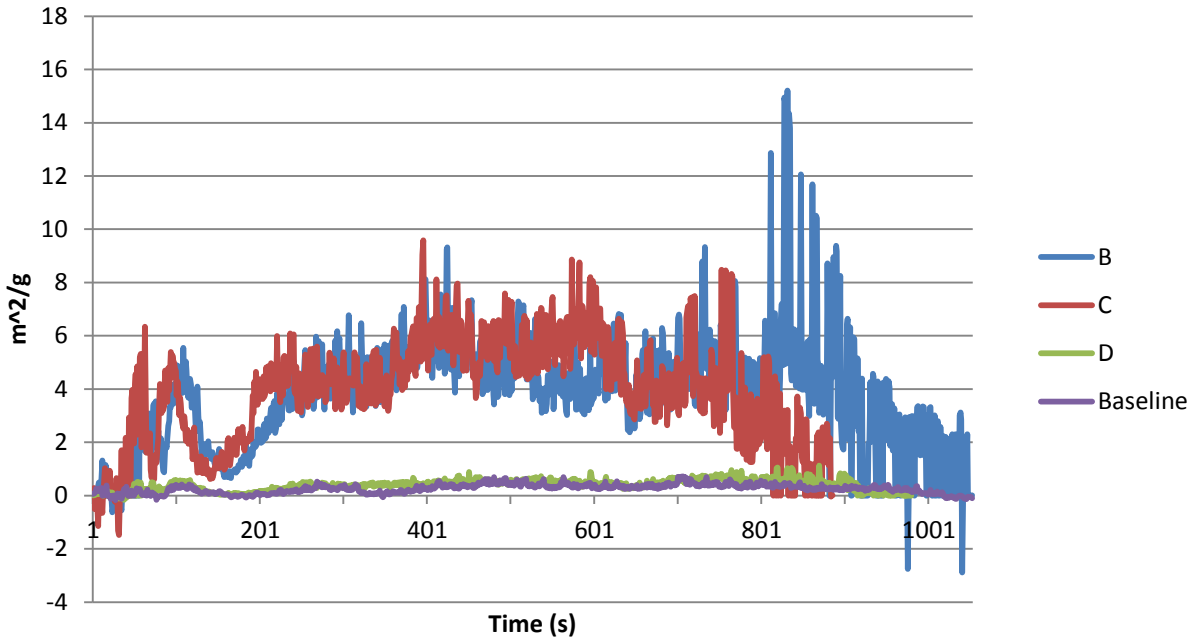
Kreysler Sample 8 SEA 50kW/m²
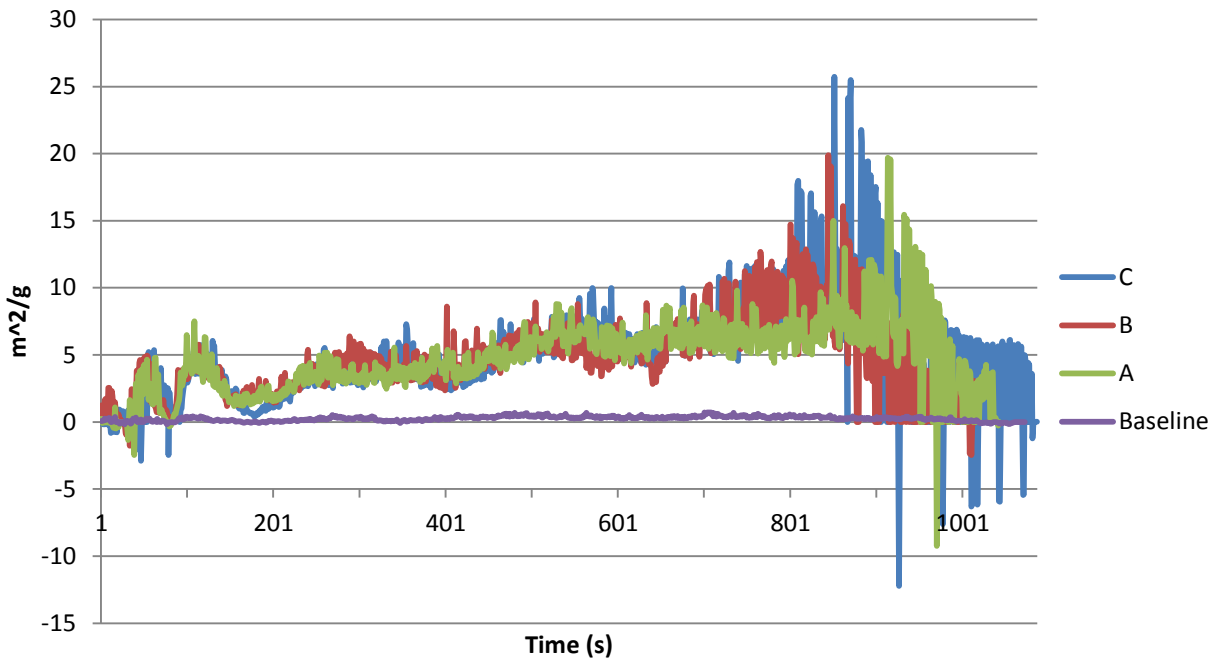
Kreysler Sample 9 SEA 50kW/m²
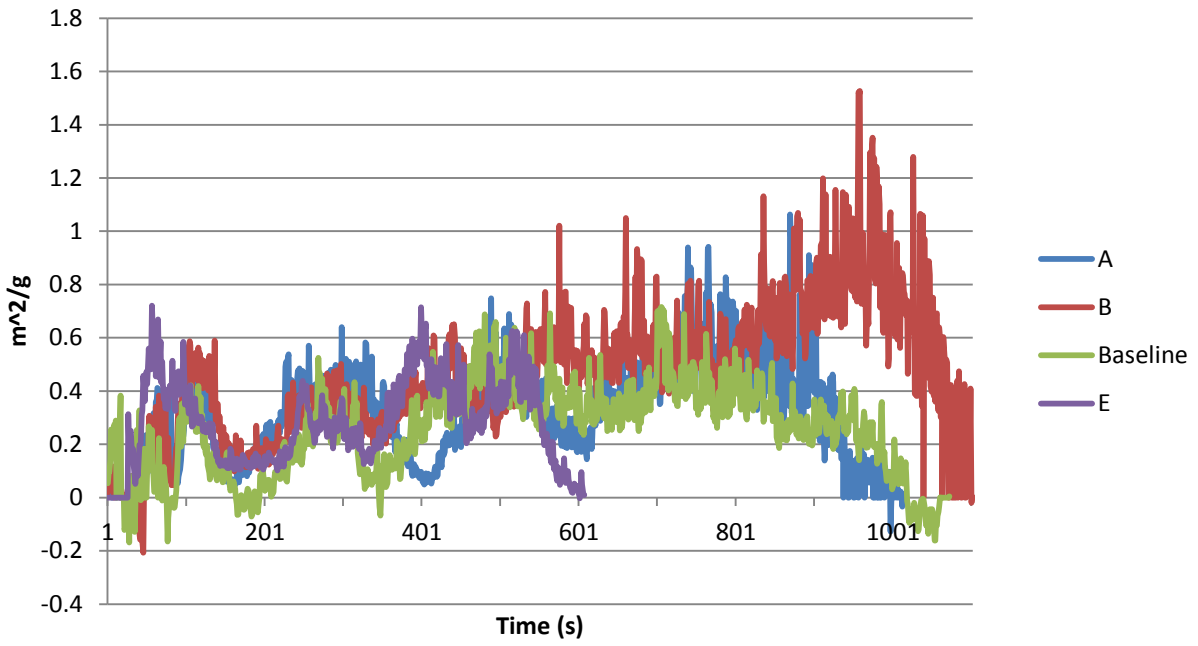

Kreysler Sample 10 SEA 50kW/m²
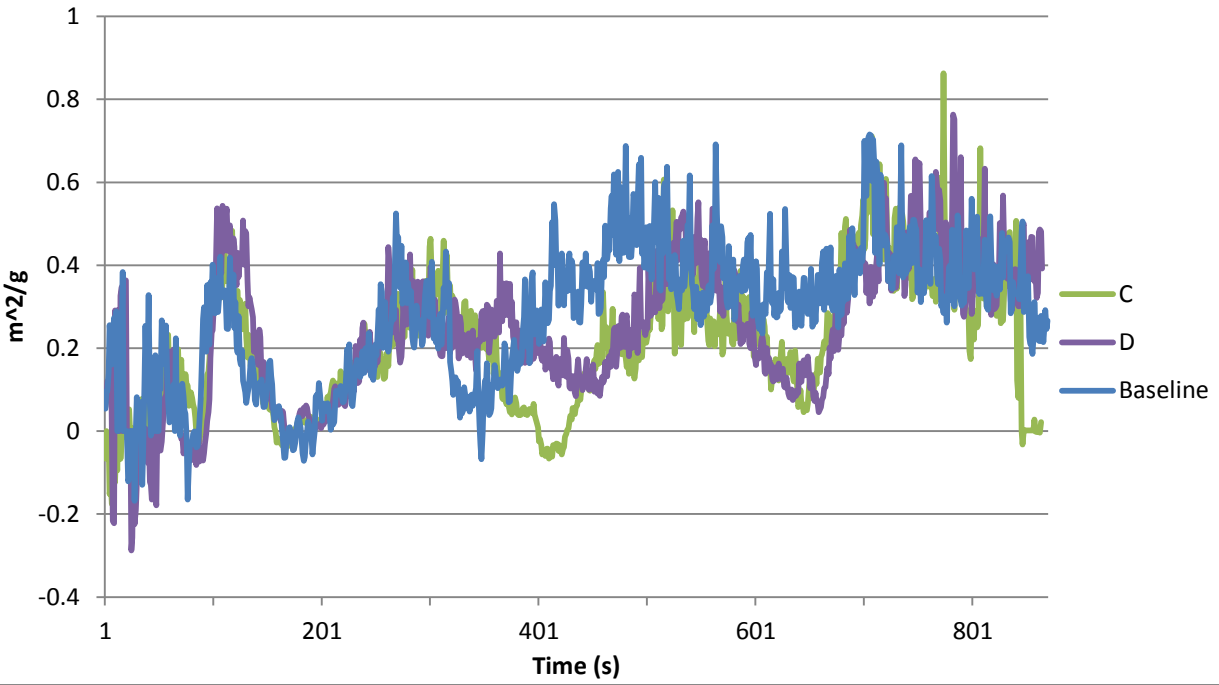
Kreysler Sample 11 SEA 50kW/m²
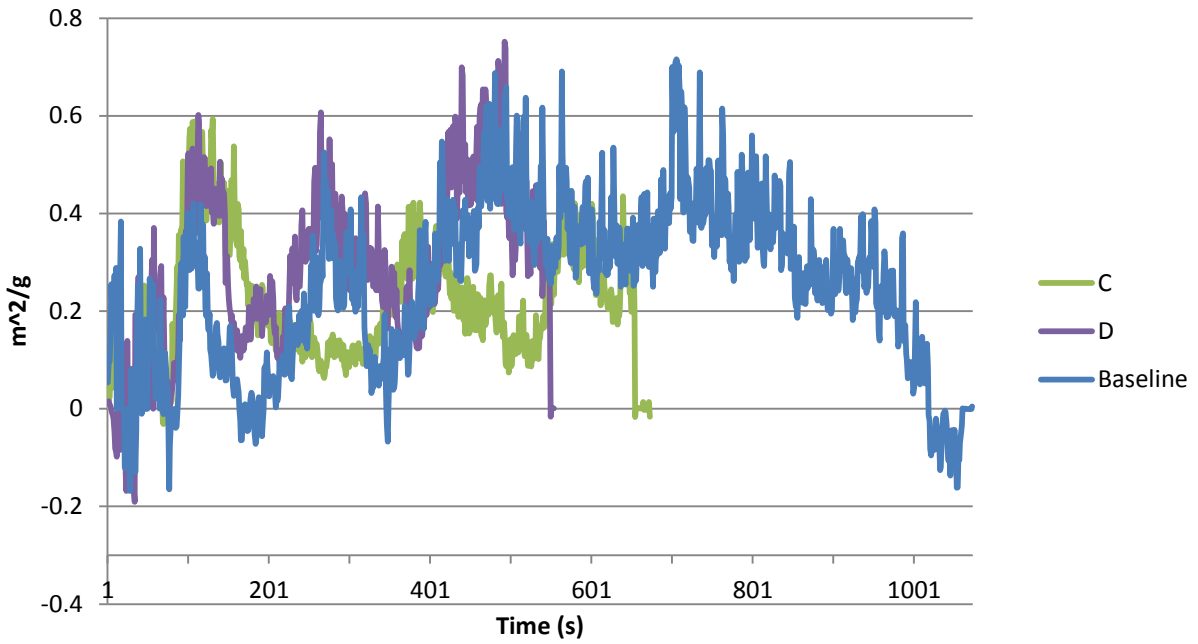
Kreysler Sample 12 SEA 50kW/m²
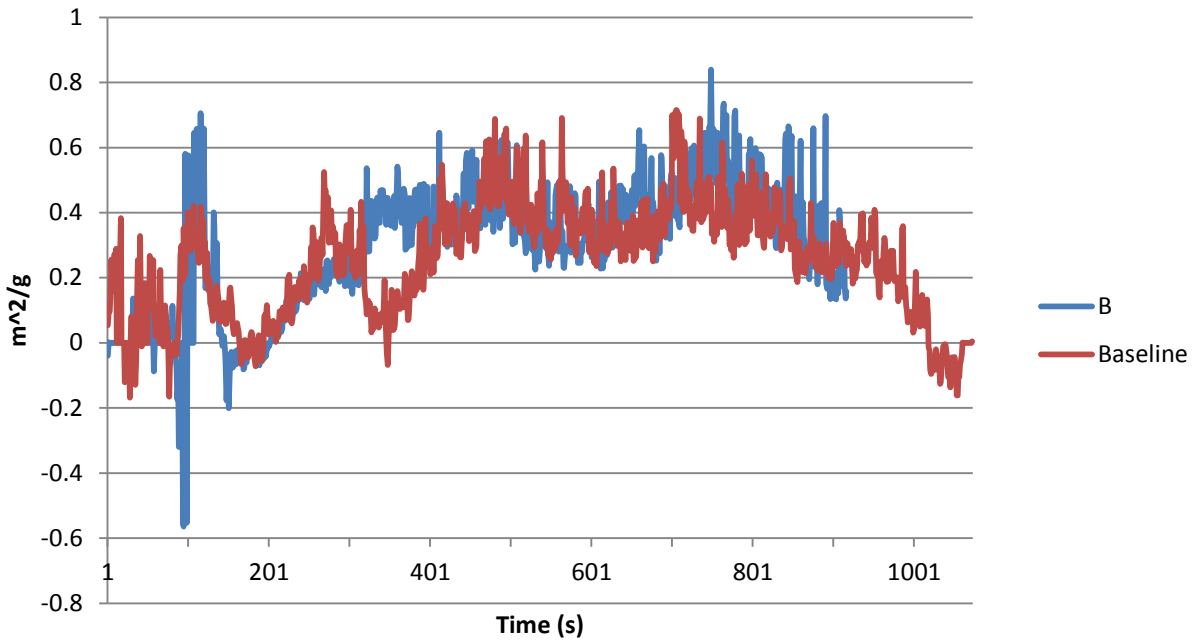
Kreysler Sample 13 SEA 50kW/m²

Legend: C, D, Baseline

Pigment SEA Comparisons 50kW/m²

Legend: (White) 7C, (Grey) 8A, (Beige) 9B, Baseline
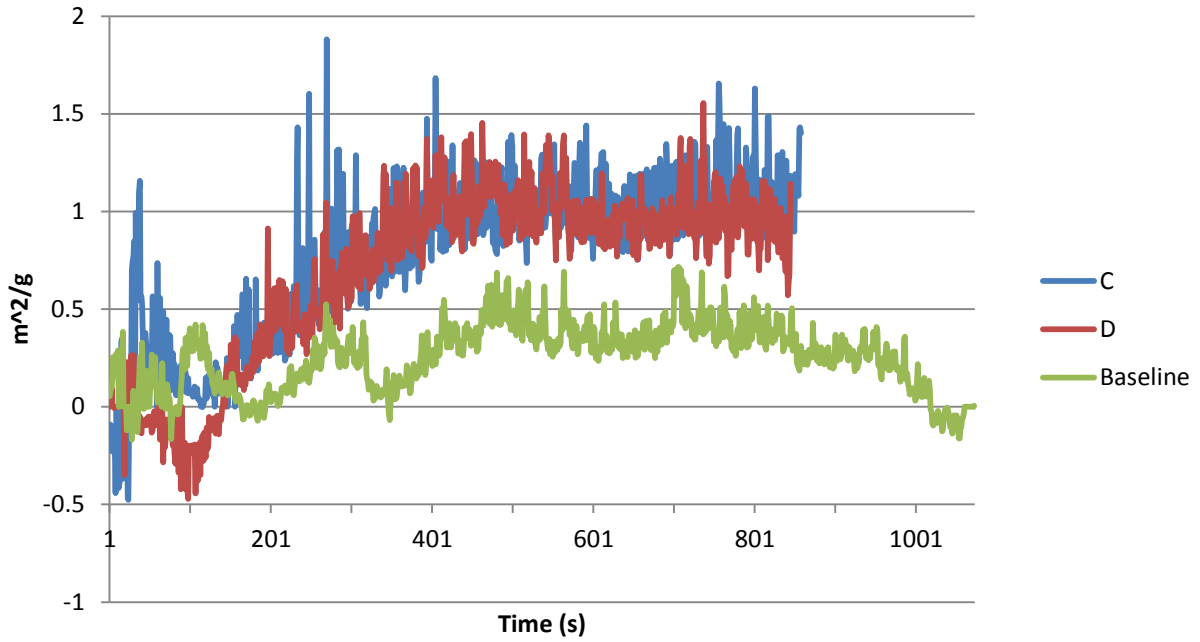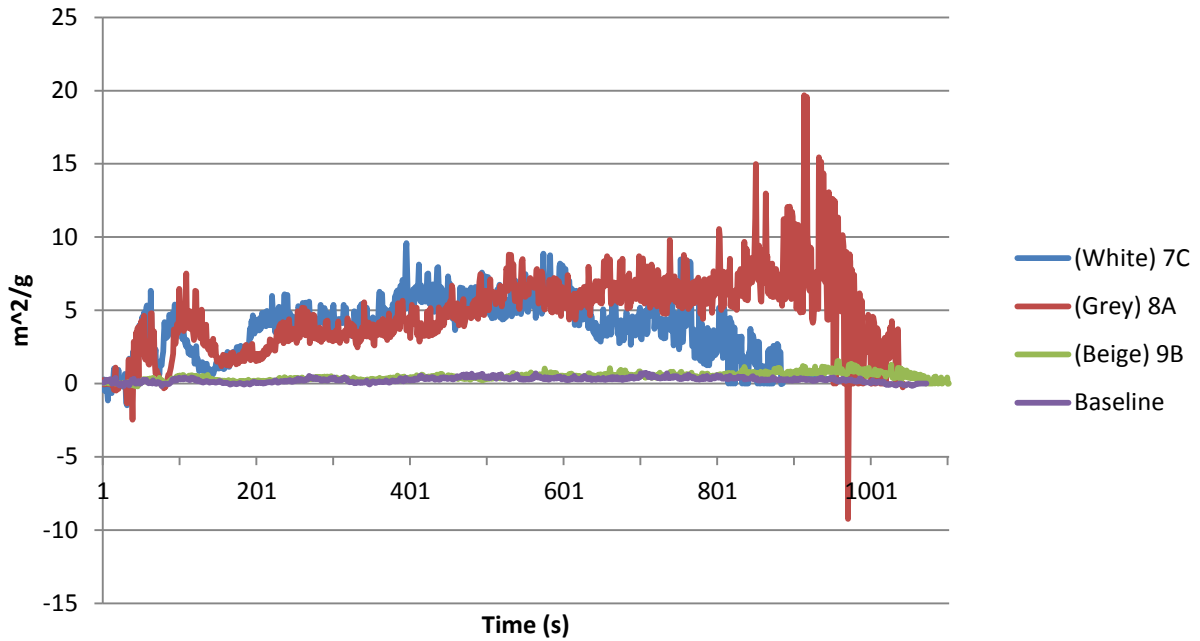
Aggregate SEA Comparison 50kW/m²

Filler SEA Comparison 50kW/m²
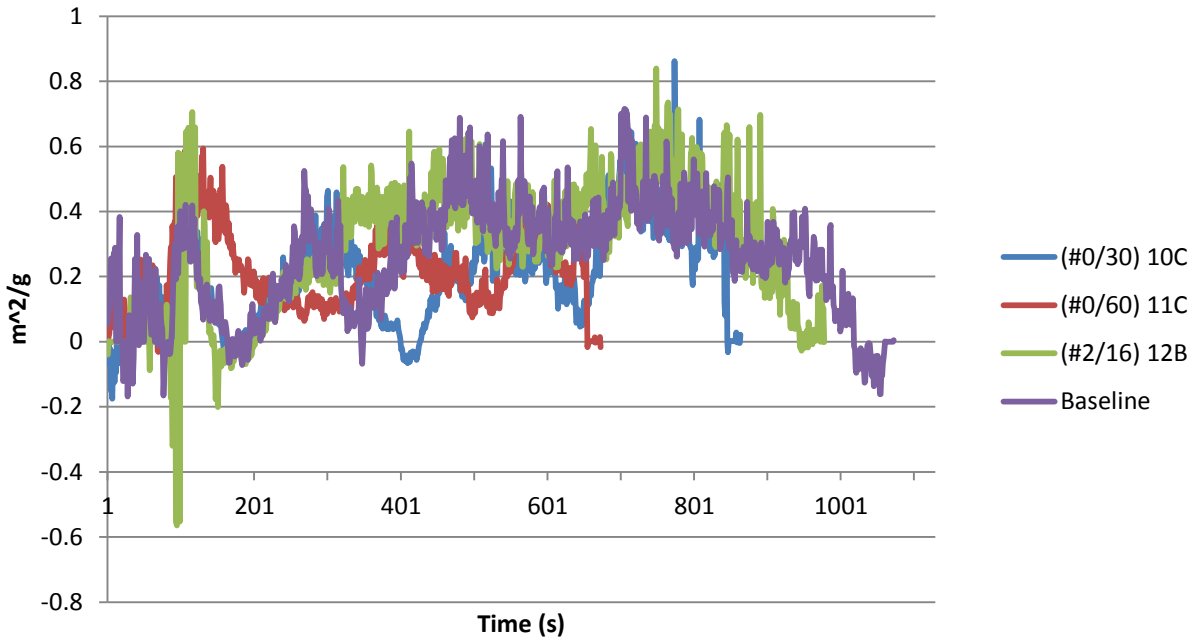
Cores SEA Comparison 50kW/m²
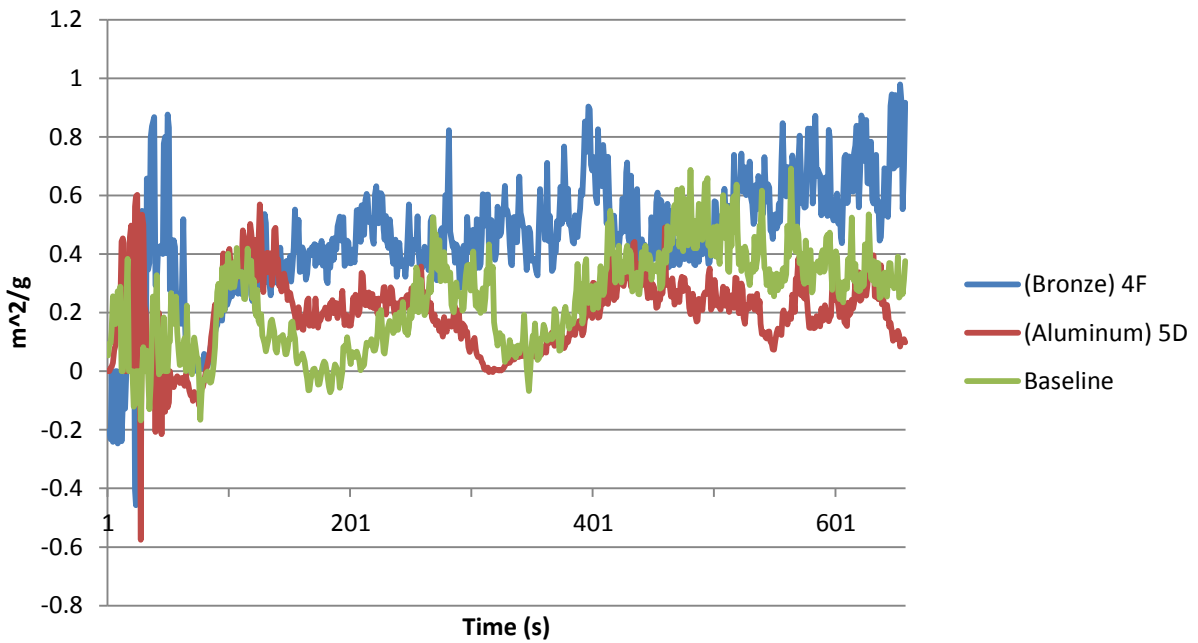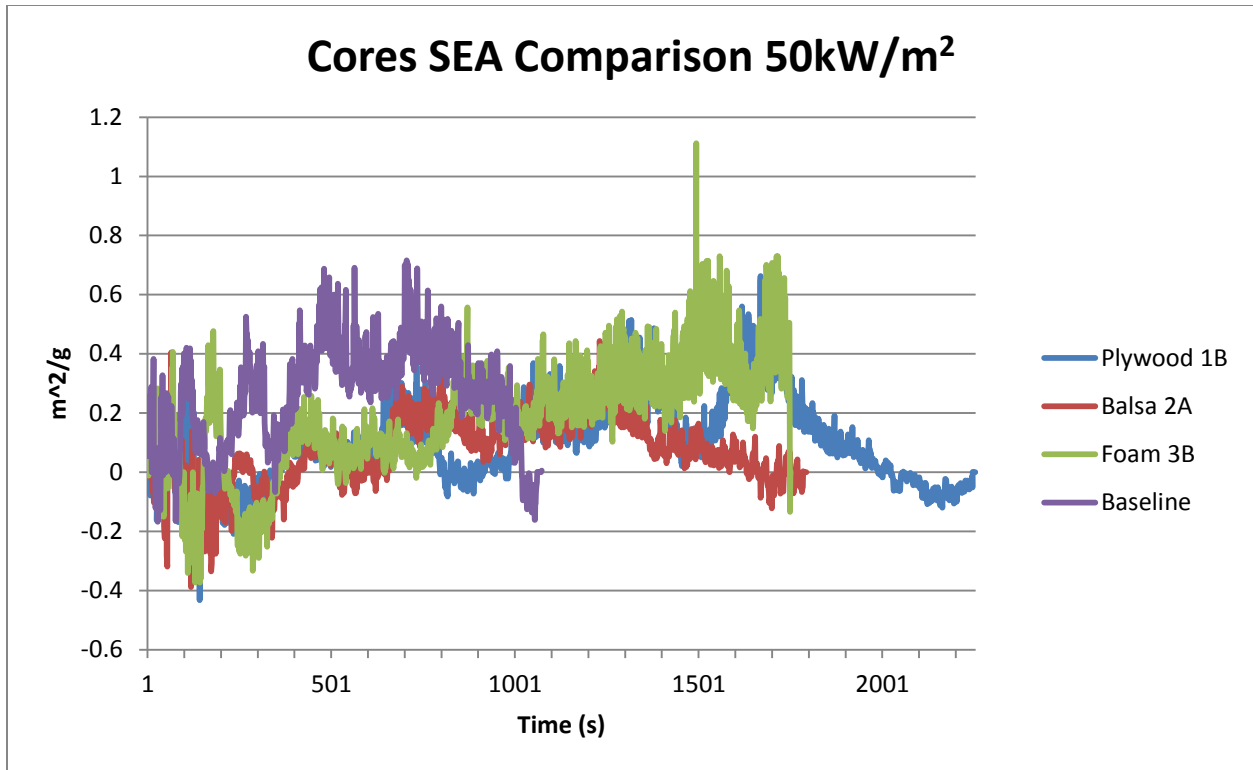
Specific Extinction Area analysis – 75kW

Thirteen FRP systems are analyzed in the context of specific extinction area. This briefing highlights all thirteen systems as well as groups the systems in terms of pigments, filler, gel, and aggregate composition for comparison purposes.

Baseline FRP System
No gelcoat
Polymer concrete: Norsodyne H 81269 TF with 6% cobalt & DDM-9
Alumina Trihydrate: 10% of resin by weight
Sand: 150% of resin by weight, split evenly between #0/30 and #2/16
1-1/2 parts sand to 1 part resin
No pigment
Approximately 60 mil thickness (aggregate dependent)
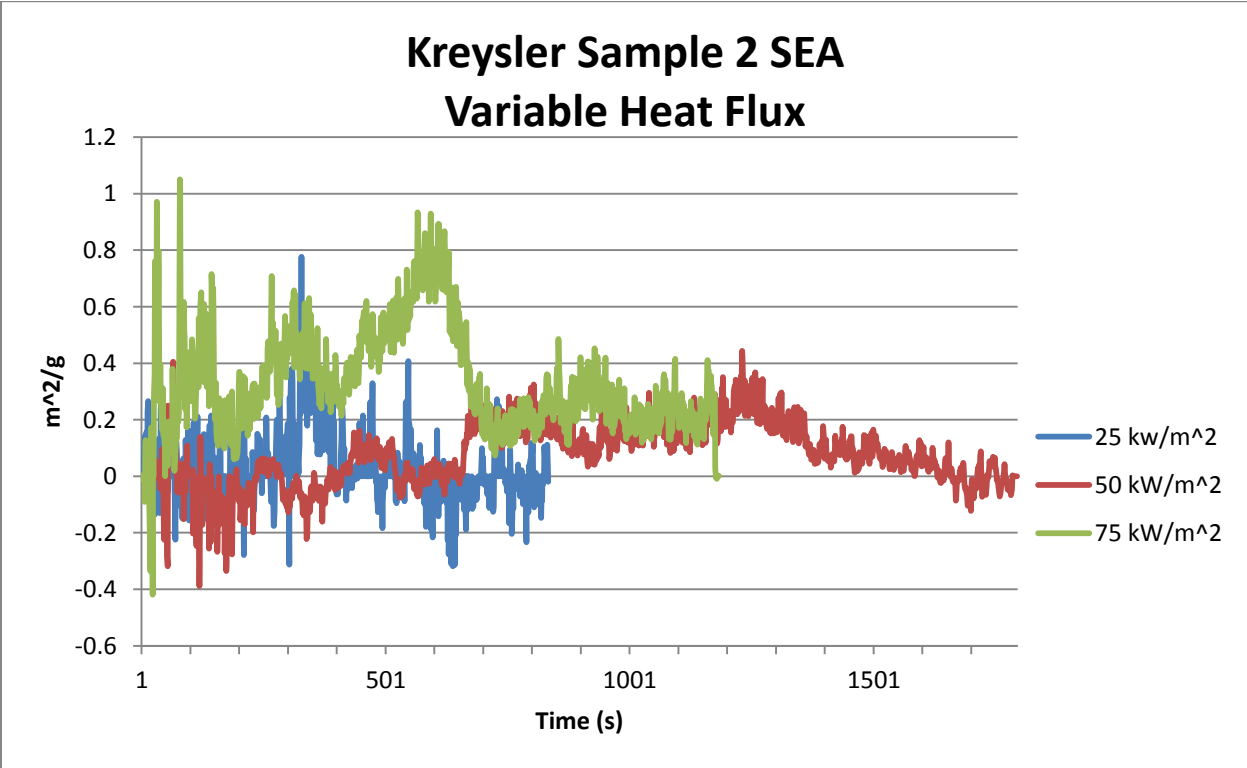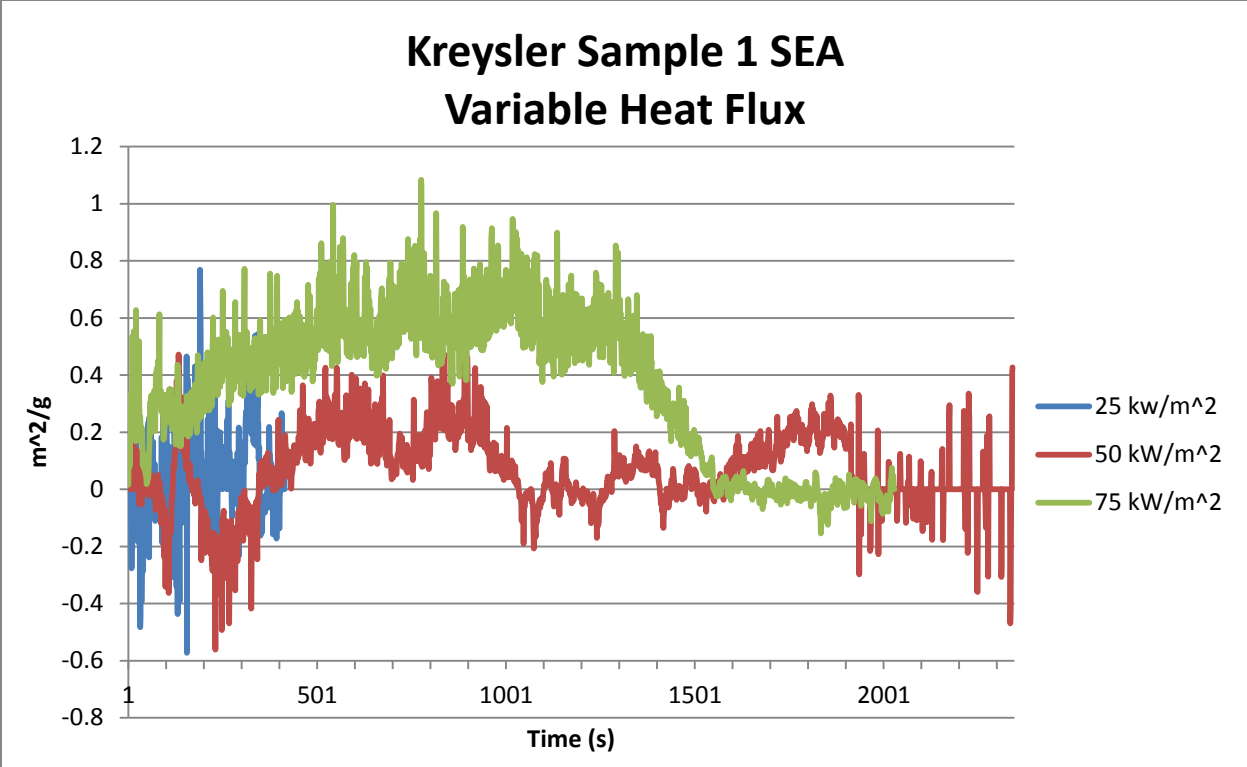3/16" single skin laminate: Norsodyne H 81269 TF with 6% cobalt & DDM-9
4 layers of 1.5 ounce chopped strand mat
Glass to resin ratio range: 25:75 to 35:65 by weight

System 1 – Addition of 1/2" plywood core & 3/16" rear skin (Note that core separation was observed in several samples)
**System 2** – Addition of 3/4" balsa core & 3/16" rear skin

System 3 – Addition of 1/2" polyurethane foam core & 3/16" rear skin

System 4 – Bronze filler instead of sand: 1 part bronze powder to 1 part resin by weight

System 5 – Aluminum filler instead of sand: 1 part aluminum powder to 2 parts resin by weight

System 6 – Straight Norsodyne H 81269 TF as gelcoat in place of resin based polymer concrete

System 7 – Addition of white pigment to polymer concrete

System 8 – Addition of grey pigment to polymer concrete

System 9 – Addition of beige pigment to polymer concrete

System 10 – #0/30 aggregate only

System 11 – #0/60 aggregate only

System 12 – #2/16 aggregate only

System 13 – DCPD Laminate resin (with 6 layers of glass) instead of Norsodyne

Baseline SEA 75kW/m²

Kreysler Sample 1 SEA 75kW/m²

Kreysler Sample 2 SEA 75kW/m²
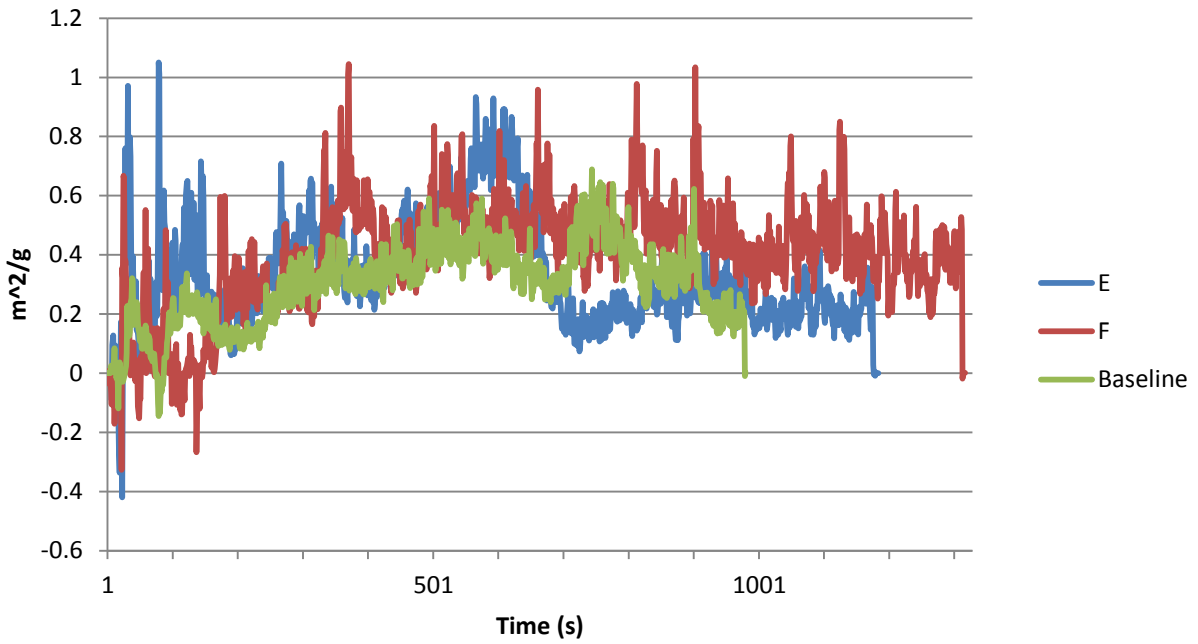
Kreysler Sample 3 SEA 75kW/m²

Kreysler Sample 4 SEA 75kW/m²

Kreysler Sample 5 SEA 75kW/m²

Kreysler Sample 6 SEA 75kW/m²

Kreysler Sample 7 SEA 75kW/m²

Kreysler Sample 8 SEA 75kW/m²

Kreysler Sample 9 SEA 75kW/m²
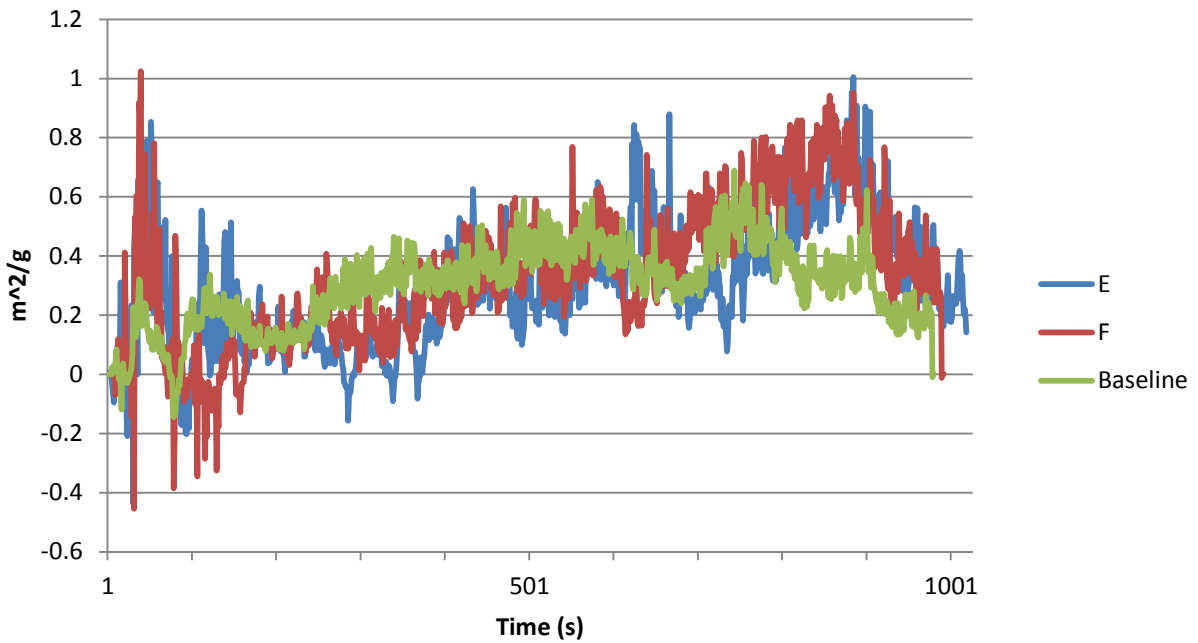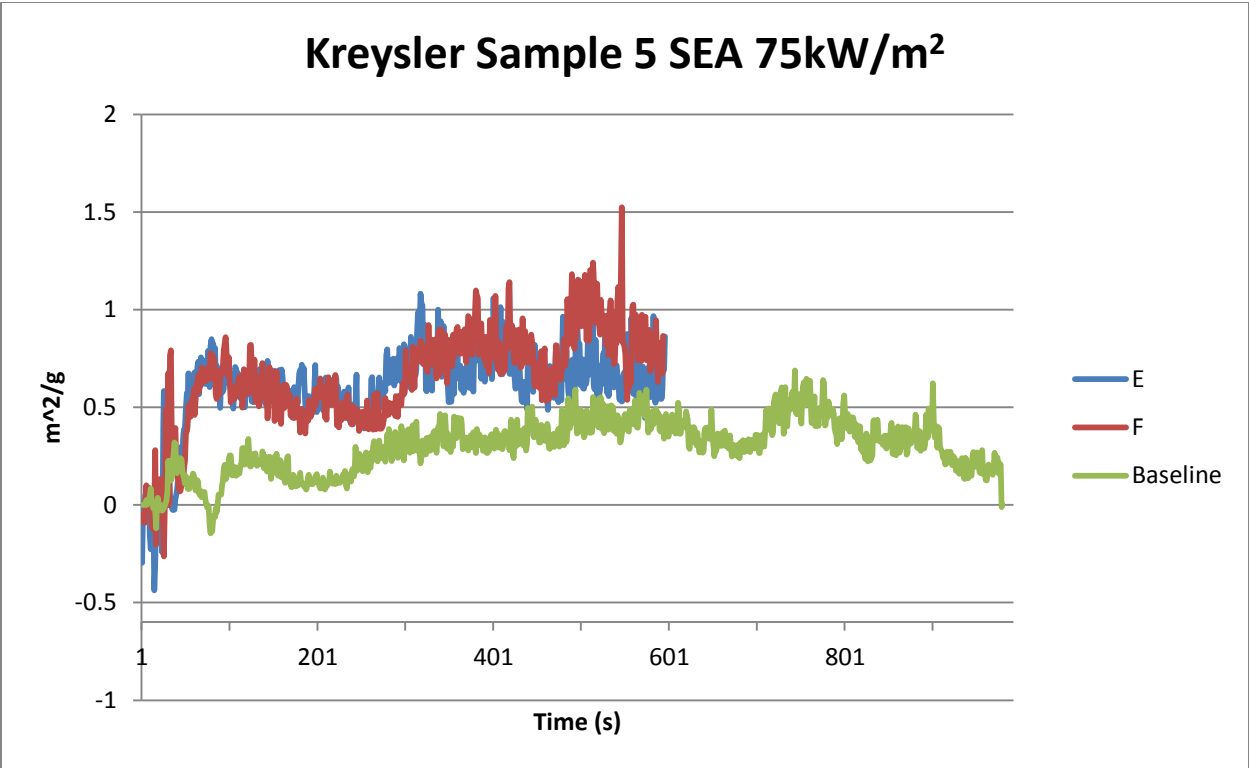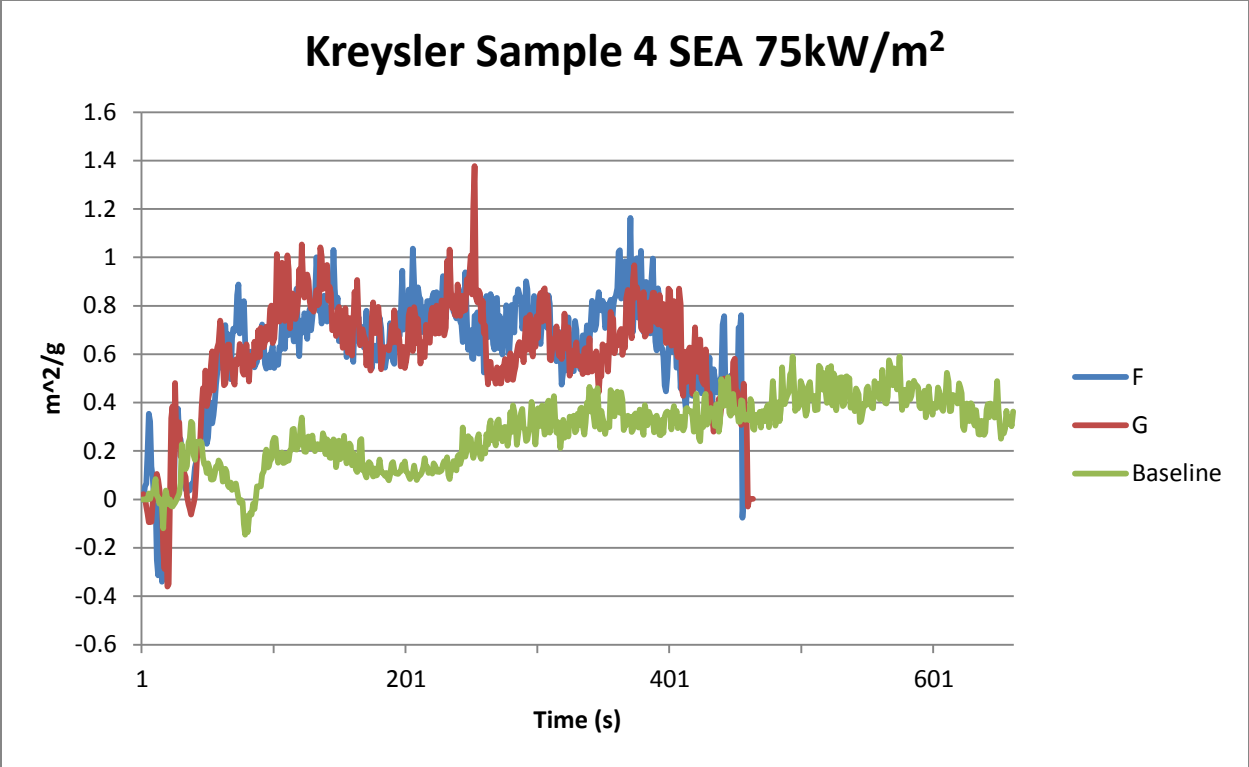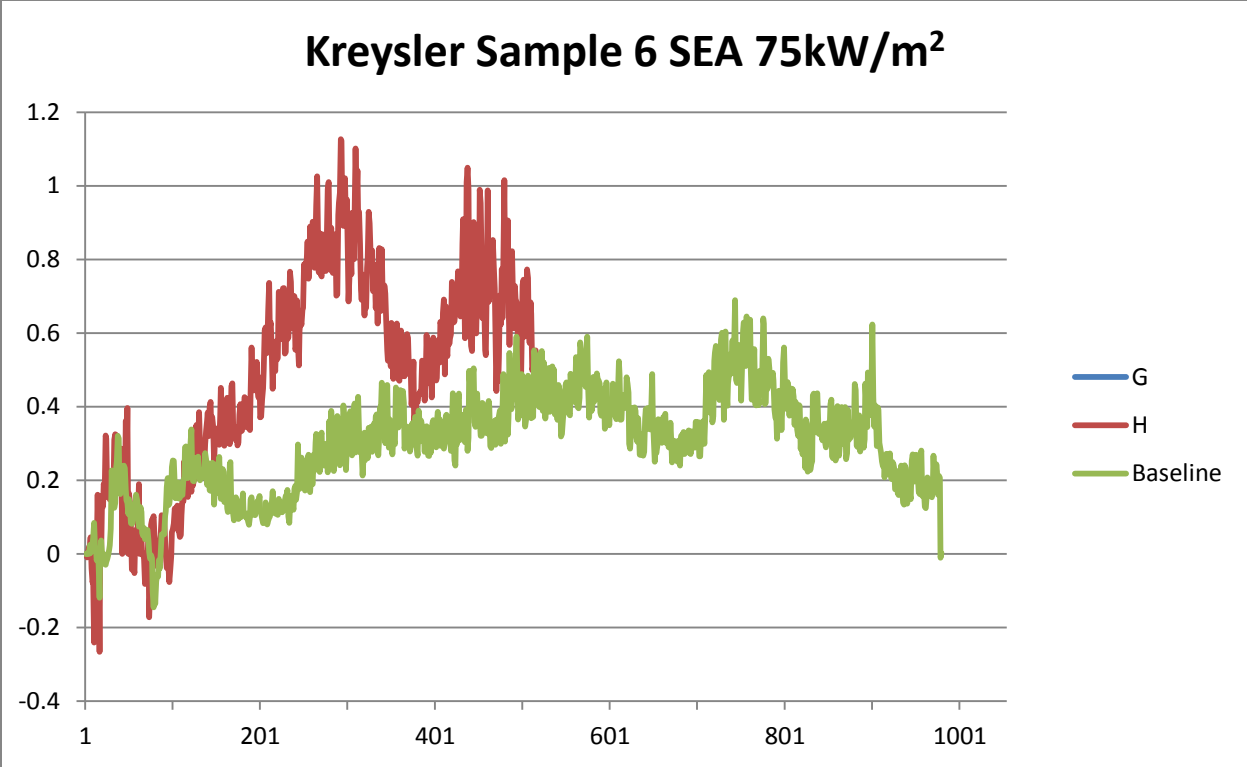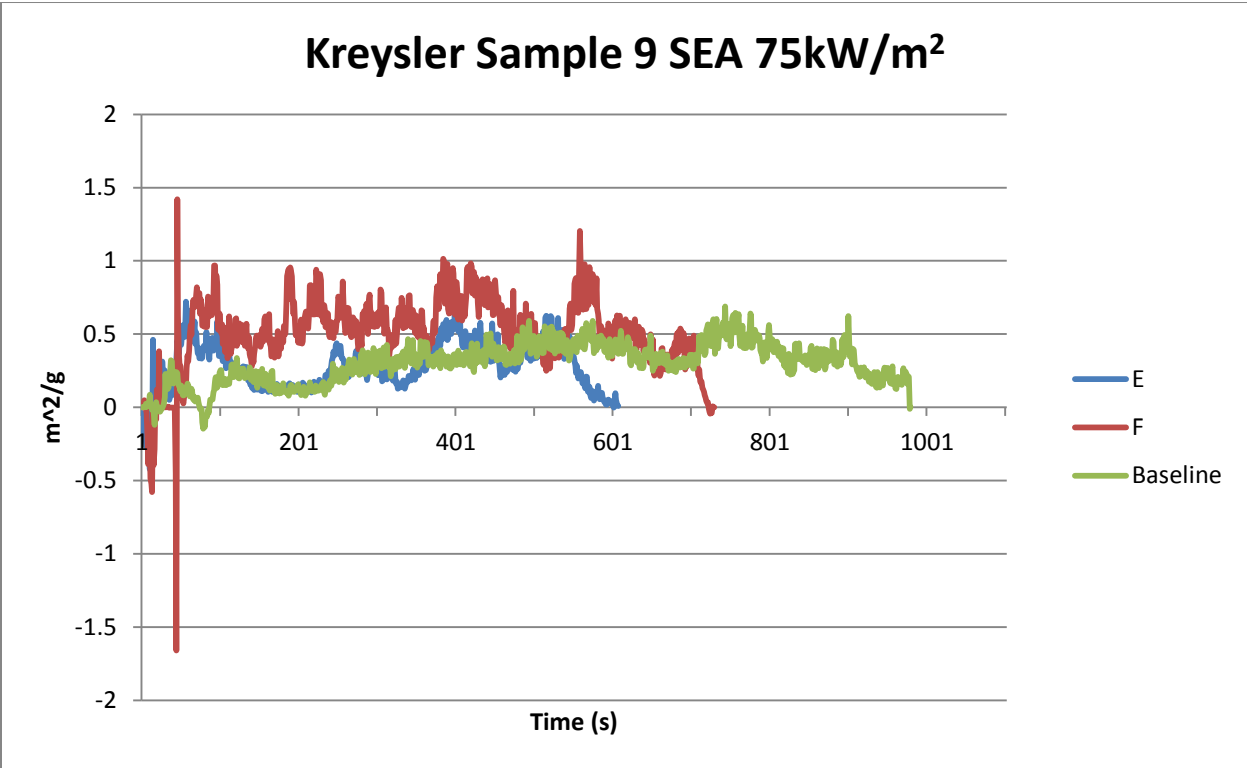
Kreysler Sample 10 SEA 75kW/m²

Kreysler Sample 11 SEA 75kW/m²

Kreysler Sample 12 SEA 75kW/m²
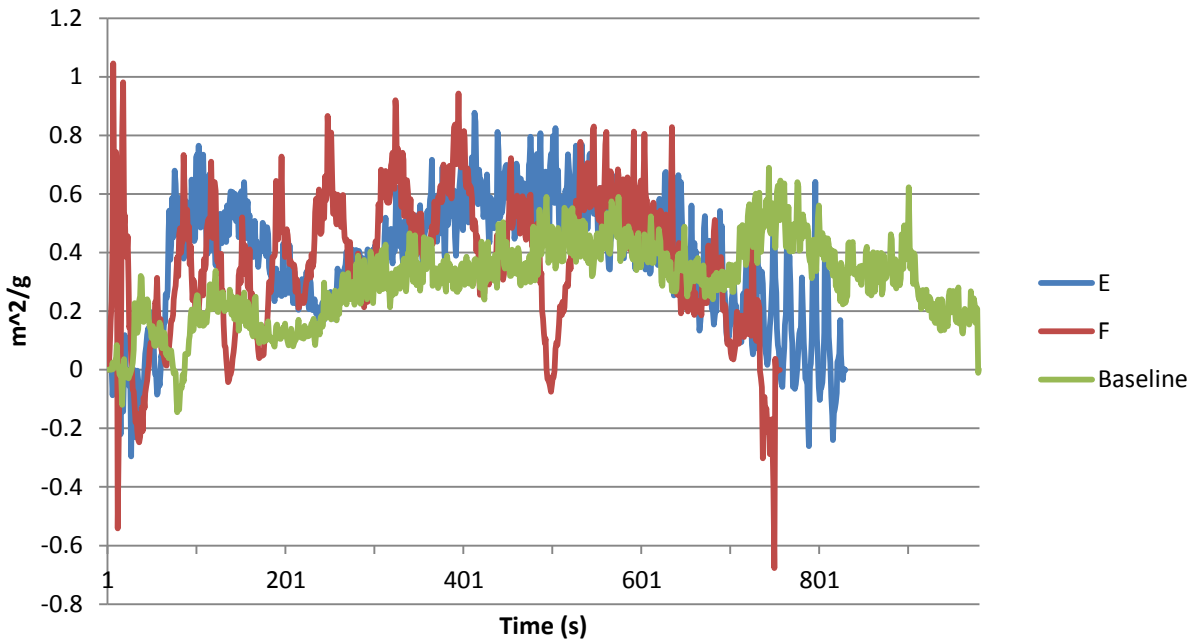
Kreysler Sample 13 SEA 75kW/m²
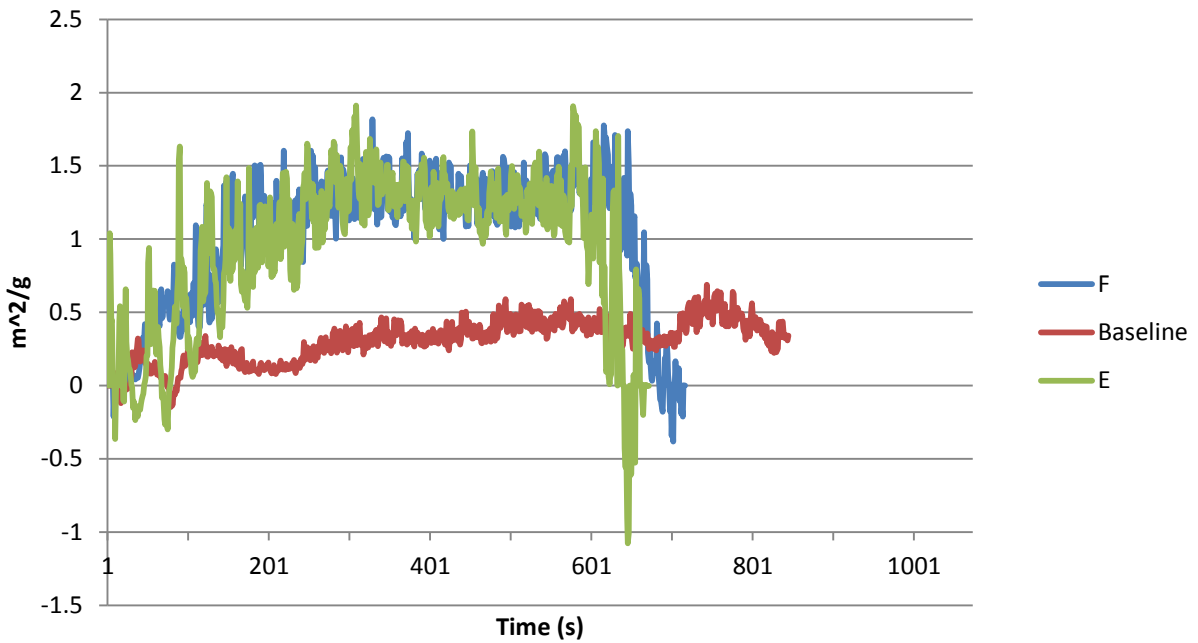
Pigment SEA Comparisons 75kW/m²
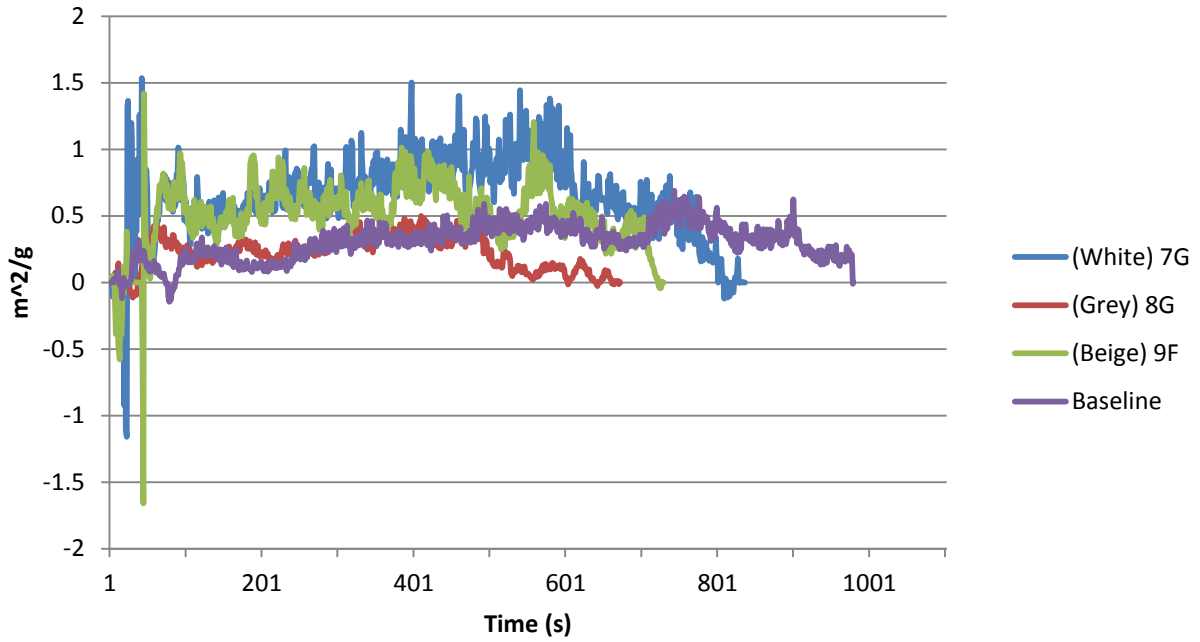
Aggregate SEA Comparison 75kW/m²
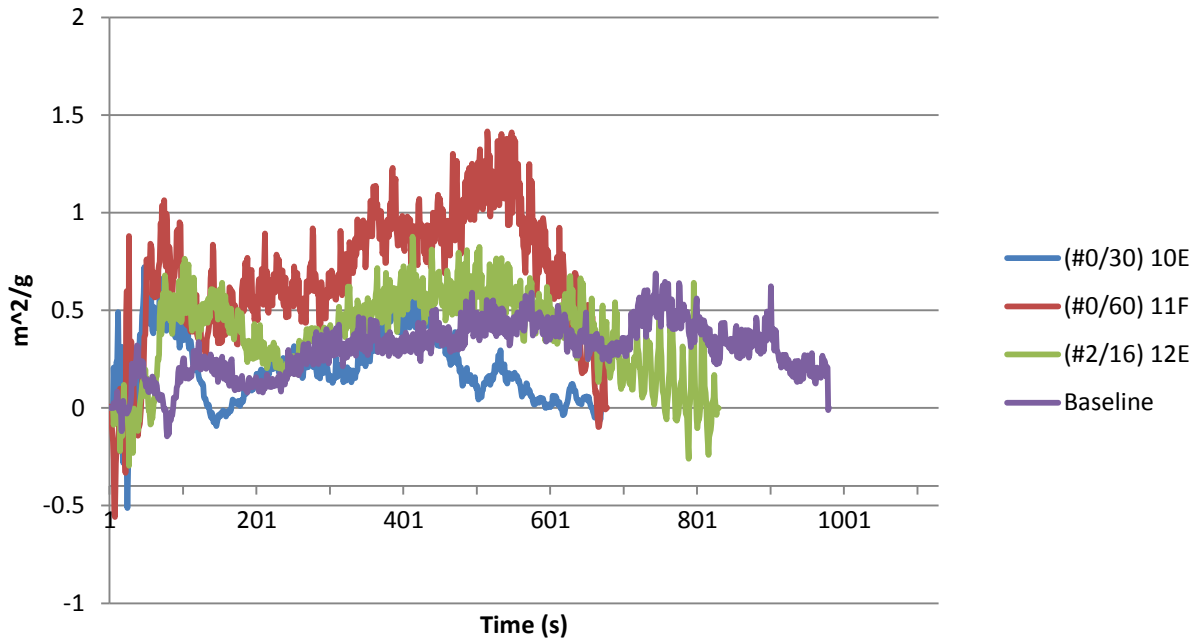
Filler SEA Comparison 75kW/m²

Gel SEA Comparison 75kW/m²

K-137
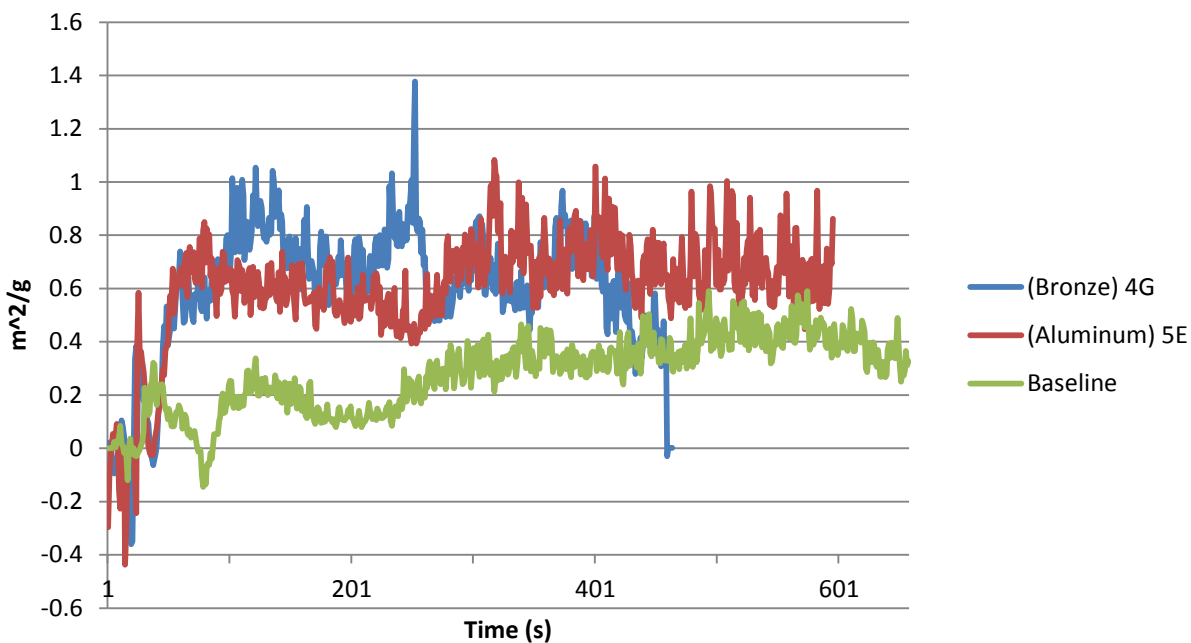
Cores SEA Comparison 75kW/m²
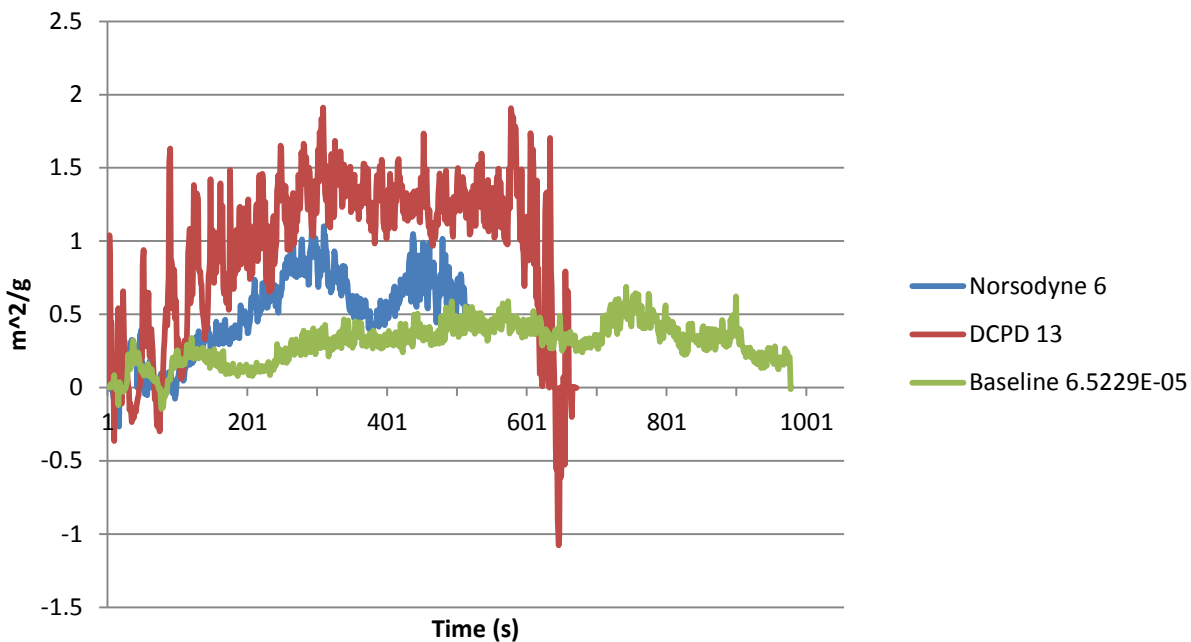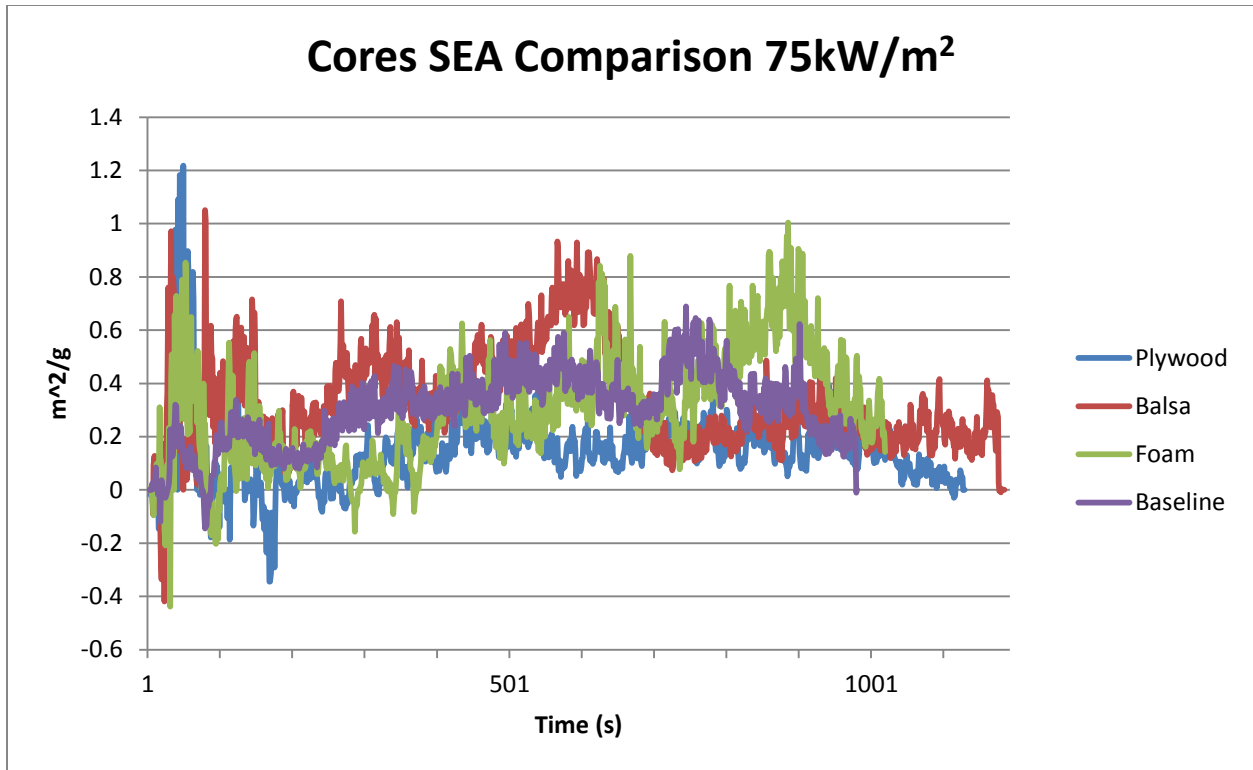
Specific Extinction Area analysis – Variable heat flux

Thirteen FRP systems are analyzed in the context of specific extinction area. This briefing highlights all thirteen systems as well as groups the systems in terms of pigments, filler, gel, and aggregate composition for comparison purposes.

Baseline FRP System
No gelcoat
Polymer concrete: Norsodyne H 81269 TF with 6% cobalt & DDM-9
Alumina Trihydrate: 10% of resin by weight
Sand: 150% of resin by weight, split evenly between #0/30 and #2/16
1-1/2 parts sand to 1 part resin
No pigment
Approximately 60 mil thickness (aggregate dependent)
3/16" single skin laminate: Norsodyne H 81269 TF with 6% cobalt & DDM-9
4 layers of 1.5 ounce chopped strand mat
Glass to resin ratio range: 25:75 to 35:65 by weight

System 1 – Addition of 1/2" plywood core & 3/16" rear skin (Note that core separation was observed in several samples)
System 2 – Addition of 3/4" balsa core & 3/16" rear skin

System 3 – Addition of 1/2" polyurethane foam core & 3/16" rear skin

System 4 – Bronze filler instead of sand: 1 part bronze powder to 1 part resin by weight

System 5 – Aluminum filler instead of sand: 1 part aluminum powder to 2 parts resin by weight

System 6 – Straight Norsodyne H 81269 TF as gelcoat in place of resin based polymer concrete

System 7 – Addition of white pigment to polymer concrete

System 8 – Addition of grey pigment to polymer concrete

System 9 – Addition of beige pigment to polymer concrete

System 10 – #0/30 aggregate only

System 11 – #0/60 aggregate only

System 12 – #2/16 aggregate only

System 13 – DCPD Laminate resin (with 6 layers of glass) instead of Norsodyne

Kreysler Sample 1 SEA
Variable Heat Flux

Kreysler Sample 2 SEA
Variable Heat Flux

Kreysler Sample 3 SEA
Variable Heat Flux
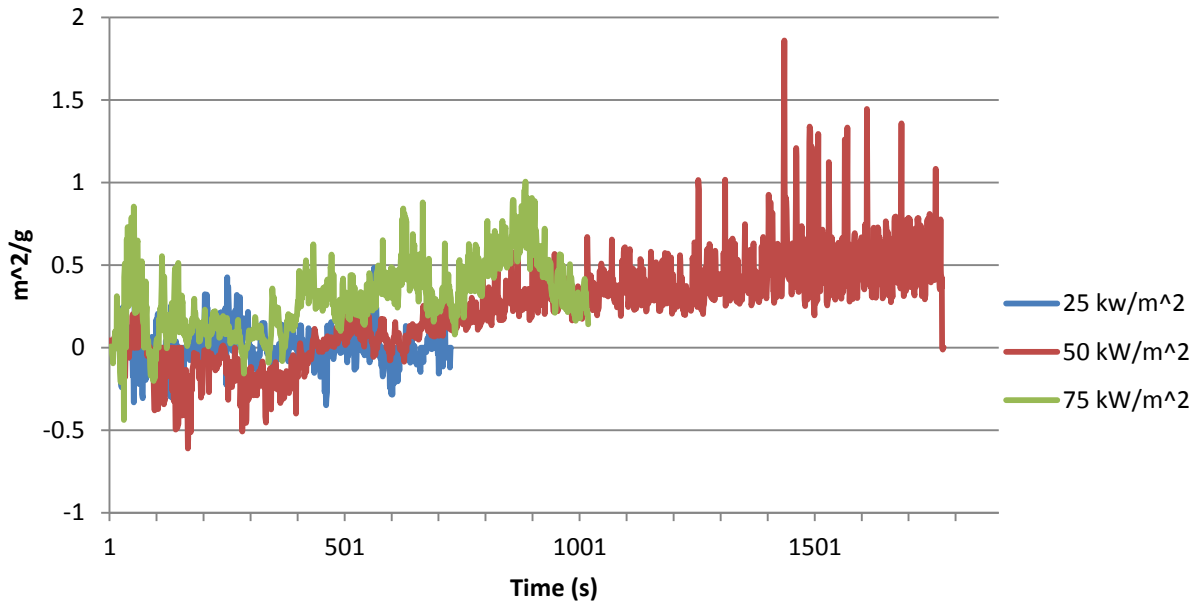
Kreysler Sample 4 SEA
Variable Heat Flux
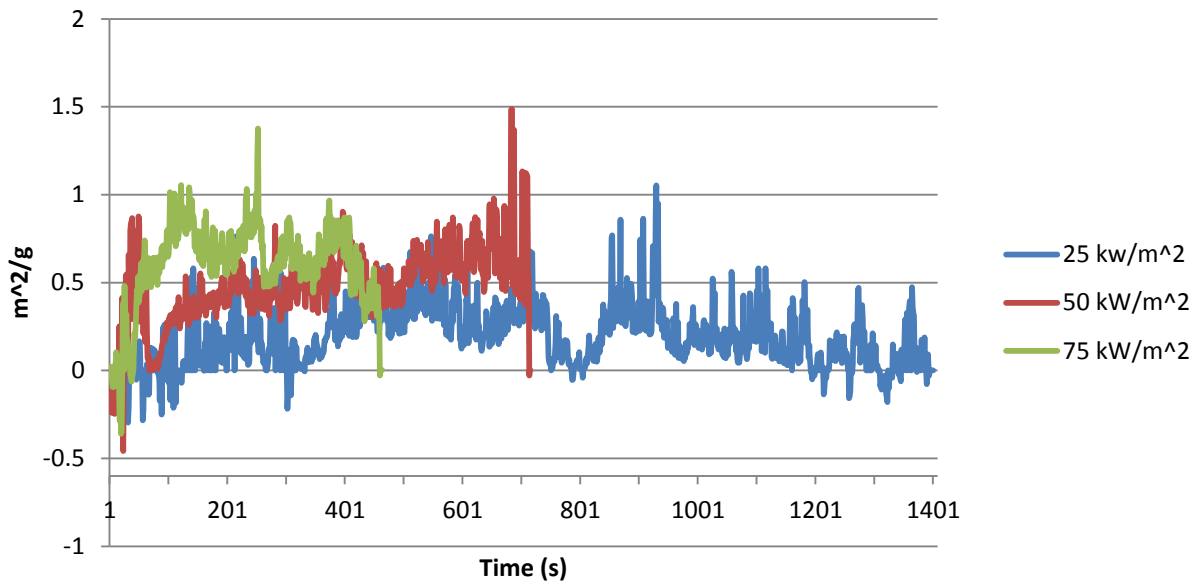
Kreysler Sample 5 SEA Variable Heat Flux

25 kw/m^2
50 kW/m^2
75 kW/m^2
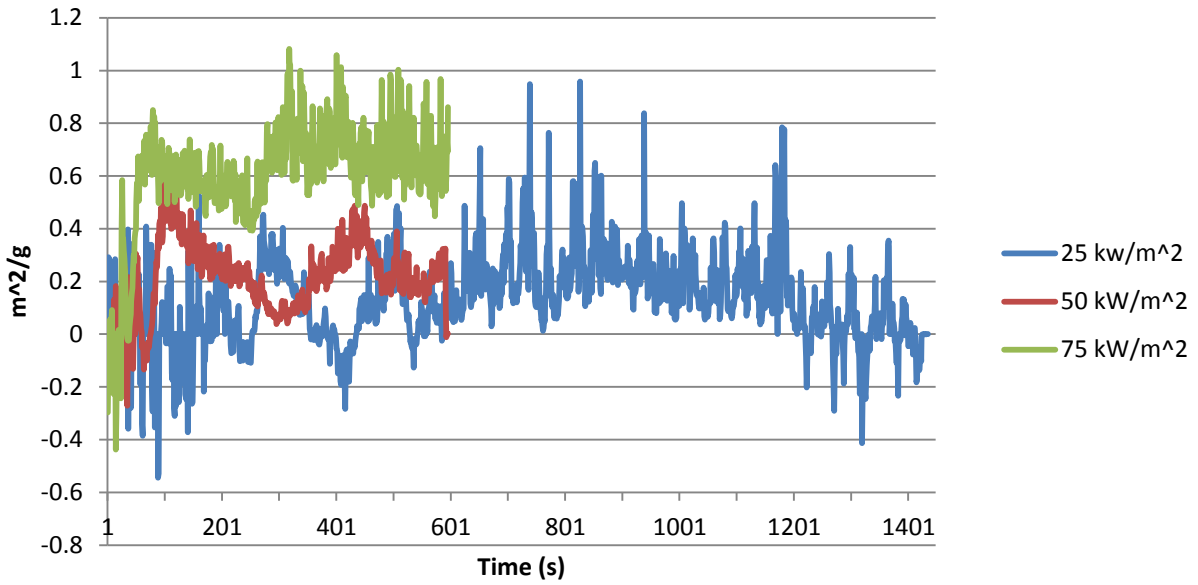
Kreysler Sample 6 SEA Variable Heat Flux

25 kw/m^2
50 kW/m^2
75 kW/m^2
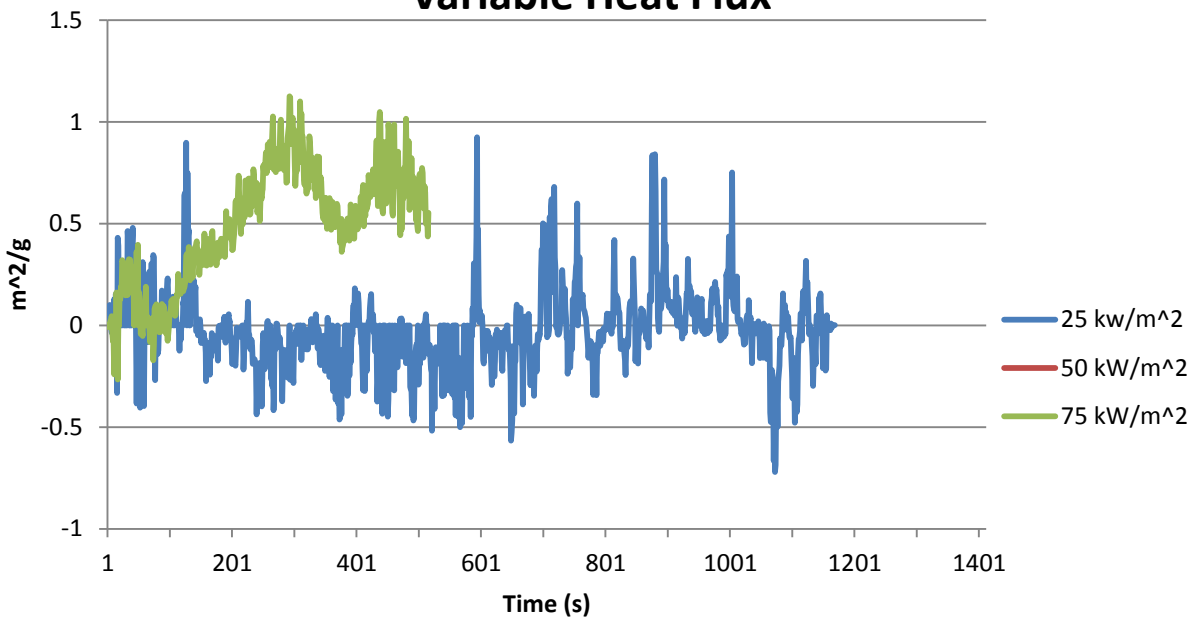
Kreysler Sample 7 SEA
Variable Heat Flux
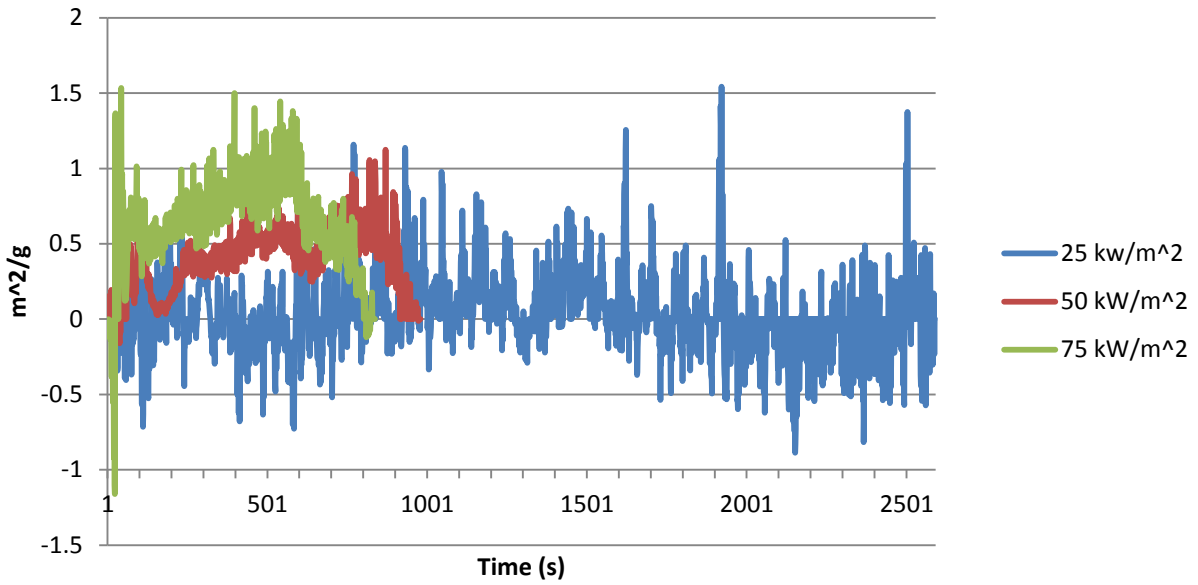
Kreysler Sample 8 SEA
Variable Heat Flux
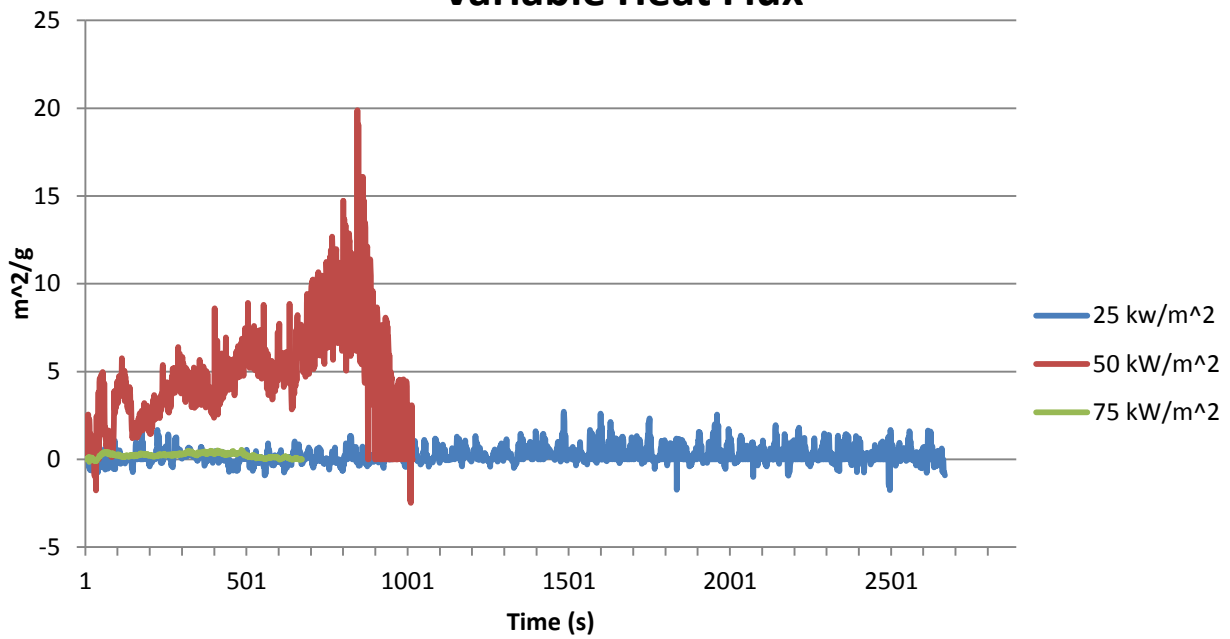
Kreysler Sample 9 SEA
Variable Heat Flux
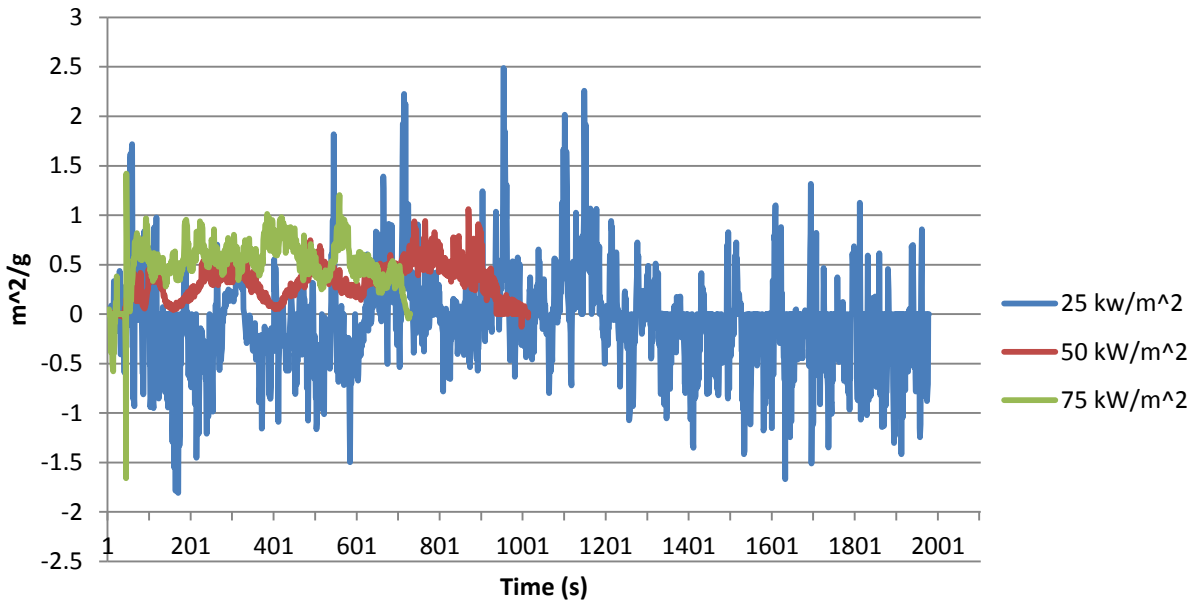
Kreysler Sample 10 SEA
Variable Heat Flux
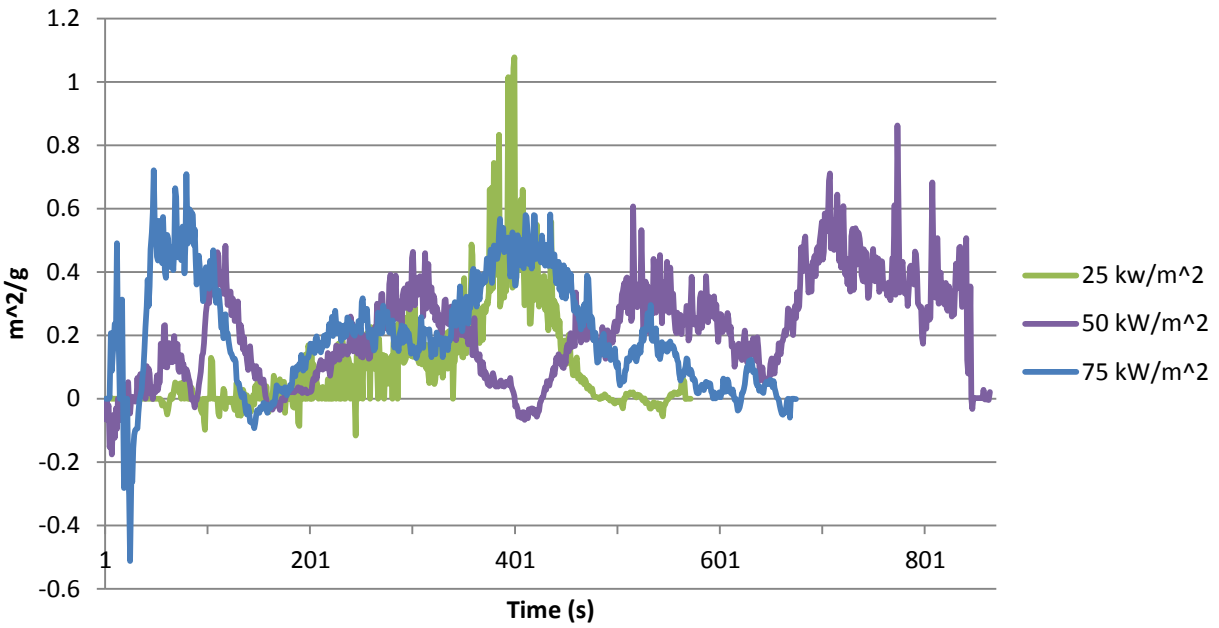
Kreysler Sample 11 SEA
Variable Heat Flux
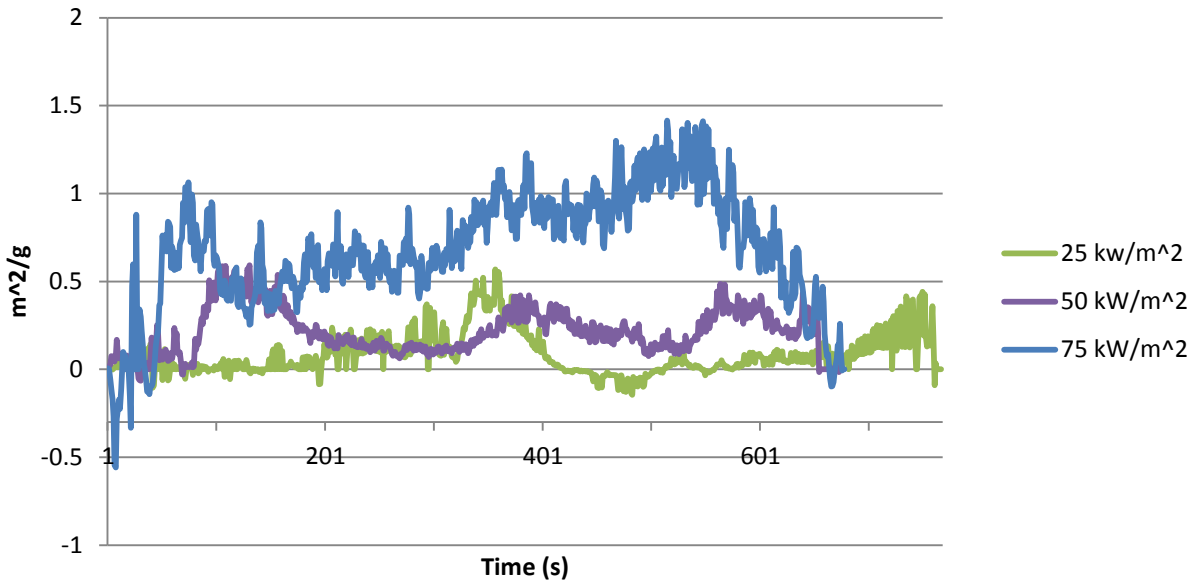
Kreysler Sample 12 SEA
Variable Heat Flux
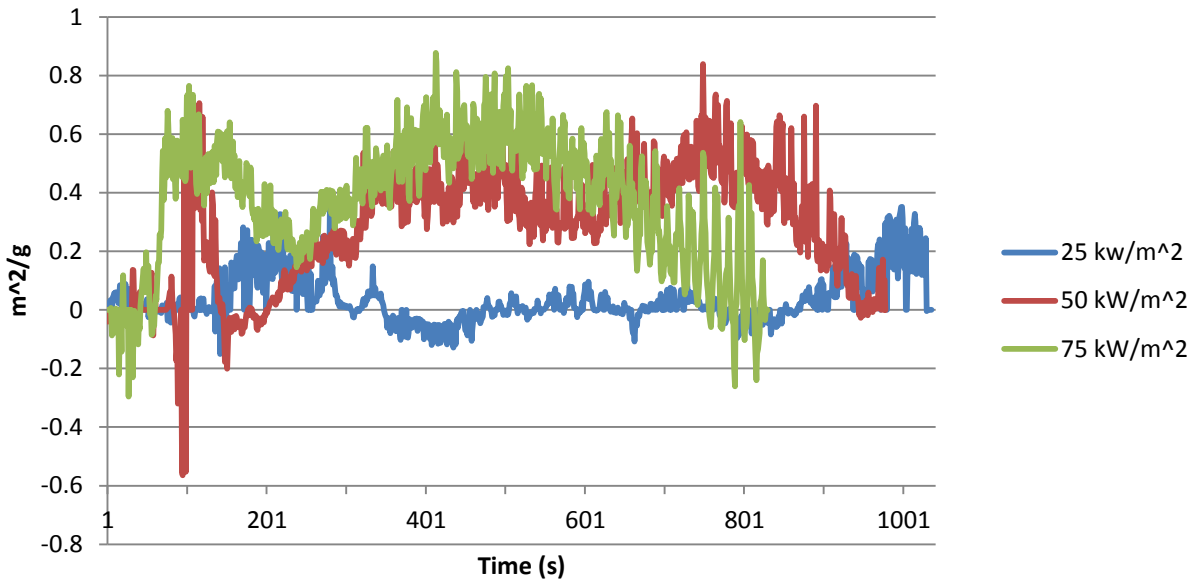
Kreysler Sample 13 SEA
Variable Heat Flux
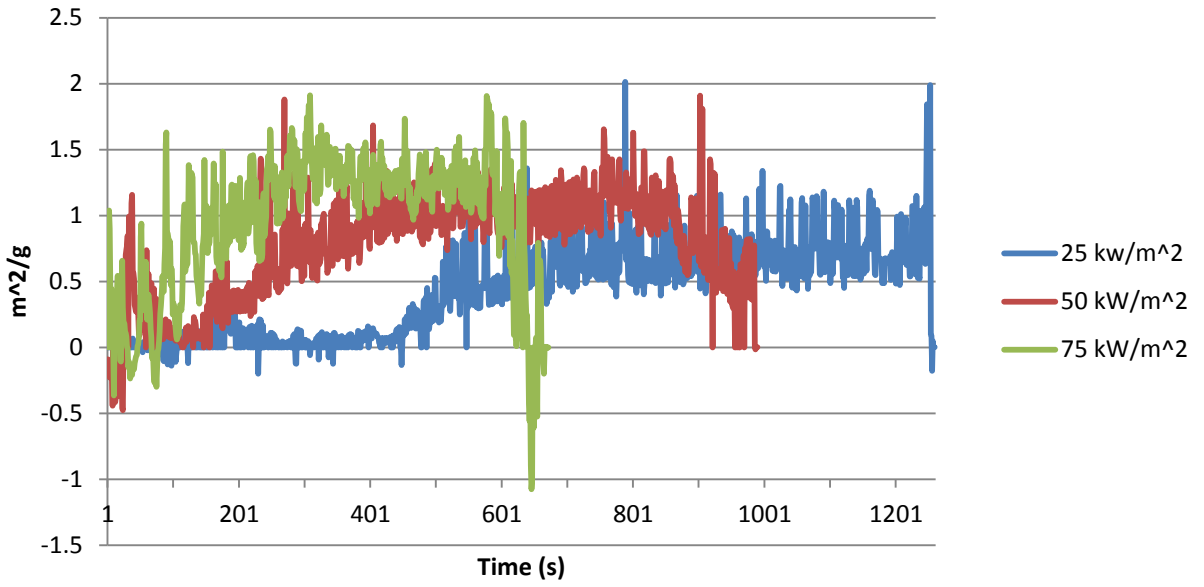
Appendix L   B-Parameter Analysis

B-Parameter Calculation

The following briefing outlines the calculations and assumptions involved in determining the B-parameter.

$$B = .01*(HRRPUA)-1-(Tig/Tb)$$

Where HRRPUA is the average heat release rate per unit area, Tig is the time to ignition, and Tb is the burn duration.

Time of Burn

To identify the most accurate burn duration, two critical points were selected from each test. These points intend to accurately locate the point where the flaming sample loses one dimensionality and begins to edge burn. The two points being considered are referred to as the short burn and the long burn. When the flame cone is reduced to multicellular flaming well below the intensity of the original peak the short burn time is noted. A long burn time is noted when the multicellular flames are further reduced to isolated, candle-like flames.

Data Analysis

With a long and short burn time identified, the remaining values are obtained from the data acquisition system to complete the analysis.

From the data acquisition summary, the following values are collected:

1. Shutter open time
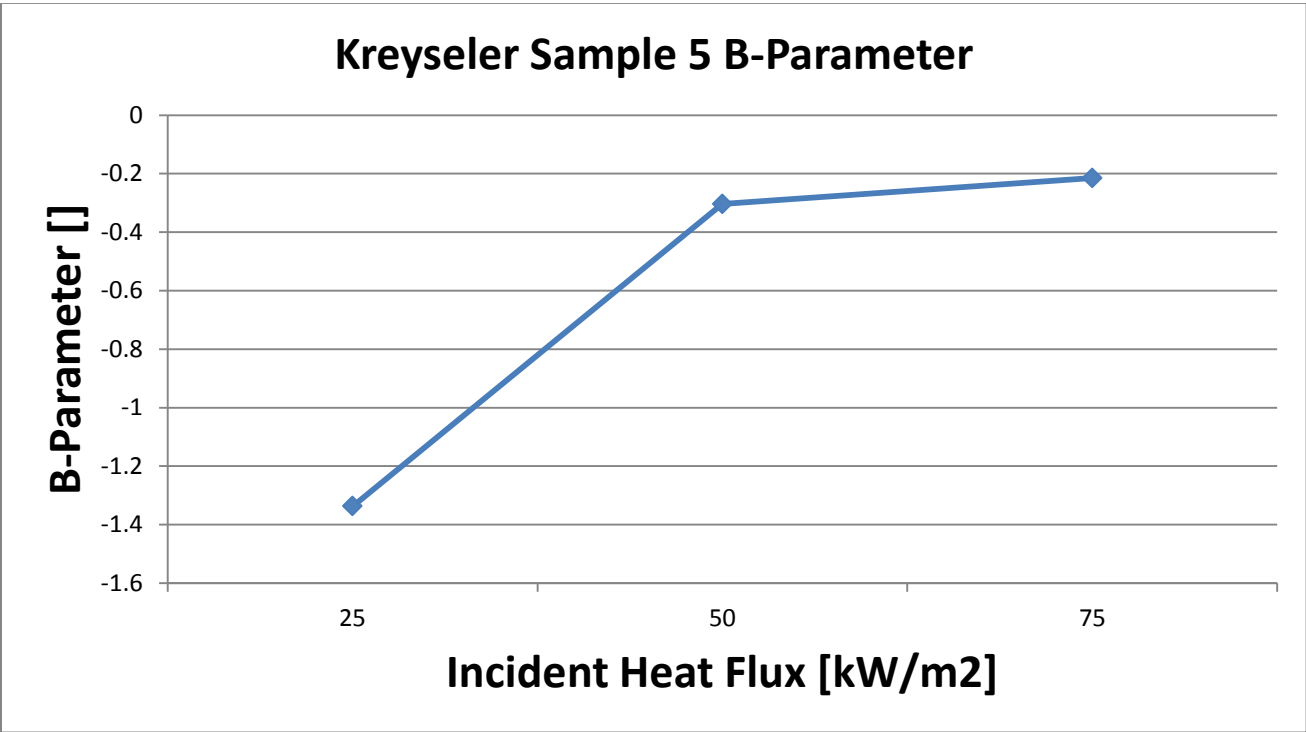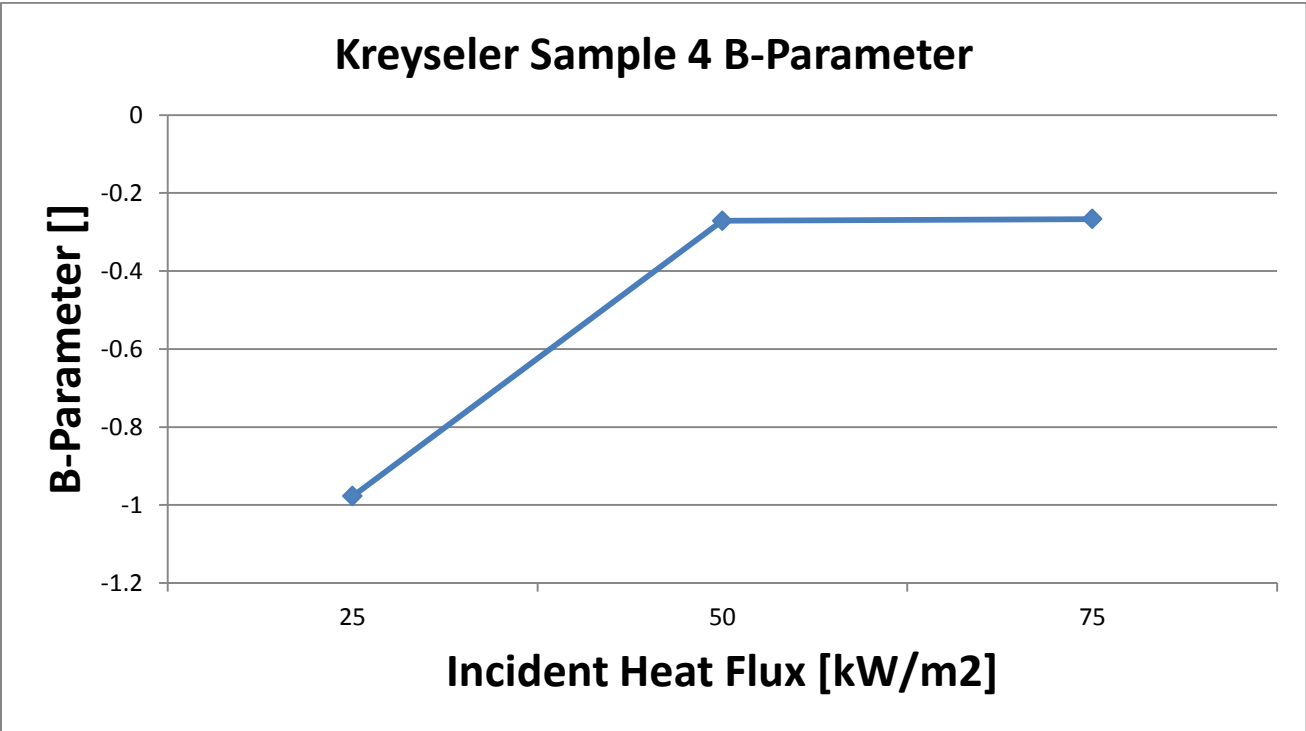2. Time to ignition
3. Short burn time
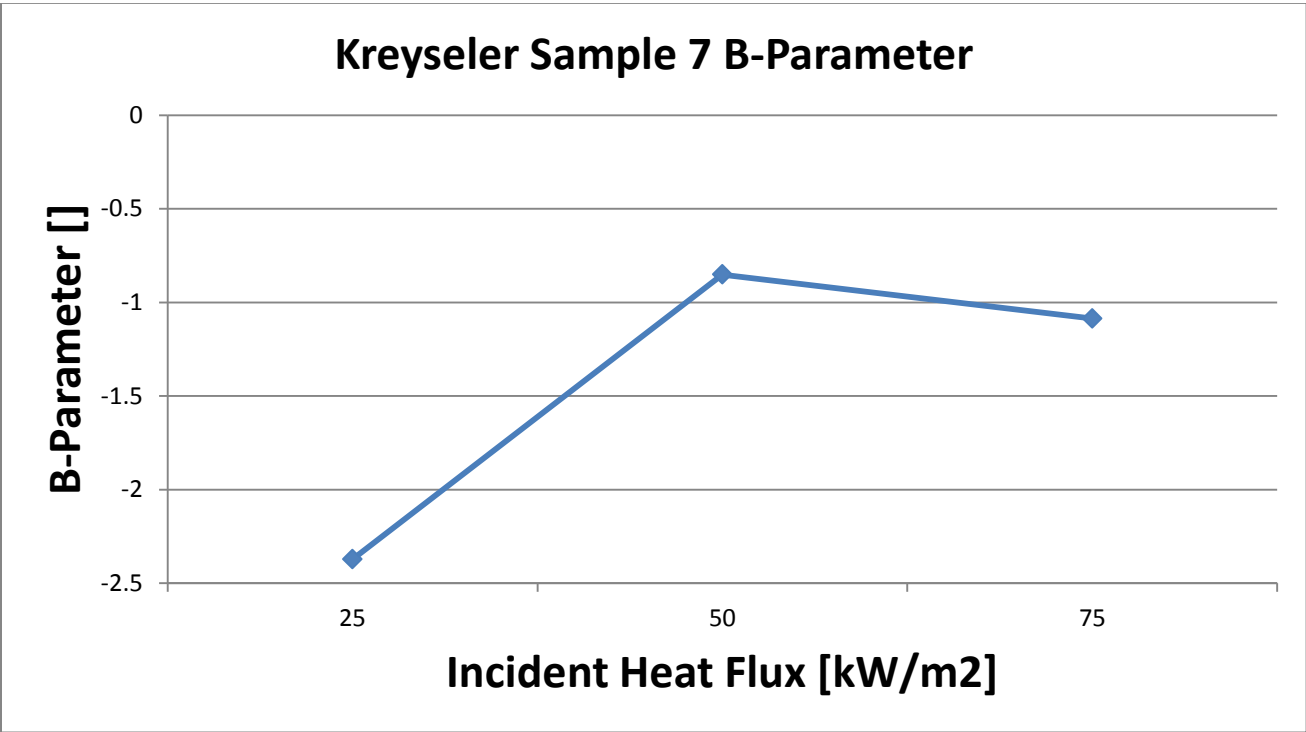4. Long burn time
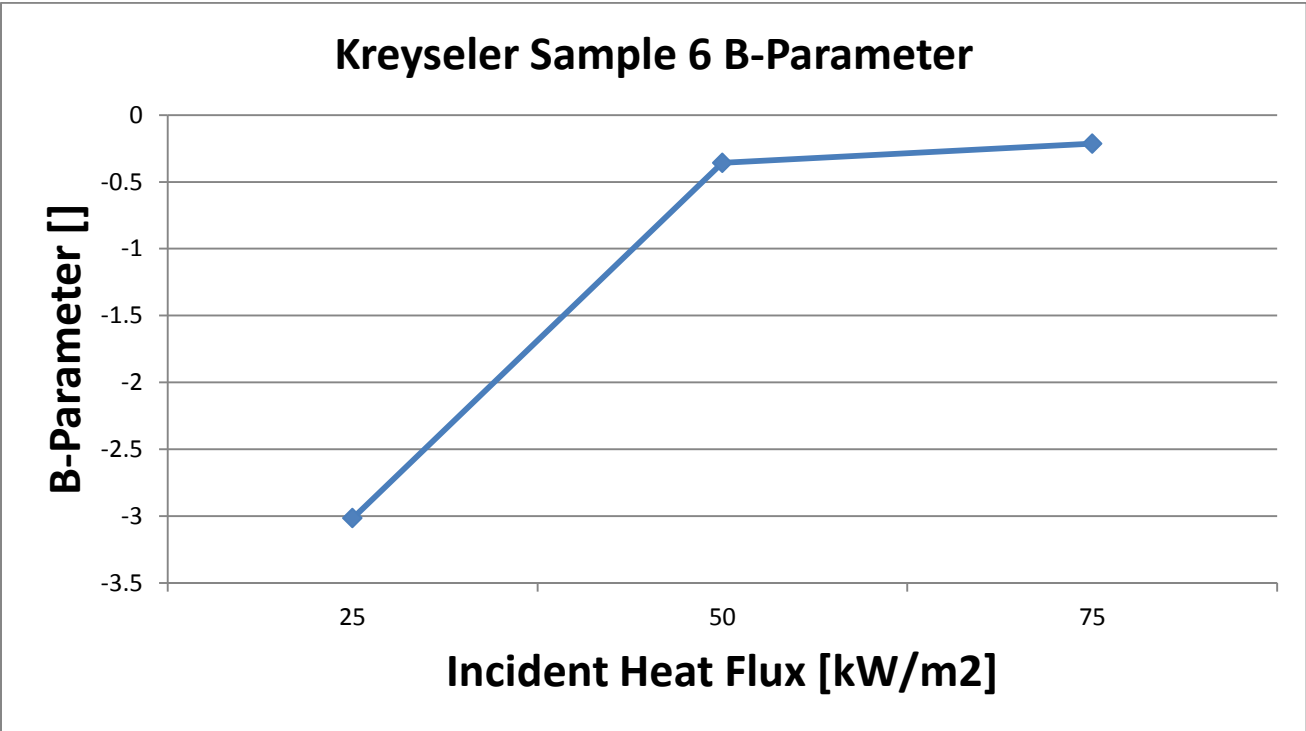
Tig = Time to ignition – Shutter open time
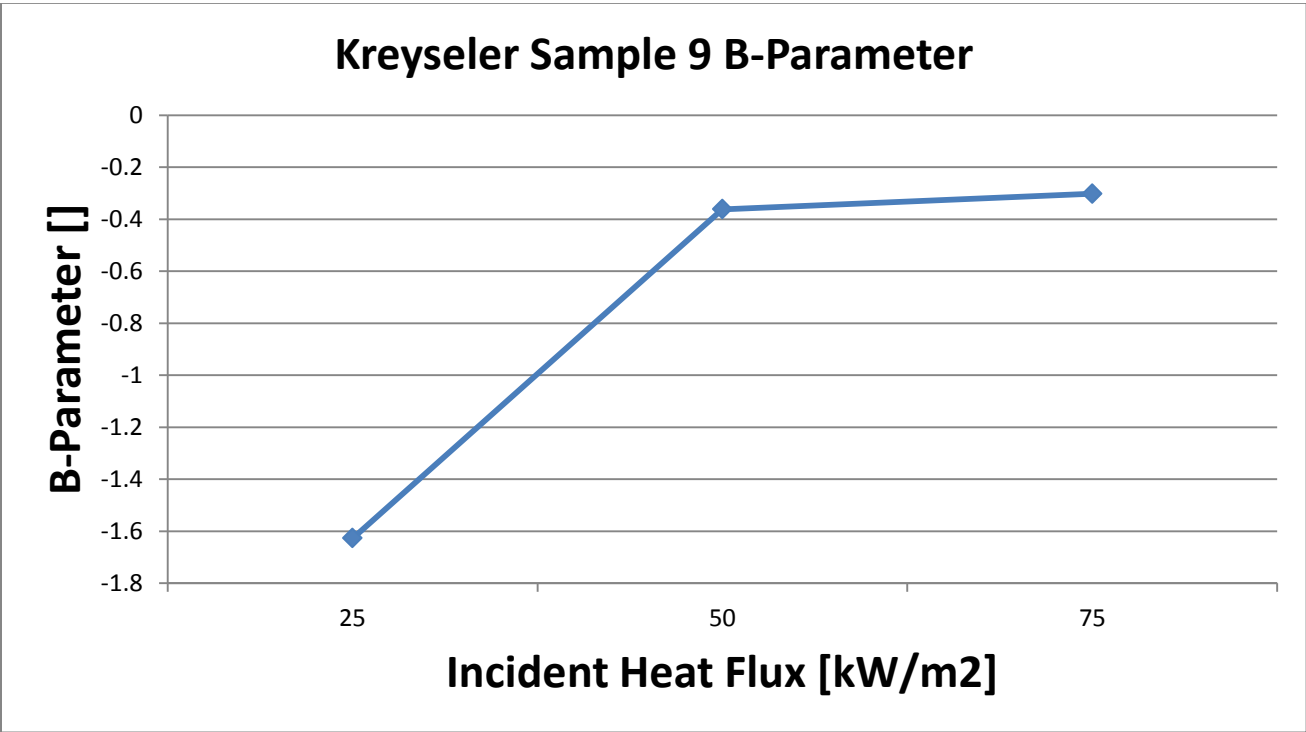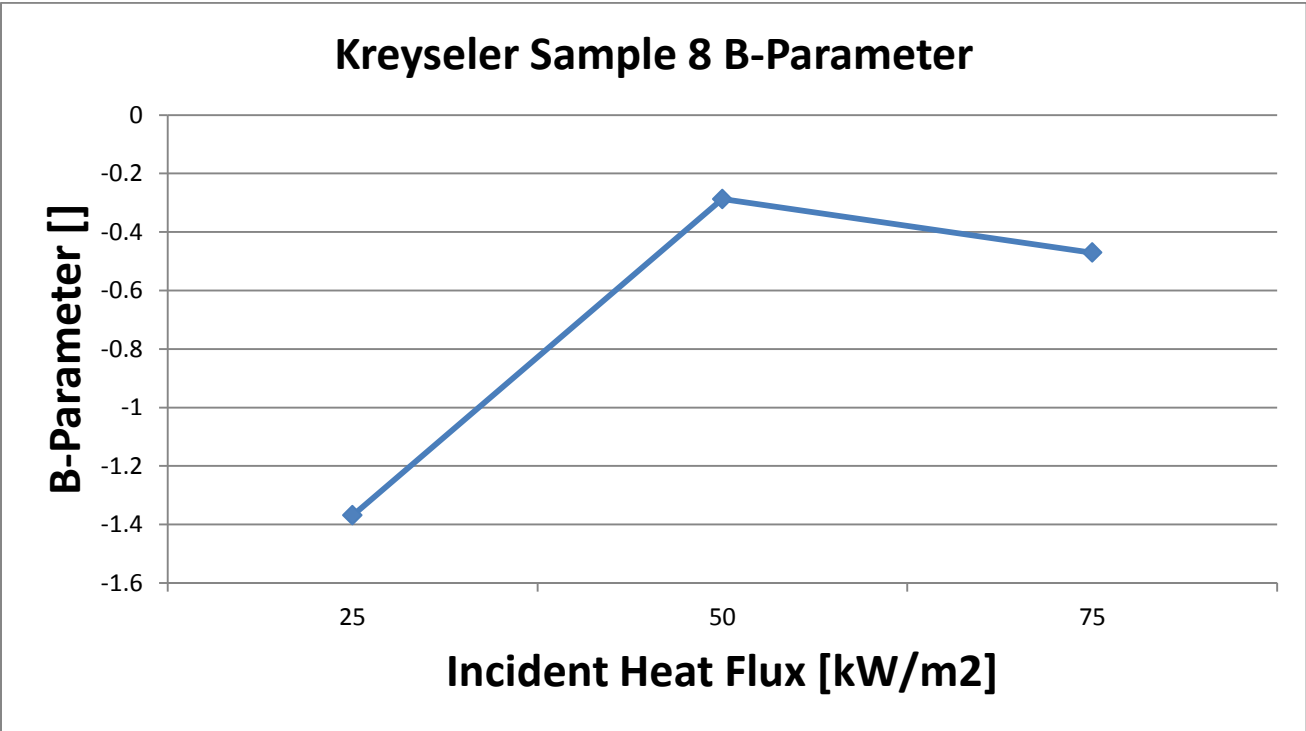**Tb** = Burn time – Time to ignition

Finally, the average HRRPUA for both the long and short burn times are calculated by averaging the HRRPUA of the calculated Burn times described above.
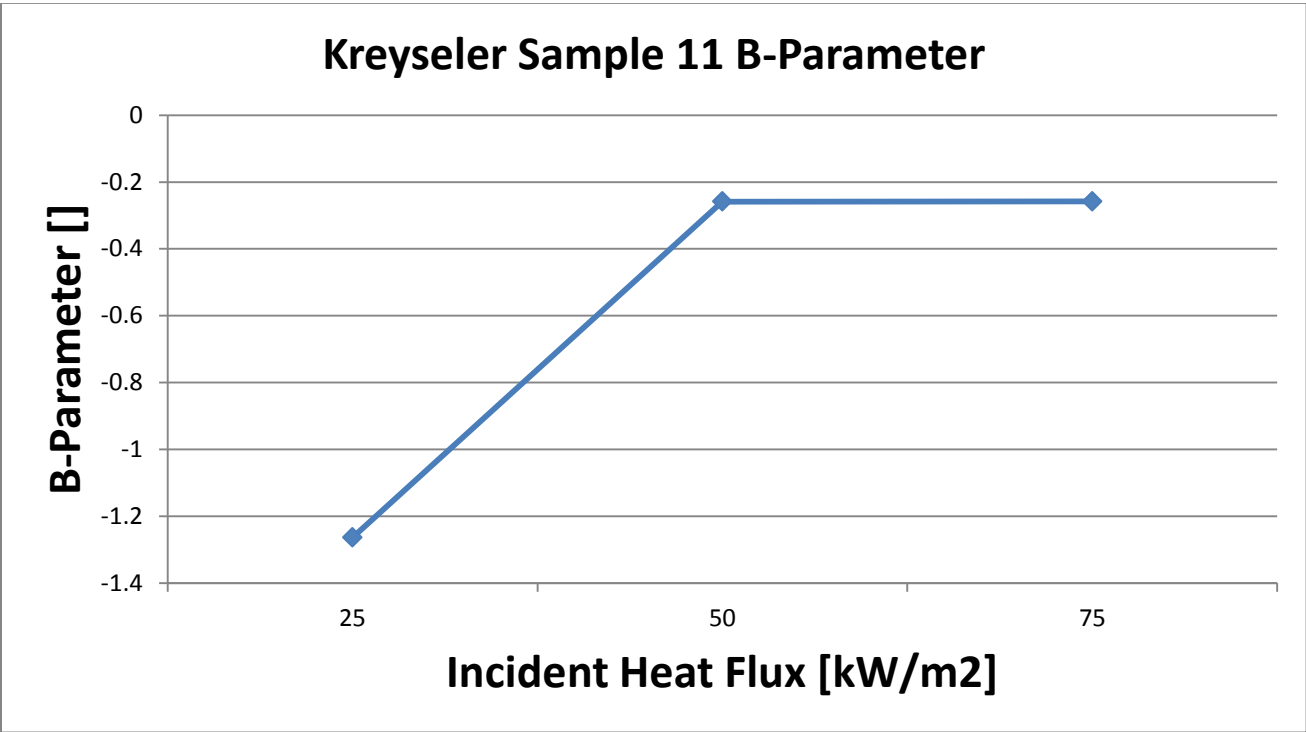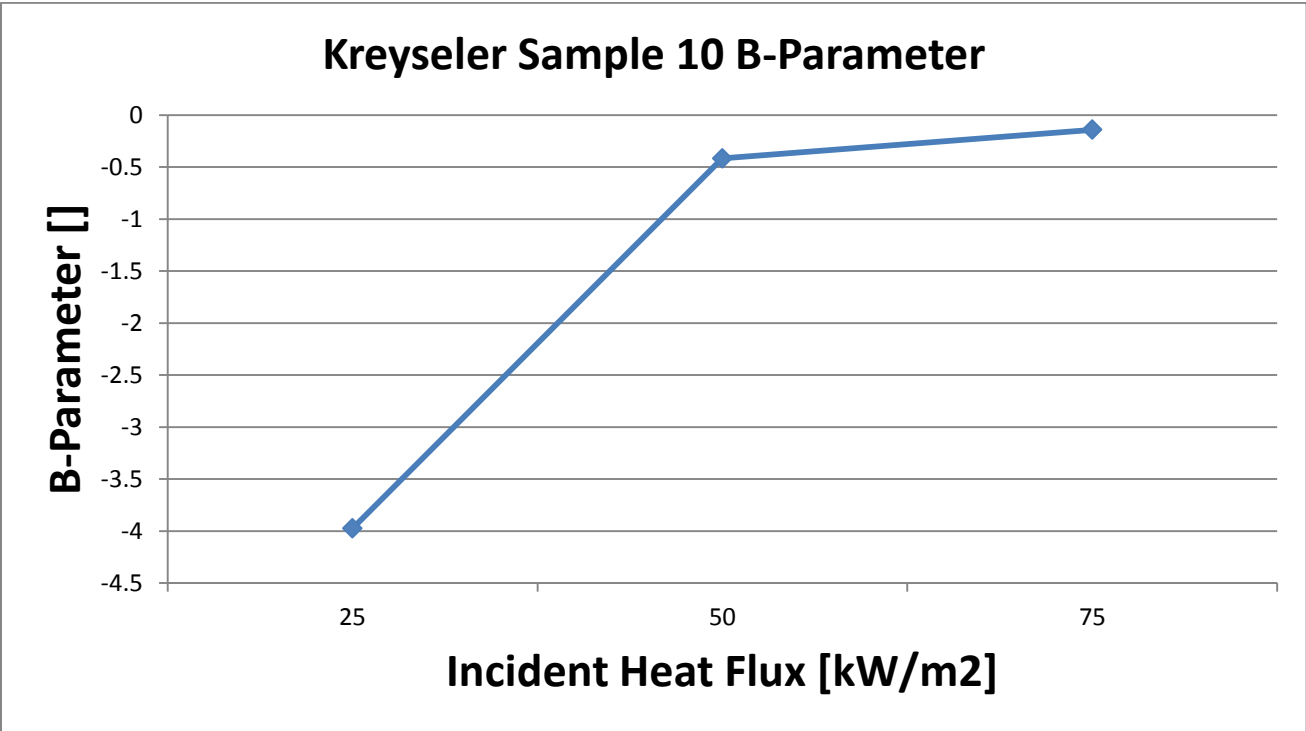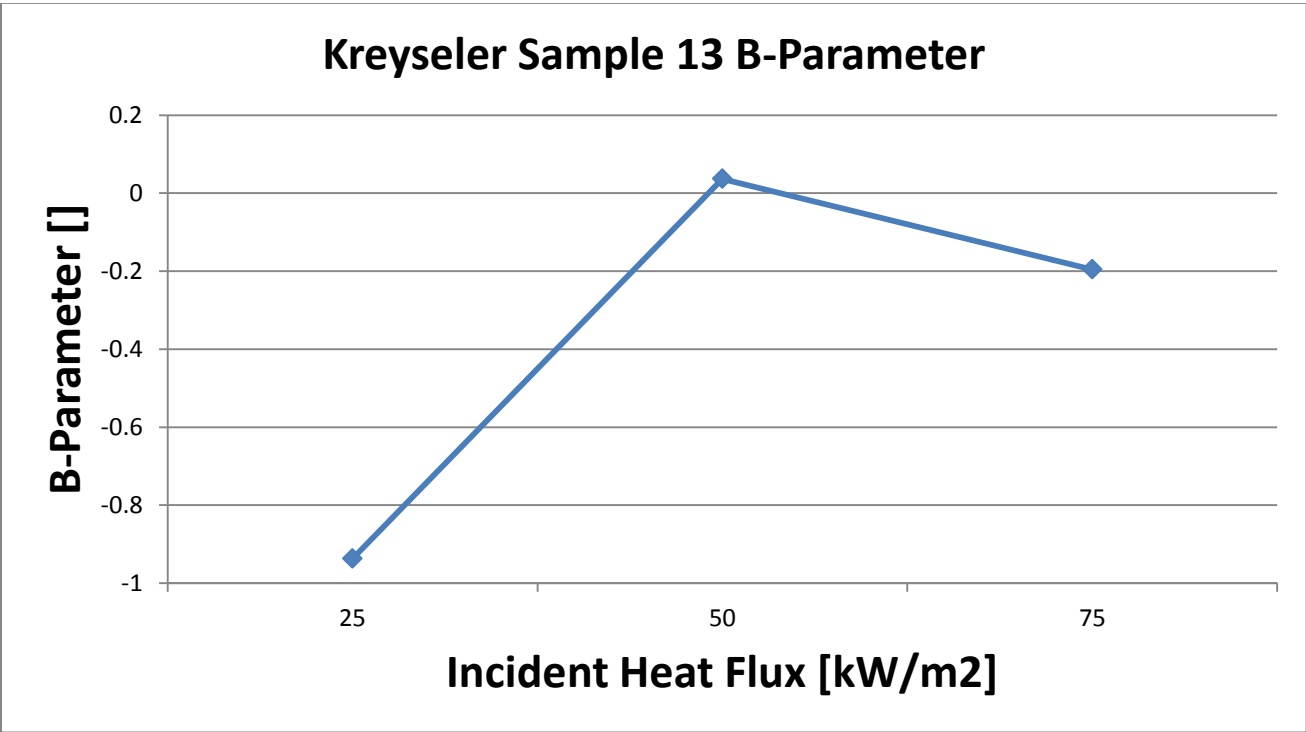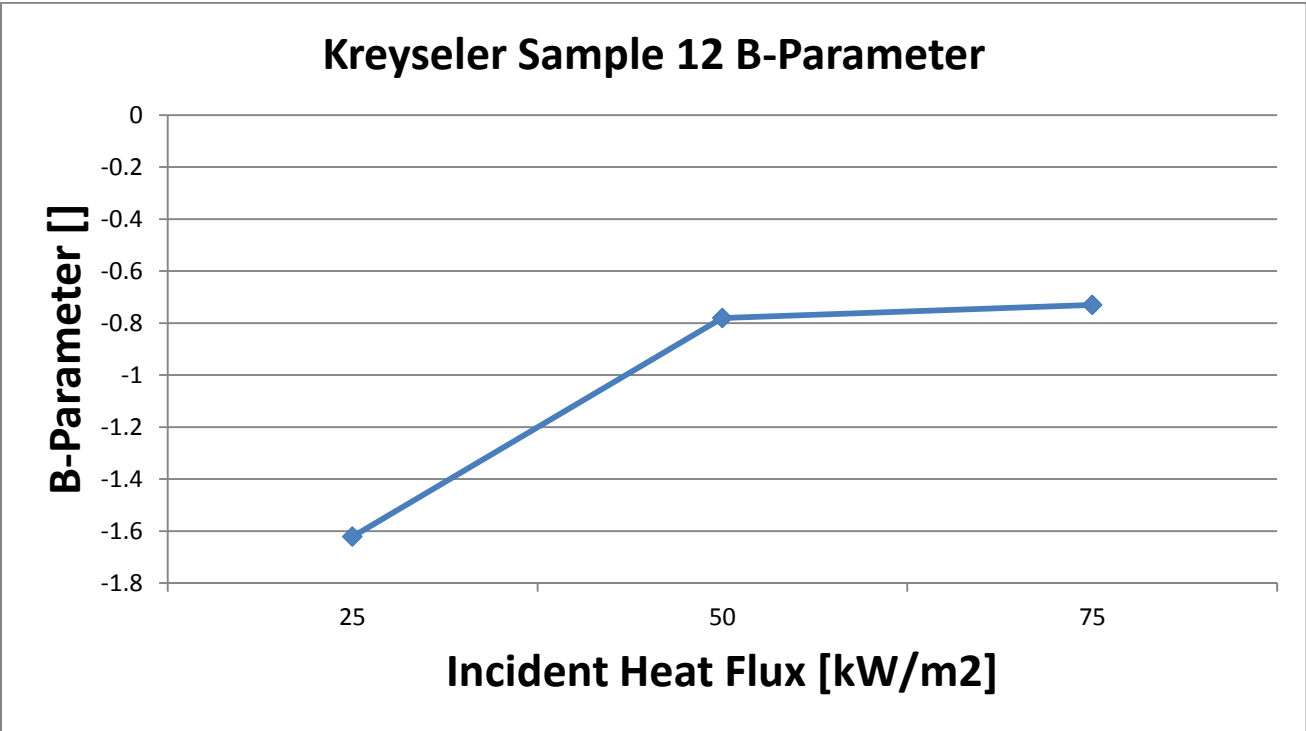

Kreyseler Baseline B-Parameter

Kreyseler Sample 1 B-Parameter

Kreyseler Sample 2 B-Parameter

B-Parameter [] vs Incident Heat Flux [kW/m2]

Kreyseler Sample 3 B-Parameter

B-Parameter [] vs Incident Heat Flux [kW/m2]

Kreyseler Sample 4 B-Parameter

Kreyseler Sample 5 B-Parameter

Kreyseler Sample 6 B-Parameter

Kreyseler Sample 7 B-Parameter

Kreyseler Sample 8 B-Parameter

Kreyseler Sample 9 B-Parameter

Kreyseler Sample 10 B-Parameter

Kreyseler Sample 11 B-Parameter

Kreyseler Sample 12 B-Parameter

Kreyseler Sample 13 B-Parameter

Kreyseler Pigment B-Parameter Comparison
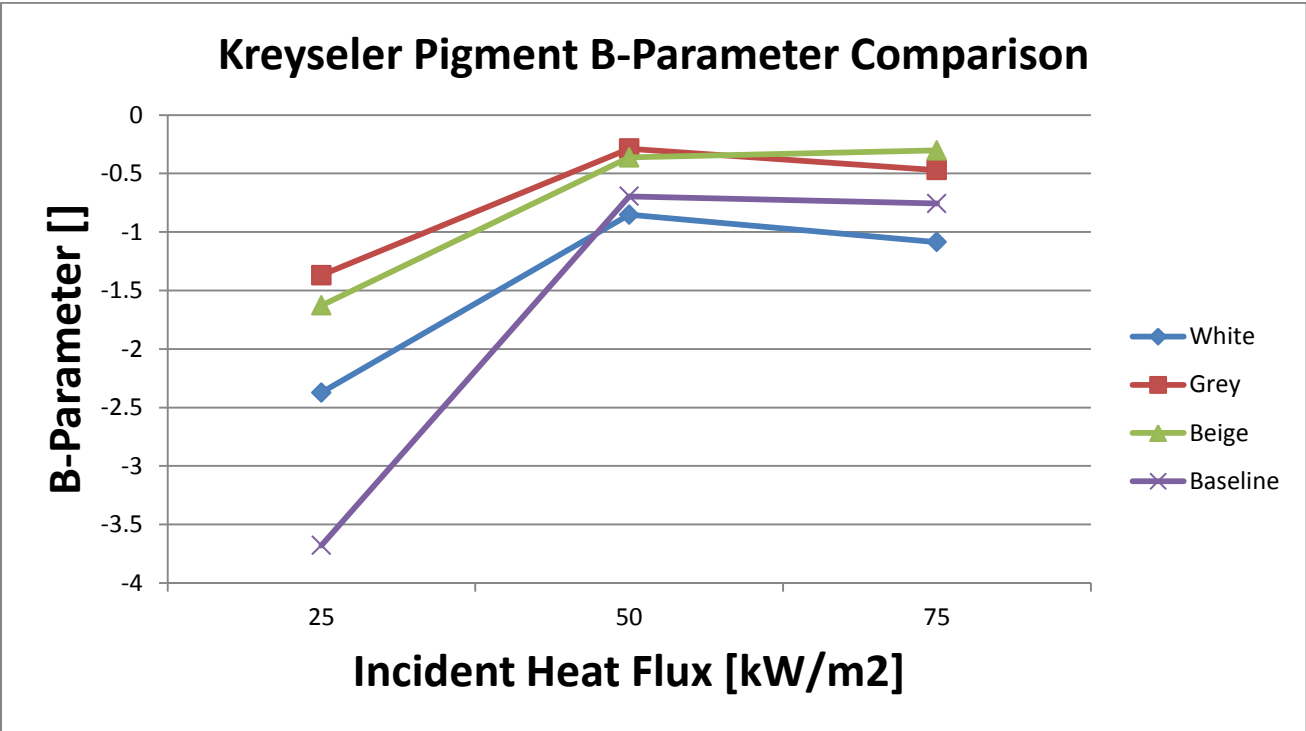

Kreyseler Aggregate B-Parameter Comparison

Kreyseler Filler B-Parameter Comparison
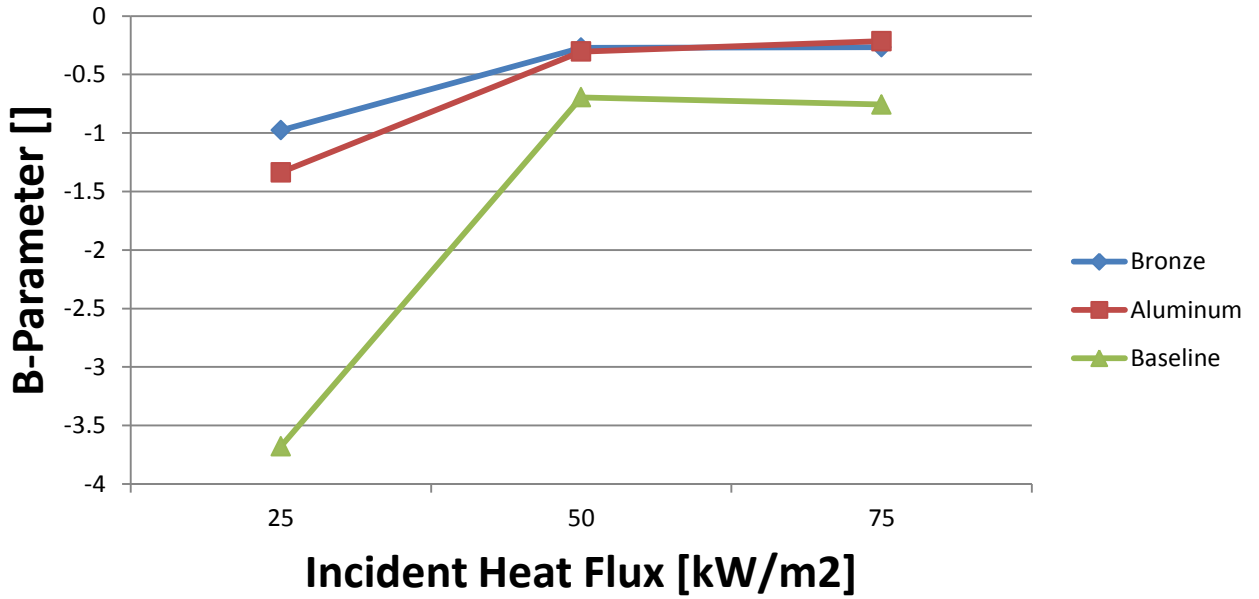
Kreyseler Gels B-Parameter Comparison

Kreyseler Cores B-Parameter Comparison
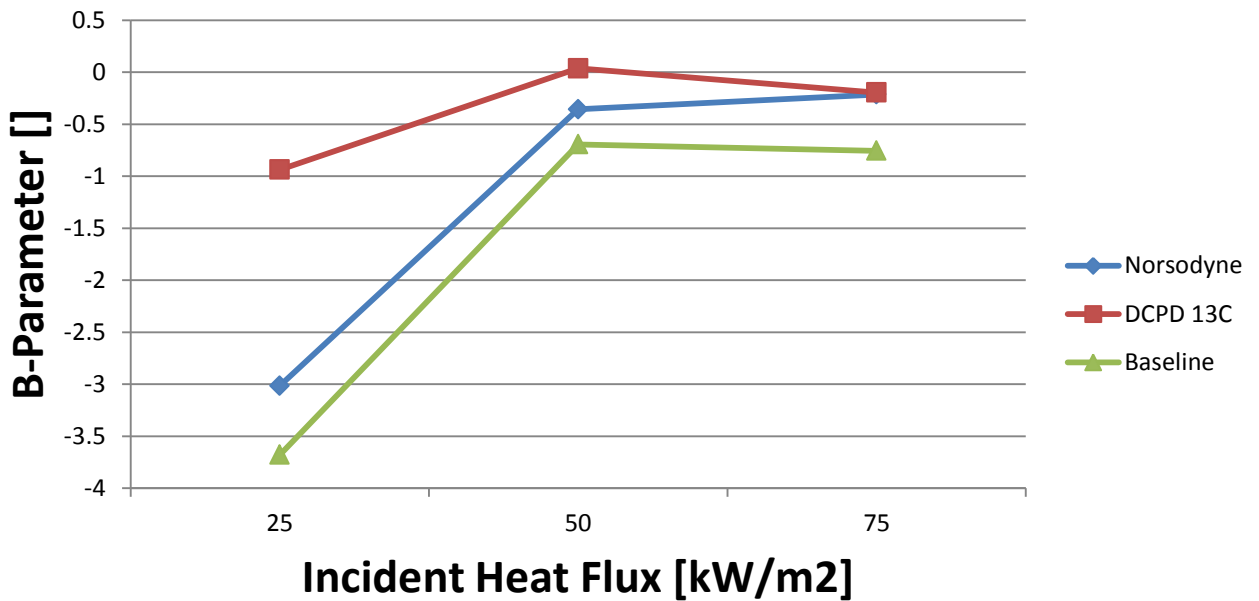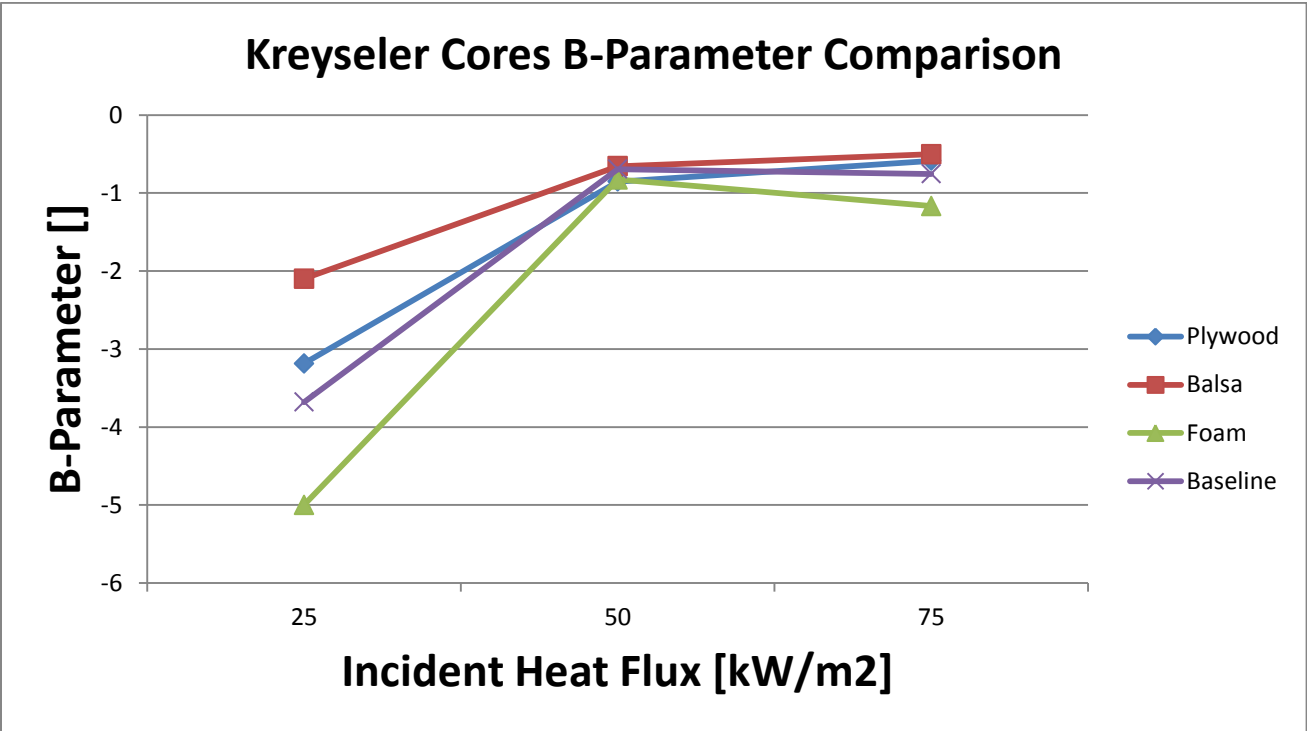
After reviewing the data, there were some questions regarding the smoke calculations for a couple of tests. Two problems were observed from the tests in question. Two tests (White Pigment and Plywood Core) showed extremely high smoke numbers while the other test (Balsa Core) had negative smoke numbers. These errors were corrected the same way. After examining the raw data, it appeared there may have been a problem with the compensating photodiode. Therefore the smoke numbers were recalculated using just the main photodiode. The equation used to calculate smoke is $= (0.1)^{-1} * ln \frac{I_o}{I}$, where I_o is the compensating photodiode and the I is the main photodiode. In the adjusted smoke calculations, the average reading of the main photodiode during the clean air burn was used instead of the compensating photodiode reading. The adjusted smoke graphs can be seen below. The shape of the graphs are the same, the adjusted calculation caused the graph to shift.

Plywood Core

Balsa Core

K-159